ASYMMETRY OF HIPPOCAMPAL FUNCTION IN MICE: LEFT-RIGHT DIFFERENCES IN MEMORY PROCESSING AND VULNERABILITY TO AMYLOID BETA

Olivia A Shipton

Thesis submitted for the degree of
Doctor of Philosophy

Magdalen College
University of Oxford
Trinity Term 2013

ABSTRACT

ASYMMETRY OF HIPPOCAMPAL FUNCTION IN MICE: LEFT-RIGHT DIFFERENCES IN MEMORY PROCESSING AND VULNERABILITY TO AMYLOID BETA

OLIVIA A SHIPTON, MAGDALEN COLLEGE, UNIVERSITY OF OXFORD
SUBMITTED FOR THE DEGREE OF D.PHIL. IN PHYSIOLOGY, TRINITY TERM, 2013

Amyloid beta (Aβ) and tau protein are both implicated in memory impairment in early Alzheimer's disease, but whether and how they interact to cause synaptic dysfunction are unknown. Consequently, I firstly investigated whether tau protein is required for the robust phenomenon of Aβ-induced impairment of hippocampal long-term potentiation (LTP), a widely accepted cellular model of memory. I demonstrate that the absence of tau prevents the Aβ-induced impairment of LTP; moreover, a specific inhibitor of the tau kinase glycogen synthase kinase 3 blocks both an Aβ-induced increase in tau phosphorylation and the Aβ-induced LTP impairment. Thus, tau protein, likely in its phosphorylated form, is required for Aβ to impair LTP. Secondly, I investigated the underlying mechanisms for this Aβ-induced impairment and find that Aβ changes the balance between the two major types of glutamate receptors involved in plasticity processes, with a specific effect on GluN2B subunit-containing NMDA receptors. Since the distribution of these receptors is asymmetric between the left and right mouse hippocampus, I accessed these different types of synapses optogenetically and found that only the GluN2B-rich synapses receiving left CA3 input show Aβ-induced changes in the balance of glutamate receptors, suggesting an asymmetry in synaptic vulnerability to Aβ. Moreover, there was a left-right difference in tetanus-induced LTP and therefore, thirdly, I investigated whether mice have a hemispheric dissociation in memory processing using acute optogenetic silencing of left or right CA3 during hippocampus-dependent memory tasks. Unilateral silencing of either the left or the right CA3 caused a deficit in short-term memory, but only left CA3 silencing impaired performance on a spatial long-term memory task. Together, these results suggest that memory may be routed via distinct left-right pathways within the mouse hippocampus, and that neural pathways subserving distinct functions may also be differentially vulnerable to pathological changes at the synaptic level.

DECLARATION

The work in this thesis is my own original work, except for: 1. the LTP recordings in **Fig. 3.6** contain some data collected by Ms. Christine Acton. 2. **Fig. 3.1**, **Fig. 3.2** and **Fig. 3.5** contain some data collected by Dr. Mariana Vargas-Caballero. 3. The Western data (**Fig. 3.7**) was collected in collaboration with Dr. Mariana Vargas-Caballero and with the guidance of Dr. Elizabeth Tunbridge. 4. To facilitate experimental blinding, Dr. Michael Kohl performed almost all the implant surgery for behavioural experiments, while Mr. Mohamady El-Gaby performed the optogenetic LTP recordings (**Fig. 4.7**) using mice in which I had performed viral injections of the optogenetic construct. 5. The Matlab scripts for acquisition, current measurement and decay-time constant measurement were written by Dr. Mariana Vargas-Caballero and the IGOR Pro scripts for acquisition and slope measurement were either general lab resources or written by Ms. Melodie Borel. 6. The P301S and their C57B/Ola controls were provided by Prof. Michel Goedert at the University of Cambridge. 7. Dr. Richard Wade-Martins at the University of Oxford generated and provided the new H1 and N296H mouse strains; the LTP data presented here is part of a wider characterisation of these lines. The work presented here has not been submitted for any other degree.

I would like to thank Prof. Ole Paulsen and Dr. David Bannerman, who have been my two supervisors for the work presented here. In addition, thanks go to Dr. Michael Kohl and Dr. Mariana Vargas Caballero for their contributions to the behavioural asymmetry and amyloid beta work respectively. I would also like to acknowledge all the members of the Neuronal Oscillations Group, past and present, who have accompanied me in the lab for the past years. It has been a pleasure to work with colleagues in the OXION Initiative, and I am particularly grateful for the opportunity given to me by Prof. Frances Ashcroft and Dr. Stephen Tucker to complete my work in the Neuronal Oscillations Group following its move to the University of Cambridge. Finally, many thanks go to the Wellcome Trust and the OXION Initiative for providing the funding for my *D.Phil.* and making this work possible.

Approximate word-count: 49,000

CONTENTS

1 Introduction **1**

1.1 Outline 2

1.2 LTP: a possible cellular substrate for learning and memory 3

1.2.1 LTP in the hippocampus as a model for associative learning 4

1.3 Pathways and mechanisms for NMDA receptor-mediated plasticity 5

1.3.1 Molecular mechanisms of NMDA receptor-dependent LTP 6

1.3.2 Molecular mechanisms of NMDA receptor-dependent LTD 8

1.4 GluN2A and GluN2B subunit-containing NMDA receptors 9

1.4.1 Bidirectional NMDA receptor-mediated plasticity 9

1.4.2 NMDA receptor composition 11

1.4.3 Functional and dynamic properties of GluN2A and GluN2B 12

1.4.4 Intracellular associations of GluN2A and GluN2B subunits 14

1.5 GluN2A and GluN2B subunit-containing NMDA receptors in plasticity 16

1.5.1 Techniques to dissociate the contribution of GluN2A and GluN2B 16

1.5.2 LTP 18

1.5.2.1 Pharmacological blockade and LTP 18

1.5.2.2 Genetic manipulations and LTP 22

1.5.3 LTD 26

1.5.3.1 Pharmacological manipulations and LTD 28
1.5.3.2 Genetic manipulations and LTD 30
1.6 GluN2A and GluN2B subunit-containing NMDA receptors in behaviour 32
1.6.1 GluN2A subunits and behaviour 32
1.6.2 GluN2B subunits and behaviour 34
1.6.3 Correlations between LTP and memory 35
1.6.4 Correlations between LTD and memory 37
1.7 Summary of NMDA receptors in plasticity and behaviour 38
1.8 Heterogeneous hippocampal synapses 41
1.8.1 Molecular and morphological characteristics of postsynaptic spines 42
1.8.2 Left-right hippocampal asymmetry of postsynaptic spines in mice 42
1.9 Alzheimer's disease 45
1.9.1 Processing of Aβ 46
1.9.2 Dysregulation of Aβ 46
1.9.3 Interaction of Aβ with neurons 49
1.9.4 Disruption of synaptic plasticity 51
1.9.5 Tau protein 52
1.10 Aim of this thesis 54
1.10.1 Objectives 54

2 Materials and Methods **56**

2.1 Mice 57
2.1.1 *In vitro* work 57
2.1.2 *In vivo* work 58
2.2 Slice preparation and storage 58

2.3 Field recording . . . 58
2.3.1 Electrophysiological protocols . . . 58
2.3.2 Data analysis . . . 60
2.4 Patch-clamp recording . . . 65
2.4.1 Electrophysiological protocols . . . 65
2.4.2 Data analysis . . . 67
2.5 Electrophysiological pharmacology . . . 69
2.5.1 Sigma-Aldrich . . . 69
2.5.1.1 Lithium chloride (L9650) . . . 69
2.5.1.2 AR-A014418 (A3230) . . . 69
2.5.2 Tocris Bioscience . . . 70
2.5.2.1 SR 95531 hydrobromide (1262) . . . 70
2.5.2.2 Amyloid β-peptide (1-42) (human) (1428) . . . 70
2.5.2.3 Amyloid β-peptide (42-1) (human) (3391) . . . 71
2.5.2.4 Ro 25-6981 maleate (1594) . . . 71
2.6 Protein extraction and Western blot analysis . . . 71
2.7 Surgery . . . 72
2.7.1 AAV vectors for optogenetic constructs . . . 72
2.7.2 CA3 virus injection surgery for *in vitro* recording . . . 73
2.7.3 CA3 implant surgery for *in vivo* behaviour . . . 73
2.8 *In vivo* light delivery . . . 74
2.9 Optrode recordings . . . 76
2.10 Behaviour . . . 78
2.10.1 Spontaneous Alternation T-Maze Task . . . 78
2.10.2 Appetitive Y-Maze Task . . . 79
2.10.3 Visual Discrimination T-Maze Task . . . 80
2.10.4 Spatial novelty Preference Y-Maze Task . . . 81

2.11 Immunohistochemistry 84
2.12 Optrode and behavioural data analysis 85

3 A role for tau in the Aβ-induced impairment of LTP 86

3.1 Introduction 87

3.1.1 Aim 90

3.2 LTP in Aβ-exposed slices from wild-type and *Tau*$^{-/-}$ mice 91

3.2.1 Synaptic properties of wild-type and *Tau*$^{-/-}$ mice 93

3.2.2 Network properties of wild-type and *Tau*$^{-/-}$ mice 95

3.3 The possible role of tau phosphorylation in LTP impairments . . . 98

3.3.1 Tau kinase inhibition with lithium 98

3.3.2 Tau kinase inhibition with AR-A014418 100

3.3.3 Tau phosphorylation changes in the presence of human $A\beta_{1-42}$ 103

3.4 Human tau mutations and LTP 105

3.5 Discussion 109

3.5.1 A role for tau in Aβ-induced toxicity 109

3.5.2 A role for GSK-3 in Aβ-induced toxicity 111

3.5.3 GSK-3 as a possible therapeutic avenue 113

3.5.4 Perspective 114

4 Synaptic mechanisms underlying the Aβ-induced effects on LTP 116

4.1 Introduction . . . 117

4.1.1 Aim . . . 120

4.2 The effect of Aβ on N/A ratios in wild-type and *Tau*$^{-/-}$ mice . . . 121

4.3 An NMDA receptor subunit-selective effect of Aβ . . . 125

4.3.1 The effect of Aβ on the NMDAR-mediated currents in wild-type and *Tau*$^{-/-}$ mice . . . 125

4.3.2 The effect of Aβ on the GluN1/GluN2B-mediated current in wild-type mice . . . 128

4.3.3 Functional GluN2B subunit-containing NMDARs in *Tau*$^{-/-}$ mice . . . 133

4.4 The role of GluN2B subunit-containing NMDARs in tetanus-induced LTP . . . 135

4.4.1 The role of GluN2B-rich synapses in tetanus-induced LTP 137

4.5 The vulnerability of GluN2B-rich synapses to Aβ . . . 141

4.5.1 The presence of GluN2B-rich synapses in *Tau*$^{-/-}$ mice . . . 143

4.6 Discussion . . . 146

4.6.1 Summary . . . 146

4.6.2 Technical considerations . . . 146

4.6.3 Possible molecular pathways . . . 151

4.6.3.1 Fyn and tau . . . 151

4.6.3.2 Extrasynaptic overactivation or synaptic underactivation . . . 152

4.6.3.3 Aβ-induced disruption in intracellular trafficking 154

4.6.4 Aβ effect at different types of synapses . . . 155

4.6.5 Perspective . . . 158

5 Left-right asymmetry in hippocampal memory processes 159

5.1 Introduction . . . 160

5.1.1 Aim . . . 163

5.2 Cell-type specific silencing and behavioural surgery . . . 164

5.2.1 Viral expression throughout the dorsal CA3 . . . 164

5.2.2 Optrode recording to test for silencing *in vivo* . . . 167

5.2.3 Behavioural surgery . . . 169

5.3 Long-term memory . . . 170

5.3.1 Appetitive spatial long-term memory task . . . 170

5.3.2 Appetitive visual discrimination long-term memory task . 173

5.4 Short-term memory . . . 176

5.4.1 Spontaneous alternation T-maze task . . . 176

5.4.2 Novelty preference Y-maze task . . . 178

5.5 Verification of expression and implant location post-testing . . . 181

5.6 Discussion . . . 183

5.6.1 Summary . . . 183

5.6.2 Unilateral lesion experiments . . . 183

5.6.3 Source of the impairments . . . 184

5.6.4 Left CA3 involvement in long-term spatial memory . . . 184

5.6.4.1 Acquisition . . . 185

5.6.4.2 Recall . . . 186

5.6.4.3 Accurate choice . . . 187

5.6.5 Left and right CA3 involvement in short-term memory . . 188

5.6.6 The development and role of asymmetry . . . 190

5.6.7 Silencing with optogenetics . . . 191

5.6.7.1 The effect of light-delivery . . . 191

5.6.7.2 Characteristics of NpHR-mediated silencing . . . 193

5.6.8 Perspective 194

6 General discussion and conclusion 197

6.1 Summary of findings 198

6.2 Use of rodents as a model system for human disease 199

6.3 Use of slices as a model system 201

6.4 Use of acute Aβ application 203

6.5 Use of pharmacology 205

6.6 Optogenetics as a technique to probe plasticity and memory . . . 208

6.7 Left-right asymmetry of mouse hippocampal function and dysfunction 210

6.8 Conclusion and perspective 213

Bibliography 215

LIST OF FIGURES

1.1 NMDAR location and subunits in synaptic plasticity 27

1.2 Left-right hippocampal asymmetry of spine distribution 44

2.1 Field recording set-up and LTP protocol 63

2.2 Details of light delivery 64

2.3 Patch-clamp recording set-up and N/A ratio measurements . . . 68

2.4 Implant surgery and light delivery 75

2.5 Optrode recordings 77

2.6 Schematics of behavioural tasks used 83

3.1 Human $A\beta_{1-42}$ does not reduce LTP in slices from *Tau*$^{-/-}$ mice . . 92

3.2 Wild-type and *Tau*$^{-/-}$ mice have similar input-output relationships and paired-pulse ratios 96

3.3 Human $A\beta_{1-42}$ does not reduce LTP in disinhibited slices from *Tau*$^{-/-}$ mice 97

3.4 Lithium effect on human $A\beta_{1-42}$-induced impairment of LTP . . . 99

3.5 The specific GSK-3 inhibitor AR-A014418 prevents the human $A\beta_{1-42}$-induced impairment of LTP in wild-type slices 101

3.6 DMSO treatment does not affect LTP results in control and human $A\beta_{1-42}$-treated slices 102

3.7 A specific inhibitor of GSK-3 reduces human $A\beta_{1-42}$-induced phosphorylation of tau 104

3.8 Mice carrying the P301S mutation do not have impaired hippocampal LTP . . . 106

3.9 Mice carrying the N269H human tau mutation do not show a human $A\beta_{1-42}$-induced LTP impairment . . . 108

4.1 Human $A\beta_{1-42}$ reduces the N/A ratio in wild-type but not *Tau*$^{-/-}$ mice . . . 124

4.2 Human $A\beta_{1-42}$ increases the contribution of the fast time constant to NMDAR-mediated current in wild-type but not *Tau*$^{-/-}$ mice 127

4.3 CA1 cells can be recorded before and after a 30 minute hold without a change in N/A ratio . . . 130

4.4 Pretreatment with human $A\beta_{1-42}$ prevents a further reduction in the N/A ratio in wild-type mice by Ro 25-6981 . . . 132

4.5 Ro 25-6981 causes a reduction in the N/A ratio in *Tau*$^{-/-}$ mice . . . 134

4.6 Ro 25-6981 does not reduce tetanus-induced LTP in slices from wild-type mice . . . 136

4.7 Tetanus-induced LTP at the CA3-CA1 pyramidal cell synapse shows hemispheric asymmetry . . . 140

4.8 Human $A\beta_{1-42}$ reduces the N/A ratio in left-injected but not right-injected wild-type mice . . . 142

4.9 Ro 25-6981 significantly reduces the N/A ratio in left-injected but not right-injected *Tau*$^{-/-}$ mice . . . 145

4.10 Table of average values for descriptive parameters in N/A ratio recordings . . . 150

5.1 Dual unilateral injection of eNpHR3.0-eYFP and YFP gives expression throughout the dorsal CA3 and its projections . . . 166

5.2 Optogenetics enables effective silencing of CA3 activity *in vivo* . . 168

5.3 Left, but not right, CA3 silencing impairs performance on a spatial long-term memory task . . . 172

5.4 Unilateral CA3 silencing does not impair performance on a visual discrimination long-term memory task . . . 175

5.5 Unilateral CA3 silencing impairs performance in a hippocampus-dependent short-term memory task 177

5.6 Unilateral CA3 silencing impairs performance in a spatial short-term memory task 180

5.7 Expression and implant placement were verified post-testing . . . 182

LIST OF TABLES

2.1 Composition of the artificial cerebral spinal fluid 59
2.2 Composition of the intrapipette solution 66

CHAPTER 1

Introduction

Deciphering how neuronal networks can robustly store information after even a single learning episode has proved to be one of the biggest challenges in neuroscience.

The possible importance of activity-driven synaptic changes to support learning and memory was proposed theoretically by Konorski (1948) and Hebb (1949). It is now forty years since the first experimental demonstration of such a phenomenon, as Bliss and Lomo (1973) showed that a high-frequency train of presynaptic stimulation delivered *in vivo* could cause a specific strengthening of a postsynaptic response to a given stimulation. Such 'synaptic plasticity' has now been found throughout the brain and encompasses both increases (long-term potentiation, LTP) and decreases (long-term depression, LTD) in synaptic strength.

1.1 Outline

In order to understand learning and memory, and how it can fail in disease, it is vital to establish the cellular mechanisms that support it. Synaptic plasticity in the hippocampus has received much experimental attention as the possible cellular substrate and therefore I will first briefly outline what is known about hippocampal synaptic plasticity and the molecular pathways that mediate input-specific increases and decreases in synaptic strength. Next, I will discuss one of the major conundrums in the field: how one type of glutamate receptor, the NMDA receptor (NMDAR), can be required to induce both directions of plasticity, and what mechanisms might exist to permit incoming neuronal activity to trigger information-rich synaptic changes. It has been proposed that the NMDAR itself may be central in facilitating this dissociation through its subunit composition, and a detailed investigation of this possibility may help elucidate learning and memory mechanisms. Therefore I will describe the evidence for and against this hypothesis in relation to synaptic plasticity and then learning and memory, and also the correlations in subunit-selectivity between these two

processes.

Dementia is a worldwide financial burden, in addition to the distressing personal consequences, and Alzheimer's disease (AD) is the leading cause. In order to understand how the failure of learning and memory might arise in this condition, it has been necessary to use a model system to probe the underlying molecular mechanisms and it is not possible to wait for an indisputable demonstration of the link between plasticity and memory. Consequently, LTP in the hippocampus has been used to investigate the possible pathological processes that destroy the ability to learn and remember. Therefore, I will outline what is known about this condition, before further exploring the pathological mechanisms in my third and fourth chapters.

Understanding the complexity of the brain remains a huge challenge, but new technologies may help approach many of the fundamental questions in neuroscience from a different angle. I will describe how one such technology, optogenetics, may enable us to harness the asymmetry of the rodent brain to investigate the mechanisms underlying LTP. In my fourth and fifth chapters, I investigate whether this asymmetry might have relevance for understanding AD pathology at the synaptic level and, finally, within the context of long-term associative spatial memory.

1.2 LTP: a possible cellular substrate for learning and memory

LTP is a particularly attractive cellular model for learning and memory because it has a number of features that suggest how memories could be acquired, stored and, later, reliably retrieved. LTP is input-specific, with increases only in the experimental pathway; this is likely to be a pre-requisite to meaningfully encode information. Not only is LTP input-specific, it is also long-lasting; for example, changes persist for at least six days in awake animals (Doyere et al., 2003). The timing requirements for pre- and postsynaptic activity in the induction of LTP (Bi and Poo, 1998) also suggest how this mechanism could form associa-

tions between occurrences in the external world. Finally, given that memories can be made after only brief experience, LTP fulfils the requirement for a learning mechanism that the increases in synaptic strength can be generated by brief tetanic stimuli. Although there is not yet causative evidence that synaptic plasticity mediates learning, there is strong circumstantial evidence. Two of the most convincing are, firstly, recordings which show that synaptic weights increase in parallel with the acquisition of a behavioural task (Whitlock et al., 2006; Gruart et al., 2006; Valenzuela-Harrington et al., 2007); secondly, that learning and LTP can both occlude each other (Gruart et al., 2006; Whitlock et al., 2006), suggesting the same mechanisms may underpin both.

1.2.1 LTP in the hippocampus as a model for associative learning

It is difficult to imagine a mechanism for learning and memory that does not involve pertinent neuronal activity leading to long-lasting changes in synaptic weights distributed throughout the network. However, more contentious is the specific hypothesis that LTP in the hippocampus supports long-term associative learning.

The hippocampus has been a brain region of interest since the famous discoveries made from the study of patient HM, who lost the ability to lay down new declarative memories after surgical removal of the medial temporal lobes (Scoville and Milner, 1957). Moreover, when pathological changes take place in the hippocampus, devastating diseases can result. One such condition is Alzheimer's disease (AD), the early stages of which are characterised by cognitive decline specifically involving impairments in learning and memory (Burns and Iliffe, 2009). It is now widely accepted that declarative memories for facts, places and events both require, and actively engage, the hippocampus in humans (Squire and Zola-Morgan, 1991; Squire et al., 1992). The hippocampus has also been extensively studied in rodents, where it was evident that hippocampal function also extends to a role in navigation, with the description of place cells

(O'Keefe and Dostrovsky, 1971). Nevertheless, a role in learning and memory is also likely, given the importance of an intact hippocampus for performance in tasks testing these cognitive abilities (Olton and Papas, 1979; Morris et al., 1982, 1990). Given that the hippocampus appears to play a fundamental role in learning and memory processes, synaptic plasticity at hippocampal excitatory synapses, especially the CA3-CA1 synapse, has become a model system to try and understand the underlying mechanisms. It is now established that most forms of hippocampal plasticity require the activation of NMDARs, for their induction (Collingridge et al., 1983). NMDARs are ideal candidates for molecular mediators of plasticity due to their Ca^{2+} permeability and also their coincidence detector properties that result from a voltage-dependent Mg^{2+} block (Bliss and Collingridge, 1993).

The first evidence that NMDAR-dependent LTP in the hippocampus might underpin associative spatial learning was the demonstration that intraventricular infusions of an NMDAR antagonist in rats both impaired this form of plasticity and also the ability to learn a spatial location across a number of trials (Morris et al., 1986). Another crucial finding was that a genetic manipulation that removed NMDARs in the CA1 region of the mouse hippocampus, albeit not without some extrahippocampal removal, blocked LTP at the CA3-CA1 synapse and slowed the rate of spatial associative learning (Tsien et al., 1996).

1.3 Pathways and mechanisms for NMDA receptor-mediated plasticity

Plastic changes at the synapse can have both short- and long-term components (Gustafsson and Wigström, 1986), and these may be supported by distinct processes and have different NMDAR subunit-dependency for their induction (Volianskis et al., 2013). Long-term plasticity is expressed by changes in AMPA receptors (AMPARs) at the postsynaptic element and/or changes in presynaptic transmitter release (Bliss and Collingridge, 2013). Ultimately, such changes

appear to be consolidated by structural alterations. Several mechanisms might contribute to plasticity in different brain regions, and some of these are NMDAR independent; examples being LTP at the mossy fibre synapse in CA3 (Zalutsky and Nicoll, 1990) and also metabotropic glutamate receptor-dependent LTD in CA1 (Oliet et al., 1997). Here, however, I will focus on NMDAR-dependent plasticity, in particular at the CA3-CA1 synapse, given its possible relevance for associative learning.

The induction of LTP is primarily characterised by phosphorylation cascades, while LTD processes are mediated by phosphatases. LTD is not simply the reverse of the mechanisms that support LTP, but there are a number of points of interaction between these two processes. Thus, a delicate balance must be maintained for appropriate synaptic function and this equilibrium would be vulnerable to pathological disruption.

1.3.1 Molecular mechanisms of NMDA receptor-dependent LTP

Ca^{2+}/calmodulin-dependent protein kinase II (CaMKII) is vital for the induction of LTP (Lisman et al., 2002), becoming activated by Ca^{2+} influx through NMDARs. There is a basal level of CaMKII present at the postsynaptic density (PSD) bound to NMDARs (Leonard et al., 1999), but this is supplemented by active, autophosphorylated CaMKII that translocates to the PSD following the induction of LTP (Otmakhov et al., 2004) and binds to NMDARs (Strack and Colbran, 1998) in the vicinity of its substrates, which include AMPARs. Protein kinase C (PKC) and mitogen activated protein kinases (MAPK) also mediate phosphorylation. The very early increases in synaptic strength are likely to be mediated by two processes. The first is an increase in conductance of AMPARs already present at the PSD (Benke et al., 1998; Lüthi et al., 2004), possibly mediated by phosphorylation of AMPARs at Ser831 (Barria et al., 1997; Lee et al., 2000) and also by capture at the PSD of mobile AMPARs already present in the membrane at extra- and perisynaptic sites (Lisman et al., 2012). The second pro-

cess is the incorporation of new AMPARs. This mechanism is more complex than simply direct insertion of AMPARs at the postsynaptic site, and Opazo and Choquet (2011) have suggested that a three-stage model might explain this increase. Firstly, LTP-inducing stimuli triggers exocytosis of GluA1-containing AMPARs to extra- and peri-synaptic regions; secondly, these diffuse laterally into synaptic sites; thirdly, receptors must be captured by the scaffolding of the PSD in order to be maintained at the synapse. CaMKII-mediated phosphorylation of AMPAR auxiliary protein stargazin appears important in this capture process (Opazo et al., 2010). Stargazin also increases the rate of AMPAR opening and decreases its deactivation rate (Tomita et al., 2005a), both of which would also contribute to an increase in synaptic strength. Nevertheless, while LTP pathways likely exert tight regulation of the initial membrane insertion stage, it has recently emerged that the subsequent steps of this process may be more flexible. Granger et al. (2013) found that, although a reserve pool of receptors was required to support synaptic strengthening in the hippocampus, the subtype identity of the AMPARs was unimportant; moreover, even the kainate receptor, a glutamate receptor not normally found at that synapse, could substitute. Following the initial recruitment of GluA1 subunit-containing AMPARs to the postsynaptic membrane, they are subsequently replaced by GluA2-containing AMPARs to support a continued enhancement of synaptic strength (Shi et al., 2001; Plant et al., 2006).

It has been suggested that LTP is maintained by persistent kinase activity. A strong candidate for this role appeared to be a kinase known as protein kinase M-ζ (PKMζ), since blocking it with a peptide called ZIP reversed both hippocampal LTP and specific spatial memories (Pastalkova et al., 2006) However, its importance has recently been questioned, since two laboratories have reported that hippocampal LTP and hippocampus-dependent learning are present in both constitutive and conditional PKMζ knock-out mice (Lee et al., 2013; Volk et al., 2013). In fact, it seems unlikely that a mechanism merely involving elevated kinase activity could maintain information storage over years,

and a better candidate to sustain enhanced synaptic strength would be structural changes at the synapse. Imaging in neuronal cultures and in animals *in vivo* has revealed two major structural changes associated with LTP. Firstly, pre-existing thin postsynaptic spines enlarge (Matsuzaki et al., 2004). Secondly, new spines appear, and LTP also correlates with the stabilisation of such nascent spines (Hill and Zito, 2013).

1.3.2 Molecular mechanisms of NMDA receptor-dependent LTD

Homosynaptic LTD of basal responses at the CA3-CA1 synapse was was first described by Dudek and Bear (1992) and Mulkey and Malenka (1992) and, in contrast to the phosphorylation cascades that mediate LTP, LTD requires phosphatase activity (Mulkey et al., 1993). Specifically, Ca^{2+} influx through NMDARs triggers activates (PP2B/calcineurin), which in turn inactivates inhibitor-1; thus, the inhibition of protein phosphatase 1 (PP1) is lifted and it can dephosphorylate its substrates to mediate LTD (Mulkey et al., 1994). The major mechanism underlying LTD is likely to be the internalisation of AMPARs, encouraged by PP1-mediated dephosphorylation of stargazin, which is one major point of bidirectional regulation of synaptic strength (Tomita et al., 2005b). There is also selective dephosphorylation of GluA1 at the protein kinase A site Ser845 (Kameyama et al., 1998; Lee et al., 1998), which controls activity-dependent AMPAR trafficking (Esteban et al., 2003) and may also be important for regulating AMPAR channel conductance (Banke et al., 2000). The type of LTD induced can also depend on the prior history of the synapse, since Lüthi et al. (2004) demonstrated that LTD was only characterised by a decreased AMPAR conductance if preceding LTP expression had involved an increase. LTD may be consolidated by structural plasticity, in the form of cofilin-mediated spine shrinkage, or even elimination, (Zhou et al., 2004; Bosch and Hayashi, 2012).

1.4 GluN2A and GluN2B subunit-containing NMDA receptors

Therefore, the downstream pathways that mediate LTP and LTD include different enzymes and recruit distinct cellular mechanisms. Moreover, additional processes exist to reinforce directional changes in synaptic strength (Peineau et al., 2007). Nevertheless, how relevant neuronal activity triggers meaningful plasticity *in vivo* remains uncertain, and one particular difficulty has arisen because NMDAR activation is the point of initiation for both LTP and LTD pathways.

A number of theories have been proposed to explain how different patterns of neuronal activity can lead to opposite effects on synaptic strength when both forms of plasticity depend on the same type of receptor. Further understanding of such mechanisms will help establish how LTP can interact with competing processes of synaptic change, in order to store relevant information *in vivo*. It may also help elucidate disease processes, since pathology might arise when the fine balance between these plasticity processes is disrupted.

1.4.1 Bidirectional NMDA receptor-mediated plasticity

The induction of NMDAR-mediated plasticity involves coupling of Ca^{2+} influx at the postsynaptic element, the 'spine', to the different intracellular signalling cascades that mediate changes in synaptic weights. It was quickly identified that the magnitude of Ca^{2+} influx through NMDARs in the traditional high frequency paradigms used to induce LTP was much greater than that during the low frequency LTD paradigms. Therefore, it was proposed that different levels of Ca^{2+} influx could couple to distinct intracellular signalling pathways to cause the molecular, and ultimately structural, changes at the synapse that underlie the two directions of plasticity (Lisman, 1989). This was also extended to the induction of plasticity by precise spike timing (Shouval et al., 2002). However, it seemed that a mechanism based on Ca^{2+} levels alone may not be sufficiently

robust, and it also could not account for some experimental observations; thus, Ca^{2+} time-course was suggested to be important (Yang et al., 1999; Rubin et al., 2005). Postsynaptic Ca^{2+} dynamics are tightly regulated by small-conductance Ca^{2+}-activated K^+ channels (Ngo-Anh et al., 2005; Tonini et al., 2013), voltage-dependent Ca^{2+} channels (Yasuda et al., 2003; Bloodgood and Sabatini, 2007) and intracellular Ca^{2+} release (Futatsugi et al., 1999); the Ca^{2+} microdomains that these generate could provide a finer level of control in the regulation of bidirectional plasticity.

In parallel to refinements in the theory linking Ca^{2+} dynamics and bidirectional plasticity arose the suggestion that the NMDAR itself could intrinsically dissociate between synaptic strengthening and weakening in response to activity patterns. NMDARs are found both pre- and post-synaptically, and evidence from neocortical areas has set a precedent that these distinct populations of NMDARs may support different plasticity mechanisms (Corlew et al., 2007; Rodríguez-Moreno et al., 2011; Sjöström et al., 2003). This might also apply in the hippocampus, since plasticity can be mediated by changes in presynaptic release probability under some experimental conditions (Emptage et al., 2003; Ward et al., 2006; McGuinness et al., 2010; Bliss and Collingridge, 2013). However, postsynaptic NMDARs could still support a variety of mechanisms, both through their location and also through their composition. NMDARs at the postsynaptic site can be found synaptically, perisynaptically and extrasynaptically (**Fig. 1.1**(**A**)). These three populations of receptors are recruited differentially by neuronal activity patterns, suggesting they may play distinct roles. However, even within the synaptic population of NMDARs there is the potential for independent functions, since NMDARs with different subunit compositions have different properties.

The distinct kinetic properties conferred by NMDAR subunits might allow the NMDAR composition to influence a finer level of control over the postsynpatic Ca^{2+} dynamics. Subunits also make distinct molecular associations, and

thus could independently couple to the downstream kinase and phosphatase pathways that have been established to regulate each direction of plasticity (Malenka and Bear, 2004). Furthermore, the relative abundance of these subunits at synaptic sites is tightly regulated throughout development, and a transition in subunit dominance correlates with changes in the ease of plasticity induction (Dumas, 2005). All this evidence converged on the attractive suggestion that the type of plasticity induced could be determined by the type of NMDAR subunit activated, perhaps by enabling transmission of distinct signals and tightly coupling them to different downstream signalling molecules. This hypothesis has been explored both *in vitro* and *in vivo*, and might also have relevance to understanding AD, since this begins as a disease of synaptic dysfunction (Selkoe, 2002).

1.4.2 NMDA receptor composition

NMDARs consist of two obligatory GluN1 subunits and two additional GluN2 or GluN3 subunits that confer the particular properties of the receptor. Each subunit consists of four major domains: the N-terminal domain containing binding sites for allosteric modulators such as Zn^{2+} and ifenprodil; the agonist-binding domain, where the binding sites for glycine/D-serine (on GluN1) and glutamate (on GluN2) are located and where competitive antagonists act; the pore domain, accessible to pore blockers such as phenycyclidine (PCP) and MK801; and, lastly, the C-terminal domain (CTD), which binds to different intracellular mediators. The two predominant GluN2 subunits in the hippocampus are GluN2A and GluN2B, although GluN2C and GluN2D are also present, in particular early in development, but also in low quantities in adulthood (Monyer et al., 1994). Hippocampal NMDARs can be diheteromeric (GluN1/GluN2A and GluN1/GluN2B) or triheteromeric (GluN1/GluN2A/GluN2B). The expression of GluN2B is high at birth but decreases into adulthood, while GluN2A expression increases with age (Monyer et al., 1994; Kirson and Yaari, 1996; Dumas, 2005; Yashiro and Philpot,

2008). The triheteromeric population is increasingly recognised to form a large proportion of the synaptic NMDARs in the adult brain (Rauner and Köhr, 2011; Gray et al., 2011; Tovar et al., 2013; Volianskis et al., 2013) but, since these receptors cannot be selectively interrogated pharmacologically, the characteristics of triheteromeric receptors can only be inferred. Thus, their precise role remains enigmatic, though likely important.

1.4.3 Functional and dynamic properties of GluN2A and GluN2B

Measurements of channel currents or postsynaptic responses to single stimuli have revealed notable differences in the kinetics of GluN2A and GluN2B subunit-containing NMDARs, and this is one way in which these channel subtypes could influence the induction of plasticity. Single-channel recordings in HEK cells showed that GluN1/GluN2A receptors have a higher probability of opening in response to glutamate and also a higher peak open probability than GluN1/GluN2B receptors (Erreger et al., 2005). These findings have been supported by whole-cell measurements in HEK cells (Chen et al., 1999) and also acute hippocampal slices (Gray et al., 2011) where channel open probability was estimated by use-dependent block of NMDAR populations with MK801. The faster activation and deactivation rates of individual NMDARs comprising GluN1/GluN2A result in whole-cell currents that rise and decay more quickly than those supported by GluN1/GluN2B, and a triheteromeric population apparently has an intermediate decay time constant (Vicini et al., 1998).

The response of NMDARs to multiple stimuli at a range of frequencies over different durations is particularly important in the context of synaptic plasticity. Measurements from single-channel recordings have been used to simulate the responses of GluN2A and GluN2B subunit-containing NMDARs to trains of presynaptic activity and this showed a relationship between stimulation frequency and total charge transfer that differed between the two subunits (Erreger et al., 2005). It was found that at the very low frequencies (0.1-0.3 Hz) used in

some plasticity protocols, GluN1/GluN2B channels supported twice as much charge transfer due to their slower deactivation rate. At the 1 Hz stimulation favoured for LTD induction, charge transfer through GluN1/GluN2B channels still exceeded that through GluN1/GluN2A, but to a lesser extent, and it was equivalent between channels at 2 Hz. Modelling also revealed that the duration of activity is important at high frequencies of stimulation; for the 100 Hz frequency often used in high-frequency induction protocols, the duration of the stimulus train dramatically changed the charge transfer through GluN2A and GluN2B subunit-containing NMDARs. The two channel subtypes permitted equivalent charge transfer for 100 ms of stimulation; however, for a 1000 ms stimulus train, the typical duration used to induce LTP, GluN1/GluN2A supported twice the charge transfer of GluN1/GluN2B (Erreger et al., 2005). Desensitisation of GluN2A and GluN2B subunit-containing NMDARs will also contribute to their ability to mediate charge transfer, but the effect will be highly influenced by the subunit composition at the postsynaptic spine; modelling has suggested that a larger fraction of GluN2A-subunit containing NMDARs will be desensitised at stimulation frequencies from 5 to 100 Hz, but that the difference between GluN2A and GluN2B will be lowest at 100 Hz for 1000 ms (Singh et al., 2011). Although these modelling studies provide useful information predicting how subunit composition and plasticity protocols may interact, further experimental investigation is essential to test their predictions under physiological conditions.

It is generally assumed that the magnitude of Ca^{2+} influx is related to charge transfer. This suggests that differences in charge transfer between channel subtypes would be important in the ability of each subunit composition to trigger distinct forms of plasticity since these require different postsynaptic Ca^{2+} dynamics. However, the relationship may be more complex, since Ca^{2+}-imaging of spines has revealed that the magnitude of Ca^{2+} influx in response to glutamate application does not necessarily correlate with NMDAR-mediated charge transfer (Sobczyk et al., 2005). Moreover, a GluN2B subunit-selective antagonist

caused a greater reduction in Ca^{2+} influx in those spines that supported a higher change in Ca^{2+} per uncaging-evoked EPSC, which led the authors to conclude that GluN2B subunit-containing NMDARs support a greater Ca^{2+} influx per unit of current (Sobczyk et al., 2005). This had previously not been observed in recombinant GluN2A or GluN2B subunit-containing NMDARs in heterologous systems (Monyer et al., 1994), which may be due to methodological differences, the presence of triheteromeric NMDARs, and/or post-translational modifications of NMDARs in acute brain slices, and so further investigation is required. If this higher Ca^{2+} influx through GluN2B subunit-containing NMDARs holds, it suggests that this subunit could exert a disproportionate influence on plasticity.

1.4.4 Intracellular associations of GluN2A and GluN2B subunits

Other ways in which NMDAR subunits could influence the direction of plasticity relate to their long CTDs, since these allow for many intracellular interactions and modifications by phosphorylation. Many of these direct and indirect molecular associations are unique, since the CTD shows a high level of sequence divergence between GluN2A and GluN2B. This permits separate regulation of their presence or absence at the synapse and could also couple each subunit to different downstream signalling cascades that support either LTP or LTD; a few key examples of these interactions with relevance to plasticity are outlined below.

The presence of GluN2A and GluN2B subunit-containing NMDARs at the synapse is stabilised by their interaction with the PSD subfamily of membrane-associated guanylate kinases, which includes PSD-95 and PSD-93, and also the synapse-associated proteins SAP102 and SAP97 (O'Brien et al., 1998). Posttranslational modifications can alter the strength with which GluN2A and GluN2B subunits bind to these PSD proteins, and this is one mechanism that regulates the availability of these subunits at the synapse; in turn, this could influence the

induction of plasticity. For example, cyclin-dependent kinase 2 (Cdk2) phosphorylates GluN2B at Ser1480, which disrupts its interaction with PSD-95 and SAP102 and leads to a reduction in synaptic GluN2B (Chung et al., 2004; Sanz-Clemente et al., 2010). Not only is this phosphorylation event unique to GluN2B (Sanz-Clemente et al., 2010), it is also regulated by synaptic activity (Chung et al., 2004). Surface levels of GluN2B can also be regulated by phosphorylation at Tyr1472 by Fyn and Src; phosphorylation prevents the clathrin adaptor protein AP-2 binding to the GluN2B internalisation motif YEKL and thus inhibits endocytosis. Cdk5 is likely to be an additional component in this regulatory cascade, since inhibiting it encourages the interaction between Src and PSD-95, and consequently increases Tyr1472 phosphorylation (Zhang et al., 2008). Another example is the endocytosis of GluN2A, which is controlled by a dileucine motif at a different site (Leu1319 and Leu1320) (Lavezzari et al., 2004), and thus its surface expression can be regulated independently. It is notable that GluN2B subunits also undergo more frequent endocytosis than GluN2A, and that these two subunits traffic into different intracellular pathways, with GluN2B trafficking into recycling endosomes and GluN2A into late endosomes (Lavezzari et al., 2004). This suggests that activity- or neuromodulatory-dependent regulation of GluN2B may be a quicker or more sensitive way to alter the state of a synapse.

In addition to separate regulatory pathways to control synaptic GluN2A and GluN2B levels, unique associations with different enzymes may also enable the subunits to contribute to opposing forms of plasticity. The most important example is probably the high affinity binding between the GluN2B CTD and the catalytic domain of CaMKII (Strack and Colbran, 1998). This interaction anchors CaMKII at the synapse in its active conformation (Bayer et al., 2001). LTP requires active CaMKII (Lisman et al., 2002); more specifically, the association between GluN2B and active CaMKII (Barria and Malinow, 2005). Therefore, the ability of GluN2B to mediate tight coupling between Ca^{2+} influx and CaMKII under basal conditions (Leonard et al., 1999) suggests that this subunit may play a crucial role in LTP. In addition, given that autophosphorylated CaMKII

translocates to the PSD after an LTP induction protocol (Otmakhov et al., 2004), it may help to maintain active CaMKII in the vicinity of its substrates to initiate the phosphorylation events that support synaptic strengthening. Another notable protein interaction at the postsynaptic spine is that between GluN2B and Ras-GRF1, a Ca^{2+}/calmodulin-sensitive Ras-specific GDP/GTP exchange factor that has been implicated in synaptic plasticity (Li et al., 2006; Jin and Feig, 2010). There are also proteins that associate indirectly with NMDARs but still retain a subunit preference, permitting an extra level of complexity in the modulation of NMDAR function by its subunit composition.

1.5 GluN2A and GluN2B subunit-containing NMDA receptors in plasticity

As illustrated thus far, there are three main ways in which varying subunit composition could affect the type of plasticity induced. Firstly, the different channel properties conferred by GluN2A and GluN2B subunits could encourage sufficiently distinct postsynaptic spine Ca^{2+} dynamics to trigger separate downstream plasticity pathways. Secondly, the unique associations made by the CTDs of these two subunits provide a direct mechanism by which GluN2A and GluN2B could couple to independent intracellular signalling cascades and thus play different roles in synaptic plasticity. Finally, changes in the quantity or subcellular location of these subunits could alter the basal state of a spine and thus affect the future induction of plasticity. Given these possibilities, it is interesting to ask to what extent experimental evidence supports the hypothesis that different NMDAR subunit compositions determine the outcome of a plasticity protocol.

1.5.1 Techniques to dissociate the contribution of GluN2A and GluN2B

A wide variety of induction protocols can be used to induce synaptic changes in the hippocampus, and these range from spike-timing dependent paradigms,

which use low-frequency stimulation and precisely timed pre- and postsynaptic spiking, to high-frequency induction protocols. Since there are considerable differences in the activity patterns used to induce even one direction of plasticity, it is possible that the synaptic changes induced by such diverse paradigms have distinct mechanistic underpinnings. Consequently, experimental results are only truly comparable when the same protocol is applied.

Various plasticity protocols have been used in combination with pharmacological and genetic manipulations to investigate the potential role of different NMDAR subunits in plasticity. The first studies into the contribution of distinct NMDAR subpopulations to bidirectional plasticity compared the possible contributions of GluN2A/B and GluN2C/D subunits using broad-spectrum antagonists (Hrabetova and Sacktor, 1997; Hrabetova et al., 2000). Subsequent studies have focussed on dissecting whether differences exist between GluN2A and GluN2B, since these are the predominant subunits present at the juvenile and adult CA3-CA1 synapse. There are currently highly selective pharmacological tools to block GluN1/GluN2B receptors, primarily ifenprodil and its more potent derivative Ro 25-6981 (Paoletti and Neyton, 2007). Nevertheless, these are activity-dependent blockers, and the agonist concentration affects the extent to which these antagonists inhibit GluN2B-subunit containing NMDARs; for example, 3 μM Ro 25-6981 achieves 93% inhibition in the presence of 100 μM NMDA but only 62% in 10 μM NMDA (Fischer et al., 1997). The study of GluN2A is even more limited by the lack of selective antagonists for this subunit. NVP-AAM077 (hereafter referred to as NVP) is commonly used as a GluN2A-preferring antagonist (Paoletti and Neyton, 2007), but it is now known to be less selective in rodents than had been assumed from recombinant human proteins, and it actually shows only a tenfold preference for GluN2A over GluN2B (Feng et al., 2004). Therefore, data collected using NVP invariably has some block of GluN2B as well, but the magnitude of this block varies considerably with the concentration used.

Pharmacological and genetic manipulations allow the investigation of different aspects of NMDAR function. Pharmacological approaches are informative about the role of the NMDAR as an ion channel and do not directly address the importance of intracellular associations. They also will indiscriminately affect a particular NMDAR subtype on all cell types, for example interneurons and pyramidal neurons, where they may play different roles. In turn, this could have repercussions for the network that manifest at a circuit as well as at a behavioural level (Hanson et al., 2013). In contrast, constitutive and inducible genetic knock-outs provide information about the combined role of the NMDAR channel properties and synaptic presence and can be directed to a particular cell type; however, given the changes in subtype composition throughout development, and even on the short timescales of metaplasticity, perturbing the balance of receptors is likely to cause other changes in the network or to recruit compensatory processes in the long-term. In addition, pharmacological manipulations have often been performed in rats, while almost all the genetic manipulations discussed below have used mice, and species differences have not been excluded.

1.5.2 LTP

1.5.2.1 Pharmacological blockade and LTP

An early study often cited to argue for the differential involvement of NMDAR subunits in the induction of LTP and LTD found that pharmacological block of GluN2A by NVP prevented tetanus- and pairing-induced LTP in 3-4 week-old rats but that antagonism of GluN2B by ifenprodil/Ro 25-6981 did not, but instead blocked LTD induction (Liu et al., 2004). Another study, using the same pharmacological concentrations and age of rats, also found that NVP completely blocked tetanus-induced LTP, though here ifenprodil and Ro 25-6981 partially blocked this form of LTP (Li et al., 2007). However, the data in both these studies were collected using a relatively high NVP concentration;

thus, in addition to the aforementioned lack of NVP specificity, the resultant NMDAR-mediated current block was much greater with NVP (reduction of current: 53 ± 3% in Liu et al. (2004) and 81 ± 3% in Li et al. (2007)) compared to the small reductions caused by Ro 25-6981 (36 ± 5% in Liu et al. (2004) and 32 ± 3% in Li et al. (2007)). Therefore, this apparently selective role of the GluN2A subunit might instead arise from a threshold effect, whereby inhibiting more total NMDAR-mediated current could block LTP, especially given that a high level of Ca^{2+} influx is traditionally thought to be required for LTP induction. Indeed, when a study in mice controlled for this by selecting antagonist concentrations to reduce NMDAR-mediated current equally (40% reduction to match that possible by Ro 25-6981), pairing-induced LTP was not impaired irrespective of the antagonist used (NVP, Ro 25-6981 or the broad-spectrum NMDAR antagonist 2-amino-5-phosphonopentanoate (AP5)) (Berberich et al., 2005). The same antagonist concentrations, as titrated for their NMDAR current reduction in the aforementioned study, also did not impair LTP induced by a theta-burst paradigm in adult mice (Romberg et al., 2009), though this low NVP concentration did partially block tetanus-induced LTP, while ifenprodil did not (Izumi et al., 2006). This suggests that tetanus-induced LTP is the most sensitive to GluN2A block. In addition to the extent of current reduction, the developmental stage is likely to account for some of the different results reported. For example, in one study using 2-week-old rats, LTP was impaired by both GluN2A and GluN2B antagonism (Bartlett et al., 2007), but this is probably because the developmental transition in subunit composition is not yet complete at this age in rats, since GluN2B antagonism reduced LTP in 2-week-old rats but not in those over 6 weeks (Köhr et al., 2003). Some pharmacological studies have also been conducted *in vivo*, where, although it is more difficult to determine the exact concentrations to which the CA3-CA1 synapse is exposed, the variability introduced by different slicing angles, techniques and incubation solutions is avoided. Intra-hippocampal infusions of both Ro 25-6981 and NVP blocked tetanus-induced LTP *in vivo* in 4-6 week-old rats (Fox et al., 2006), whereas,

when drugs were delivered intraperitoneally, only NVP blocked LTP with Ro 25-6981 having no effect (Fox et al., 2006; Ge et al., 2010); this apparent discrepancy is likely to result from different levels of NMDAR block. Therefore, even *in vivo* studies have not yielded a clear conclusion.

Since these pharmacological studies have provided little convincing evidence for a highly selective role of either subunit in LTP induction, an alternative hypothesis should be considered, whereby either subunit can support LTP providing they allow sufficient Ca^{2+} entry, but the subunit that mediates most of the Ca^{2+} influx will have a greater importance. *In vivo* this subunit bias will be affected by neuronal activity patterns, whilst the induction protocol will influence the subunit bias in plasticity studies. The charge transfer modelling of Erreger et al. (2005) suggests that the frequency of stimulation affects which subunit predominates; specifically, GluN2A should carry a majority of the current in tetanically-induced LTP, while GluN2B might carry more current in lower frequency protocols (Erreger et al., 2005). Indeed, Ro 25-6981 blocked the induction of spike-timing dependent LTP (t-LTP) in acute hippocampal slices from adult mice (Zhang et al., 2008; Kohl et al., 2011), which is induced by a low-frequency paradigm, while it did not impair tetanus-induced LTP (Zhang et al., 2008). However, complicating this interpretation, Zhang et al. (2008) found, albeit with a high and thus less selective concentration, that NVP also blocked t-LTP. Furthermore, Gerkin et al. (2007) found that an equivalent concentration of Ro 25-6981 did not block t-LTP in cultured hippocampal neurons, but NVP did; performing pre-post pairings at 1 Hz, rather than 0.1-0.2 Hz, and the use of cultured neurons, might account for this different result. Other studies have provided further evidence for a subunit bias due to charge transfer. For example, a pairing protocol should limit the importance of subunit kinetics, as the post-synaptic neuron is held at a depolarised potential to remove the Mg^{2+} block. Therefore, neither subunit would be predicted to dominate, and any bias would rather be determined by the numbers of each subunit present at the synapse. Indeed, Berberich et al. (2007) found that pairing-induced LTP was not blocked

by NVP, Ro 25-6891 or AP5 when used at sufficiently low concentrations to have a minimal impact on charge transfer during induction; however, when antagonist concentrations were increased to a level that significantly reduced charge transfer, both GluN2A and GluN2B antagonists caused an equivalent reduction in the magnitude of LTP. It is also important to consider the complication introduced by the large triheteromeric population of NMDARs; a recent study found that only high concentrations of Ro 25-6981 could impair theta burst-induced LTP, possibly because the antagonist starts inhibiting these triheteromers (Volianskis et al., 2013).

Overall, therefore, the conclusion from the current pharmacological data, with the caveat that no subunit-selective GluN2A antagonist exists, is that either subunit is capable of supporting LTP induction, provided they can mediate sufficient charge transfer (and associated Ca^{2+} influx). Which subunit mediates most charge transfer will be influenced by age, since the relative abundance of these two subunits changes over development (Monyer et al., 1994; Dumas, 2005; Yashiro and Philpot, 2008). Within a given age range, the induction protocol used may bias which subunit makes a greater contribution because of the different kinetics of the two subunits. Specifically, at the two extremes of frequency, t-LTP might have a greater contribution from GluN2B subunit-containing NMDARs, while tetanus-induced LTP could have a bigger contribution from GluN2A subunit-containing NMDARs (Erreger et al., 2005). The greater ability of GluN2A subunit-containing NMDARs to drive the induction of tetanic LTP has received additional support from modelling work (Santucci and Raghavachari, 2008). The potential importance of stimulation frequency during induction means that, in order to fully explore the role of GluN2A and GluN2B in plasticity, it is vital to investigate further the types of activity patterns that drive synaptic changes in behaving animals.

1.5.2.2 Genetic manipulations and LTP

Pharmacological antagonists only block the ligand binding and channel properties of the NMDAR and therefore pharmacological studies do not directly address whether the physical presence of NMDAR subunits at the synapse could play a role additional to that mediating Ca^{2+} influx. The most important other function in plasticity is likely to be related to the direct and indirect intracellular associations made by the GluN2 CTD. Genetic manipulations that remove or alter the GluN2 subunits may shed some light on whether subunit selectivity in LTP induction could arise through these interactions; of particular interest is whether the GluN2B subunit plays a crucial role due to its association with CaMKII.

A conditional knock-out of GluN2B subunits in the CA3 subfield abolished tetanus-induced LTP at the commissural-CA3 and commissural/associational-CA3 synapses (Akashi et al., 2009). In mice lacking GluN2B in the CA1 and neocortex, LTP induced by two tetani was impaired, but this deficit could be overcome by giving multiple tetani (Brigman et al., 2010). A smaller effect on LTP was seen in another forebrain-specific GluN2B knock-out mouse, where LTP was deficient only when induced by a pairing protocol, and not by a stronger protocol using two tetani (von Engelhardt et al., 2008). Other genetic manipulations that indirectly affect the levels of GluN2B have also shown considerable LTP impairments. For example, kinesin-like protein KIF17 transports GluN2B subunit-containing NMDARs to the synapse, and KIF17 knock-out mice (Yin et al., 2011), or mice carrying mutations in KIF17 that disrupt its loading or unloading of GluN2B (Yin et al., 2012), show reduced synaptic GluN2B and also abolished (KIF17 knock-out) or impaired (KIF17 mutant) LTP induced by a single tetanus. However, when interpreting results from genetic manipulations as evidence for a role of GluN2B in LTP, it must be remembered that such long-term manipulations could trigger compensatory changes at the cellular level, such as increased recruitment of CaMKII by GluN1, or even at the network

level, through changes in inhibition, for example. Of particular note, GluN2B knock-out lines also show small reductions in either GluN2A (Yin et al., 2011, 2012), GluN1 (Akashi et al., 2009), or spine density (Akashi et al., 2009; Brigman et al., 2010). Given that GluN2B subunits therefore contribute to the regulation of NMDAR levels and postsynaptic structural integrity, it is difficult to attribute fully the LTP impairments found following chronic reduction of GluN2B to a unique structural/interaction role of the GluN2B CTD in LTP.

Therefore, it is interesting that shorter-term manipulations, despite only reducing the GluN2B content, have produced stronger effects than complete genetic knock-outs. For example, GluN2B knock-down with RNA interference (RNAi) caused a profound reduction in the magnitude of LTP induced in 2-month-old rats, even though a very strong LTP protocol (4 tetani) was used (Clayton et al., 2002). LTP was also abolished in slices incubated for 2 hours with a membrane-permeable GluN2B C-terminal peptide that disrupted the GluN2B-PSD interaction and caused a consequent decrease in synaptic GluN2B content (Gardoni et al., 2009). Nevertheless, since mice with reduced synaptic GluN2A (Ng et al., 2009) or GluN2A knock-out (Sakimura et al., 1995) also exhibit reduced LTP, which can be recovered by a stronger induction protocol with multiple tetani (Kiyama et al., 1998), these experiments alone do not provide convincing evidence for a unique role of the intracellular interactions made by GluN2B.

The converse experiments, using subunit-selective overexpression, show that LTP is enhanced in adult (Tang et al., 1999) and aged (Cao et al., 2007) mice and adult rats (Wang et al., 2009) by increasing GluN2B. Cdk5 knock-out mice with elevated levels of synaptic GluN2B also show enhanced LTP (Hawasli et al., 2007). In contrast, GluN2A-overexpressing mice do not show increased LTP (Cui et al., 2013), suggesting that GluN2B may play a unique role. However, since elevated LTP was observed in dysbindin knock-out mice that had enhanced GluN2A-mediated currents (Tang et al., 2009), it is not completely

clear whether the enhanced LTP in GluN2B-overexpressing rodents arises from higher levels of Ca^{2+} influx due to the increased NMDAR-mediated current or because of an important contribution of the GluN2B subunit itself. Therefore, data from knock-out and overexpression studies suggest that the GluN2B subunit is important for the induction of LTP, but do not convincingly distinguish between a unique role of GluN2B at the synapse or a general threshold effect. In the latter case, the reduction or increase in synaptic NMDAR content produced by these genetic manipulations would alter the magnitude of LTP simply because of non-specific changes in the amount of Ca^{2+} influx during induction.

Rather than attempt to demonstrate a unique role for GluN2B by excluding this threshold possibility, studies have instead focused on manipulating the distinguishing features of the GluN2B subunit, in particular its intracellular interactions. The most convincing evidence for a uniquely important role for the interaction between GluN2B and CaMKII in LTP comes from experiments directly perturbing this association. The first data came from work by Barria and Malinow (2005); they showed that LTP was blocked in organotypic hippocampal slices transfected with a GluN2B construct impaired in binding to CaMKII. Moreover, the LTP impairment caused by transfecting recombinant GluN2A, which drives a switch in synaptic NMDAR content from GluN2B to GluN2A, could be ameliorated by transfecting a mutated form of GluN2A with an enhanced ability to bind CaMKII (Barria and Malinow, 2005). This further suggests that an important function of wild-type GluN2B is to maintain sufficient CaMKII at the synapse. These findings have since been extended to acute slices; an inducible mutation that weakens the GluN2B-CaMKII interaction impaired LTP induced by both a tetanic and 10 Hz protocol (Zhou et al., 2007), while a knock-in mouse with two point mutations that decrease the GluN2B-CaMKII interaction also showed a large reduction in two-tetani-induced LTP (Halt et al., 2012). This interaction is regulated by both components since inhibiting CaMKII, which initially disrupts the GluN2B-CaMKII association, leads to downregulation of synaptic GluN2B content within two hours and

a concomitant impairment in LTP (Gardoni et al., 2009). Inhibition of CaMKII was removed, and hence CaMKII kinase activity restored, before LTP was induced, and therefore the LTP deficit observed by Gardoni et al. (2009) could be attributed to an altered synaptic subunit composition.

One reason why the GluN2B-CaMKII interaction is so important for LTP might be its effect on AMPARs. Phosphorylation of Ser831 on GluA1 by CaMKII may be necessary for AMPAR insertion, and this phosphorylation does not occur when the GluN2B-CaMKII interaction is blocked (Halt et al., 2012), which may hinder synaptic strengthening. Thus, through its strong affinity for CaMKII, GluN2B may play a special role at the synapse additional to its function as an ion channel. This was particularly clear when, at an age when pharmacological inhibition of GluN2B with Ro 25-6981 no longer blocked pairing-induced LTP, LTP was impaired by RNAi knockdown of GluN2B (Foster et al., 2010). This difference seems directly related to a unique role of the GluN2B CTD since, following RNAi knockdown of GluN2B and the resultant LTP impairment, LTP could be restored either by an RNAi resistant GluN2B or by a chimera of GluN2A with the GluN2B tail, but not the chimera of GluN2B with the GluN2A tail (Foster et al., 2010). Thus, the physical presence of GluN2B may be important irrespective of its contribution to Ca^{2+} influx. This explains how GluN2B could have a unique and fundamental role in LTP induction, despite pharmacological block of GluN2B not impairing LTP induced by certain paradigms.

However, this does not mean that the GluN2A CTD makes no contribution to LTP. It has been shown that GluN2A subunit-containing NMDARs alone can trigger a form of LTP dependent on the Ras-GRF2/Erk Map Kinase pathway (Jin and Feig, 2010), suggesting that unique interactions may occur. Indeed, a mouse line with a GluN2A C-terminal truncation showed impaired tetanus-induced LTP, with the remaining LTP supported by GluN2B-subunit containing NMDARs (Köhr et al., 2003; Sprengel et al., 1998). However, since the truncation mutation also caused an overall reduction in GluN2A levels in this mouse

line, as well as a possible switch to a pure triheteromeric NMDAR population, it is possible that the LTP impairment arose from a threshold effect from reduced Ca^{2+} influx rather than a unique role of the GluN2A CTD. Supporting the threshold interpretation, stronger induction protocols expected to promote higher levels of Ca^{2+} influx could overcome the LTP deficits in mice with a GluN2A C-terminal truncation both in this (Köhr et al., 2003) and another study (Moody et al., 2011). Thus the evidence for a privileged role of GluN2A in LTP induction is weaker.

In summary, the most parsimonious conclusion from the available evidence is that both GluN2A and GluN2B subunits can support the requisite Ca^{2+} influx to induce LTP in the hippocampus. However, which subunit predominates in mediating this Ca^{2+} influx, and thus contributes more to LTP induction, depends on the protocol and also developmental stage, as the latter affects subunit abundance at the postsynaptic spine. Providing the NMDARs present can support sufficient Ca^{2+} influx, the GluN2B subunit seems to play a unique additional role because of its association with CaMKII (**Fig. 1.1**(**B**)). This interaction targets CaMKII to the vicinity of Ca^{2+} influx at the PSD under basal conditions and also provides a binding site for the additional activated CaMKII recruited following an LTP induction protocol. Finally, GluN2B helps maintain CaMKII activation and localise it at the PSD in the vicinity of its cellular substrates, enabling it to trigger the downstream pathways that mediate the expression of LTP.

1.5.3 LTD

Given the possible bias towards an important contribution of the GluN2B subunit to LTP induction, an opposite bias might have been expected for LTD. However, studies into the NMDAR subunit dependence of LTD have produced even more contradictory results than those for LTP, making it hard to draw unifying conclusions. The different types of findings are illustrated below and possible

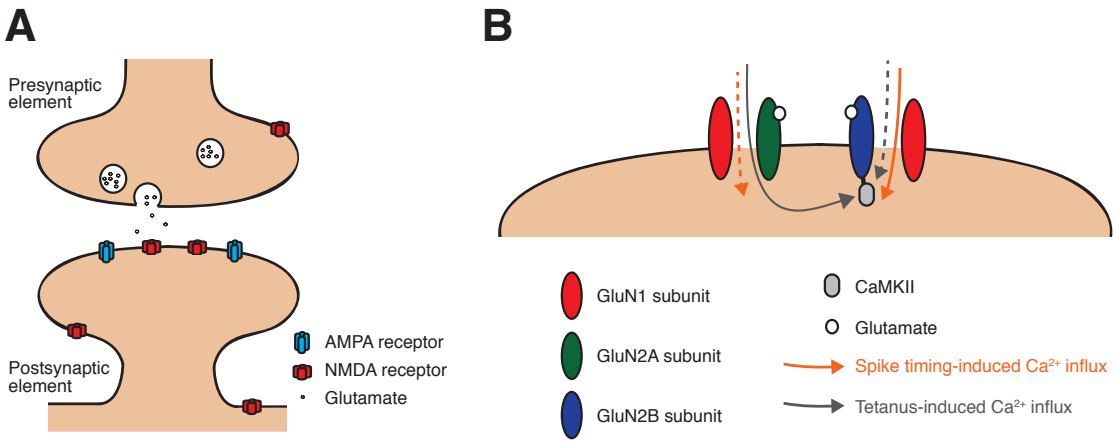

Figure 1.1: NMDAR location and subunits in synaptic plasticity. (**A**) NMDARs are found both pre- and postsynaptically, and these two NMDAR populations might play different roles in synaptic plasticity. In the postsynaptic membrane, NMDARs are found synaptically, perisynaptically and extrasynaptically, where they are also likely to perform different functions. (**B**) During induction of spike timing-dependent LTP, Ca^{2+} influx through GluN2B subunit-containing NMDARs (orange arrow) directly activates CaMKII to elicit LTP. Tetanic activation triggers a larger Ca^{2+} influx through GluN2A subunit-containing NMDARs (grey arrows), which reaches and activates CaMKII anchored at the postsynaptic density by the C-terminal of the GluN2B subunit. In both cases, it is CaMKII activation that triggers downstream signalling cascades mediating LTP expression, suggesting that the presence of the GluN2B subunit at the postsynaptic density is important for LTP induction irrespective of whether or not it supports a majority of the Ca^{2+} influx.

explanations for the controversies are offered. One major complication in this field is the strong dependence of LTD induction on developmental age, since small changes in age affect the magnitude or even presence of LTD (Ku et al., 2008). Nevertheless, this may provide information about the mechanisms involved, especially given the changing pattern of subunit expression across development (Dumas, 2005; Yashiro and Philpot, 2008).

1.5.3.1 Pharmacological manipulations and LTD

Groups investigating LTD have often drawn opposing conclusions about subunit-specificity, despite using very similar experimental preparations. For example, some pharmacology-based studies have found that a concentration of NVP with which they can block LTP does not impair LTD in culture (Gerkin et al., 2007), acute slices (Liu et al., 2004) or *in vivo* (Ge et al., 2010), suggesting that GluN2A subunits are not required for LTD induction. In contrast, other studies have found that NVP concentrations which impair LTP also block LTD (Bartlett et al., 2007; Li et al., 2007). It is possible that NVP causes a substantial reduction in NMDAR-mediated current that prevents LTP and, depending on the precise concentrations used, sufficient Ca^{2+} influx remains to trigger the downstream molecular cascades that mediate LTD. The importance of antagonist concentration in determining experimental conclusions is illustrated by the findings of Fox et al. (2006), where, of two NVP concentrations administered intraperitoneally that blocked LTP *in vivo*, only the higher concentration blocked LTD. Overall, therefore, the extent to which GluN2A subunits are engaged in LTD induction under physiological circumstances is not yet clear, but there certainly is no pharmacological evidence that they play a mandatory or unique role.

There has been a particular focus on a possible role of GluN2B-subunit containing NMDARs in LTD. Some groups found that the GluN2B-specific antagonists Ro 25-6981 and ifenprodil block LTD in acute slices (Izumi et al., 2006; Liu et al., 2004), in culture (Gerkin et al., 2007), and *in vivo* (Fox et al., 2006; Ge et

al., 2010), even when a larger NMDAR-mediated current reduction by NVP has no effect (Liu et al., 2004; Fox et al., 2006; Ge et al., 2010). However, as with the contradictory findings reported with GluN2A antagonism, many other studies have reported that the same manipulation has no effect on LTD induction in acute slices, despite using equivalent or higher concentrations of GluN2B antagonists (Bartlett et al., 2007; Li et al., 2007; Morishita et al., 2007; Kollen et al., 2008). The slice orientation used may partially explain the discordance between these findings, since Bartlett et al. (2011) found that coronal slices (as used by Liu et al. (2004)) had a form of LTD that was sensitive to Ro 25-6981, whereas sagittal slices (as used in Bartlett et al. (2007)) had a GluN2B-independent form of LTD, likely due to the stronger preservation of cholinergic projections with a sagittal cutting angle. Indeed, when the authors blocked muscarinic acetylcholine receptors, it unmasked a GluN2B-dependent LTD (Bartlett et al., 2011). The contradictory results found in slices cut in the transverse angle, where studies have found either GluN2B-dependence (Izumi et al., 2006; Li et al., 2006) or GluN2B-independence (Morishita et al., 2007; Kollen et al., 2008) of LTD, might result from subtle variations in the integrity of cholinergic fibres.

One further factor contributing to the variability in the sensitivity of LTD to GluN2B antagonism may be the extent to which extrasynaptic GluN2B subunit-containing receptors are recruited. The traditional low-frequency induction protocol is sometimes combined with application of the glutamate-uptake inhibitor *threo*-β-hydroxyaspartate (TBOA), which would likely increase activation of the extrasynaptic receptor population. Contrasting effects have been reported following TBOA application: it has not affected GluN2B involvement in LTD (Bartlett et al., 2007), it has produced a GluN2B-dependent LTD (Duffy et al., 2008), or it has even decreased the magnitude of LTD (Kollen et al., 2008). The last finding suggests that extrasynaptic, possibly GluN2B subunit-containing, receptors could exert a negative modulatory role on LTD under some experimental conditions. This suggestion is supported by a study finding that ifenprodil block of GluN2B actually enhanced the magnitude of LTD (Hendricson et al., 2002).

However, it cannot be excluded that the discrepancy between these findings results from the complex mode of action of the non-competitive GluN2B antagonists used, since the extent of their block varies with agonist concentration (Fischer et al., 1997), and such concentrations are likely more variable when glutamate uptake is blocked. Overall, therefore, the contradictory findings mean the precise nature of the role played by GluN2B subunit-containing NMDARs in LTD is anything but clear, and the induction of LTD may be particularly sensitive to experimental conditions.

1.5.3.2 Genetic manipulations and LTD

Transgenic approaches have also not provided conclusive support for a unique role of either subunit in LTD and, in fact, most of the findings have been negative. A reduction in synaptic GluN2B levels, achieved by disrupting the association of GluN2B with PSD-95 in an acute manner, did not alter LTD, despite being sufficient to impair LTP (Gardoni et al., 2009). The GluN2A knock-out mouse also showed no LTD impairment, though the same study also found no reduction in LTP (Longordo et al., 2009). Furthermore, overexpression of GluN2B did not affect the magnitude of traditional 1 Hz stimulation-induced LTD (Wang et al., 2009), and neither did direct (Cui et al., 2013) or indirect (Tang et al., 2009) GluN2A overexpression, although GluN2A overexpression did reduce LTD induced by 3 or 5 Hz stimulation without affecting LTP (Cui et al., 2013). The only clear positive findings have been that GluN2B knock-out mice (Brigman et al., 2010) and KIF17 knock-out mice, which have a consequent reduction in synaptic GluN2B (Yin et al., 2011), both had impaired LTD. However, this is not evidence for a subunit-selective role of GluN2B in LTD since these manipulations also caused reduced LTP. Overall, there is no clear evidence from transgenic approaches that either subunit plays an irreplaceable role in LTD induction, though impairments have been more frequently associated with GluN2B-specific manipulations.

A final possibility is that one subunit makes a more important contribution to LTD through its unique intracellular interactions. This may be because it facilitates coupling of Ca^{2+} influx to the downstream pathways that mediate a reduction in synaptic strength. Alternatively, NMDARs could play a different role in LTD, where their activation is still required to trigger downstream signalling cascades, but not to mediate Ca^{2+} influx. Evidence for this latter proposal is the demonstration that NMDAR-dependent LTD could still be induced despite NMDAR-mediated ion flux being blocked (Nabavi et al., 2013). This suggests that the basal level of Ca^{2+}, rather than Ca^{2+} influx through NMDARs, is necessary for LTD induction, and may explain why no clear findings have emerged from studies using subunit-specific pharmacological antagonists. It also implies that any subunit selective function of NMDARs would emerge solely through their unique intracellular associations. As predicted by the requirement for CaMKII being in LTP induction alone, genetic disruption of the GluN2B-CaMKII association did not impair LTD (Zhou et al., 2007). However, other interactions have been identified that could be important. For example, LTD alone was impaired in mice with a genetic knock-out of the p75 neurotrophin receptor (Woo et al., 2005). The specific mechanism responsible for this deficit was reported to be that pro-brain derived neurotrophic factor (pro-BDNF) could not activate the p75 neurotrophin receptor to enable LTD and, since the mouse line also had an overall reduction in GluN2B levels, it suggests a possible signalling role of GluN2B. Another important association might be that between Ras-GRF1 and the GluN2B CTD, since LTD is impaired in Ras-GRF1 knock-out mice (Li et al., 2006). The level of Ras-GRF1 may determine the type of depression induced under physiological conditions, since LTD is GluN2B-dependent when this association predominates (Bartlett et al., 2011). Furthermore, acetylcholine concentration is inversely correlated with the level of the GluN2B-Ras-GRF1 interaction (Bartlett et al., 2011), suggesting that activity of the cholinergic system could modulate the subunit dependence of LTD induction.

In summary, the data are inconclusive, but neither the GluN2A nor the GluN2B subunit seems to play a mandatory role in the induction of LTD. Nevertheless, the GluN2B subunit has been implicated more frequently, perhaps because of its unique associations with components of pathways that modulate or mediate LTD.

1.6 GluN2A and GluN2B subunit-containing NMDA receptors in behaviour

Synaptic plasticity is widely considered a cellular model for learning and memory (Bliss and Collingridge, 1993), and there were early indications that NMDARs might play an important role in certain forms of learning and memory (Morris 1986). Moreover, it has been shown that synaptic weights increase in parallel with the acquisition of a behavioural task (Whitlock et al., 2006; Gruart et al., 2006; Valenzuela-Harrington et al., 2007), and both learning and LTP can occlude each other (Gruart et al., 2006; Whitlock et al., 2006).

Therefore, in parallel to investigations into whether there is a subunit-selective contribution to LTP and LTD, the same pharmacological and genetic subunit-specific manipulations have also been used to interrogate whether GluN2A and GluN2B subunits are important for behavioural tasks with different cognitive demands. In some cases, impairments in one direction of plasticity could be correlated with performance deficits.

1.6.1 GluN2A subunits and behaviour

GluN2A knock-out mice were the first to be studied behaviourally. The initial characterisation of these mice suggested relatively pervasive memory deficits compared to C57BL/6 controls (Sakimura et al., 1995), but this was later attributed to the high degree of CBA strain character remaining in their genetic background, a line known to perform worse on the Morris water maze (MWM) task (Schimanski and Nguyen, 2004). Once on an almost pure C57 background,

the behavioural deficits found were relatively limited: GluN2A knock-out mice and mice lacking the GluN2A CTD showed no evidence of long-term memory deficits, since mice were not impaired on spatial tasks acquired over a number of days (the MWM and radial arm maze) (Bannerman et al., 2008). Mice with a knock-out of Neuropilin toiloid-like 1 (Neto1), a component of the NMDAR protein complex, have an approximately one third reduction in GluN2A at the PSD and an LTP impairment, but also acquired the MWM at a normal rate (Ng et al., 2009). Furthermore, pharmacological manipulations have produced a similar result; Ge et al. (2010) used the GluN2A subunit-preferring antagonist NVP injected intraperitoneally at a concentration that impaired LTP *in vivo*, and saw no deficits of NVP-treated rats either in MWM acquisition or consolidation. Thus, GluN2A does not seem necessary for incrementally acquired long-term memory tasks.

However, GluN2A manipulations have been associated with short-term spatial memory deficits, since GluN2A knock-out mice and mice lacking the GluN2A CTD were impaired on a non-matching-to-place T-maze task, and also in their ability to distinguish between arms based on how recently they had been visited within a trial on the radial maze (Bannerman et al., 2008). In further support of a role of GluN2A in short-term spatial memory, infusion of NVP into the CA1 impaired performance on a delayed-alternation T-maze task (Zhang et al., 2013). It also seems that GluN2A subunit-containing NMDARs may contribute to the rapid formation of context or object representations. GluN2A knock-out mice, which had an increased threshold for LTP induction, were only impaired in a hippocampus-dependent contextual fear conditioning paradigm when the task demands were increased by reducing context exposure before shock delivery (Kiyama et al., 1998), suggesting a deficit in fast learning about the context. Neto1 knock-out mice were impaired in a displaced object recognition task, but not in a novel object recognition task (Ng et al., 2009); both these tasks require relatively rapid learning about an object, but only the displacement task has a spatial component and clear hippocampal involvement (but also see (Broad-

bent et al., 2010)). Overall, mice with no, or reduced, GluN2A do show some learning impairments, which are limited to short-term memory and the rapid acquisition of spatial information. In order to test whether this is a particular role of GluN2A or a non-specific effect of reduced NMDAR-mediated currents (especially given the lack of NVP selectivity), these results should be compared to those from mice with equivalent genetic and pharmacological manipulations of GluN2B levels.

1.6.2 GluN2B subunits and behaviour

There is considerable evidence that pharmacological and genetic manipulations of the GluN2B subunit produce similar impairments to those described for GluN2A, suggesting that the short-term memory deficits observed in GluN2A-deficient mice are primarily due to a general reduction in NMDAR-mediated current. For example, mice with postnatal GluN2B knock-out in pyramidal neurons of CA1 and the dentate gyrus (DG) of the hippocampus showed very similar impairments to global GluN2A knock-out mice, namely a short-term spatial memory deficit in spontaneous alternation in the T-maze but normal performance in the MWM (von Engelhardt et al., 2008). This finding is supported by pharmacological data from rats, where infusion of Ro 25-6981 or ifenprodil into the CA1 region of the hippocampus impaired performance in tasks requiring short-term spatial memory, though long-term memory was not tested (Zhang et al., 2013). Rats were impaired on a delayed alternation T-maze task with 5- and 30-second delays, but they only made significantly more win-shift errors than controls after a 30-second delay. Rats also had longer escape latencies on trial 2 of a delayed matching-to-place water maze task, but only when the retention interval was 10 minutes, not 30 seconds (Zhang et al., 2013). These two findings suggest that GluN2B subunits may become more important when delay times increase. It should be noted, though, that pharmacological antagonism of NMDARs will also affect interneurons (Hanson et al., 2013). In general, the similar short-term memory impairments caused by manipulations that remove or

reduce either the GluN2A or GluN2B subunit suggest that this phenotype is primarily due to a decrease in NMDAR-mediated currents rather than a selective contribution of either subunit.

Nevertheless, there is evidence that GluN2B subunits could play a role in learning and memory additional to that shared with GluN2A in short-term memory, since other studies have found more pervasive impairments following GluN2B disruption. For example, KIF17 knock-out mice, which have reduced synaptic GluN2B levels due to a transport impairment, performed worse on the MWM task (Yin et al., 2011, 2012), a novel object test with long delays (Yin et al., 2011) and contextual dependent fear conditioning (Yin et al., 2011). A CA1 and neocortical GluN2B knock-out mouse line was deficient in MWM acquisition, fear conditioning and T-maze spontaneous alternation (Brigman et al., 2010). However, these impairments might be attributable to extra-hippocampal deficits (von Engelhardt et al., 2008). Therefore, it is reassuring that a more acute manipulation involving RNAi-mediated knock-down of GluN2B in the hippocampi of rats also showed slower acquisition of the MWM task (Clayton et al., 2002). The authors also found a correlation between GluN2B level and MWM performance within an aged population of rats (Clayton et al., 2002). However, the nature of the GluN2B involvement cannot be correlated with one direction of plasticity since RNAi caused an LTP deficit but LTD was not investigated, while both the aforementioned genetically altered mouse lines had deficits in both LTP and LTD. Nevertheless, these studies suggest that GluN2B may play a role in long-term memory that was not seen in mice with GluN2A knock-out or reduction, though additional studies using acute manipulations restricted to the hippocampus are required to verify this conclusion.

1.6.3 Correlations between LTP and memory

To dissect further the possibly unique role of GluN2B in learning and memory, it is useful to investigate the behavioural deficits associated with a selective im-

pairment of one direction of plasticity. For LTP, a selective impairment arises if the association between CaMKII and GluN2B is weakened. This manipulation has been found to cause deficits in acquisition of both the MWM task, which could be overcome by extended training, and also in a delayed spatial win-shift eight-arm radial maze task, where mice had to remember the baited arms from the first session and then avoid them in the next trial to find the food reward (Zhou et al., 2007). The authors ascribed this deficit to an impairment in forming a spatial map. Another mouse line with genetic disruption of the CaMKII-GluN2B interaction engineered in a different way showed fewer behavioural impairments, being normal in MWM acquisition and probe trial performance at 1-2 hours post-training but, interestingly, did exhibit long-term consolidation deficits, as they performed worse in a probe test 24 hours after training (Halt et al., 2012).

Furthermore, in contrast to the impairments seen following GluN2A overexpression (Cui et al., 2013), GluN2B overexpression has been shown to improve performance of adult (Tang et al., 1999) and aged mice (Cao et al., 2007) and rats (Wang et al., 2009) in a battery of tests including context and cued fear-conditioning, object recognition memory at longer retention intervals, MWM acquisition and spatial working memory. Cdk5 knock-out mice, which have increased synaptic GluN2B due to a reduction in its degradation, were also found to have improved contextual learning in a context-dependent fear-conditioning paradigm (Hawasli et al., 2007). All these behavioural improvements were associated with increased LTP, while LTD, when investigated, was found not to change (Wang et al., 2009). Stronger evidence for a link between subunit-specificity in LTP and learning comes from tasks where learning and postsynaptic responses can be measured simultaneously. Using the trace-conditioning paradigm in rats, Valenzuela-Harrington et al. (2007) showed that acquisition of this task was associated with an increased strength of the medial perforant pathway-DG synapse of the hippocampus. Moreover, systemic Ro 25-6981 application blocked both task acquisition and the changes in synaptic strength.

Therefore, possibly through its contribution to LTP induction via CaMKII, GluN2B seems to have an important role in learning and memory.

1.6.4 Correlations between LTD and memory

Some behavioural deficits have also been related to a GluN2B-dependent LTD impairment. Ge et al. (2010) administered Ro 25-6981 intraperitoneally to rats, which impaired LTD but not LTP *in vivo*, and found that, while acquisition of a MWM task was not impaired by this manipulation, rats that received Ro 25-6981 on the training day could not recall the platform location 24 hours later which was attributed to a consolidation-related deficit. This compromised performance could be mimicked by injection of a peptide that prevented AMPAR endocytosis (Tat-GluA2$_{3Y}$), suggesting the impairment was related to an LTD-like process. However, an alternative interpretation is that this manipulation disrupted homeostatic resetting of the network and that this process is required for consolidation.

A finding reported by a number of groups is a possible link between LTD and reversal learning. Duffy et al. (2008) found that subcutaneous administration of Ro 25-6981 blocked LTD and impaired reversal learning in mice, and deficient reversal learning in the MWM was also found in mice with GluN2B knock-out in the hippocampus, though LTD was not tested (von Engelhardt et al., 2008). In rats, GluN2B-dependent LTD could not be induced in naïve animals *in vivo*, but was possible after animals experienced MWM training; when rats that had previously acquired the MWM were tested on a reversal phase, those rats treated with either Ro 25-6981 or the Tat-GluA2$_{3Y}$ peptide were impaired in reversal learning (Dong et al. 2013). In further support of a role of GluN2B-dependent LTD in reversal learning, enhancing LTD by subcutaneous administration of D-serine increased the rate at which the mice learnt the reversal phase in the MWM (Duffy et al., 2008), while a mouse line with enhanced GluN2B-mediated currents showed no improvement in the acquisition of a MWM task, but did

show faster reversal learning (Hawasli et al., 2007). Thus, many of the studies investigating a role of NMDAR subunits in behaviour have found a 'perseverance phenotype' that correlates with an impairment in GluN2B-dependent LTD.

1.7 Summary of NMDA receptors in plasticity and behaviour

The hypothesis that different GluN2 subunits selectively mediate different directions of plasticity is not supported by the available studies. Although the lack of specific GluN2A antagonists prohibits the conclusive testing of this hypothesis, when manipulations control for the magnitude of NMDAR-mediated current reduction, there is no clear evidence, as yet, that either subunit plays an irreplaceable role in LTP induction. Nevertheless, the different kinetics conferred on the NMDAR by the GluN2A and GluN2B subunits means the contribution of each subunit to charge transfer during induction may vary, and therefore they may not play an equal role in potentiation under physiological conditions and naturalistic activity.

Irrespective of the induction paradigm used, however, most evidence suggests that the GluN2B subunit has a greater importance for LTP induction. If GluN2B subunit-containing NMDARs were found to carry more Ca^{2+} influx per unit of current (Sobczyk et al., 2005), this is one possible explanation for why GluN2B can exert a strong influence on LTP in the adult hippocampus, despite comprising a smaller proportion of GluN2 subunits than early in development. An alternative explanation, which is more in line with the prevailing evidence, is that GluN2B is particularly important for LTP induction because its presence at the spine anchors CaMKII at the PSD. Thus, GluN2B subunit-containing NMDARs enable activation of the downstream signalling cascades that mediate synaptic strengthening, irrespective of whether they support a majority of the Ca^{2+} influx. This suggests that GluN2B is a necessary factor for LTP induction under naturalistic conditions, but, importantly, whether or not it is sufficient to support the requisite Ca^{2+} influx may depend on the pattern

of presynaptic activity. Moreover, although spine-based imaging studies and asymmetry studies have suggested that small spines, which tend to be GluN2B-rich, have a greater propensity for the induction and maintenance of LTP, the presence of GluN2B may not be sufficient if downstream signalling pathways and structural changes are already saturated.

The LTD literature is ambiguous, although a greater number of studies and the developmental profile of LTD would support a more integral role of GluN2B in its induction. Exactly why this may be is not clear, but could relate to intracellular associations distinct from that with CaMKII. Most plasticity studies investigate the response to induction protocols at either the cellular or extracellular field potential level, and thus record the summed changes at many synapses. However, synapses are not equal, and instead have different structural and molecular signatures, and this may help explain at least some of the contradictory findings in the plasticity literature. Overall, given that GluN2B seems important for both LTP and LTD, a parsimonious hypothesis is that this subunit confers the synapse with malleable properties.

Given the contradictory conclusions of plasticity studies, it is unsurprising that neither subunit has yet been found to have a clear role in learning and memory. Moreover, while there is a large body of evidence to suggest that synaptic plasticity supports learning and memory (Morris et al., 1986; Whitlock et al., 2006; Gruart et al., 2006; Valenzuela-Harrington et al., 2007), the link is not yet resolved (Bannerman et al., 2012; Gallistel and Matzel, 2013). Therefore, studies that correlate plasticity and behaviour have been informative, irrespective of whether the underlying, possibly subunit-selective, mechanisms are known. Nevertheless, correlations between plasticity deficits and learning and memory impairments do not provide a causative link. Moreover, we should be cautious in concluding that such studies provide definitive evidence, given the possible compensatory mechanisms and network changes that may be triggered by the experimental manipulations described here. Of course, even if plasticity does

support learning and memory, we still do not know what types of plasticity would be engaged in tasks with different cognitive demands and thus, with all this considered, it is no surprise that the findings from these studies are complex and often apparently contradictory. What the current literature does suggest is that both GluN2A and GluN2B support short-term memory processes. However, studies investigating the interactions between GluN2B and CaMKII have suggested that GluN2B subunit-containing NMDARs appear to make a greater contribution to learning when information must be retained during a delay or when there is incremental task acquisition across a number of days.

It may seem surprising that short-term memory tasks often appear the most susceptible to genetic lesions or pharmacological block of NMDARs, especially in light of the proposal that NMDAR-dependent LTP supports task acquisition through incremental learning (Morris, 2013). However, a number of factors make it premature to conclude that this necessitates a revision of the theory linking plasticity and learning. Firstly, NMDARs are not only involved in plasticity; a global knock-out would also remove NMDARs located on interneurons, and hence may alter the network dynamics important for short-term memory (Korotkova et al., 2010). Secondly, in the few studies where the subunit knock-out is restricted to pyramidal cells or by region, navigation systems may still be affected, and how that could interact with the cognitive demands of short- and long-term memory tasks is not known. Thirdly, even localised manipulations have been chronic and so compensatory mechanisms are likely to be recruited; it is conceivable that short-term memory requires greater online processing power or rapid, large-scale network changes, either of which might need a higher level of Ca^{2+} influx to drive them, and thus would be more sensitive to manipulations that reduce NMDARs and hence total Ca^{2+} influx. Finally, the fact that these manipulations also often impair LTP does not necessarily imply a link between LTP and short-term memory, it shows only that both processes rely on NMDARs. Indeed, short-term potentiation also requires NMDARs and may have subunit preference (Volianskis et al., 2013).

In some studies it has been possible to relate a behavioural impairment to a selective deficit in one direction of plasticity. In particular, there is evidence that the gradual acquisition and consolidation of information may be supported by the GluN2B-CaMKII interaction, which is also important for LTP. Another common finding is that the mechanisms that support reversal learning may involve a GluN2B-dependent LTD-like process. One caveat of studies relating learning impairments with LTD deficits is that many laboratories find they cannot induce LTD in adult rodents, despite rodents of that age still being able to perform the associated memory task. This suggests that either the low frequency paradigms used to induce LTD do not successfully mimic the type of activity that triggers reduction of synaptic weights *in vivo* or, even, that synapse-specific reductions in strength do not underlie learning; instead, they may be more important for circuit refinement during development. One way to reconcile these observations would be that synaptic strengthening always supports acquisition of new information, but a concomitant depression is necessary in behavioural tasks that require re-learning (reversal learning, extinction) or refinement of learning (recognition memory) to increase the gain of the potentiated synapses above noise or 'background'. In this scenario, a limited number of synapses would potentiate and carry new information, but an overall depression would be observed in extracellular field or whole-cell measurements that record populations of synapses. Such a form of synaptic depression would be functionally distinct from purely homeostatic mechanisms, as it would contribute to information coding.

1.8 Heterogeneous hippocampal synapses

There are many controversial findings in the studies that have set out to investigate if there is a subunit-selective involvement of NMDARs in plasticity and behaviour. One vital consideration when interpreting the results of these studies is that CA3-CA1 synapses are not a uniform population. Consequently, experi-

ments that measure changes in the extracellular field or whole-cell response to a plasticity protocol are, therefore, measuring the summed changes from a heterogeneous population of synapses that may have divergent responses to the same activity pattern. Moreover, these different types of synapses may have different functions *in vivo*. Given that AD is thought to begin as a disease of synaptic dysfunction (Selkoe, 2002), it may also be valuable to investigate whether the pathological changes in AD differentially affect these distinct types of synapse.

1.8.1 Molecular and morphological characteristics of postsynaptic spines

Two major types of postsynaptic spine morphology are the large, 'mushroom-shaped' spines and the small, 'thin' spines. Mushroom spines have a bulbous spine head and a constricted neck and have been considered as a mature spines, since they are stable for months (Holtmaat et al., 2005) and show no permanent morphological changes following an LTP protocol (Matsuzaki et al., 2004). These characteristics have led to the suggestion that this type of spine may represent permanent memory traces that are resistant to disruption (Kasai et al., 2003; Bourne and Harris, 2007). In contrast, thin spines have a smaller size and a higher rate of turnover, but can be strengthened and stabilised by the addition of AMPARs and enlarge following an LTP protocol (Matsuzaki et al., 2004). Consequently, it has been proposed that these spines may be responsible for the acquisition of new information (Kasai et al., 2003; Bourne and Harris, 2007). Furthermore, the molecular signatures of these two types of spine seem to vary, since single spine imaging has shown that the GluN2B antagonist Ro 25-6981 selectively reduced glutamate uncaging-evoked EPSCs and Ca^{2+} transients in small spines (Sobczyk et al., 2005).

1.8.2 Left-right hippocampal asymmetry of postsynaptic spines in mice

Surprisingly, there is an asymmetric distribution of these two types of spine in the mouse hippocampus. Shinohara et al. (2008) injected a lentiviral vector

carrying GFP into either the left or the right CA3 of the mouse hippocampus, and used electronmicroscopy and immunolabelling to identify the type of postsynaptic spine contacted by the CA3 in each hemisphere. The authors found that, irrespective of whether they were located in the left or right hemisphere, spines on CA1 pyramidal neurons that received projection from the left CA3 tended to be morphologically characteristic of thin spines and were densely populated with GluN2B subunit-containing NMDARs (**Fig. 1.2**). In contrast, those CA1 spines that were contacted by input from the right CA3 were mainly mushroom-shaped spines, with a high proportion of GluA1 subunits, but a low proportion of GluN2B subunits (**Fig. 1.2**). This is in agreement with the electrophysiological work of Kawakami et al. (2003), in which they transected the ventral hippocampal commissure (VHC) to cause the contralateral commissural projections to degenerate and hence isolate the ipsilateral Schaffer collateral projections to CA1. The apical dendrites in the left hemisphere were found to have a greater GluN2B content, since there was a smaller relative NMDAR-mediated current in the presence of Ro 25-6981 in the left than in the right hemisphere. Moreover, it was demonstrated this asymmetry held in GluN2A knock out mice and was specific to pyramidal neurons (Wu et al., 2005).

The nature of the asymmetry, with the two populations of postsynaptic CA1 spines receiving right or left input being distributed across both hemispheres, means that viral targeting, as used by Shinohara et al. (2008), is a useful technique to access these different synaptic populations. VHC transection risks triggering the growth of new spines to compensate for the degeneration of those that received commissural projections. The advent of optogenetics, which is the ability to control the activity of a regionally- and genetically-defined neuronal population with light, has allowed viral targeting to be combined with electrophysiology in living tissue. Therefore, Kohl et al. (2011) tested whether or not there may be a hemispheric asymmetry in LTP using viral injection of a construct containing a cre-dependent Channelrhodopsin2 into the left or right hemisphere of CaMKIIα-cre mice. This allowed selective recruitment of the left

or right excitatory CA3 input onto CA1. This study confirmed the findings of Kawakami et al. (2003) that Ro 25-6981 caused a greater reduction in NMDAR-mediated currents when the postsynaptic neuron received left CA3 input than when the input came from the right CA3. Furthermore, it showed that this asymmetric distribution of GluN2B subunits had a functional correlate, since only left-injected mice showed spike timing-dependent LTP (tLTP) using induction protocols with pairing at either baseline or at theta frequency, which was blocked by Ro 25-6981 (Kohl et al., 2011). This lends further support to the importance of GluN2B subunit-containing NMDARs in LTP, and provides a model that could be used to test the relationship between NMDAR subunits, LTP and learning and memory in health and disease.

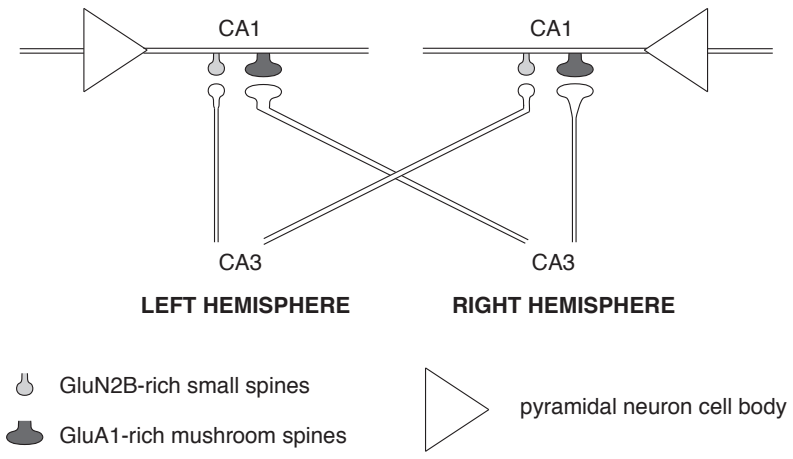

Figure 1.2: Left-right hippocampal asymmetry of spine distribution. The CA3 projects both ipsilaterally (Schaffer collaterals) and contralaterally (commissural fibres). Irrespective of whether the CA1 neuron is found in the left or right hemisphere, postsynaptic spines on CA1 neurons that receive input from left CA3 tend to be small, thin spines that are rich in GluN2B subunit-containing NMDA receptors. In contrast, those spines receiving right CA3 input are mainly mushroom shaped spines with a lower density of GluN2B subunit-containing NMDA receptors but a high proportion of GluA1-containing AMPA receptors.

1.9 Alzheimer's disease

There is much more to discover about the processes that support learning and memory, especially regarding whether or not synaptic plasticity is at the core of their mechanistic underpinnings. A particular motivation for understanding this aspect of brain function is that learning and memory are central to our sense of identity, and devastating diseases result when they fail.

Alzheimer's disease (AD) is the leading cause of dementia worldwide and the early stages of this disease are characterised by loss of memory, especially episodic memory. AD comes in two forms, early-onset familial AD and late-onset sporadic AD. Early-onset AD is heritable, and associated with rare mutations in amyloid precursor protein (APP), presenilin-1 (PSEN1) and presenilin-2 (PSEN2) (Tanzi, 2012). However, the vast majority of AD cases are sporadic, and very little is known about the aetiology of this disease. Nevertheless, genetic heritability may be as high as 80% (Bettens et al., 2013) and major risk factors include the allele of the apolipoprotein-E (APOE) gene, with the APOε4 allele being a major genetic determinant (Liu et al., 2013; Rhinn et al., 2013).

The post-mortem pathology observed in sufferers of familial and sporadic AD is indistinguishable, and is characterised by amyloid plaques and tau neurofibrillary tangles (NFTs) and extensive neuronal loss and brain atrophy. These pathologies are first found in the entorhinal cortex and then the hippocampus (Braak and Braak, 1995) but, as the disease progresses, they become pervasive throughout the brain. The genetic risk factors and pathologies have established amyloid beta (Aβ) and tau as the molecular mediators of AD. Nevertheless, despite huge advances in our understanding of AD processes, there are currently only two available drugs for AD sufferers, the cholinesterase inhibitors and the NMDAR antagonist memantine, both of which only alleviate symptoms rather than halt disease progression. Therefore, much remains to uncover about this disease.

1.9.1 Processing of Aβ

Aβ is formed by sequential cleavage of APP. APP can enter many pathways in the cell but there are two primary pathways (Ling et al., 2003). The first involves processing by α-secretase, which generates non-amyloidogenic fragments. The second, alternative pathway, involves initial cleavage by β-secretase; the C-terminal fragment that this cleavage produces is membrane-bound and is then further processed by γ-secretases to release the small peptides of Aβ that can be either 40 ($A\beta_{1-40}$) or 42 ($A\beta_{1-42}$) amino acids in length (Ling et al., 2003).

Notably, there is not conversion of $A\beta_{1-42}$ to $A\beta_{1-40}$ as they are generated by independent pathways, with the final length of the peptide being determined by the precursors and the site of γ-secretase cleavage (Qi-Takahara et al., 2005; Takami et al., 2009). Moreover, it is even possible that the processing which generates $A\beta_{1-40}$ and $A\beta_{1-42}$ could take place in different cellular compartments (Hartmann et al., 1997). Therefore, the concentration and length of Aβ peptides in the brain could be regulated by the rate of APP production, APP processing by α-secretase or β- and γ-secretases, Aβ secretion and also the rate of clearance.

1.9.2 Dysregulation of Aβ

It appears that the regulation of Aβ production is under activity-dependent control, since the concentration of Aβ increases as neuronal activity increases (Kamenetz et al., 2003; Bero et al., 2011) via an Arc-mediated pathway (Wu et al. 2011). The function of Aβ is not known, but it may play an important role in the cell in healthy individuals. Aβ has been implicated in the regulation of presynaptic vesicle release (Puzzo et al., 2008; Abramov et al., 2009), which may in turn modulate Aβ levels (Cirrito et al., 2005). Thus, combined with its concentration-dependent effects on LTP (Puzzo et al., 2008) and enhancement of LTD (Shankar et al., 2008), Aβ may play a homeostatic role, with high levels of Aβ leading to synaptic depression and the restoration of the network to a less potentiated state. Aβ may also increase the gain of the network by pro-

moting enhanced release probabilities, especially in cells with low firing rates (Abramov et al., 2009). Although such effects would increase the sensitivity of a network if carefully regulated, when such control is lost neurons may produce high levels of Aβ that could lead to the pathological changes underlying early AD. Moreover, activity-dependent Aβ clearance by neprilysin fails over time in AD-transgenic neurons (Tampellini et al., 2011). What is clear is that brain regions with higher activity have higher Aβ levels overall, and such regions are the most vulnerable to Aβ deposition (Vlassenko et al., 2010; Bero et al., 2011). For example, the entorhinal cortex, with constitutive grid cell activity (Hafting et al., 2005), acts as an attractor network, which may explain why it is one of the first regions to be affected in AD.

Thus, we still need to understand more about how Aβ levels are regulated and which rate-limiting steps are the most important in determining its concentration. In particular, activity-dependent fluctuations in Aβ have been shown to occur naturally diurnally *in vivo* (Bero et al., 2011) and on a timescale of hours in organotypic slices, where extreme manipulations involving tetrodotoxin and picrotoxin were used to block and enhance neuronal activity respectively (Kamenetz et al., 2003). However, it remains to be seen how tightly Aβ concentration at synapses is linked to physiological changes in neuronal activity in the order of minutes and seconds. A greater understanding of this will help determine how regulation fails and dysequilibria arise and, moreover, which is the best rate-limiting step controlling Aβ concentration to target therapeutically.

It is not only the concentration of Aβ that is important, but also the form in which it is found. The Aβ monomer can oligomerise rapidly to form β-sheet structures under aqueous conditions (Barrow et al., 1992). It is still not resolved whether dimers, oligomers or fibrils are the most toxic form, although dimers and low-n oligomers are currently favoured (Selkoe, 2002). It is likely that there is interconversion between these various forms (Bitan et al., 2003). This equilibrium is dependent on Aβ concentration since a shift from a low Aβ concen-

tration, when Aβ is primarily in the monomeric form thought to be non-toxic, and even potentially neuroprotective (Giuffrida et al., 2009), to a higher concentration may trigger the assembly process (Hellstrand et al., 2010) and the start of pathological changes at the synapse. The plaques that form at very high Aβ concentrations will sequester these toxic Aβ oligomers, but it is not yet resolved whether they are inactive (Shankar et al., 2008) or could provide a source of toxic oligomers. Irrespective of whether or not plaques act as a reservoir for toxic species, amyloid plaques could still play a role in AD progression; this might be through an interaction with microglia and inflammatory responses, which are known to mediate pathology (Heneka et al., 2013), or even by physical displacement of nearby synapses.

A further consideration is that the a difference of one or two amino acids in the length of the Aβ peptide can have huge implications for the toxicity of the peptide. Most focus has been on $A\beta_{1-40}$ and $A\beta_{1-42}$ because these peptides are the most prevalent in the diseased human brain and mouse models. However, $A\beta_{1-42}$ has emerged as better associated with AD progression, since mutations that cause an increased $A\beta_{1-42}/A\beta_{1-40}$ ratio are associated with early onset AD, and $A\beta_{1-42}$ shows greater toxicity in LTP (Nomura et al., 2012) and neurodegeneration experiments. In fact, it has been suggested that $A\beta_{1-40}$, which is ten times more abundant in the healthy brain, should be the focus of studies into the physiological function of Aβ (Mucke and Selkoe, 2012); it remains possible that the production of $A\beta_{1-42}$ could be a byproduct of titrating the reactions required to generate the appropriate level of $A\beta_{1-40}$. For example, the $A\beta_{1-42}/A\beta_{1-40}$ ratio can be altered by the activity history (Dolev et al., 2013). The differential importance of $A\beta_{1-42}$ and $A\beta_{1-40}$ in AD may result from the greater hydrophobicity of $A\beta_{1-42}$, such that these two forms exist in different secondary structures as monomers (Lührs et al., 2005; Tycko, 2006), and so generate distinct intermediates during the fibrillisation process (Bitan et al., 2003); this could explain the toxicity differences. For example, the higher propensity of $A\beta_{1-42}$ to assemble into β-sheet structures would push the equilibrium towards

the toxic oligomeric forms of the peptide. However, other forms of Aβ must not be overlooked. Despite its lower levels in the brain, $A\beta_{1-43}$ is more common in amyloid plaque cores than $A\beta_{1-42}$ (Welander et al., 2009), suggesting it is better able to seed oligomerisation. Recent evidence suggests that $A\beta_{1-43}$ may be even more neurotoxic than $A\beta_{1-42}$ (Saito et al., 2011). Finally, post-translational modification of Aβ may also be important. In particular, N-terminally modified pyroglutamate-Aβ (pE3-Aβ) has been suggested to play an important role in seeding Aβ aggregation, and hence neurotoxicity, *in vivo* (Alexandru et al., 2011; Nussbaum et al., 2012).

Overall, while the cleavage steps that generate Aβ monomers are irreversible, important equilibria exist in the assembly process and differences in Aβ aggregation propensity can promote different mechanisms of fibrillisation (Pellarin et al., 2010), which, in turn, determines which intermediates are formed and their toxicity. It appears that the ability to tightly regulate Aβ levels and maintain them in the appropriate form is lost in the progression towards AD. This failure in homeostasis may be accelerated by stress, insult and injury. The consequence is two major and interconnected disequilibria, which manifest as higher Aβ levels and a disproportionate increase in the toxic forms, and hence trigger pathological changes.

1.9.3 Interaction of Aβ with neurons

In order to exert its neurotoxic effects in the progression towards AD, it is likely that Aβ has some type of interaction with the neuronal membrane. Aβ is found both intra- and extracellularly, and can exert toxic effects from both locations. It is possible that intracellular Aβ is more toxic (Zhang et al., 2002), but extracellular Aβ is more abundant and easier to target therapeutically. This makes it vital to identify how its extracellular presence is transduced into intracellular pathologies and synaptic degeneration.

The way in which Aβ interacts with neurons is still contentious; it is possi-

ble the peptide is taken up (Bahr et al., 1998), and it has even been suggested that truncated fragments of $A\beta_{1-42}$ form channels in the membrane (Jang et al., 2010). Nevertheless, most evidence points to extracellular Aβ binding to the neuronal plasma membrane. Given the hydrophobicity of $A\beta_{1-42}$, one possibility is that oligomers bind directly to lipid rafts in the membrane itself (Lai and McLaurin, 2010). Nevertheless, many different membrane binding-partners have been proposed, including metabotropic glutamate receptors (mGluRs) (Um et al., 2013), α7-nicotinic acetylcholine receptors (Wang et al., 2000), ephrin B2 (Cissé et al., 2011), paired immunoglobulin-like receptor B and its human ortholog the leukocyte immunoglobulin-like receptor B2 (Kim et al., 2013). One recent addition to this list of binding partners is the cellular prion protein (Laurén et al., 2009), possibly in combination with mGluR5 (Um et al., 2013). Although this remains controversial (Kessels et al., 2010; Balducci et al., 2010), there is increasing evidence that this target of Aβ leads to pathological changes at the synapse (Barry et al., 2011; Freir et al., 2011; Resenberger et al., 2011). It is also possible that some of the proposed partners may not provide direct binding sites but are still required for Aβ targeting, for example membrane cholesterol (Nicholson et al., 2011), NMDARs (Decker et al., 2010a) or AMPARs (Zhao et al., 2010).

The concentration of Aβ used in binding assays varies considerably, and it is important to identify whether pathological changes result from Aβ binding with new, additional partners as its concentration increases, or simply from overactivation of those already used in the healthy human brain. Nevertheless, these possibilities are not mutually exclusive and, since Aβ binding might be in equilibrium, reducing the extracellular Aβ concentration could prevent both. Competitive antagonists are also possible, but to use this strategy to design drugs would require knowing the identity of the binding partners and the contribution each makes to pathological changes. An alternative treatment could be to modulate the number of Aβ binding sites, perhaps using signalling downstream of insulin receptors (De Felice et al., 2009). Nevertheless, if binding sites

are synaptic receptors, reducing these may have too many detrimental side effects.

1.9.4 Disruption of synaptic plasticity

The toxic effects of Aβ have been studied at many levels, from changes in the balance of glutamate receptors at the postsynaptic density and functional effects on synaptic plasticity, to outright synapse and cell loss, all the way through to cognitive impairments in behaving animals, as well as in AD patients. The disruption in glutamate receptor distribution and synaptic plasticity are described in greater detail in the subsequent chapters, but it is worth noting that Aβ appears to shift the balance between LTP and LTD induction to favouring the induction of LTD.

Aβ from many different sources can impair or completely block LTP; synthetic Aβ inhibits LTP in slices (Lambert et al., 1998) and also *in vivo* (Cullen et al., 1997; Kim et al., 2001) and Aβ derived from cells expressing mutated APP is particularly potent in triggering deficits in LTP (Walsh et al., 2002; Wang et al., 2004). Moreover, samples of cerebrospinal fluid from AD patients, but not controls, also induce an impairment in LTP (Klyubin et al., 2008; Shankar et al., 2008). Alongside these LTP deficits, it has also been reported that Aβ facilitates the induction of LTD (Kim et al., 2001; Li et al., 2009). An Aβ-induced enhancement of LTD has been reported for both NMDAR-dependent LTD (Kim et al., 2001) and mGluR-dependent LTD (Chen et al., 2013) in the hippocampus. Furthermore, there is much evidence suggesting that Aβ might recruit similar pathways to depress transmission as those used physiologically in the cell to mediate LTD, since calcineurin, which is central in the induction of LTD (Mulkey et al., 1994), is also implicated in the molecular cascades that mediate the effect of Aβ (Hsieh et al., 2006; Shankar et al., 2007; Zhao et al., 2010; D'Amelio et al., 2011). It is possible that this disruption in the plasticity mechanisms would then lead to synapse elimination (Lacor et al., 2007; Shankar et al., 2007; Tackenberg and

Brandt, 2009; Wei et al., 2010), which is the first major change in the AD progression (DeKosky and Scheff, 1990; Terry et al., 1991). However, whilst much emphasis has been put on the recruitment of LTD pathways by Aβ, it is also possible that homeostatic mechanisms are recruited pathologically to cause a general reduction in synaptic strength.

1.9.5 Tau protein

The other major pathology in AD is NFTs, and these comprise tau protein (Goedert et al., 1989). Unlike Aβ, the role of tau in the healthy brain is well established; tau belongs to the family of microtubule-associated proteins, and functions to promote microtubule assembly and stabilise the fully formed microtubules. In the healthy brain, its hydrophilic nature and intrinisically disordered and dynamic structure promotes binding to a range of intracelullar molecules (Mandelkow and Mandelkow, 2012). This is necessary to maintain cell shape, correctly localise intracellular organelles and for the function of intracellular transport systems. However, in AD, tau becomes hyperphosphorylated, and it appears this reduces its affinity for microtubules. This prevents tau from fulfilling its physiological functions, and an age-dependent increase in microtubule dynamics has been observed in tau transgenic mouse models of AD (Barten et al., 2012). Moreover, either as a by-product of this dissociation, or through an active process, tau starts to aggregate. It has been shown that this aggregation is pathological, since animal models with pro-aggregant versions of tau directed to the hippocampus by inducible expression under CaMKII control show synapse loss, LTP impairments, deficits in the MWM and context-dependent fear conditioning all in the absence of increased levels of Aβ (Hochgräfe et al., 2013).

The dissociation of tau from microtubules might also promote mislocalisation of the protein. In the mature healthy brain, tau is primarily present in the axonal compartment of neurons, but is also found in dendrites in small quanti-

ties (Papasozomenos and Binder, 1987). However, a higher level of tau is found in dendrites in AD models (Mandelkow and Mandelkow, 2012). Once in high quantities in dendrites, tau may disrupt vital physiological processes that are required for the integrity and appropriate functioning of the synapse. For example, Merino-Serrais et al. (2013) have reported that dendrite alterations and atrophy were only visible in post-mortem tissue from AD patients when aggregated tau was present at the dendrite; the presence of phosphorylated tau alone was not sufficient to promote pathology.

Another change to tau that occurs during the progression of AD is an increased level of proteolytic cleavage; this could encourage aggregation (Gamblin et al., 2003) or may even generate particularly pathological fragments (Park and Ferreira, 2005).

It remains contentious as to whether or not tau itself initiates AD pathology. Mutations in tau do not cause AD, but instead produce other tauopathies such as frontotemporal dementia (FTD) (Goedert et al., 2012), suggesting that tau may act downstream of Aβ. Therefore, studies in which tau aggregation has been studied in the hippocampus in the absence of Aβ pathology have been artificially induced (Hochgräfe et al., 2013). Such models help investigate tau mechanisms but do not recapitulate the progression of the human disease. Nevertheless, once the function of tau becomes disrupted, it is likely this sets in motion a process of pathological events that are no longer dependent on the presence of Aβ and which would need to be targeted for a treatment to be effective.

Overall, there has been highly significant progression in our understanding of AD, but our best hope to advance this knowledge further might be to elucidate the mechanisms and cellular pathways that underlie the early stages of this disease. Later in AD progression it appears that multiple additional pathological pathways are set in motion, and thus the disease process becomes even more difficult to dissect.

1.10 Aim of this thesis

The distinct types of spines, with their different NMDAR subunit compositions, may engage differently in plasticity processes and thus could play independent roles in the mature brain. Much controversy currently surrounds the role of NMDAR subunits in the induction of plasticity and possible contribution to learning and memory. However, it appears that NMDAR subunit composition alone is not sufficient to mediate selectively one direction of plasticity; the precise nature of synaptic context of the NMDAR may also be vital to enable a synapse to translate efficiently incoming activity to appropriate changes in strength. We have previously used optogenetics to access the left-right hippocampal asymmetry in mice (Kohl et al., 2011) and this provides a tool to utilise the variability in synapse structure and NMDAR composition, which may be a fruitful additional way to study the role of NMDAR subunits in plasticity and information processing in general.

The pathological changes in AD are thought to originate at the synapse, and hippocampal LTP at the CA3-CA1 synapse has been used as a model to further understand these changes. Nevertheless, there are many unanswered questions about how Aβ causes synaptotoxicity. It is possible that Aβ may disrupt synaptic function, and hence cognitive function, by destabilising the fine balance between LTP and LTD that is maintained in the healthy brain. Given the possible importance of LTP in learning and memory, it may be helpful to investigate whether Aβ differentially affects those spines where the balance is shifted towards favouring the induction of LTP.

1.10.1 Objectives

The objectives of this thesis are to:

1. Use a model of hippocampal LTP dysfunction in the presence of Aβ to investigate the possible interaction between Aβ and tau in pathological

changes at the synapse.

2. Investigate the synaptic mechanisms underlying the LTP findings with Aβ and tau (see Objective 1) and place them in the context of the left-right asymmetry in GluN2B subunit-containing NMDARs and plastic properties.

3. Translate the findings in asymmetry of LTP and synaptic properties to investigate whether there are any manifestations of the left-right differences at the behavioural level.

CHAPTER 2

Materials and Methods

2.1 Mice

Animal care and experimental procedures were conducted in accordance with U.K. Home Office regulations under the Animals (Scientific Procedures) Act of 1986 under appropriate personal and project licences. Mice were housed in polycarbonate cages of 5-10 animals and had access to food and water *ad libitum*, except when on food restriction during appetitively-motivated behavioural tasks. Holding facilities were maintained at approximately 22 °C, 60-70% humidity, and with a 12-hour light-dark cycle (7 a.m. to 7 p.m.).

2.1.1 *In vitro* work

For the field recording experiments presented in Chapter 3, 4-6 month old male *Tau*$^{-/-}$ mice on a C57BL6-J background (Dawson et al., 2001) and age-matched control male C57BL6-J mice were used. For the voltage-clamp experiments presented in Chapter 4 comparing the effect of amyloid β, 2-4 month old *Tau*$^{-/-}$ male mice and their age-matched male C57BL6-J controls were used. For all *in vitro* work, male C57BL6-J mice were purchased from Charles River Laboratories (Margate, U.K.), and *Tau*$^{-/-}$ mice were bred in-house. All mice were housed in the same animal facility under the same conditions for at least one week before experiments commenced. For the other voltage-clamp and field recording experiments presented in Chapter 4, mice were 2-6 months old when recordings were made. Any mice purchased from Charles River Laboratories that underwent surgery were housed in the animal facility for at least one week before surgery commenced.

In addition, unless otherwise described, all experiments presented together in the same figures have all been performed interleaved between genotypes and experimental conditions.

2.1.2 *In vivo* work

Male C57BL6-J mice were purchased from Charles River Laboratories (Margate, U.K.) or Harlan Laboratories (Wyton, U.K.) at 8-10 weeks and were housed in the animal facility for at least one week before surgery commenced.

2.2 Slice preparation and storage

Mice were deeply anaesthetised by inhalation of isoflurane. Upon cessation of pain reflexes (tested by paw withdrawal to firm fingernail pinch), the animals were decapitated. The brain was swiftly removed in ice-cold (0 to 1 °C) artificial cerebral-spinal fluid (aCSF, **Table 2.1**), that had been bubbled with carbogen gas (95% O_2 and 5% CO_2) for at least 30 minutes before use. Coronal hippocampal slices were prepared for optogenetic experiments by removing the cerebellum and then making an anterior cut, which was glued to a microtome plate using cyanoacrylate adhesive. For all other field-recording and voltage-clamp experiments, parasagittal hippocampal slices were prepared by separating the hemispheres and gluing the cut side of both hemispheres to the microtome plate.

Coronal slices (350 μm) and parasagittal slices (400 μm) were cut with a vibratome (Leica VT 1000S or Leica VT 1200S) in ice-cold aCSF. In all cases, further tissue was removed to leave a smaller section containing each hippocampus (**Fig. 2.1**(**A**)). After sectioning, slices were transferred to a submerged-style holding chamber for at least one hour and then incubated in drug solutions when applicable.

2.3 Field recording

2.3.1 Electrophysiological protocols

For field recording experiments, slices were transferred to an interface-style recording chamber maintained at 31-34 °C and superfused with aCSF at a rate

Compound	Final concentration (mM)
NaCl	126
KCl	3
NaH_2PO_4	1.25
$MgSO_4$	2
$CaCl_2$	2
$NaHCO_3$	26
Glucose	10
pH	7.2-7.4
Osmolarity	285 to 300 mOsm l^{-1}

Table 2.1: Composition of the artificial cerebrospinal fluid The concentration of each compound used in making artificial cerebrospinal fluid as well as the final pH and osmolarity.

of 0.5-2 mL min^{-1}. Recordings were started at least 15 minutes after the slices were transferred. Extracellular field recordings of the field excitatory postsynaptic potential (fEPSP) were performed with glass recording electrodes (3 to 5 MΩ) made from standard borosilicate glass capillaries (outer ∅: 1.2 mm, inner ∅: 0.68 mm; World Precision Instruments, Hitchin, U.K.) using a horizontal P-97 pipette puller (Sutter Instruments, Novato, U.S.A.). Recording electrodes were filled with aCSF. Monopolar tungsten stimulation electrodes (2 MΩ; A-M Systems, Sequim, U.S.A.) were used, and connected to a stimulus isolator unit (ISO-Flex, A.M.P.I, Jerusalem, Israel). Stimulation and recording electrodes were positioned in the stratum radiatum of CA1 (**Fig. 2.1**(**B**)). For the optogenetic field recording experiments, an optical fibre (200 μm, 0.39 NA; Thorlabs, Ely, U.K.) was also placed in the stratum radiatum, as close as possible to the stimulation electrode to ensure maximal overlap of fibres recruited (**Fig. 2.1**(**B**); **Fig. 2.2**(**A**)). The optical fibre was connected to a blue (470 nm) fibre-coupled high-power LED (Thorlabs) to enable optical stimulation.

Extracellular field recordings were made with an Axoclamp-2A amplifier

in bridge mode and data were acquired with an Instrutech ITC-16 A/D board (Instrutech Corp., Port Washington, U.S.A.) using Igor Pro software (WaveMetrics, Lake Oswego, U.S.A.). Before LTP recording commenced, an input-output curve was recorded by measuring the maximum amplitude of the field EPSP (fEPSP) at a stimulation current range from 100 to 0 μA in 10 μA decremental steps. To measure the paired-pulse ratio both before and after LTP induction, two 50 μs pulses with an inter-pulse interval of 40 ms were given at a low stimulation strength and the maximum fEPSP amplitude of each response was measured. For LTP recordings, stimulation strength was set to elicit a fEPSP of half-maximal amplitude. Synaptic efficacy was then monitored by stimulating the Schaffer collaterals at 0.2 Hz, (50 μs, 20-100 μA); for optogenetic experiments, stimulation was alternated between the electrical and optical (5 ms, 1-3 mW) stimulation, both at 0.2 Hz. The fEPSPs were recorded for a baseline period of at least 15 minutes (**Fig. 2.1**(**C**)), and when synaptic transmission was stable (<15% change in fEPSP slopes over 15 minutes), a single high-frequency stimulation train was delivered (100 Hz for 1 s) (**Fig. 2.1**(**C**),(**D**)). In the optogenetic experiments, the stimulus train was delivered by electrical stimulation alone, since the kinetics of ChR2 mean it cannot be used to drive pyramidal neurons at frequencies greater than ∽ 20 Hz. In addition, in the optogenetic experiments, the electrical stimulus duration was increased to 100 μs during delivery of the tetanus in order to maximise the recruitment of fibres activated by this electrical stimulation that would also be activated by the optical stimulation. In all field-recording experiments, the fEPSPs were then monitored for a further 45 minutes (**Fig. 2.1**(**C**)).

2.3.2 Data analysis

All slope and amplitude measurements were performed using custom-written procedures in Igor Pro (Wavemetrics). Firstly, the average fEPSP for the last minute of baseline recording was compared to the average fEPSP for 44-45 minutes post-induction to verify that the presynaptic fibre volley and stimulation

artefact overlapped and therefore that there had been no change in the recording conditions. The fEPSP slope estimates were then measured using the middle third of the slope; two time points corresponding to these values were assigned on the fEPSP average for the last minute of baseline recordings and slopes were measured by linear interpolation. Given the increase in slope following LTP induction, it was also checked that these values captured an appropriate slope measurement on the average fEPSP 44-45 minutes post-tetanus. Changes in synaptic efficacy were estimated using the mean fEPSP slopes for the last 5 minutes of recording, normalised to the mean fEPSP slope during the last 5 minutes of the baseline recording. For the optogenetic LTP experiment, due to increased variability in fEPSP slopes, data were normalised to the whole 15 minute baseline, and thus instead the average fEPSP slope during the last 15 minutes of recording (30-45 minutes post-tetanic stimulation) was used to estimate the magnitude of LTP. The input-output curve measurements were made using both fEPSP slope and amplitude. Paired pulse values were obtained by dividing the second fEPSP amplitude by the first fEPSP amplitude, and measurements were an average of 5 paired pulse values.

A subset (approximately half) of the LTP experiments comparing wild-type and *Tau*$^{-/-}$ mice were performed blind to drug and genotype. As the average and variability of blind and non-blind experiments were similar, these data were pooled. All the optogenetic LTP experiments in left- and right-injected mice were performed with the experimenter blind to injected hemisphere. For all optogenetic experiments, data from left- and right-injected mice were collected using slices both ipsilateral and contralateral to the injection site. Since there was no difference in the magnitudes of electrical or optical LTP between slices recorded ipsilaterally or contralaterally to the injection site, as has also been found previously for timing-dependent LTP (Kohl et al., 2011), the results were pooled. The level of overlap between the optical and electrical pathways was estimated using linear summation. Linear summation was measured by stimulating the electrical and optical pathways independently at the stimula-

tion strength used for the LTP recording. Both optical and electrical pathways were then triggered simultaneously and the amplitude of the resulting fEPSPs measured. The degree of linear summation was quantified as:

$$\frac{(optical\,fEPSP\,amplitude + electrical\,fEPSP\,amplitude) - simultaneous\,fEPSP\,amplitude}{optical\,fEPSP\,amplitude}$$

whereby an overlap index of 0 would suggest no overlap and 1 would suggest complete overlap. This measure was found not to differ between right- and left-injected mice (LS left: 0.47 ± 0.10, n = 10; LS right 0.40 ± 0.09, n = 11; Student's t-test P = 0.602). Statistical analyses were performed using SPSS and significance was assessed by Student's t-test, one-way ANOVA with a between subjects factor of treatment (with three or four levels) or by two-way ANOVA with two between subject factors of genotype and treatment (each with two levels). Significant interactions were explored by simple main effects. All values are given as mean ± s.e.m., and numbers (n) refer to the number of slices, with each condition obtained from at least six animals. All data presented together in the same figure have been collected interleaved between the different genotype/hemisphere and treatment conditions, unless otherwise stated.

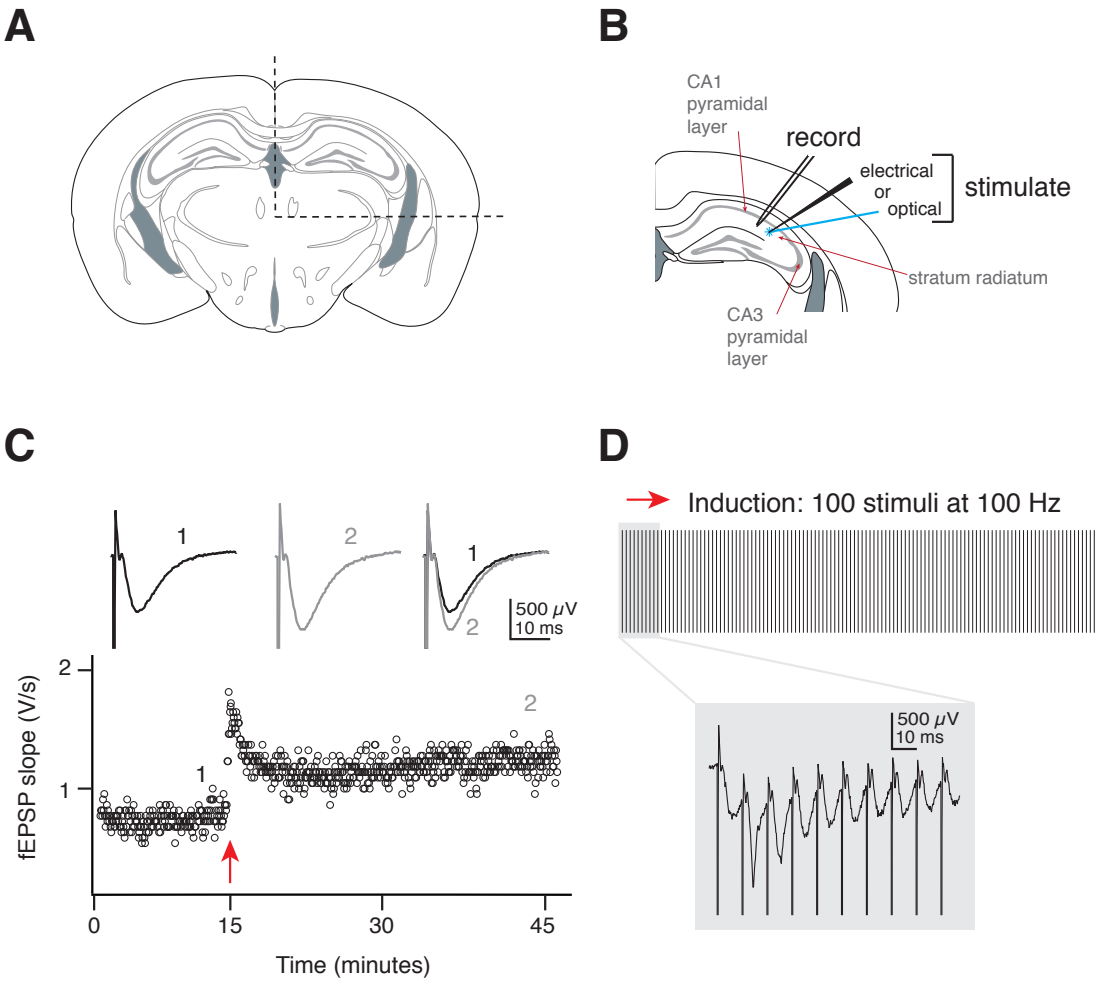

Figure 2.1: Field recording set-up and LTP protocol. (**A**) A coronal slice illustrating the further dissection that took place (dotted lines represent cuts) after slicing on the vibratome. The smaller sections containing each hippocampus were transferred to storage. (**B**) The hippocampal Schaffer collateral/commissural-CA1 pathway was activated by either electrical or electrical and optical stimulation in the stratum radiatum. The fEPSP response was monitored by a glass recording pipette that contained aCSF and was placed in the stratum radiatum. (**C**) A 15 minute stable baseline was recorded, the induction protocol was applied (red arrow) and fEPSP responses were monitored for a further 45 minutes. Following induction, a post-tetanic potentiation was observed and then fEPSP responses gradually decayed and stabilised at a new level. The insets show example traces of fEPSPs before and after induction of LTP. (**D**) The induction protocol consisted of a tetanus of 100 electrical stimulations at 100 Hz. The grey inset window shows the example field response to the first 10 stimuli of the high-frequency induction protocol.

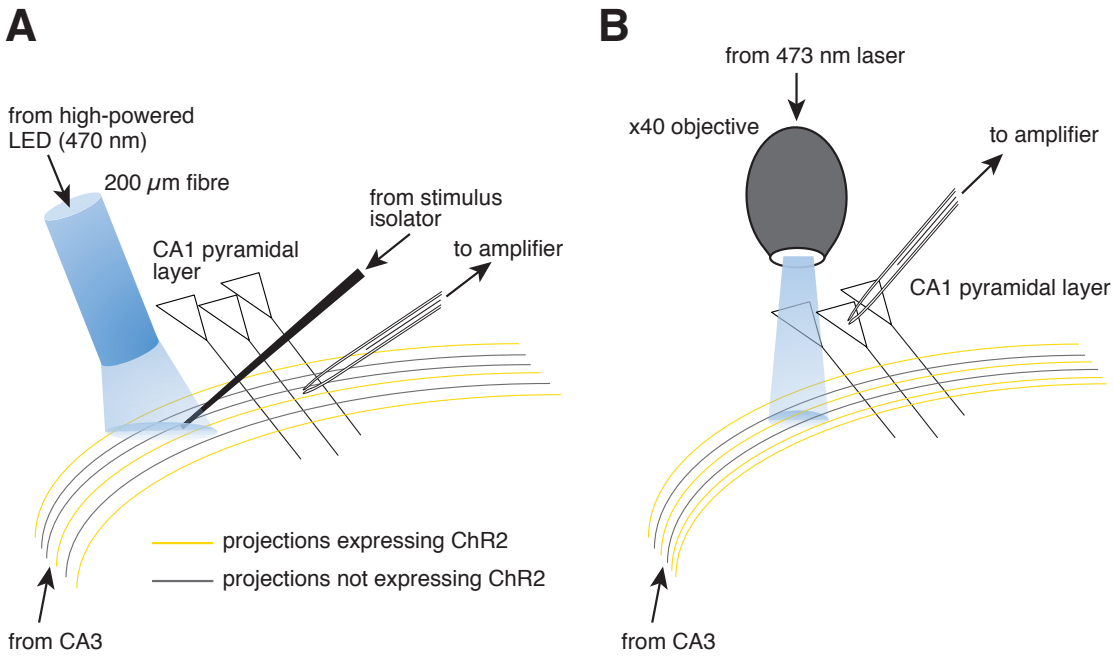

Figure 2.2: Details of light delivery. (**A**) Projections from the CA3 in the injected hemisphere that expressed ChR2 were activated by optical stimulation in the stratum radiatum via 470 nm wavelength light delivered from a high power LED coupled to a 200 μm fibre. These projections were either hippocampal Schaffer collateral or commissural projections depending on whether the slice used was ipsilateral or contralateral to the injected hemisphere. Electrical stimulation recruits expressing and non-expressing projections indiscriminately. The optical fibre and stimulation electrode were placed as closely as possible so that light and electrical stimulation recruited some of the same projections. The fEPSP response was monitored by a glass recording pipette that contained aCSF and was placed in the stratum radiatum. (**B**) Projections from the CA3 in the injected hemisphere that expressed ChR2 were activated by optical stimulation in the stratum radiatum via 473 nm wavelength light generated by a laser and delivered through the objective. These projections were either hippocampal Schaffer collateral or commissural projections depending on whether an ipsilateral or contralateral slice was used. A CA1 pyramidal neuron was patched and the EPSC response was monitored in voltage-clamp.

2.4 Patch-clamp recording

2.4.1 Electrophysiological protocols

For voltage-clamp experiments, slices were transferred to a submerged-style recording chamber at room temperature, and superfused with aCSF at 1-2 mL min^{-1}. Whole-cell voltage-clamp recordings were performed with glass pipettes (3 to 5 MΩ) made from standard borosilicate glass capillaries (outer ∅: 1.2 mm, inner ∅: 0.68 mm; World Precision Instruments) using a horizontal P-97 pipette puller (Sutter Instruments). A caesium methylsulphonate-based intracellular solution (**Table 2.2**) based on that in Snyder et al., 2005, was used for voltage-clamp recordings. In order to measure the NMDA receptor- /AMPA receptor-mediated current ratio (N/A ratio), the bath solution routinely contained 3 μM SR 95531 (gabazine) to block inhibitory postsynaptic currents. Before transferring the slice to the recording chamber, afferents from CA3 were cut, in order to prevent epileptiform activity.

Cells with a pyramidal-shaped soma in the stratum pyramidale of CA1 were selected for recording using infrared, differential interference contrast optics (**Fig. 2.3**(**A**)). Voltage-clamp recordings were not started until at least 10 minutes after breakthrough to allow diffusion of Cs^+ into the dendrites for improved space clamp. Series resistance was not corrected for but was monitored continuously during recordings and a range of 10-16 MΩ was used. Cells in which the series resistance rose above 18 MΩ were not considered for analysis. For long-term recordings comparing the N/A ratios before and after drug application, recordings were rejected if the series resistance changed by more than 25%.

Excitatory postsynaptic currents (EPSCs) were evoked either by a 50 μs pulse (80-300 μA) delivered by an extracellular stainless steel electrode (5 MΩ; A-M Systems) connected to a stimulus isolator unit (DS3, Digitimer Ltd., Welwyn Garden City, U.K.) or by a 5 ms pulse of blue laser light (473 nm, 1-5 mW at objective entry; Rapp OptoElectronic, Hamburg, Germany) (**Fig. 2.3**(**A**);

Fig. 2.2(**B**)). A 50 μm fibre (0.22 NA) was used to couple the laser to the microscope. In both types of experiments, stimulation strength was adjusted to yield 100-200 pA EPSC peak amplitude at a holding potential of -70 mV. EPSCs were evoked in the stratum radiatum every 14 seconds, alternating between a holding potential of -70 mV, 5 mV and +65 mV for 3 s steps, but returning to -70 mV in between, as illustrated in (**Fig. 2.3**(**B**)). Measured voltages were not corrected for the liquid junction potential of approximately -15 mV. If polysynaptic responses were observed then the slice was rejected. Data were low-pass filtered at 2 kHz and acquired at 20 kHz with an Axon Multiclamp 700B amplifier (Molecular Devices, Sunnyvale, U.S.A.) using the Matlab acquisition software (Mathworks, Natick, U.S.A.) and custom software (MatDAQ, Hugh P.C. Robinson 1995-2013).

Compound	Final concentration (mM)
$CsCH_3SO_3$	120
CsCl	20
EGTA	0.2
HEPES	10
QX-314	10
Mg-ATP	4
GTP	0.3
Final pH	7.2-7.3 adjusted with CsOH
Osmolarity	285 to 300 mOsm l^{-1}

Table 2.2: Composition of intrapipette solutions. The concentration of each compound used in making intrapipette solution for voltage-clamp recordings as well as the final pH and osmolarity.

2.4.2 Data analysis

Estimates of AMPA and NMDAR-mediated current were made using Matlab (Mathworks). The AMPAR-mediated current estimate was made using the peak current recorded at a holding potential of -70 mV (**Fig. 2.3**(**C**)). The NMDAR-mediated current estimate was measured at +65 mV during a period of 55-57 ms after stimulation, at a time when the fast AMPAR-mediated component of the current had decayed to less than 5% of its peak value (**Fig. 2.3**(**C**)). The average value of NMDAR- and AMPAR-mediated current was calculated per cell, and then normalised by dividing the NMDA value by the AMPAR value to give the N/A ratio. In order to estimate whether the decay time constant of the current recorded at +65 mV changed in different treatment conditions, a fixed fast time constant value (40 ms) and a fixed slow time constant value (275 ms) were assigned according to the weighted time constant values that have been measured for GluN1/GluN2A and GluN1/GluN2B homodimers (Vicini et al., 1998). The data was fitted with the double exponential equation of the form: fit = $A_f e^{(-t/\tau_f)}$ + $A_s e^{(-t/\tau_s)}$ where A_f and A_s = amplitude of fast and slow components respectively, t = time, τ_f and τ_s are the fast and slow time constant values respectively (**Fig. 2.3**(**D**)). Paired pulse values (measured at -70 mV) were obtained by dividing the peak amplitude of the second EPSC by the peak amplitude of the first EPSC, and measurements were an average of 5 paired pulse values. Statistical analyses were performed using SPSS and statistical significance was assessed by Student's *t*-test or by two-way ANOVA, with two between subjects factors with two levels (genotype: wild-type vs. *Tau*$^{-/-}$; hemisphere: left vs. right; basic treatment: control vs. hA$\beta_{1\text{-}42}$; acute treatment: control vs. hA$\beta_{1\text{-}42}$ or control vs. Ro 25-6981). Significant interactions were explored with simple main effects. All values are given as mean ± s.e.m., and numbers (*n*) refer to the number of cells. All data presented together in the same figure have been collected interleaved between the different genotype/hemisphere and treatment conditions.

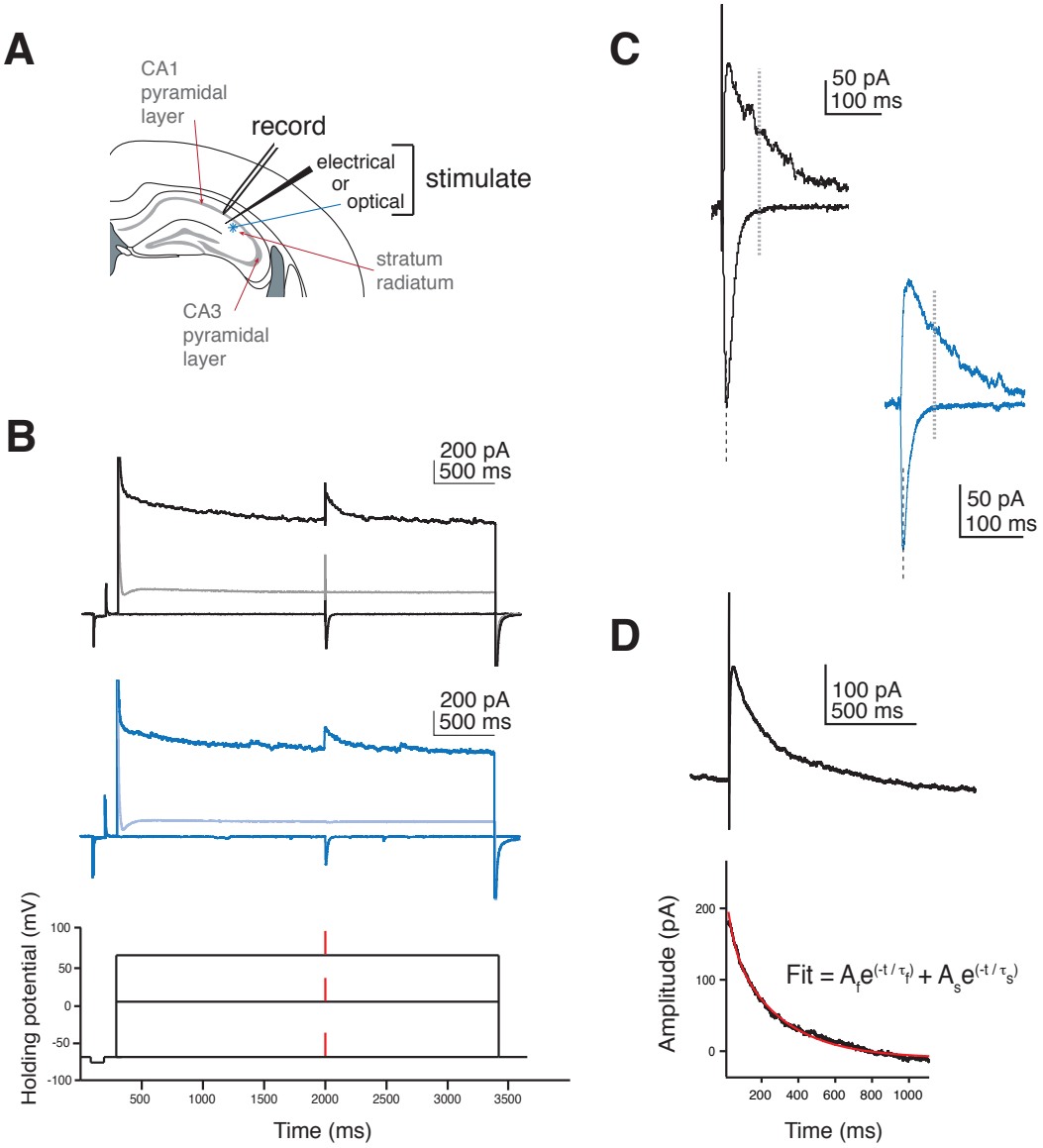

Figure 2.3: Patch-clamp recording set-up and N/A ratio measurements. (**A**) The hippocampal Schaffer collateral/commisural-CA1 pathway was activated by either electrical or optical stimulation in the stratum radiatum. A cell in the CA1 pyramidal layer was recorded in whole-cell mode and the EPSC response recorded. (**B**) The voltage-clamp recording protocol consisted of alternating 3 second steps to -70 mV, 5 mV and 65 mV, returning to -70 mV in between. Each recorded sweep was 4 seconds, and there was 14 seconds between each stimulation (red line), which was delivered 2 seconds into each sweep to evoke an EPSC. In order to measure series resistance, a 5 mV test pulse of 100 ms duration was delivered at the start of each recording sweep. (**C**) The AMPAR-mediated current was estimated using the peak amplitude at -70 mV (black dashed line) and the NMDAR-mediated current was estimated at a time window of 55-57 ms after stimulation (grey dashed line), at a time when the AMPAR-mediated component had decayed to less than 5% of its peak value. (**D**) The decay time constant was estimated from the slope of the current recorded at +65 mV; A_f and A_s = amplitude of fast and slow components respectively, t = time, τ_f and τ_s are the fast and slow time constant values respectively, here fixed to 40 ms and 275 ms.

2.5 Electrophysiological pharmacology

Pharmacological agents were used in both field recording and patch-clamp recordings experiments.

2.5.1 Sigma-Aldrich

The following pharmacological agents were purchased from Sigma-Aldrich (Poole, U.K.) and the catalogue numbers are stated in parentheses. The method of application is also described.

2.5.1.1 Lithium chloride (L9650)

Chemical name: LiCl. Lithium chloride is an unspecific inhibitor of glycogen synthase kinase 3 (GSK3) (Klein and Melton, 1996), a serine/threonine kinase. LiCl was added to a stock solution used to make up aCSF to give a final concentration of 5 or 10 mM Li^+. In order to maintain an appropriate osmolarity of the aCSF, the NaCl concentration used was reduced to give a final concentration of 120 or 115 mM respectively.

2.5.1.2 AR-A014418 (A3230)

Chemical name: N-(4-Methoxybenzyl)-N'-(5-nitro-1,3-thiazol-2-yl)urea. This is a highly selective competitive GSK3 inhibitor. It inhibits GSK3 with an IC_{50} value of 104 nM, but does not significantly inhibit cdk2 or cdk 5 (IC_{50} > 100 μM) or 26 other kinases (Bhat et al., 2003). AR-A014418 was dissolved in DMSO at 100 mM concentration and stored in frozen aliquots. For slice incubation, single aliquots of AR-A014418 were defrosted and diluted to a final concentration of 1 μM in ACSF. Slices were incubated for between 30 to 45 minutes in AR-A014418 before the addition of h$A\beta_{1\text{-}42}$ or control ACSF.

2.5.2 Tocris Bioscience

The following pharmacological agents were purchased from Tocris Bioscience (Bristol, U.K.) and the catalogue numbers are stated in parentheses. The method of application is also described.

2.5.2.1 SR 95531 hydrobromide (1262)

Alternative name: Gabazine. Chemical name: 6-Imino-3-(4-methoxyphenyl)-1(6H)-pyridazinebutanoic acid hydrobromide. Gabazine is a selective, competitive $GABA_A$ receptor antagonist that displaces [^{3}H]-GABA from rat brain membranes with a K_i of 150 nM (Heaulme et al., 1986). A stock solution of 6 mM was prepared and stored in frozen aliquots. Single aliquots were defrosted on the day of use and diluted to the final concentration in aCSF. For field recordings, gabazine was bath-applied at 100 nM concentration to slices from which the CA3 had been removed. For voltage-clamp recordings, gabazine was included in the circulating aCSF at a concentration of 3 μM, with afferents from CA3 cut before the slice was transferred into the recording chamber.

2.5.2.2 Amyloid β-peptide (1-42) (human) (1428)

Human form of the predominant amyloid β-peptide that is found in the brains of patients with Alzheimer's disease and is known to be neurotoxic (Hardy and Selkoe, 2002). Human $A\beta_{1-42}$ was freshly prepared on the day of experiment. It was initially dissolved in aCSF to a concentration of 5 mM. Aliquots were then sonicated for 11 minutes before final dilution to 220 nM in aCSF. Hippocampal slices were incubated in a submerged-style holding chamber in aCSF with or without human $A\beta_{1-42}$ for 1-3 hours before recording. Superfusion with half concentration of the drug continued after slices were transferred to the interface chamber or recording chamber.

2.5.2.3 Amyloid β-peptide (42-1) (human) (3391)

This is the reverse, inactive control peptide for amyloid β-peptide (1-42). It was prepared and used in the same way as human $A\beta_{1-42}$, as described above.

2.5.2.4 Ro 25-6981 maleate (1594)

Chemical name: (*αR*,*βS*)-*α*-(4-Hydroxyphenyl)-β-methyl-4–(phenylmethyl)-1-piperidinepropanol maleate. This is a highly selective antagonist at NMDA receptors containing the GluN2B subunit (IC_{50} values are 0.009 and 52 μM for cloned receptor subunit combinations of GluN1C/GluN2B and GluN1C/GluN2A respectively) (Fischer et al., 1997). It is a derivative of ifenprodil and is a non-competitive and activity-dependent antagonist. A stock solution of 5 mM was prepared and stored in frozen aliquots. Single aliquots were defrosted on the day of use and diluted to the final concentration of 0.5 μM in aCSF.

2.6 Protein extraction and Western blot analysis

Parasagittal slices from wild-type and *Tau*$^{-/-}$ mice were prepared as described for electrophysiological experiments and incubated in aCSF with or without 220 nM $hA\beta_{1\text{-}42}$ for two hours. A subset of slices were pre-incubated in 1 μM AR-A014418 for 30 minutes. The hippocampus was dissected from each slice and immediately frozen in dry ice and maintained at -80 °C. Total protein was extracted by homogenising hippocampal slices in radioimmunoprecipitation assay (RIPA) buffer (Sigma Aldrich, Poole, U.K.), supplemented with phosphatase inhibitors (PhosSTOP, Roche, Burgess Hill, U.K.) and protease inhibitors (Complete Mini Protease Inhibitor Cocktail, Roche), followed by brief microcentrifugation. Protein concentrations were determined using the Bradford Protein Assay method (Bradford, 1976). Two μg total protein was separated on 3-8% Tris Acetate polyacrylamide gels (Invitrogen, Paisley, UK) and transferred to

polyvinylidine fluoride membrane. Membranes were blocked in phosphate buffered saline (PBS) containing 0.1% Tween 20 and 10% milk and probed with primary antibody. Membranes were probed initially with an anti-phospho tau primary antibody (AT8; 1:1000 Thermo Fisher Scientific, Cramlington, U.K.), before stripping in Restore buffer (Thermo Fisher Scientific) and reprobing with a primary antibody to detect total tau (Tau5; 1:1000; Fitzgerald, Acton, U.S.A.). Primary antibody binding was detected using an anti-mouse HRP-conjugated secondary antibody (Biorad; Hemel Hempstead, U.K.) and ECL Plus reagent (GE Healthcare; Chalfont St Giles, U.K.), apposed to photographic film (CL-Xposure film, Thermo Fisher Scientific). Films were scanned, digitised and optical densities determined using ImageJ (v1.43u; National Institutes of Health). In order to control for between-membrane variation, all samples from an individual mouse were run on a single gel, and optical densities were expressed as ratios of phospho/total tau normalised to the respective aCSF-only condition. Values presented are the mean of duplicate Western blots.

2.7 Surgery

2.7.1 AAV vectors for optogenetic constructs

For field recording and voltage-clamp experiments, channelrhodopsin2 (ChR2) was used to evoke fEPSPs or EPSCs. ChR2 is a cation channel that is responsive to blue light. hChR2(E123T/T159C) was fused in-frame to enhanced yellow fluorescent protein (eYFP) (Berndt et al., 2011) and driven by a CaMKIIα promoter in order to ensure expression only in CaMKIIα-expressing neurons, which are primarily excitatory. Adeno-associated viral particles of serotype 5 were produced by the Vector Core Facility at The University of North Carolina at Chapel Hill.

For behavioural work, halorhodopsin (NpHR) was used to silence pyramidal neurons. NpHR is a chloride ion pump that hyperpolarises and thus si-

lences neurons upon activation with yellow-green wavelength light. eNpHR3.0 was fused in-frame to enhanced yellow fluorescent protein (eYFP) (Gradinaru et al., 2010) and driven by a CaMKIIα promoter (**Fig. 2.4** (**A**)). Adeno-associated viral particles of serotype 5 were produced by the Vector Core Facility at The University of North Carolina at Chapel Hill.

2.7.2 CA3 virus injection surgery for *in vitro* recording

Wild-type mice (2-4 months old) were anaesthetised with 2-4% isoflurane at 0.6-1.4 L min^{-1}. Using stereotactic apparatus (Kopf Instruments, Tujunga, U.S.A.), the head was levelled and a small craniotomy was made 2.3 mm anterior and 2.2 mm lateral (either left or right) from the skull surface at bregma. Through a small durotomy, 0.6 µL virus suspension (AAV5-CaMKIIα-ChR2(E123T/T159C)-eYFP, 1-4 x 10^{12} viral molecules $^{-1}$; University of North Carolina Vector Core, U.S.A.) were delivered at a rate of 0.1 µL min^{-1} 2.25 mm below the skull surface at bregma through a 33-gauge needle using a Hamilton Microlitre syringe (Esslab, Hadleigh, U.K). Following a five minute wait after bolus injection, the needle was retracted by 0.2 mm and after another five minutes slowly retracted fully. The scalp incision was sutured, and post-injection analgesic (0.03 mg kg^{-1} buprenorphine) was administered intraperitoneally to aid recovery.

2.7.3 CA3 implant surgery for *in vivo* behaviour

Wild-type male mice (10-12 weeks old) were anaesthetised with 2-4% isoflurane at 0.6-1.4 L min^{-1}, placed on a heating pad to aid body temperature maintenance and their head fixed in a stereotactic apparatus (Kopf Instruments). The head was levelled and three small craniotomies were made above either the left or right dorsal hippocampus. At sites 1 and 3 (site 1: anteriorposterior [AP]: -1.46 mm, mediolateral [ML]: 1.25 mm left or right, dorsoventral [DV]: -2.00 mm; site 3: AP: -2.46 mm, ML: 2.40 mm left or right, DV: -2.30, all coordinates from skull surface at bregma) 0.75 µL virus suspension (AAV5-CaMKIIα-eNpHR3.0-

eYFP-WPREpA, 4 x 10^{12} viral molecules $^{-1}$ for experimental mice and AAV5-CaMKIIα-eYFP, 6 x 10^{12} viral molecules $^{-1}$ for control mice; University of North Carolina Vector Core) were delivered at a rate of 0.1 µL min^{-1} through a 33-gauge needle using a Hamilton Microlitre syringe (Esslab) (**Fig. 2.4**(**B**)). Following a six-minute wait after bolus injection, the needle was retracted by 0.20 mm and after another four minutes slowly retracted fully. At site 2 (AP: -1.94 mm, ML: 2.00 mm left or right) a fibre-optic cannula, 200 µm diameter, 0.22 NA (Doric Lenses, Quebec, Canada) that had been cut with a diamond blade (Thorlabs) to approximately 2.2 mm, was lowered to a depth of -1.80 mm (DV tip of fibre-optic) and secured to the skull using dental cement (CB Metabond; Prestige Dental, Bradford West, U.K. and Simplex; Claudius Ash, Stevenage, U.K.) (**Fig. 2.4**(**B**),(**C**)). The scalp incision was sutured, and anti-inflammatory and analgesic drugs (2 mg kg^{-1} meloxicam; 0.1 mg kg^{-1} buprenorphine) were administered subcutaneously to aid recovery. Mice were returned to their home cages and left for at least 8 weeks for expression of eNpHR3.0-eYFP or eYFP to develop after surgery.

2.8 *In vivo* light delivery

Green laser light (532 nm) from a solid-state laser diode (Laser 2000, Ringstead, U.K.) assembled on a breadboard set-up (optical components from Thorlabs and Doric Lenses) was collimated into an aperture-matched fibre-optic patchcord (Doric Lenses). During testing, this was connected to the fibre-optic implants with a cubic zirconia sleeve (**Fig. 2.4**(**D**),(**E**)). In order to allow the animal free rotation, a rotary joint (Doric Lenses) was used as an intermediary between the patchcord attached to the laser and the patchcord connected to the implants. The rotary joint was attached to the ceiling in the centre of the room to allow equal movement in all directions. In addition, the equipment was all used from a sufficient height to ensure a mouse would never encounter strain to the patchcord while in the mazes. The output from the laser was regularly measured

using a thermosensor (Thorlabs) to ensure that the light delivered was sufficient for silencing, but did not increase to potentially damaging levels, and was adjusted to maintain a reading of 24 ± 3 mW at the fibre tip. Light delivery was controlled using a low vibration shutter combined with a shutter controller (Stanford Research Systems, Sunnyvale, U.S.A.).

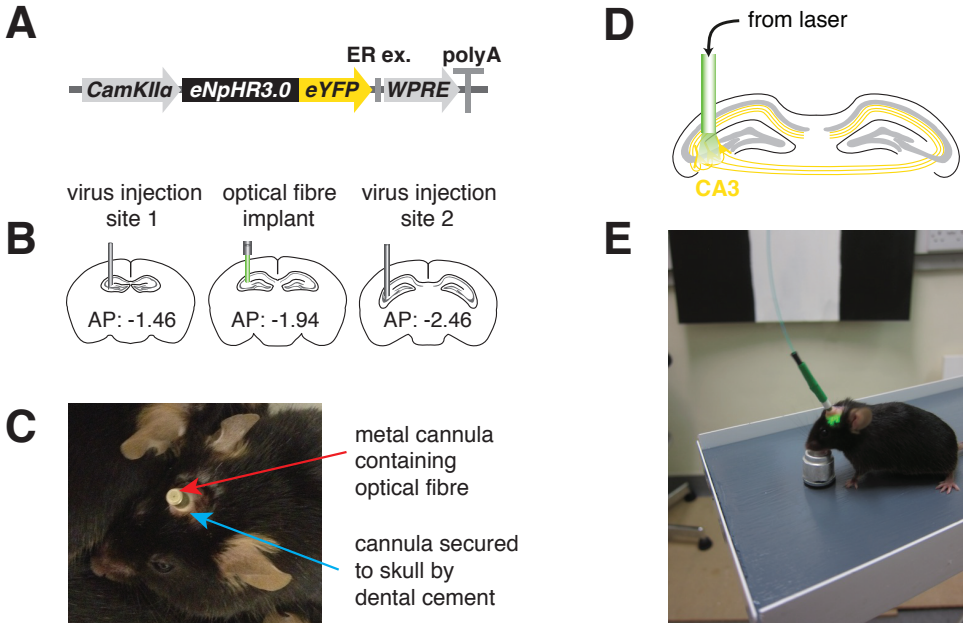

Figure 2.4: Implant surgery and light delivery. (**A**) An adeno-associated viral construct of serotype 5 was used to express eNpHR3.0 in CA3 pyramidal neurons under the control of a CaMKIIα promoter. The construct contained a woodchuck hepatitis post-transcriptional regulatory element (WPRE) to enhance gene expression and an export sequence (ER ex.) to increase the level of functional protein in the cell membrane. (**B**) Virus was delivered at two injection sites in the dorsal hippocampus in one hemisphere, and the fibre-optic cannula was implanted in between. (**C**) A 0.22 NA optical fibre was contained in a metal cannula (50 mm by 7.5 mm, red arrow), which was secured to the skull using dental cement (blue arrow). (**D**) Approximately 8 weeks after surgery, expression of eNpHR3.0 was sufficient to enable pyramidal neurons in the injected hemisphere (labelled CA3) to be silenced by green laser light (see (**Fig. 2.5**). (**E**) During behavioural testing, mice were securely connected to a fibre-optic patch cord carrying laser light via a cubic zirconia sleeve.

2.9 Optrode recordings

Adult male mice received dual injections of AAV5-CaMKIIα-driven eNpHR3.0 at sites 1 and 3, as described above but without the fibre-optic implant. Following at least 8 weeks for expression to develop, mice were anaesthetised with intraperitoneal injections of urethane (1.2 g kg^{-1}), ketamine (100 mg kg^{-1}), and xylazine (10 mg kg^{-1}) and their head fixed in a stereotactic apparatus (Kopf Instruments). Heating pads were used to aid body temperature maintenance. The head was levelled and a craniotomy was made above the injected hemisphere at the site used for the implant in behavioural surgery (AP: -1.94 mm, ML: 2.00 mm left or right, coordinates from Bregma).

Simultaneous optical silencing and electrical recording in CA3 were performed using an optrode consisting of an extracellular parylene-C insulated tungsten microelectrode (127 μm diameter, 1 MΩ; A-M Systems) tightly bundled with a stripped optical fibre (200 μm, 0.22 NA; Doric Lenses) that had been cut with a diamond blade (Thorlabs). The tip of the electrode protruded 0.5-0.7 mm beyond the fibre tip to ensure illumination of the recorded neurons (**Fig. 2.5**(**A**),(**B**)). A new optrode was made for each mouse. The optical fibre was coupled to the laser and light output adjusted to 20-25 mW at the fibre tip (please see '*In vivo* light delivery'). The optrode was initially placed above CA3 (DV: -1.80 mm from Bregma) and gradually lowered in 0.1 mm increments.

Signals were recorded and band-pass filtered between 300 Hz and 5 kHz using a microelectrode amplifier (1800 Microelectrode AC Amplifier, A-M Systems) and acquired using Spike2 (Cambridge Electronic Design, Cambridge, U.K.) in order to detect single and multi-unit spike activity (**Fig. 2.5**(**C**)). Recordings of both short-term light illumination and longer-term light illumination were made in order for results to be comparable with behaviour tasks of different duration trials. For short-term recordings, when clear spikes were detected, a baseline of 1 minute was recorded, followed by continuous laser light illumination for 30 s, followed by at least 1 minute recording without light. This

was repeated 1-4 times within each recording. For longer-term recordings, a baseline of 2 minutes was recorded, followed by continuous laser light illumination for 3 minutes, followed by 2 minutes of recording without light. Surgery was terminal and, after recordings were made, coronal slices were prepared and visualised under fluorescence brightfield optics to verify eNpHR3.0-eYFP expression and optrode site.

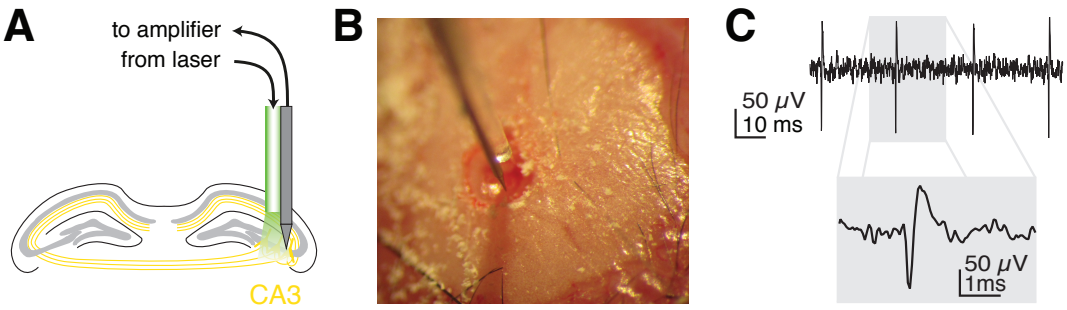

Figure 2.5: Optrode recordings. (**A**) At least 8 weeks after mice received dual virus injection, eNpHR3.0 was expressed by pyramidal neurons in the injected CA3 (labelled CA3), and their ipsilateral and contralateral projections. An optrode, consisting of an optical fibre tightly bundled to an extracellular microelectrode, could be used to record neuronal spiking activity and a possible silencing response to green laser light delivery. (**B**) The optrode was lowered through a craniotomy (∽ 0.4mm in diameter) into the brain until the extracellular microelectrode tip was in the CA3 pyramidal cell layer. Once the microelectrode was in the CA3 pyramidal cell layer, single or multiple units could be recorded spiking repeatedly. The grey inset window shows an example unit recorded.

2.10 Behaviour

Prior to starting behavioural testing, mice were handled to habituate them to the experimenter and accustom them to the connection of the implant. All behavioural testing was done during the light phase of the light-dark cycle and with the experimenter blind to condition. All mice were used first in the spontaneous alternation T-maze task and then in the appetitive Y-maze task. The last batch of 36 mice was additionally used in the visual discrimination T-maze task and supplemented by a group of experimentally naïve mice. This latter group of mice then went on to perform the novelty preference Y-maze task.

2.10.1 Spontaneous Alternation T-Maze Task

The T-maze was black painted wood and had two sliding doors to enclose the two choice arms (30 cm by 10 cm, 20 cm high walls) and a removable central barrier (extending 5 cm into central arm). During each trial the floor was covered with wood chipping litter. Mice received two self-contained trials each day, one in the morning and one in the afternoon. Mice were started in a psuedorandom order within the cage, which varied across trials. Before the start of each trial, the implant was connected to the laser. For 'Light on' trials, the illumination was started before the mouse was placed in the maze and light was then on continuously during the trial; light was turned off once the mouse was removed from the maze at the end of the trial. 'Light off' trials were interleaved, during which mice were still connected to the laser but no light was delivered. Mice were started facing outwards and given a free choice of arm (**Fig. 2.6**(**A**)). The central barrier was in position so mice received sensory input from only the chosen side before they could enter the arm. Once they had entered an arm, a black painted wooden block was positioned so they experienced a 30 second exploratory period in their chosen arm. The central barrier was removed, then the mouse was removed from the explored arm and immediately replaced in the start arm facing outwards (**Fig. 2.6**(**A**)). The subsequent arm choice was recorded, and if it

was the novel one this was scored as a correct alternation. A mouse was judged to have entered an arm when the tip of the tail passed the arm block holder when the mouse was moving in a forward direction. Since it has been reported that delay times can affect performance on short-term memory tasks (Zhang et al., 2013), if mice had not made an arm decision after 20 seconds in the second phase of the trial, the trial was aborted.

2.10.2 Appetitive Y-Maze Task

The Y-maze was constructed of grey painted wooden arms (50 cm by 13 cm bordered by 1 cm high white plastic walls), extending from a central triangle. Metal food wells (1.5 cm high) were positioned 5 cm from the distal end of the arms. The maze was elevated 82 cm from the floor. Mice were put on a restricted feeding schedule, allowing them to maintain at least 85% of their free-feeding body weight. Mice were introduced to the food reward (0.1 ml of sweetened condensed milk diluted 50:50 with water) in their home cages to overcome neophobia and then pre-trained on the elevated Y-maze in a room different to where behavioural testing would occur until they were highly motivated to search for food and running freely on the Y-maze (reaching the food reward in under 15 seconds for three consecutive trials).

The testing room contained visual cues made from black-and-white painted cardboard, which were positioned so that they did not coincide with the end of the arms. Mice were assigned a rewarded target arm (designated A, B and C according to its fixed position relative to extramaze cues). Target arm designations were counterbalanced such that approximately equal proportions of each experimental group were assigned to each arm. Mice were started facing outwards from the centre of the maze in either the left or right arm relative to the target arm (**Fig. 2.6**(**B**)) and received ten trials per day for eleven consecutive days. On each day they had five starts from the left of the target arm and five starts from the right in a pseudorandom order with no more than three consecutive starts

from the left or right. Mice were started in a pseudorandom order within the cage that varied across trials and the inter-trial interval (ITI) was approximately 15 minutes. Before being placed on the maze, the implant was connected to the laser and illumination started, light was then on continuously during the trial and was turned off once the mouse was removed from the maze. An arm entry was defined by all four paws being within the chosen arm. Mice would almost always move to the respective food well once an arm had been entered. If a mouse made the correct choice it was allowed to consume the reward. To prevent arm re-entry errors that could otherwise provide an additional source of learning impairment (Schmitt et al., 2003), the trial was ended if mice chose the incorrect arm and after they had seen the empty food well (i.e. they were not allowed to self-correct) (**Fig. 2.6**(**B**)). The maze was pseudorandomly rotated either clockwise or anticlockwise between trials to ensure that olfactory, tactile or visual cues on the maze itself (intramaze cues) did not provide information that could be used to solve the task. On the last day of testing, food was only delivered once the mouse reached the food well to confirm that mice did not use the reward odour to solve the task (post-choice baiting). When not performing the task, mice were kept behind a screen to minimise exposure to the testing room and cues in the absence of laser light.

2.10.3 Visual Discrimination T-Maze Task

The visual discrimination T-maze consisted of two painted wooden interchangeable arms, one grey and one black-and-white striped (30 cm by 10 cm, 30 cm high walls). The starting arm, central area and back wall were all brown. Mice were put on a restricted feeding schedule, allowing them to maintain at least 85% of their free-feeding body weight and re-introduced to the food reward (0.1 ml of sweetened condensed milk diluted 50:50 with water). Mice were assigned a target arm (with numbers trained to the grey or striped arm counterbalanced across each experimental group). Before the testing commenced, mice received four forced pre-trials to overcome any potential neophobia to the goal arms. In

these forced trials, one arm was blocked off so that they experienced each possible combination across the four trials (grey-left, grey-right, striped-left and striped-right), and the reward contingencies applied as they would for the rest of the experiment. For training, mice received ten trials per day for eight consecutive days and were always started facing outwards in the central arm, which remained in a fixed position (**Fig. 2.6**(**C**)). To ensure that there was no spatial solution to the task, the grey and the striped arm were interchanged such that each day mice received five trials where the rewarded arm was on the left and five where it was on the right (**Fig. 2.6**(**C**)). Reward arm location was assigned in a pseudorandom order, with no more than three consecutive positions of the rewarded arm being the same. Mice were started in a pseudorandom order within the cage, which varied across trials, and the ITI was approximately 15 minutes. Before being placed in the maze, the implant was connected to the laser and illumination started, light was then on continuously during the trial. The light was turned off once the mouse was removed from the maze. An arm entry was defined by all four paws being within the chosen arm. Mice would almost always move to the respective food well once an arm had been entered. If a mouse made the correct choice it was allowed to consume the reward, but if an incorrect choice was made the mouse was removed from the maze immediately after it had seen the empty food well analogous to the appetitive Y-maze task (**Fig. 2.6**(**C**)). On the last day of testing, food was only delivered once the mouse reached the food well to confirm that mice did not use the reward odour to solve the task (post-choice baiting).

2.10.4 Spatial novelty Preference Y-Maze Task

The spatial novelty preference Y-maze consisted of three transparent colourless Perspex arms, 8 cm wide and 25 cm tall, mounted onto a painted white wooden board. During each trial the floor was covered with wood chipping litter. Each arm could be closed off with a block made of opaque Perspex. Mice were assigned a 'novel' arm and a 'start ' arm (in relation to extramaze cues).

Arm designations were counterbalanced such that approximately equal proportions of each experimental group were assigned to each novel arm. During the first exploration phase of the trial, the novel arm was blocked off. Mice were placed facing outwards in the start arm, and were given 5 minutes to explore the 'start' and 'other' arms; timing was started once the mouse left the start arm (**Fig. 2.6**(**D**)). Before being placed in the maze, the implant was connected to the laser and illumination started, light was then on continuously during the first part of the trial. The light was turned off once the mouse was removed from the maze and the implant disconnected. Mice were then placed back in their home cage for 1 minute (**Fig. 2.6**(**D**)). The arm block was then removed and wood chipping shuffled. Mice were reconnected to the laser and illumination started, light was then on continuously during the second part of the trial. Mice were then placed back in the start arm facing outwards and given 2 minutes to explore all three arms, and the time spent in each arm was recorded; timing started once the mouse left the start arm (**Fig. 2.6**(**D**)). A mouse was defined as being in an arm when all four paws were within the arm. Mice received two separate novelty preference tests, each in a different testing room.

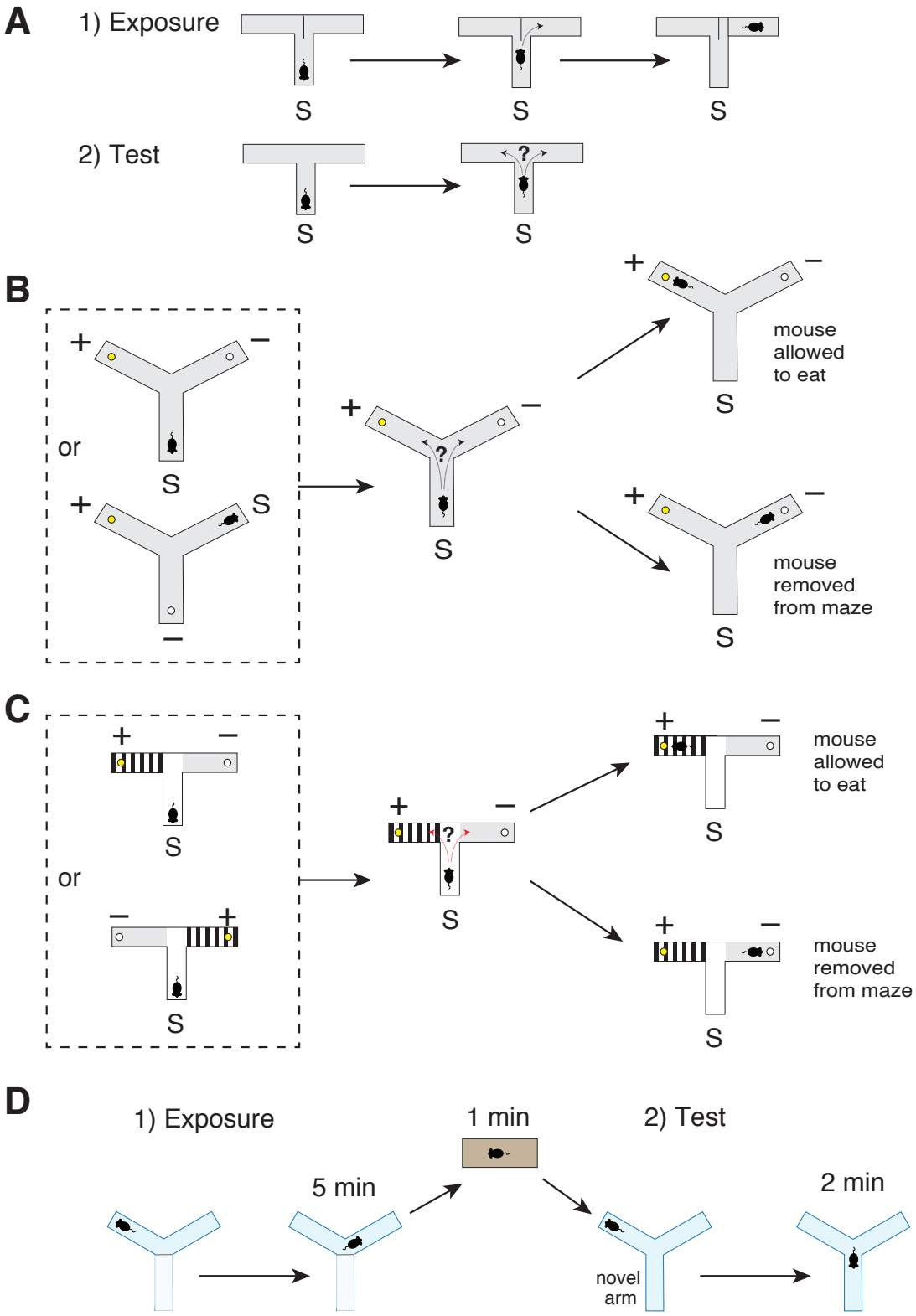

Figure 2.6: Schematics of behavioural tasks used. (**A**) The T-maze alternation task used to test short-term memory. (**B**) The appetitive spatial Y-maze task used to test long-term memory. (**C**) The appetitive visual discrimination task that was used as a hippocampus-independent control long-term memory task. (**D**) The novelty preference Y-maze task used to test short-term memory. For all tasks, start arm is denoted by 'S', rewarded arm (where applicable) is denoted by '+', and unrewarded arm (where applicable) is denoted by '-'.

2.11 Immunohistochemistry

In order to verify expression levels and implant placement, all mice used in behavioural experiments were anaesthetised by intraperitoneal injection of pentobarbital (533 mg kg^{-1}) and then transcardially perfused with cold PBS (pH 7.4) followed by 4% (w/v) paraformaldehyde (PFA) in PBS. Brains were post-fixed for 36 hours at 4 °C in PFA in PBS, then rinsed and subsequently kept in 30% (w/v) sucrose in PBS for at least 48 hours until the brain had sunk indicating sufficient sucrose infiltration. Coronal sections of 40 μm thickness along the entire dorsal-ventral axis of the hippocampus were cut using a microtome (Spencer Lens Co., Buffalo, U.S.A.) and divided into three series. The first series was immunostained to visualise expression of the YFP tag. Sections were rinsed for 3 x 10 minutes in PBS and incubated for 1 hour in PBS with 0.2% (w) Triton X-100 (PBS-T) containing 1% (w/v) bovine serum (Sigma). They were then incubated for 15 hours at 4 °C in PBS-T containing 1 % bovine serum and anti-GFP (goat, 1:1000, Abcam). The sections were then rinsed for 3 x 10 minutes in PBS and incubated in PBS-T containing 1% bovine serum and Alexa 488-labeled secondary antibody (donkey anti-goat; 1:1000, Invitrogen) for 90 minutes at room temperature. After three 10-minute rinses in PBS, slices were mounted in DAPI VectaShield (Vector Labs). In order to image the level of NpHR or control YFP expression, fluorescence images were taken using a Zeiss Axioskop 2 microscope with a 1.25x lens and acquired with FluoView software. The exposure and gain settings were kept constant in order to facilitate comparison of expression levels between mice.

In order to determine implant placement, sections containing evidence of the implant were separated from each of the three series. These sections were then imaged unmounted in bright-field mode. For each mouse, the image where the implant location appeared deepest was then used to plot implant location on the Mouse Brain Atlas. For this, all implants were plotted on the left hemisphere.

All imaging and scoring of the presence of expression and implant loca-

tion were performed blind. The two criterion set were expression of either eNpHR3.0-eYFP or eYFP in the injected CA3 of the dorsal hippocampus and an implant position that would have been able to illuminate the CA3.

2.12 Optrode and behavioural data analysis

Optrode recording data were analysed using Spike2 (CED) or custom procedures in Matlab (Mathworks) and Igor Pro (Wavemetrics). For short duration silencing, a voltage threshold was set and spike templates were produced during the baseline in Spike2 (CED) and counted. Data were then binned (5 s) and normalised to a 30 s baseline. For longer duration silencing recordings, individual spikes were counted using a voltage threshold. Data were then binned (30 s) and normalised to a 2 minute baseline. The normalised means during silencing were compared to 100% using a one-sample *t*-test.

For the appetitive Y-maze and the visual discrimination T-maze, arm choices were scored during the behavioural tasks. For the spontaneous alternation T-maze task, arm choices in the test part of the trial were scored during the behaviour but also some arm choices were verified *post-hoc* using video recordings made during each trial. The time spent in each arm for the novelty-preference Y-maze task was scored using videos filmed during each trial. The behavioural results were analysed by two-way ANOVA in SPSS, with two between subjects factors with two levels: transgene (NpHR vs. YFP) and hemisphere (left vs. right). In addition, the appetitive Y-maze and visual discrimination T-maze task had a within subjects factor of block (11 levels and 8 levels, respectively). Significant interactions were explored by simple main effects.

CHAPTER 3

A role for tau in the Aβ-induced impairment of LTP

3.1 Introduction

Alzheimer's disease (AD) is characterised by a progressive failure of learning and memory. The degree of cognitive impairment in AD correlates with the extent of synaptic loss (DeKosky and Scheff, 1990; Terry et al., 1991). Since pathological changes at the synaptic level are present before neuronal loss, this has led to the hypothesis that synaptic dysfunction underlies the cognitive deficits in patients with early AD and its precursor, mild cognitive impairment (MCI) (Selkoe, 2002).

Considerable evidence has accumulated that the pathological changes which occur in the hippocampus at the very early stages of the disease process are not mediated by two hallmark pathologies of amyloid plaques and tau neurofibrillary tangles (NFTs) but, instead, by their molecular constituents, amyloid beta (Aβ) and tau. Aβ in particular is thought to play a central role in pathogenesis (Hardy and Selkoe, 2002). Plaque formation is preceded by elevated levels of soluble, low-N oligomers of $A\beta_{1-42}$, and it is these that appear responsible for synaptic dysfunction (Selkoe, 2002; Lue et al., 1999) since acute exposure to synthetic or naturally secreted $A\beta_{1-42}$ peptides has been shown to impair hippocampal LTP in rodents (Cullen et al., 1997; Lambert et al., 1998; Walsh et al., 2002; Wang et al., 2004). Longer exposure triggers the loss of synapses (Wei et al., 2010) and eventually neurodegeneration, all in the absence of plaques.

Tau protein may also play a crucial role in the cognitive decline in early AD, although its precise contribution to pathology is less clearly defined than that of Aβ. NFTs are elevated in the medial temporal lobe of AD patients, and their numbers in the hippocampal CA1 correlate with memory decline (Markesbery et al., 2006). However, tau intermediates have been suggested as more important in actually mediating such cognitive decline than the tangles themselves (SantaCruz et al., 2005). Tau protein, through its interaction with microtubules, plays an important role in cytoskeletal dynamics under control conditions. For example, increased microtubule turnover is important for LTP at hippocampal

synapses (Fanara et al., 2010). However, the hyperphosphorylation of tau that occurs during disease progression is thought to weaken its interactions with microtubules, and thus may prevent it performing its necessary functions. Zempel et al. (2010) showed that the decreased stability of microtubules following tau dissociation causes structural networks to break down, reduces numbers of dendritic mitochondria, and finally culminates in spine loss. Tau may also actively promote pathology through gain-of-function effects. The level of tau in the somatodendritic compartment is low in healthy cells, but this dendritic level is increased in AD models (Mandelkow and Mandelkow, 2012). This missorting, likely following dissociation from axonal microtubules, has a range of damaging effects on the synapse. For example, tau aggregates can completely displace organelles to inhibit cellular function (Waxman and Giasson, 2011). It is not yet known whether the damaging effects of tau arise primarily through its ability to aggregate (Sydow et al., 2011) or through specific pathological effects of tau intermediates (SantaCruz et al., 2005). It has even been proposed that a specific 17 kDa fragment of tau causes pathology (Park and Ferreira, 2005; Nicholson and Ferreira, 2009). Nevertheless, a pathological role for tau seems indisputable.

Thus, Aβ and tau are both fundamental in the development of pathology at the early stages of AD. Each may exert synaptotoxic effects through parallel downstream pathways (Small and Duff, 2008), especially since Aβ is primarily found extracellularly, but tau protein is intracellular. Nevertheless, an alternative, but not mutually exclusive, possibility exists, whereby Aβ and tau could interact to trigger pathology. The steps from the binding or uptake of Aβ to the synaptotoxic downstream changes are yet to be fully elucidated, but it is notable that many of the downstream signalling cascades implicated in the pathology that develops following Aβ expsoure, such as those involving Wnt (De Ferrari et al., 2007; Cerpa et al., 2010) and mTOR (Ma et al., 2010, 2011b), are likely to culminate in changes in the balance between tau kinase and phosphatase activity, and hence a dysequilibruim in the phosphorylation status of tau. Evidence that Aβ might itself trigger tau pathology comes from the observation that CSF

extracts from AD patients containing Aβ can promote tau pathology in primary culture of hippocampal neurons (Jin et al., 2011) or when infused intracerebrally in rodents (Bolmont et al., 2007).

There is also direct evidence for an important interaction between Aβ and tau in triggering pathological changes. Firstly, tau-depleted neurons are protected from Aβ-induced neurodegeneration in culture (Rapoport et al., 2002). Secondly, the cognitive deficits seen in mice that overexpess the human amyloid precursor protein (hAPP), and hence Aβ (Hsiao et al., 1996), are absent in hAPP-overexpressing mice with a genetic knockout of tau protein (Roberson et al., 2007, 2011).

Given that NFTs containing hyperphosphorylated tau are a defining pathology of AD, and hyperphosphorylated tau is even found in amyloid plaques (Moechars et al., 1999), it is possible that a tau kinase could mediate a possible interaction between Aβ and tau, by enhancing the level of tau phosphorylation. One candidate for this role is glycogen synthase kinase-3 (GSK-3), which is a serine/threonine kinase that phosphorylates tau protein (Ishiguro et al., 1993) and is active in tangle-bearing neurons (Pei et al., 1999). If GSK-3 is involved in an interaction between Aβ and tau, inhibiting GSK-3 may be a promising therapeutic strategy for slowing the onset of AD.

3.1.1 Aim

Whether, and how, Aβ and tau interact is not yet fully established, but such a pathway might mediate the pathological synaptic changes that are thought to underlie the cognitive decline in early AD. The hippocampus is one of the earliest regions affected in AD and LTP at the CA3-CA1 synapse has provided a useful cellular model of the synaptic changes that may support learning and memory. Therefore, to further investigate a possible interaction between Aβ and tau, I asked whether tau is required for the Aβ-induced impairment of LTP in the hippocampus. For this, I used both wild-type mice and mice with a genetic knockout of tau protein (*Tau*$^{-/-}$ mice) (Dawson et al., 2001). In order to investigate a possible molecular pathway for the interaction between Aβ and tau, I tested whether tau phosphorylation by GSK-3 could be involved in the Aβ-induced impairment of LTP. Finally, I compared the effect of Aβ on LTP in *Tau*$^{-/-}$ mice that had either the human tau gene introduced, or a version containing a human tau mutation that is known to impair microtubule assembly.

3.2 LTP in Aβ-exposed slices from wild-type and *Tau*$^{-/-}$ mice

In order to investigate a possible interaction between Aβ and tau, I tested the effect of Aβ on LTP in wild-type and *Tau*$^{-/-}$ mice using extracellular field recordings in acute parasagittal hippocampal slices interleaved between genotypes and treatment conditions.

I first wanted to confirm that, under my experimental conditions, I could replicate the well-established impairment of LTP caused by acute exposure to human $A\beta_{1-42}$ ($hA\beta_{1-42}$) (Walsh et al., 2002; Wang et al., 2004; Townsend et al., 2006). I monitored fEPSPs evoked by extracellular stimulation of the Schaffer collateral/commissural pathway and, once I had recorded a stable baseline for at least 15 minutes, I induced LTP using high-frequency stimulation (100 Hz for 1 s). I then recorded the fEPSP responses for a further 45 minutes following the induction protocol. Some slices were incubated for 1-3 hours in 220 nM human $hA\beta_{1-42}$ before being transferred to the field recording chamber, where $hA\beta_{1-42}$ exposure continued at half concentration. I found that $hA\beta_{1-42}$ strongly impaired LTP in wild-type mice (control: 137 ± 5%, n = 11; $hA\beta_{1-42}$: 115 ± 5%, n = 9; **Fig. 3.1**(**A**),(**C**)). This was a specific effect of $hA\beta_{1-42}$ because slices pre-treated with a control peptide containing the hAβ peptide sequence in the reverse order ($hA\beta_{42-1}$) showed a synaptic potentiation (137 ± 7%, n =13; **Fig. 3.1**(**A**),(**C**)) equivalent to that in control slices (t-test P = 0.98). In contrast, while slices from *Tau*$^{-/-}$ mice incubated in control solution showed normal levels of LTP, slices that had been pre-incubated in $hA\beta_{1-42}$ also showed a similar magnitude of LTP (control: 138 ± 5%, n = 15; $hA\beta_{1-42}$: 138 ± 7%, n = 9; **Fig. 3.1**(**B**),(**C**)). ANOVA confirmed a main effect of treatment ($F_{1,40}$ = 4.27, P = 0.045) and genotype ($F_{1,40}$ = 5.03, P = 0.031) and, importantly, showed a genotype by treatment interaction ($F_{1,40}$ = 4.52, P = 0.04) due to a significant effect of $hA\beta_{1-42}$ in wild-type slices ($hA\beta_{1-42}$ $F_{1,40}$ = 8.25, P = 0.006). This dissociation between the effect of $hA\beta_{1-42}$ in wild-type and *Tau*$^{-/-}$ mice suggests that acute application of $hA\beta_{1-42}$ impairs one or more of the cellular mechanisms necessary to support LTP, but it requires

tau protein to do so. Moreover, the same result was also found with the rodent version of Aβ_{1-42} (Shipton et al., 2011), suggesting the lack of Aβ effect in *Tau$^{-/-}$* mice is a robust phenomenon.

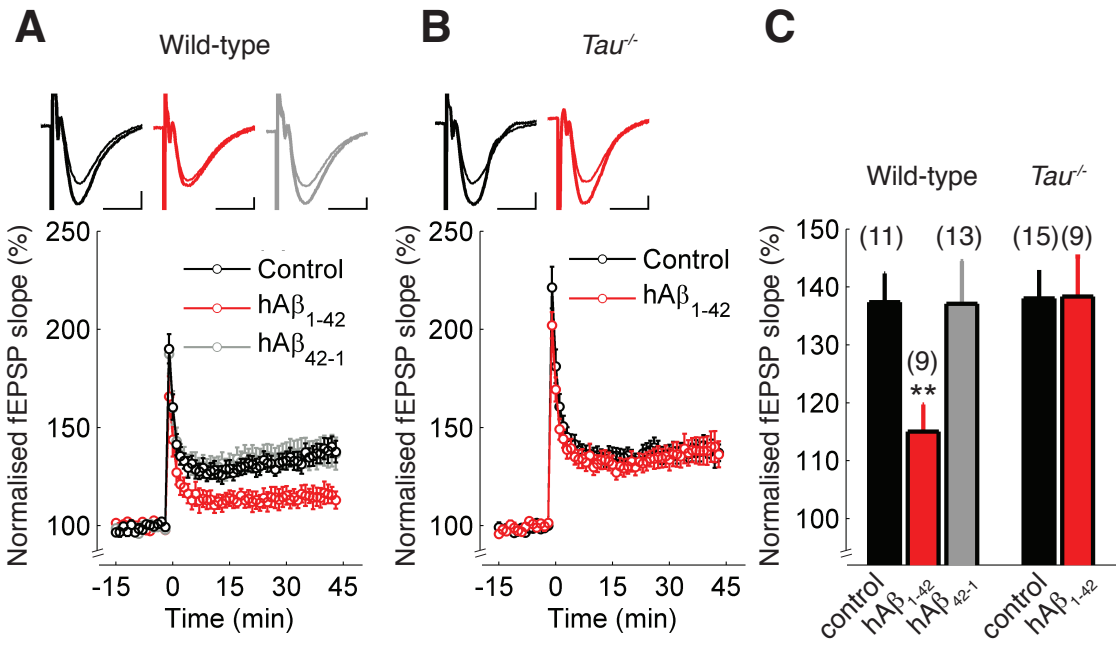

Figure 3.1: Human Aβ_{1-42} does not reduce LTP in slices from *Tau$^{-/-}$* mice. (**A**),(**B**) Hippocampal Schaffer collateral/commissural-CA1 LTP in wild-type (**A**) and *Tau$^{-/-}$* mice (**B**) in control aCSF (black), after incubation with hA$\beta_{1\text{-}42}$ (red) or after incubation with the reverse control peptide hAβ_{42-1} (grey). The insets show superimposed example traces before and 40 minutes after high-frequency stimulation for each condition. Scale bars: 5 ms, 200 μV. (**C**) Summary of results 40-45 minutes after high-frequency stimulation. The numbers of slices are shown in parentheses. Error bars are s.e.m. ** $P < 0.01$.

3.2.1 Synaptic properties of wild-type and *Tau*$^{-/-}$ mice

To investigate whether the differential ability of slices from wild-type and *Tau*$^{-/-}$ mice to express LTP in the presence of hA$\beta_{1\text{-}42}$ could be explained by different basic synaptic properties between the two genotypes, I measured the synaptic input-output relationship and the paired-pulse ratio (PPR). In order to measure the input-output relationship, I varied the extracellular stimulation strength from 100 μA to 0 μA in decrements of 10 μA and recorded the fEPSP responses in both wild-type and *Tau*$^{-/-}$ mice before starting the LTP recording. Both the slope and the amplitude of the fEPSPs recorded at each stimulation strength were used to measure the magnitude of the field response. There was no difference in synaptic input-output relationships between wild-type and *Tau*$^{-/-}$ mice for either the fEPSP slope or amplitude, indicating equivalent basal synaptic transmission (**Fig. 3.2**(**A**)) and this was confirmed by repeated measures ANOVA with genotype as the between-subjects factor and stimulus intensity as the within-subjects factor, which revealed no effect of genotype (wild-type n = 18, *Tau*$^{-/-}$ n = 20; fEPSP amplitude: $F_{1,36}$ = 0.33, P = 0.57; fEPSP slope: $F_{1,36}$ = 0.19, P = 0.66). Therefore, the equivalent input-output curves suggests that there should be no difference between the genotypes in the ability to induce LTP when the baseline fEPSP amplitude was set at half the maximum fEPSP before a population spike occurred.

It has been reported that, under some conditions, LTP at the hippocampal CA3-CA1 synapse can be mediated by presynaptic mechanisms (Ward et al., 2006; McGuinness et al., 2010). Therefore, in order to investigate whether there could be a difference in the presynaptic properties between the two genotypes that might account for the dissociation in the response to hA$\beta_{1\text{-}42}$, I also measured the PPR before and after LTP induction. I found no difference in the PPR between wild-type and *Tau*$^{-/-}$ mice and, moreover, the values did not vary before and after the induction of LTP (wild-type PPR before LTP: 1.67 ± 0.05, PPR after LTP: 1.68 ± 0.10, n = 12; *Tau*$^{-/-}$ PPR before LTP: 1.63 ± 0.11, PPR after LTP:

1.72 ± 0.06, n = 10; **Fig. 3.2**(**B**)). Repeated measures ANOVA revealed no effect of genotype (between-subjects factor $F_{1,17}$ = 0.323; P = 0.58) on the PPR before or after LTP induction (within-subjects factor $F_{1,17}$ = 0.55; P = 0.47). A change in the PPR following the induction of LTP suggests there is a presynaptic contribution to the LTP expression mechanism. Therefore, since the PPR remained constant, there is no indication that LTP was mediated by a purely presynaptic mechanism in either genotype under the experimental conditions used. Most importantly, the lack of any difference between wild-type and *Tau*$^{-/-}$ mice under any of the experimental conditions suggest that presynaptic differences under control conditions could not account for the distinct effect of hA$\beta_{1\text{-}42}$ in each genotype.

To further confirm this, I measured synaptic currents directly by performing whole-cell recordings of CA1 pyramidal neurons and measuring the amplitude of the evoked response whilst the cell was voltage-clamped at -70 mV. The PPR measured from excitatory postsynaptic currents (EPSCs) was also equivalent between the two genotypes (wild-type: 2.01 ± 0.23, n = 10; *Tau*$^{-/-}$: 1.81 ± 0.15, n = 8; t-test P = 0.50; **Fig. 3.2**(**C**)). Moreover, these paired-pulse measurements in control aCSF were interleaved with those made following incubation in hA$\beta_{1\text{-}42}$ for 1-3 hours, as had been used in LTP recordings. Even in the presence of hA$\beta_{1\text{-}42}$, no difference emerged between the two genotypes (wild-type: 1.97 ± 0.16, n = 10; *Tau*$^{-/-}$: 2.00 ± 0.18, n = 8, t-test P = 0.89, **Fig. 3.2**(**C**)). These measurements also showed that hA$\beta_{1\text{-}42}$ did not cause changes in the PPR within either genotype (ANOVA: no effect of genotype $F_{1,32}$ = 0.19, P = 0.67; no effect of treatment $F_{1,32}$ = 0.13, P = 0.72; and no genotype by treatment interaction $F_{1,32}$ = 0.38, P = 0.54; **Fig. 3.2**(**C**)). Overall, therefore, the PPR data provides no indication that presynaptic changes could explain the different effect of hA$\beta_{1\text{-}42}$ in wild-type and *Tau*$^{-/-}$ mice. It also suggests that Aβ does not exert its effect via an impairment of presynaptic mechanisms with the experimental conditions used here.

It is thought that the prominent increase in fEPSP amplitude and slope observed immediately following a high-frequency induction stimulation paradigm, known as post-tetanic potentiation (PTP), is a presynaptic phenomenon caused by increased vesicular release. Therefore, to further characterise the basic synaptic properties of the two genotypes, I also investigated whether the magnitude of the PTP varied between the two genotypes. However, no significant difference between wild-type and *Tau*$^{-/-}$ mice was found (wild-type PTP: 193 ± 9%, n = 28 mice; *Tau*$^{-/-}$ PTP: 211 ± 10%, n =18 mice, t-test P = 0.18; **Fig. 3.1**(**A**),(**B**)).

3.2.2 Network properties of wild-type and *Tau*$^{-/-}$ mice

In addition to possible differences in synaptic properties, the dissociation between wild-type and *Tau*$^{-/-}$ mice in the effect of hA$\beta_{1\text{-}42}$ on LTP could also be caused by distinct inhibitory network properties, either pre-existing under baseline conditions or arising following incubation in hA$\beta_{1\text{-}42}$. It is known that long-term exposure to hA$\beta_{1\text{-}42}$ may cause reduced $GABA_A$ mediated currents (Limon et al., 2012) and alter circuit mechanisms (Verret et al., 2012; Palop et al., 2007; Palop and Mucke, 2010), but whether differences could arise following acute exposure to hA$\beta_{1\text{-}42}$ is not yet clear. To confirm that differences in GABAergic inhibition could not account for the LTP results, I repeated the experiments in the presence of 100 nM gabazine. This concentration is sufficient to block phasic inhibition; a higher concentration was not possible due to a high frequency of epileptiform activity emerging after the induction of LTP, which could affect fEPSP slope measurements. To limit epileptiform activity even under 100 nM conditions, the CA3 was removed before slices were transferred to the field recording chamber. I obtained equivalent results in disinhibited slices, with a an hA$\beta_{1\text{-}42}$-induced impairment of LTP in wild-type mice (wild-type control: 140 ± 7%, n = 11; wild-type hA$\beta_{1\text{-}42}$: 114 ± 4%, n = 11; t-test P = 0.006; **Fig. 3.3**). However, as had been found previously, there was no effect of Aβ in *Tau*$^{-/-}$ mice (*Tau*$^{-/-}$ control: 145 ± 5%, n = 7; *Tau*$^{-/-}$ hA$\beta_{1\text{-}42}$: 142 ± 11%, n = 6; t-test P = 0.79; **Fig. 3.3**). This suggests that under the conditions of these experiments, with

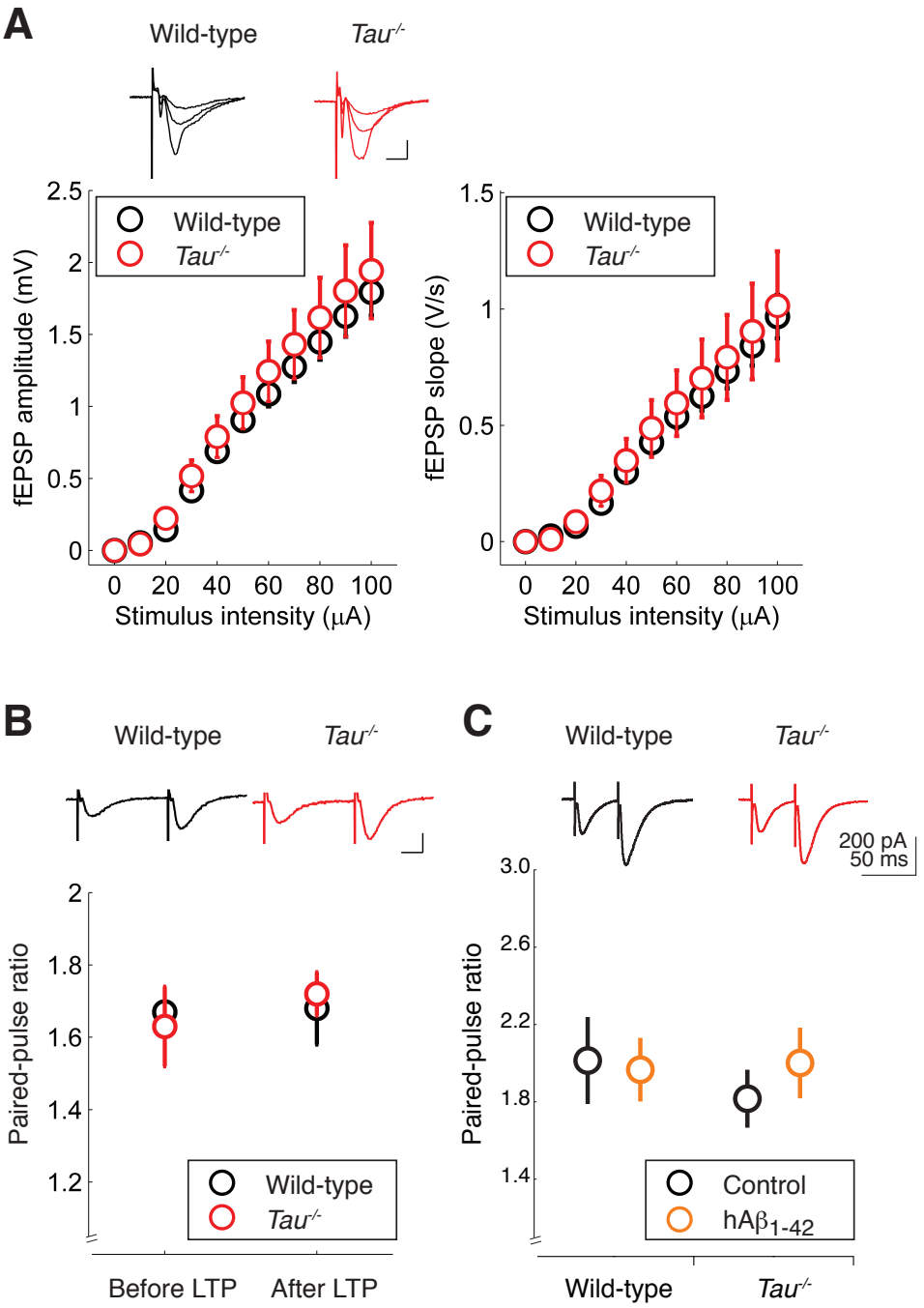

Figure 3.2: Wild-type and *Tau*$^{-/-}$ mice have similar input-output relationships and paired-pulse ratios. (**A**) Left panel: the fEPSP amplitude for wild-type (black) and *Tau*$^{-/-}$ mice (red) recorded at different strengths of stimulation of the Schaffer collateral/commissural input to CA1; right panel: the fEPSP slope at different stimulation strengths. Inset shows example traces corresponding to 20, 60 and 100 μA stimulation. Scale bars: 5 ms, 500 μV. (**B**) Paired-pulse ratio for wild-type (black) and *Tau*$^{-/-}$ mice, before and after LTP induction. Inset shows example traces for paired pulse responses before LTP. Scale bars: 5 ms, 500 μV. (**C**) Paired-pulse ratio for wild-type and *Tau*$^{-/-}$ mice measured from EPSCs, in both control aCSF (black) and following incubation in hAβ$_{1\text{-}42}$ (orange). Insets show example traces for paired pulse responses in control aCSF. Error bars are s.e.m.

acute exposure to Aβ, changes to interneuron network function can not explain the requirement for tau in the Aβ-induced LTP impairment.

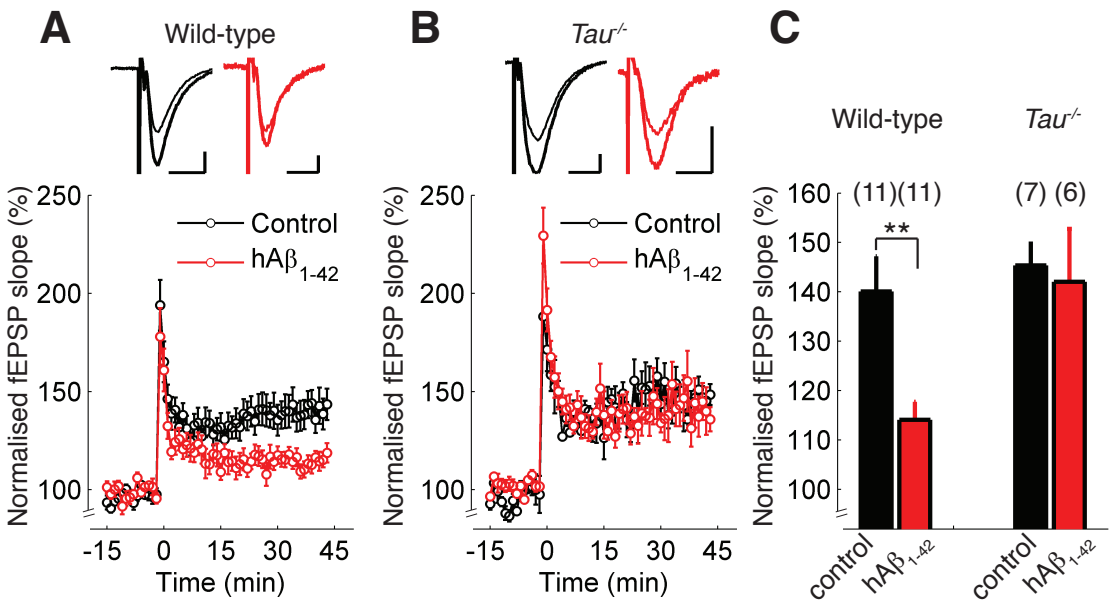

Figure 3.3: Human Aβ_{1-42} does not reduce LTP in disinhibited slices from *Tau*$^{-/-}$ mice. (**A**),(**B**) Hippocampal Schaffer collateral/commissural-CA1 LTP in wild-type (**A**) and *Tau*$^{-/-}$ mice (**B**) in the presence of 100 nM gabazine in control aCSF (black) or after incubation with hA$\beta_{1\text{-}42}$ (red). The insets show superimposed example traces before and 40 minutes after high-frequency stimulation for each condition. Scale bars: 5 ms, 200 μV. (**C**) Summary of results 40-45 minutes after high-frequency stimulation. The numbers of slices are shown in parentheses. Error bars are s.e.m. ** $P < 0.01$.

3.3 The possible role of tau phosphorylation in LTP impairments

Given that NFTs comprising hyperphosphorylated tau are a prominent pathology alongside Aβ plaques in AD, I asked whether the hA$\beta_{1\text{-}42}$-induced impairment of LTP requires the activity of a tau kinase and is associated with changes in the level of tau phosphorylation. For this work, I used wild-type mice, since I wanted to further explore the LTP impairment caused by hA$\beta_{1\text{-}42}$, and focused on the tau kinase GSK-3, since this has previously been implicated in Aβ-triggered cell death (Tackenberg and Brandt, 2009).

3.3.1 Tau kinase inhibition with lithium

Lithium inhibits the tau kinase activity of GSK-3 (Klein and Melton, 1996) and hence can reduce tau phosphorylation (Hong et al., 1997; Lovestone et al., 1999); it also has been shown to prevent neurodegeneration (Alvarez et al., 1999). Moreover, lithium is already approved for therapeutic use in humans with bipolar depression. Therefore, I performed an exploratory study to test whether lithium might reduce the effect of hA$\beta_{1\text{-}42}$ on LTP in wild-type mice. Since the presence of LiCl in the aCSF altered the osmolarity, I adjusted the Na^+ concentration used in order to maintain an osmolarity of approximately 300 mOsm L^{-1}.

Slices were kept in control aCSF or pre-incubated in aCSF containing 5-10 mM lithium for 30 minutes to inhibit GSK-3; in some cases, hA$\beta_{1\text{-}42}$ was then added for the 1-3 hour incubation, as had been done previously. There was a trend for lithium to rescue LTP in the presence of hA$\beta_{1\text{-}42}$ (control: 135 ± 6%, n = 6; Li^+: 130 ± 5%, n = 19; Li^+ + hA$\beta_{1\text{-}42}$: 125 ± 6%, n = 8; hA$\beta_{1\text{-}42}$: 117 ± 3%, n = 6; **Fig. 3.4**(**B**),(**C**)), however, there was not a significant effect of treatment between the groups (ANOVA: $F_{3,35}$ = 1.07, P = 0.375; **Fig. 3.4**). Moreover, results were not conclusive because the magnitude of LTP appeared lower in the presence of lithium. This may be caused by lithium reducing slice health, especially since I

made a qualitative observation that fewer slices met the criterion for use in LTP experiments that the fEPSP amplitude exceeded the pre-volley following incubation in aCSF containing LiCl. Alternatively, it may be because lithium, which is known to block many other kinases in addition to GSK-3, interfered with other cellular pathways that are required for LTP. Nevertheless, given the trend towards recovery, an alternative, more specific, GSK-3 inhibitor was sought to test whether blocking tau phosphorylation would prevent the hA$\beta_{1\text{-}42}$-induced LTP impairment.

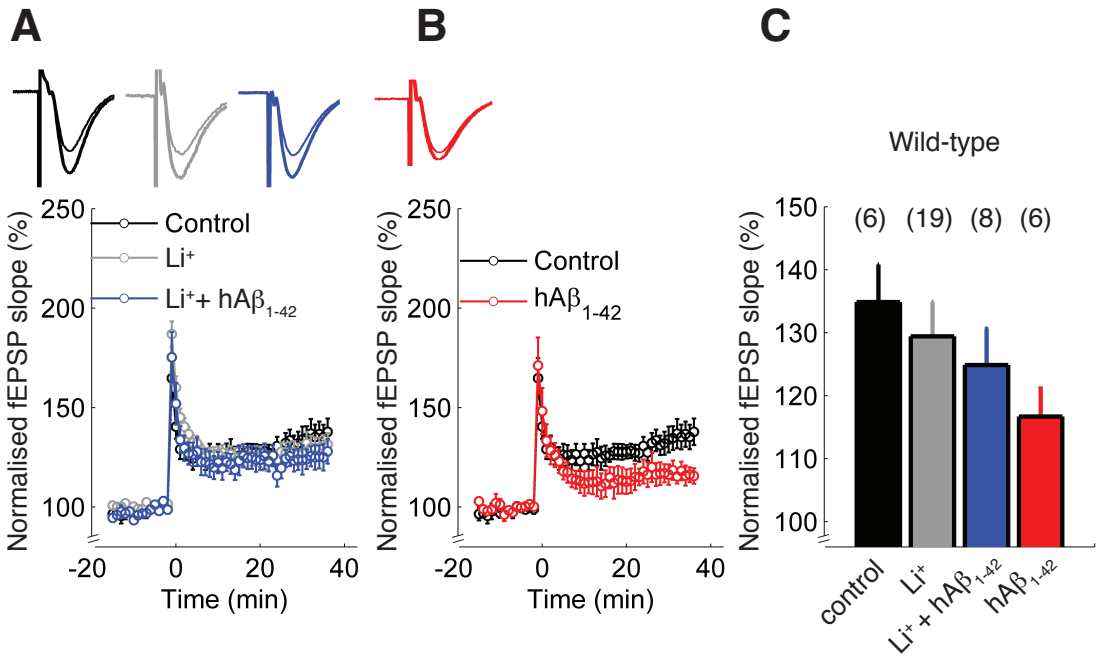

Figure 3.4: Lithium effect on human Aβ_{1-42}-induced impairment of LTP. (**A**) Hippocampal Schaffer collateral/commissural-CA1 LTP in wild-type mice in control aCSF (black), after incubation with 5-10 mM lithium alone (grey), lithium incubation followed by incubation with hA$\beta_{1\text{-}42}$ (blue) or hA$\beta_{1\text{-}42}$ treatment alone (red). All experiments were performed interleaved. The insets show superimposed example traces before and 35 minutes after high-frequency stimulation for each condition. Scale bars: 5 ms, 200 μV. (**B**) Summary of results 33-38 minutes after high-frequency stimulation. The numbers of slices are shown in parentheses. Error bars are s.e.m.

3.3.2 Tau kinase inhibition with AR-A014418

Since the exact nature of the effect with lithium was inconclusive, I tested whether an alternative tau kinase inhibitor might provide clearer results about whether tau phosphorylation could be involved in the hA$\beta_{1\text{-}42}$ impairment of LTP.

I used AR-A014418, which is a highly specific GSK-3 inhibitor that does not significantly inhibit closely related kinases such as Cdk2 or Cdk5 (Bhat et al., 2003). I pre-exposed slices from wild-type mice to 1 μM AR-A014418 for 30 minutes prior to the addition of hA$\beta_{1\text{-}42}$ to a final concentration of 220 nM. With this AR-A014418 pre-treatment prior to incubation in hA$\beta_{1\text{-}42}$, the magnitude of LTP that I observed was equivalent to that in control slices (control: 134 ± 6%, n = 9; hA$\beta_{1\text{-}42}$ + AR-A014418: 135 ± 5%, n = 9; **Fig. 3.5**). It is possible that this recovery effect could arise because exposure to AR-A014418 and subsequent block of GSK-3 activity itself causes an enhancement of LTP that masks the impairment by hA$\beta_{1\text{-}42}$. However, since slices exposed to AR-A014418 alone also showed an equivalent level of potentiation (134 ± 10%, n = 9; **Fig. 3.5**), this explanation is unlikely. Instead, given that ANOVA confirmed no difference between the three treatment groups ($F_{2,24}$ = 0.013, P = 0.99), the data suggests that inhibition of GSK-3 by AR-A014418 acted to rescue the impairment caused by hA$\beta_{1\text{-}42}$.

However, since AR-A014418 was prepared in DMSO, I wanted to confirm that the recovery of LTP was attributable to the activity of the drug and not because the vehicle affected the magnitude of LTP or interfered with the action of hA$\beta_{1\text{-}42}$. A particular concern would be that DMSO could interfere in the oligomerisation of Aβ monomers and hence the formation of the toxic low-N oligomeric Aβ. Therefore I tested LTP in wild-type slices pre-exposed to vehicle (0.01% DMSO) for 30 minutes prior to incubation with hA$\beta_{1\text{-}42}$ and to vehicle alone. I found that DMSO did not affect the toxicity of hA$\beta_{1\text{-}42}$, indicating that the recovery of LTP could be attributed to the action of AR-A014418, and, moreover, vehicle alone did not affect the magnitude of LTP (control: 138 ± 10%, n = 8; DMSO + Aβ: 112 ± 5%, n = 9; DMSO: 136 ± 7%, n = 10; ANOVA $F_{2,24}$ = 3.87,

P = 0.035; **Fig. 3.6**).

Therefore, overall, these data show that blocking tau kinase activity can prevent the LTP impairment caused by hA$\beta_{1\text{-}42}$. A hypothesis parsimonious with this data is that tau phosphorylation is required for hA$\beta_{1\text{-}42}$ to exert its synaptotoxic effects.

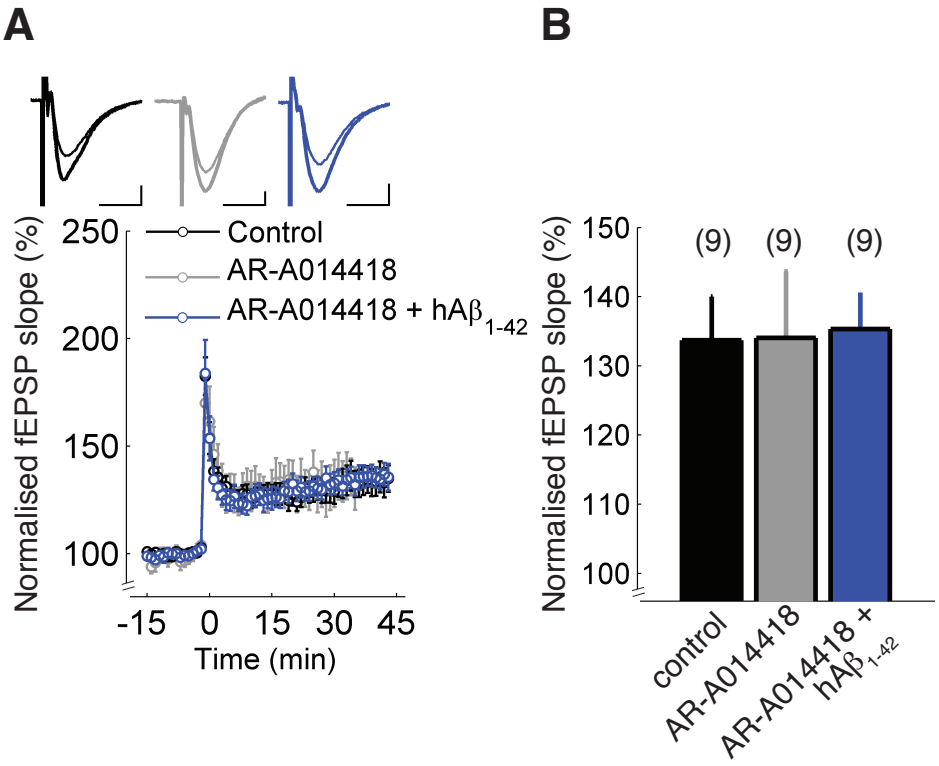

Figure 3.5: The specific GSK-3 inhibitor AR-A014418 prevents the human Aβ_{1-42}-induced impairment of LTP in wild-type slices. (**A**) Hippocampal Schaffer collateral/commissural-CA1 LTP in wild-type mice in control aCSF (black), or after incubation with AR-A014418 alone (grey) or AR-A014418 followed by incubation with hA$\beta_{1\text{-}42}$ (blue). The insets show superimposed example traces before and 35 min after high-frequency stimulation for each condition. Scale bars: 5 ms, 200 μV. (**B**) Summary of results 30-35 min after high-frequency stimulation. The numbers of slices are shown in parentheses. Error bars are s.e.m.

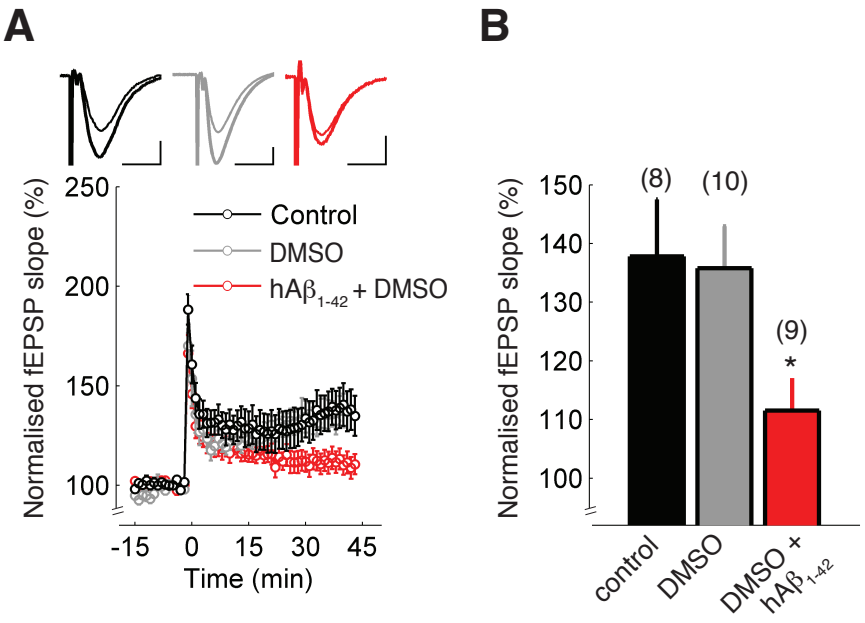

Figure 3.6: DMSO treatment does not affect LTP results in control and human Aβ_{1-42}-treated slices. (**A**) Hippocampal Schaffer collateral/commissural-CA1 LTP in wild-type mice in control aCSF (black), or after incubation with 0.01 % DMSO alone (grey) or 0.01 % DMSO and hA$\beta_{1\text{-}42}$ (red). The insets show superimposed example traces before and 40 min after high-frequency stimulation for each condition. Scale bars: 5 ms, 200 μV. (**B**) Summary of results 35-40 min after high-frequency stimulation. The numbers of slices are shown in parentheses. Error bars are s.e.m. * $P < 0.05$.

3.3.3 Tau phosphorylation changes in the presence of human Aβ_{1-42}

In order to investigate whether tau phosphorylation could be involved in mediating the impairment of LTP by hA$\beta_{1\text{-}42}$, I wanted to investigate whether changes in the level of tau phosphorylation occurred under my experimental conditions of hA$\beta_{1\text{-}42}$ exposure and, furthermore, whether they were restored to baseline levels by pre-incubation with AR-A014418. Thus I performed Western blot analysis of hippocampal tissue from wild-type slices that had been prepared in the same way as in the LTP experiments. Slices were incubated in aCSF with or without 220 nM hA$\beta_{1\text{-}42}$, and a subset of slices in each of these groups had been pre-treated with 1 μM AR-A014418 for 30 minutes to inhibit GSK-3 activity. These concentrations and incubation times were identical to those used in the electrophysiology experiments so that they could be directly compared. Phosphorylation of tau was detected using the AT8 antibody, and was normalised to the total level of tau using the Tau5 antibody. A significant effect of treatment on the ratio of phosphorylated to total tau was found (ANOVA $F_{2,22} = 3.99$, $P < 0.05$; **Fig. 3.7**). Specifically, incubation with hA$\beta_{1\text{-}42}$ increased tau phosphorylation compared to that observed in control slices (AT8/Tau5 ratio = 1.53 ± 0.26, $n = 10$; one sample *t*-test compared to 1, $P < 0.05$), and the phosphorylation ratio in slices pre-incubated with AR-A014418 before exposure to hA$\beta_{1\text{-}42}$ was significantly lower than those incubated with hA$\beta_{1\text{-}42}$ alone (AT8/Tau5 ratio = 0.72 ± 0.14, n =9; two-sample *t*-test $P < 0.01$). Finally, slices exposed to 1 μM AR-A014418 alone showed equivalent tau phosphorylation to that observed in control conditions (AT8/Tau5 ratio = 0.96 ± 0.16, $n = 4$).

These results suggest that hA$\beta_{1\text{-}42}$ increases the level of tau phosphorylation, and this correlates with the impairment in LTP. Moreover, not only does pre-incubation with AR-A014418 block the synaptotoxic effect of hA$\beta_{1\text{-}42}$, it restores tau phosphorylation to baseline levels. Altogether, this is consistent with the hypothesis that the activation of GSK-3 and its phosphorylation of tau are required for the inhibitory effect of hA$\beta_{1\text{-}42}$ on LTP, though alternative interpre-

tations are possible.

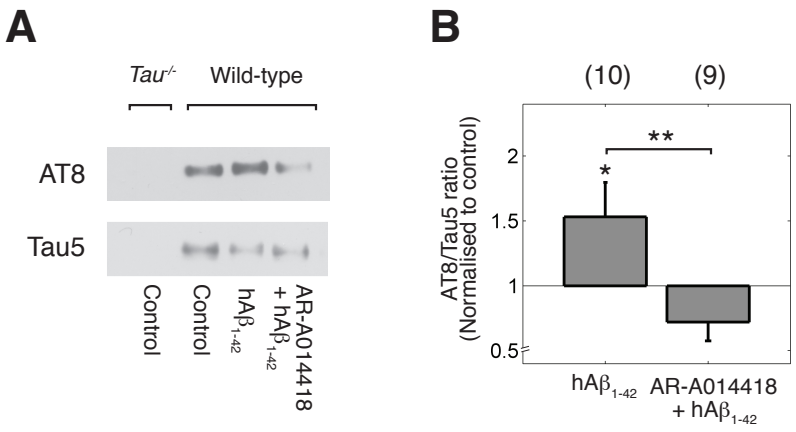

Figure 3.7: A specific inhibitor of GSK-3 reduces human Aβ_{1-42}-induced phosphorylation of tau. (**A**) Example Western blot showing immunoreactivity to Tau5 (total Tau) and AT8 (phosphorylated Tau). (**B**) Pooled data for AT8/Tau5 ratios normalised to the immunoreactivity observed in control conditions in each mouse. The numbers of mice are shown in parentheses. Error bars are s.e.m. * $P < 0.05$; ** $P < 0.01$.

3.4 Human tau mutations and LTP

Mutations in APP, PSEN 1 and PSEN 2 are known to cause early onset AD in humans (Tanzi, 2012), and late onset AD still has a strong heritable component (Bettens et al., 2013). Thus, given the prevalence of tau in AD pathology, it might be predicted that mutations in the MAPT gene would cause early onset AD and/or contribute to late onset AD. However, MAPT mutations instead produce frontotemporal dementia (FTD), which lacks any Aβ pathology (Goedert et al., 2012). Therefore, this further suggests that tau may be downstream of Aβ in the chain of events leading to early AD pathology and, hence, further investigating FTD may enhance our understanding of the pathological process once tau is recruited. It is possible that, despite AD and FTD having a different initiating factor, and thus originating in distinct brain regions, these conditions could have a shared molecular pathway downstream from tau.

In order to investigate whether it would be valid to measure the effect of $hA\beta_{1\text{-}42}$ on LTP in mice containing a mutated MAPT gene, I first investigated whether hippocampal LTP was observed in a well-established mouse line carrying the P301S mutation (Allen et al., 2002). The P301S-T43 mice were 5-6 months old and were compared to aged matched control mice of the C57BL/Ola line, all provided by Professor Michel Goedert at the University of Cambridge. Despite an overt motor disruption, this mouse line had a magnitude of hippocampal LTP equivalent to that in the control mice (P301S-T43: 134 ± 7%, n = 14; C57BL/Ola: 137 ± 7%, n = 11; t-test P = 0.76; **Fig. 3.8**(**A**),(**B**)).

Therefore, I investigated the effect of acute exposure to $hA\beta_{1\text{-}42}$ on LTP in two recently developed mice lines that carry the N296H mutation. This is a different human MAPT mutation associated with FTD, and is know to impair microtubule assembly (Yoshida et al., 2002). The two mice lines had the mutant human tau gene introduced onto a $Tau^{-/-}$ background (N24 and N51 lines), and they were compared to age-matched $Tau^{-/-}$ mice that had the wild-type form of human tau introduced (H1 line). The mice were 3-5 months old at testing. The

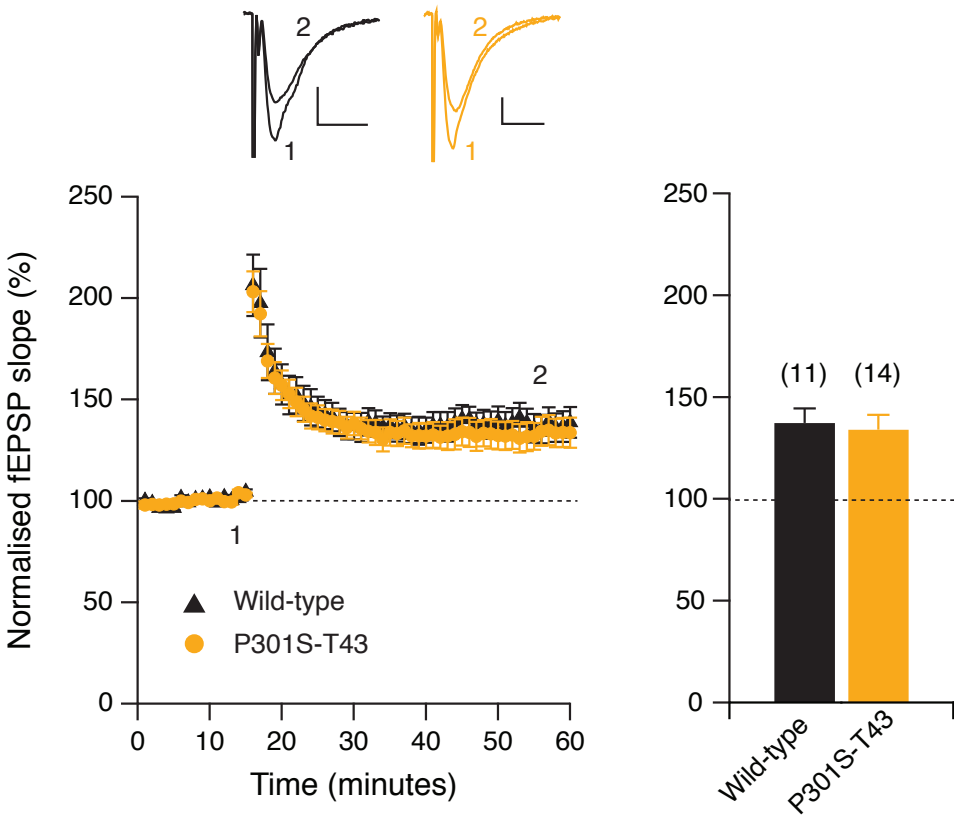

Figure 3.8: Mice carrying the P301S mutation do not have impaired hippocampal LTP. (**A**) Hippocampal Schaffer collateral/commissural-CA1 LTP in C57BL/Ola control mice (black) or in P301S-T43 mice (orange). The insets show superimposed example traces before (1) and after (2) high-frequency stimulation for each condition at the representative time points; scale bars: 10 ms, 500 μV. (**B**) Summary of results 35-40 min after high-frequency stimulation. The numbers of slices are shown in parentheses. Error bars are s.e.m.

Wade-Martins group at the University of Oxford generated these mice, and the LTP work is part of a broader characterisation of these new lines.

I first tested whether the H1 mouse line was equivalent to wild-type mice in showing an hA$\beta_{1\text{-}42}$-induced impairment in LTP. There was a reduction in the magnitude of LTP in the presence of hA$\beta_{1\text{-}42}$ in H1 mice (control: 162 ± 8%, n = 11; hA$\beta_{1\text{-}42}$: 133 ± 5%, n = 9; t-test P = 0.002; **Fig. 3.9**(**A**),(**C**)). Therefore, since the H1 line shows the same hA$\beta_{1\text{-}42}$-induced LTP impairment as wild-type mice, it suggests that human tau protein was expressed and functioning in an equivalent manner to the mouse tau. Interleaved with these experiments, I also tested the effect of hA$\beta_{1\text{-}42}$ on LTP in the N51 mice line. In contrast to the effect of hA$\beta_{1\text{-}42}$ in the H1 line, although a normal magnitude of LTP was seen in the N51 mice under control conditions, no impairment in the presence of hA$\beta_{1\text{-}42}$ was observed (control: 157 ± 13%, n = 9; hA$\beta_{1\text{-}42}$: 161 ± 8%, n = 11; **Fig. 3.9**(**B**),(**C**)). Overall, therefore, a comparison between the H1 and N51 mouse lines showed a very similar pattern of results to the comparison between wild-type and *Tau*$^{-/-}$ mice, and ANOVA revealed a genotype by treatment interaction ($F_{1,44}$ = 4.12, P = 0.049) due to an effect of hA$\beta_{1\text{-}42}$ in H1 mice alone ($F_{1,44}$ = 6.70, P = 0.013; **Fig. 3.9**(**A**),(**B**),(**C**)).

In order to confirm that this lack of hA$\beta_{1\text{-}42}$ effect was robust in mice carrying the N296H mutation, I also tested the second mouse line generated alongside the N51 line that contained the same human tau mutation, the N24 line. No effect of hA$\beta_{1\text{-}42}$ was observed on LTP in this line either (control: 139 ± 5%, n = 5; hA$\beta_{1\text{-}42}$: 138 ± 5%, n = 5; **Fig. 3.9**(**D**),(**E**)).

The similar lack of effect of hA$\beta_{1\text{-}42}$ in the *Tau*$^{-/-}$ and N296H tau mutant mice further emphasises the possible importance of tau in mediating the hA$\beta_{1\text{-}42}$-induced impairment of LTP.

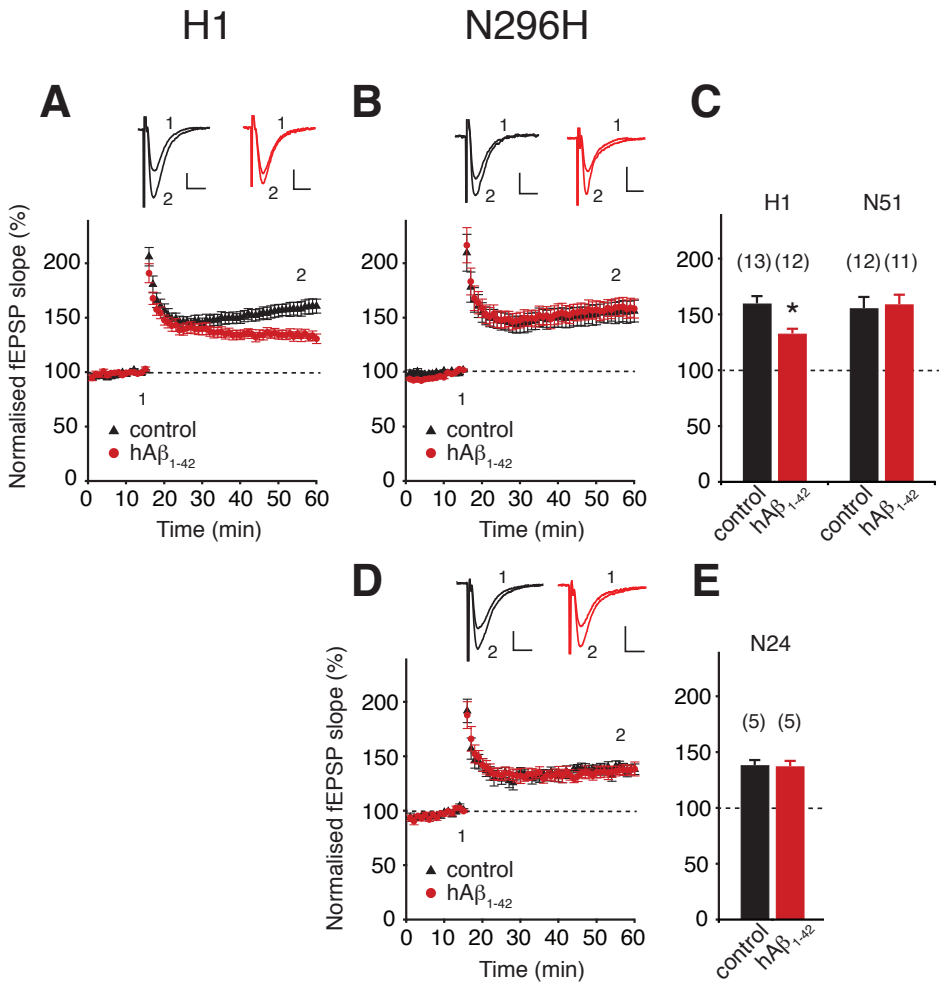

Figure 3.9: Mice carrying the N269H human tau mutation do not show a human Aβ_{1-42}-induced LTP impairment. (**A**),(**B**),(**D**) Hippocampal Schaffer collateral/commissural-CA1 LTP in H1 (**A**), N51 mice (**B**) and N24 (**D**) in control aCSF (black), or after incubation with hA$\beta_{1\text{-}42}$ (red). Recordings in H1 and N51 mice were performed interleaved but recordings in N24 mice were made independently. The insets show superimposed example traces before (1) and after (2) high-frequency stimulation for each condition at the representative time points; scale bars: 10 ms, 500 μV. (**C**),(**E**) Summary of results 40-45 minutes after high-frequency stimulation. The numbers of slices are shown in parentheses. Error bars are s.e.m. * $P < 0.05$

3.5 Discussion

Three principal findings emerge from the work presented in this chapter. Firstly, in *Tau*$^{-/-}$ mice, hA$\beta_{1\text{-}42}$ did not impair hippocampal LTP, in contrast to the robust impairment of LTP it caused in wild-type mice. Secondly, a specific inhibitor of the tau kinase GSK-3 prevented both the augmented tau phosphorylation and the impairment of LTP that were otherwise seen following hA$\beta_{1\text{-}42}$ treatment in wild-type mice. Thirdly, mouse lines carrying a mutated human tau associated with FTD behave as *Tau*$^{-/-}$ mice in their lack of response to hA$\beta_{1\text{-}42}$.

Since cognitive decline in early AD is associated with pathology in the medial temporal lobe, I investigated LTP at the hippocampal CA3-CA1 synapse, a widely accepted cellular model for learning and memory (Bliss and Collingridge, 1993). My confirmation that hA$\beta_{1\text{-}42}$ impaired LTP in slices from wild-type mice is in agreement with a wealth of previous reports (Cullen et al., 1997; Lambert et al., 1998; Walsh et al., 2002; Wang et al., 2004; Townsend et al., 2006) showing that soluble Aβ oligomers have an inhibitory effect on LTP. It also suggests that, under my experimental conditions, Aβ assembled into the oligomeric complexes thought to be the synaptotoxic form of the peptide; this has since been confirmed in two labs independently using atomic force microscopy (please see General Discussion). This then provided me with a model to test in the *Tau*$^{-/-}$ mouse to investigate the hypothesis that tau may be required for Aβ to exert its toxic effects.

3.5.1 A role for tau in Aβ-induced toxicity

In contrast to the effect in wild-type mice, the magnitude of LTP was not reduced in slices from *Tau*$^{-/-}$ mice exposed to hA$\beta_{1\text{-}42}$. This suggests that tau protein is required for the synaptotoxic effects of hA$\beta_{1\text{-}42}$, consistent with the finding that tau-depleted neurons do not degenerate in the presence of Aβ (Rapoport et al., 2002), and also that tau reduction can alleviate the memory im-

pairments in mice overexpressing Aβ (Roberson et al., 2007, 2011). Nussbaum et al. (2012) have also suggested a role for tau in mediating the cytoxicity of a pyroglutamylated form of Aβ that displays prion like behaviour. The similar synaptic input-output relationships and unchanged paired-pulse ratios following either LTP induction or incubation in $hA\beta_{1\text{-}42}$ in wild-type and *Tau*$^{-/-}$ mice suggest that this result is not caused by different basal presynaptic properties in *Tau*$^{-/-}$ mice, nor a distinct presynaptic change between the two genotypes following acute Aβ exposure. Instead, the results are most consistent with the conclusion that the absence of tau uncouples Aβ from its downstream effects that impair the postsynaptic mechanisms required for LTP. In support of this postsynaptic interpretation, a dendritic role for tau in mediating Aβ toxicity has been reported (Ittner et al., 2010). Nevertheless, this does not exclude a contribution of presynaptic mechanisms, for example Aβ-induced deficits in axonal transport are prevented in cultured *Tau*$^{-/-}$ neurons (Vossel et al., 2010) or in neurons where GSK-3 is inhibited (Decker et al., 2010b). It is also possible that the reduced mitochondrial function found in some AD models (Yao et al., 2011; Ma et al., 2011a, 2012) could impair the efficacy of presynaptic release and glutamate recycling at the presynaptic terminal, which would also potentially impair LTP. Moreover, Aβ does not only effect excitatory neuronal activity, but can also target interneurons. However, the data here does not provide any evidence that a reduction in $GABA_A$-mediated currents, as has been found in membranes from AD brains (Limon et al., 2012), nor an impairment the hippocampal inhibitory network, as is found in animal models of AD with longer exposure to Aβ (Verret et al., 2012; Palop et al., 2007; Palop and Mucke, 2010) could explain either the LTP impairment in wild-type mice or the discrepancy between genotypes. Therefore, overall, it appears that tau may be required in its wild-type form for Aβ-induced synaptotoxicity, which is further supported by the demonstration that there is no $hA\beta_{1\text{-}42}$-induced LTP impairment in mice carrying the N296H MAPT mutation.

3.5.2 A role for GSK-3 in Aβ-induced toxicity

It is a priority to establish the molecular pathways that underlie the Aβ-induced impairment of LTP to inform drug development aimed at slowing the progression of MCI and the early stages of AD. It is known that overactivation of GSK-3 causes tau hyperphosphorylation, neurodegeneration (Lucas et al., 2001) and spatial learning deficits (Hernandez et al., 2002), and the data presented here are consistent with the hypothesis that exposure to Aβ may set this pathological process in motion. In support of this interpretation, I demonstrate that Aβ increases the ratio of phosphorylated to total tau, but that this augmented tau phosphorylation is blocked by inhibiting GSK-3. Furthermore, the specific GSK-3 inhibitor AR-A014418 prevented the impairment of LTP by $hA\beta_{1\text{-}42}$ in wild-type slices, which suggests that GSK-3, via its subsequent phosphorylation of tau (Ishiguro et al., 1993), is a key component in the pathway by which Aβ exerts its pathogenic downstream effects on LTP. Moreover, additional characterisation of the H1 and N51 lines has revealed that there is a lower level of phosphorylated to total tau (AT8/Tau5 ratio) in the N51 line compared to the H1 line under baseline conditions, and that, while the AT8/Tau5 ratio increases following $hA\beta_{1\text{-}42}$ exposure in the H1 line, no such increase in tau phosphorylation occurs in the N51 line (pers. comm. Dr. Mariana Vargas-Caballero). All this is consistent with a requirement for tau in its hyperphosphorylated form to mediate the $hA\beta_{1\text{-}42}$-induced LTP impairment.

Nevertheless, GSK-3 appears to play an important role in synaptic plasticity itself under control conditions (Bradley et al., 2012), which could be a potential confounding factor for the interpretation of these experiments. Peineau et al. (2007) concluded that GSK-3 is required to prevent recently potentiated synapses from undergoing future long-term depression (LTD), since GSK-3 activity is reduced following LTP induction and inhibiting GSK-3 prevents the induction of LTD. A reduction in GSK-3 activity following potentiation induced *in vivo* was also reported by Hooper et al. (2007). However, these changes oc-

cur following the induction of LTP; although I cannot yet conclude whether the hA$\beta_{1\text{-}42}$ effect arose from an impairment in the induction or expression of LTP (please see the next chapter for evidence supporting an impairment in induction), there was no effect of GSK-3 inhibition on the magnitude of LTP induced with the AR- A014418 concentration used here. This suggests that a mechanism involving GSK-3 modulation of synaptic plasticity is unlikely to account for the recovery of LTP in the presence of hA$\beta_{1\text{-}42}$. Notably, the slices used in the Western measurement of phosphorylated tau were sampled following incubation and so the results are indicative of the phosphorylation status of tau (and thus GSK-3 activity) during baseline conditions, and hence the background on which LTP would be induced.

The phosphorylation sites detected by the AT8 antibody used do not completely overlap with those phosphorylated by GSK-3, meaning that other kinases previously implicated in the Aβ-induced impairment of LTP, including c-Jun N-terminal kinase, cdk5, p38 MAPK (Wang et al., 2004) and PKA (Vitolo et al., 2002) could also be involved in mediating the effect of Aβ via tau phosphorylation. In addition, Mairet-Coello et al. (2013) have recently implicated AMP-activated kinase as a mediator of the synaptoxic interaction between Aβ and tau in APP overexpressing mice, in a pathway that incudes CAMKK2. Nevertheless, the complete recovery of LTP magnitude in the presence of AR-A014418 is striking, suggesting that GSK-3 may be a primary kinase in the experimental conditions used here. The involvement of GSK-3 in the hA$\beta_{1\text{-}42}$-induced impairment of LTP has been confirmed independently using a different experimental set-up and GSK-3 inhibitor (Jo et al., 2011); the authors also further characterised the possible molecular pathway, revealing an involvement of caspase-3 and Akt1. In addition, $BAX^{-/-}$ mice do not exhibit an Aβ-induced LTP impairment (Olsen and Sheng, 2012), and BAX is upstream of caspase-3 in an apoptosis pathway linked to mitochondria (Youle and Strasser, 2008). This suggests a possible unified pathway that could mediate the Aβ-induced LTP impairment, and one that may also be relevant later in the disease process, since GSK-3 has also

been implicated in Aβ-induced and tau-mediated neurodegeneration (Tackenberg and Brandt, 2009). However, it remains uncertain whether the results described here are explained by engagement of this cell death pathway after acute exposure to Aβ or alternatively, given that GSK-3 is a hub in many different molecular pathways, whether the findings here are actually mediated by a distinct pathway involving tau. Nevertheless, there is accumulating evidence that GSK-3 may play a central role in mediating an interaction between Aβ and tau to cause synaptic changes that impair LTP.

3.5.3 GSK-3 as a possible therapeutic avenue

Inhibition and knock-down on GSK-3 can reduce amyloid plaques and NFTs in mouse models of AD (Hurtado et al., 2012) and, given the protective effects on LTP described here, GSK-3 may seem an ideal candidate for a treatment to slow AD progression. However, tau kinase inhibitors have not proved successful treatments for AD in human clinical trials. The only GSK-3 inhibitor currently under investigation, Tideglusib, was recently found not to improve end-points in phase II of a clinical trial (Zeltia, 2012). The ineffectiveness of GSK-3 inhibition for improving cognitive symptoms is likely due to a combination of reasons. Firstly, a wide range of possible membrane binding partners and cellular pathways have been linked to the effects of Aβ, indicating the interaction is likely to be more complex than described here. For example, an indirect route, where Aβ activates microglia that in turn activate a p38 MAPK cascade that increases tau phosphorylation (Bhaskar et al., 2010), could also work in parallel; other links between Aβ and tau may also exist, such as that involving heat shock protein70 (Oddo et al., 2008). Secondly, blocking a link between Aβ and tau is unlikely to be successful as a treatment late in the disease process, which is usually the stage when patients are recruited for clinical trials. The model used here involves acute exposure to Aβ in order to identify the mechanisms that mediate the early synaptic changes; with chronic exposure, many parallel and additional pathological processes occur, which include excitotoxicity, in-

flammation and cell death. Once such independent changes are set in motion, preventing an interaction between Aβ and tau may no longer be able to slow the disease progression. Thirdly, cognitive symptoms are also far-removed from cellular pathology. Finally, the molecular pathways involved in humans may not be identical to those in rodents.

3.5.4 Perspective

Tau protein is required to see a range of pathological changes triggered by exposure to Aβ, including synaptic impairments, neurodegeneration and behavioural deficits. This suggests that an important interaction between Aβ and tau might exist, with tau, likely in its hyperphosphorylated form, mediating the toxic changes downstream from Aβ. Nevertheless, a primarily dual pathway model leading to pathological changes (Small and Duff, 2008), in which both Aβ and tau target cellular processes independently or synergistically, remains a possibility, especially given the complex aetiology of late-onset AD. Indeed, Tackenberg and Brandt (2009) conclude that Aβ promotes spine pathology, while tau mediates neurodegeneration, and the common effector is actually NMDA receptor activity. Even if Aβ and tau can act separately, it does not exclude a linear pathway being the primary mechanism by which the pathological changes associated with early AD arise. Therefore, dissociating these pathways, and identifying their relative contribution to disease progression, is an important goal for future research.

In addition, it is also vital to establish what role tau itself is playing in synaptotoxicity following exposure to Aβ. As discussed, my results show that changes in tau phosphorylation correlate with the effects of Aβ on LTP, but they do not provide conclusive evidence that tau phosphorylation is necessary for Aβ to exert its synaptotoxic effects. I currently cannot exclude the possibility that Aβ causes an LTP impairment through changing GSK-3 activity, which subsequently both alters its role in LTP and the phosphorylation state of tau simul-

taneously. Therefore, to investigate the importance of tau phosphorylation as a driving mechanism for synaptotoxicity in future experiments, I would induce LTP when tau is either constitutively phosphorylated or cannot be phosphorylated. If tau phosphorylation is required to mediate the effect of hA$\beta_{1\text{-}42}$, a constitutively phosphorylated form of tau should occlude the impairment of LTP after exposure to Aβ. In contrast, a non-phosphorylatable form would block the Aβ-induced impairment of LTP and show similar results to *Tau*$^{-/-}$ mice, or those containing the N296H mutation. To this end, I would use stereotaxic surgery to inject adeno-associated virus containing the mutated forms of tau into *Tau*$^{-/-}$ mice.

A different way to understand whether tau may itself be playing an important role in Aβ-induced LTP impairments, would be to investigate the underlying synaptic changes in wild-type mice that are not present in *Tau*$^{-/-}$ mice. This is the approach I will pursue in the next chapter.

CHAPTER 4

Synaptic mechanisms underlying the Aβ-induced effects on LTP

4.1 Introduction

It is widely held that memory formation is associated with changes in synaptic strength. Hippocampal LTP has provided a useful model to study the memory impairments associated with Alzheimer's disease (AD), since Aβ-induced impairments in potentiation at the CA3-CA1 synapse *in vitro* and *in vivo* (Cullen et al., 1997; Lambert et al., 1998; Stéphan et al., 2001; Walsh et al., 2002; Shankar et al., 2008) correlate with spatial learning deficits in transgenic mouse models of AD (Chapman et al., 1999), and therefore it provides a more amenable experimental system in which synaptic changes and molecular pathways can be probed in greater detail. However, despite this very reproducible LTP deficit, the mechanism(s) underlying this effect of Aβ remains unclear.

The earliest Aβ-induced synaptic changes that could impair LTP are likely to involve changes in presynaptic release and/or postsynaptic receptors, since both can have immediate effects on the ability to induce or express LTP. The synapse is a dynamic system, with constant movement of receptors between the postsynaptic density (PSD) and extrasynaptic sites (Alcor et al., 2009), combined with an equilibrium between receptor insertion and internalisation. Thus there are many regulatory pathways which together finely tune the synapse to provide meaningful information processing and storage, and such regulatory mechanisms might be vulnerable to the application of Aβ. Although the importance of NMDA receptor (NMDAR) subunit composition in the induction of synaptic potentiation and depression remains contentious, the importance of the NMDAR itself in triggering many forms of these two directions of plasticity is unrefuted. Thus, the induction of plasticity will be affected by any changes that alter how efficiently NMDAR-mediated Ca^{2+} influx couples to its different downstream effectors. In addition, AMPA receptors (AMPARs) are required for the expression of either synaptic strengthening or weakening; dysregulation of AMPAR receptor content at, or supply to, the PSD would also alter synaptic strength or the expression of plasticity respectively. Therefore, if Aβ triggers

pathways that disrupt the delicate synaptic balance, it explains how impairments in LTP, and possibly also cognitive function, could arise even before the synapse loss and neurodegeneration that are apparent later in the disease process.

There is evidence that Aβ does indeed interfere with the synaptic receptor content from both antibody labelling of cell surface receptors and voltage-clamp measurement of evoked-excitatory postsynaptic excitatory currents (EPSCs) mediated by AMPARs and NMDARs. Nevertheless, such studies have revealed contrasting effects, from selective up- or downregulation of one receptor type to a combination of changes in both. Various studies have found a selective reduction in AMPARs at the cell membrane (Shemer et al., 2006; Ting et al., 2007; Gu et al., 2009; D'Amelio et al., 2011). D'Amelio et al. (2011) further demonstrated that it was the GluR1 subunit that was internalised under the experimental conditions, which accounted for the Aβ-induced deficits in LTP and behaviour, while NMDAR-mediated currents and subunits in the PSD remained relatively constant. The reduction in AMPAR-mediated currents in the presence of Aβ may also be due to a decrease in the open channel probability of AMPARs (Parameshwaran et al., 2007).

Equally, however, there are reports that Aβ has selective effects on NMDARs, though the direction of such effects appears conflicting. Reduced cell surface expression of NR1 (Goto et al., 2006) and GluN2B subunits has been found in the APP[V717] (Dewachter et al., 2009), 3xTg-AD (Zhang et al., 2010) and Tg2576 (Kurup et al., 2010) mouse models of AD. In support of such expression studies, Chen et al. (2002) and Snyder et al. (2005) showed that acute application of Aβ reduces NMDAR-mediated currents presumed to be synaptic. It has also been suggested that plasticity deficits could arise from overactivation of NMDARs, specifically GluN2B subunit-containing receptors, at extrasynaptic sites causing excitotoxicity (Rammes et al., 2011; Rönicke et al., 2011) during the pathological changes leading to AD. Indeed, Li et al. (2011) found that Aβ ap-

plication enhanced GluN2B-mediated NMDA currents, which they concluded were extrasynaptic in origin and responsible for excitotoxicity.

Other studies have reported changes in both types of glutamate receptors following exposure to Aβ. Hsieh et al. (2006) found fewer AMPARs in the PSD and a reduction in AMPAR-mediated evoked currents. They also found a suppression of NMDAR currents following Aβ exposure, but that this was dependent on the endocytosis of GluR2-containing AMPARs. The reduction in NMDARs observed could either be a by-product of spine shrinkage or an active mechanism targeting NMDARs. In support of the latter possibility, Cerpa et al. (2010) found that both AMPAR- and NMDAR-mediated currents decreased following Aβ application, but that the reduction in the NMDAR-mediated current was larger, suggesting an additional active process regulating these receptors. One explanation could be the finding of Renner et al. (2010) that an Aβ-dependent reduction in surface expression of NMDARs is linked to mGluR5.

The differences between the synaptic changes reported in these studies may result from the preparation technique and Aβ concentration used. In particular, discrepancies may also be caused by the length of time that cells were exposed to Aβ, since early pathological changes at the synapse may trigger either compensatory changes or positive feedback loops. It remains possible that more than one pathological process, with different synaptic outcomes, could occur simultaneously. However, another possible explanation is that different synapses or neurones may be differentially vulnerable to the effects of Aβ, and affected by different pathways. It is clear that neurons in different brain regions will experience different basal levels of activity, and synapses with high or low activity may be more susceptible to distinct changes, for example overactivation of receptors compared to receptor loss. Many of these studies have been conducted in different brain regions, which may explain some of the variability in the findings. Nevertheless, even within the same brain region, synapses are not equivalent. Thus, another possible reason for the discrepancies between re-

sults is that studies using electrical stimulation to measure EPSCs will recruit a diverse population of synapses, which have different presynaptic release probabilities, morphologies and numbers and composition of glutamate receptors at the PSD. These types of synapse may be differentially vulnerable to the pathological processes triggered by acute exposure to Aβ, and such variability could make it hard to detect important, and possibly distinct, changes occurring at individual synapses.

4.1.1 Aim

Changes in postsynaptic receptor content are very likely to contribute to an Aβ-induced LTP deficit, but there are conflicting reports in the type of glutamate receptors affected, and even the direction of change. Consequently, I wanted to make a direct comparison between an incubation protocol known to impair LTP and the possible glutamate receptor changes it may trigger, in order to try and understand the mechanism underlying the plasticity deficit I had observed. Moreover, I aimed to investigate why there was no such impairment in *Tau*$^{-/-}$ mice, since understanding how a lack of tau can uncouple Aβ exposure to downstream synaptoxicity may be important to inform therapies aimed at slowing disease progression. Given that there may be a subunit selective contribution to opposing directions of plasticity, I also aimed to investigate whether I could detect any NMDAR subunit selectivity in the effect of Aβ.

4.2 The effect of Aβ on N/A ratios in wild-type and *Tau*$^{-/-}$ mice

NMDARs play a crucial role in LTP induction, and AMPARs are vital for the expression of LTP. Therefore, in order to investigate a possible mechanism underlying the LTP deficit following 1-3 hour incubation in 220 nM Aβ, I tested whether there were changes in the ratio of currents mediated by these two types of ionotropic glutamate receptors in postsynaptic CA1 pyramidal neurons.

It is possible to isolate NMDAR- and AMPAR-mediated currents pharmacologically, using CNQX or NBQX to block AMPARs and AP5 to block NMDARs. However, in order to reduce variability, it is important to measure the current mediated by these two types of glutamate receptor in the same cell, and wash-on and long wash-off periods are required to do so pharmacologically. Since I do not know the timescale of the Aβ effect, it is possible that changes may occur during the time taken to carry out the recordings, especially if more than one treatment condition is required, and hence the conditions under which each receptor-mediated current were measured would not be equivalent. Therefore, instead, I estimated the AMPAR- and NMDAR-mediated contribution to the total excitatory postsynaptic potential by varying the holding potential of the patched postsynaptic neurons using voltage-clamp, since this permits alternating measurement of the AMPAR- and NMDAR-mediated currents to account for changes in experimental conditions over time. Moreover, it allows one current estimate to be used as a normalisation factor in order to control for differences in stimulation strength. It is well established that the current mediated by each of these glutamate receptors can be estimated from measurements taken at different holding potential due to the distinct current-voltage (I-V) relationships of these two receptors. The predominant form of AMPARs, GluA2-containing AMPARs, display a linear I-V relationship and so carry high levels of current at negative and positive holding potentials, and the direction of the current reverses from an inward to outward current at approximately 0 mV; GluA2-lacking AMPARs do not pass current at positive potentials (Verdoorn et

al., 1991). In contrast, the overall I-V curve of the NMDAR is non-linear and the current through NMDARs is very limited at potentials more negative than -60 mV due to block of the channel by Mg^{2+}. Therefore, an AMPAR-mediated current dominates when the cell is held at -70 mV and so this current can be estimated by measuring the peak EPSC amplitude at this negative holding potential. Nevertheless, the I-V curve for the NMDAR is near linear above -30 mV; therefore, when recording at positive holding potentials the EPSC contains both AMPAR- and NMDAR-mediated current. However, the contribution of these two receptors can still be distinguished due to the distinct kinetics of the current flow through these two types of receptors. The AMPAR-mediated current is fast, while the NMDAR-mediated current peaks later and decays much more slowly. Therefore, an estimate of NMDAR-mediated current can be made at a time point after stimulation when the remaining AMPAR-mediated current is negligible; here, this time point was taken at 55-57 ms post-stimulation.

Therefore, I patched visually identified CA1 pyramidal neurons using a caesium methylsulphonate-based intrapipette solution and recorded the current following extracellular stimulation of the Schaffer-collateral/commissural inputs, alternating between +65 mV and -70 mV to enable me to estimate an NMDAR- to AMPAR-mediated current ratio (N/A ratio). In addition, I also recorded at 0 mV to confirm that the 3 μM gabazine included in the aCSF superfusing the slices was sufficient to block inhibitory $GABA_A$ receptors, since these could otherwise contaminate the current measurements mediated by the glutamatergic receptors.

Given the importance of the NMDAR for LTP induction, I first wanted to investigate whether there might be any difference in the N/A ratio between wild-type and *Tau*$^{-/-}$ mice that could explain the selective LTP deficit in wild-type mice following exposure to $hA\beta_{1\text{-}42}$. Therefore, I incubated slices from wild-type and *Tau*$^{-/-}$ mice of the same age range that had been used in the LTP experiments in either control aCSF or 220 nM $hA\beta_{1\text{-}42}$, again with the same incubation

concentrations and duration as for the LTP experiments, and measured the N/A ratio. I found that the N/A ratio was lower in cells that had been incubated in hA$\beta_{1\text{-}42}$ in wild-type mice (control: 0.61 ± 0.03, n = 46 cells; hA$\beta_{1\text{-}42}$: 0.49 ± 0.02, n = 51; **Fig. 4.1**). In contrast, in *Tau*$^{-/-}$ mice, which show no hA$\beta_{1\text{-}42}$-induced LTP impairment, the N/A ratio did not change in the presence of hA$\beta_{1\text{-}42}$ (control: 0.59 ± 0.03, n = 49 cells; hA$\beta_{1\text{-}42}$: 0.59 ± 0.03, n = 42; **Fig. 4.1**). ANOVA revealed a main effect of treatment ($F_{1,184}$ = 4.47, P = 0.036) and a treatment by genotype interaction ($F_{1,184}$ = 4.45, P = 0.036) due to an effect of hA$\beta_{1\text{-}42}$ in wild-type mice ($F_{1,184}$ = 9.23, P = 0.003). Overall, therefore, the N/A ratio measurement showed a strikingly similar pattern of results to the magnitude of LTP, and this suggested that a difference in the effect of hA$\beta_{1\text{-}42}$ on N/A ratio might explain the LTP results. Nevertheless, this measurement is a ratio and, therefore, could result from a relative reduction in the NMDAR content, an increase in AMPAR, or changes in both receptor types in the postsynaptic spine. Although a reduction in NMDAR-mediated current would be a favoured explanation for an LTP impairment, given that NMDARs are required for the induction of LTP, further exploration of this hypothesis was required.

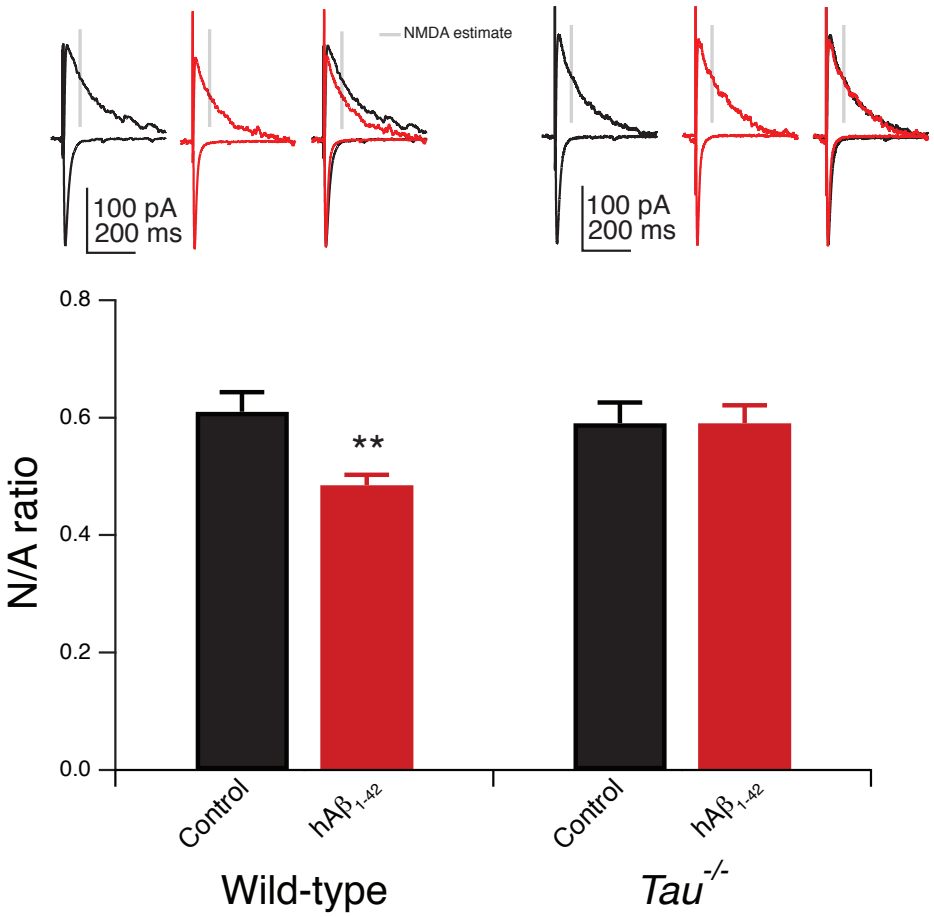

Figure 4.1: Human Aβ_{1-42} reduces the N/A ratio in wild-type but not *Tau*$^{-/-}$ mice. Activation of hippocampal Schaffer collateral/commissural projections to CA1 pyramidal neurons allows an N/A ratio to be measured at the CA3-CA1 synapse under control conditions (black) and following incubation with hA$\beta_{1\text{-}42}$ (red). Insets show representative traces of AMPAR- and NMDAR-mediated currents in wild-type (left) and *Tau*$^{-/-}$ mice (right), before (black) and after (red) incubation with hA$\beta_{1\text{-}42}$. Representative traces from different cells are shown both individually and superimposed to facilitate comparison. Error bars are s.e.m. ** $P < 0.01$.

4.3 An NMDA receptor subunit-selective effect of Aβ

The proposal that one NMDAR subunit composition mediates synaptic strengthening, whilst another mediates synaptic weakening, has not stood up to further experimental investigation. Nevertheless, evidence has accumulated that GluN2B subunit-containing NMDARs may make an important, and unique, contribution to the induction of LTP. Since the hA$\beta_{1\text{-}42}$-induced reduction in N/A ratio in wild-type mice could reflect a reduction in the NMDAR-mediated current, I wanted to explore whether there could be subunit selectivity in this effect.

4.3.1 The effect of Aβ on the NMDAR-mediated currents in wild-type and *Tau*$^{-/-}$ mice

It is known that the decay time constants of NMDARs with different subunit compositions vary. Specifically, GluN1/GluN2A receptors have a faster decay time constant than that of GluN1/GluN2B receptors (Vicini et al., 1998). Therefore, a change in NMDAR-mediated current decay kinetics might provide an indication as to whether or not hA$\beta_{1\text{-}42}$ could differentially affect NMDARs with different subunit compositions. NMDAR-mediated currents are best fitted by a double exponential with a fast and slow tau (Vicini et al., 1998). Therefore, using values from Vicini et al. (1998) to provide an estimate of the weighted decay time constant for that mediated by GluN1/GluN2A (40 ms) and GluN1/GluN2B (275 ms), I tested whether the contribution made by each of these time constants to the overall fit varied between control and hA$\beta_{1\text{-}42}$ incubation in each genotype. I found a decrease in the contribution of the component with the slow time constant to the double exponential fit in wild-type mice following incubation in hA$\beta_{1\text{-}42}$ (control: 42 ± 2%, n = 49 cells; hA$\beta_{1\text{-}42}$: 37 ± 1%, n = 53; **Fig. 4.2**), which suggests there was a reduction in the contribution from GluN1/GluN2B NMDARs to the NMDAR-mediated current following exposure to Aβ. There was, however, no change in the percentage contribution of the component with

the slow time constant in *Tau*$^{-/-}$ mice (control: 41 ± 2%, n = 47 cells; hA$\beta_{1\text{-}42}$: 42 ± 2%, n = 41; **Fig. 4.2**). ANOVA showed a treatment by genotype interaction ($F_{1,186}$ = 3.99, P = 0.047) due to an effect of hA$\beta_{1\text{-}42}$ in wild-type mice ($F_{1,186}$ = 5.62, P = 0.019). This implies that, not only does the N/A ratio not change in *Tau*$^{-/-}$ mice following hA$\beta_{1\text{-}42}$ treatment, but also, there is no underlying shift in the NMDAR subunit composition either.

The change in percentage contribution of the component with a slow time constant was a small effect, but this may be because the time constant values in Vicini et al. (1998) were determined from data recorded in transfected HEK cells using L-glutamate pulses to activate the channels. However, I have measured synaptic currents using electrical stimulation in slices whilst recording at the soma. Therefore, I am not measuring the pure decay of currents at the synapse and instead such values will be filtered. The extent of filtering will vary according to the series resistance and how far the synaptic currents are from the recording site. Moreover, the different time constants of GluN2A and GluN2B will be filtered differently, increasing the variability. In addition, a substantial proportion of GluN2B subunits are present as triheteromers in the adult hippocampus, and the decay time constant of these receptors is thought to be intermediate between that mediated by a pure GluN2A or GluN2B diheteromer with GluN1. However, only two fixed values have been used here to fit the curve. Consequently, due to these various limitations, I decided to explore this possible subunit selective change using a pharmacological approach.

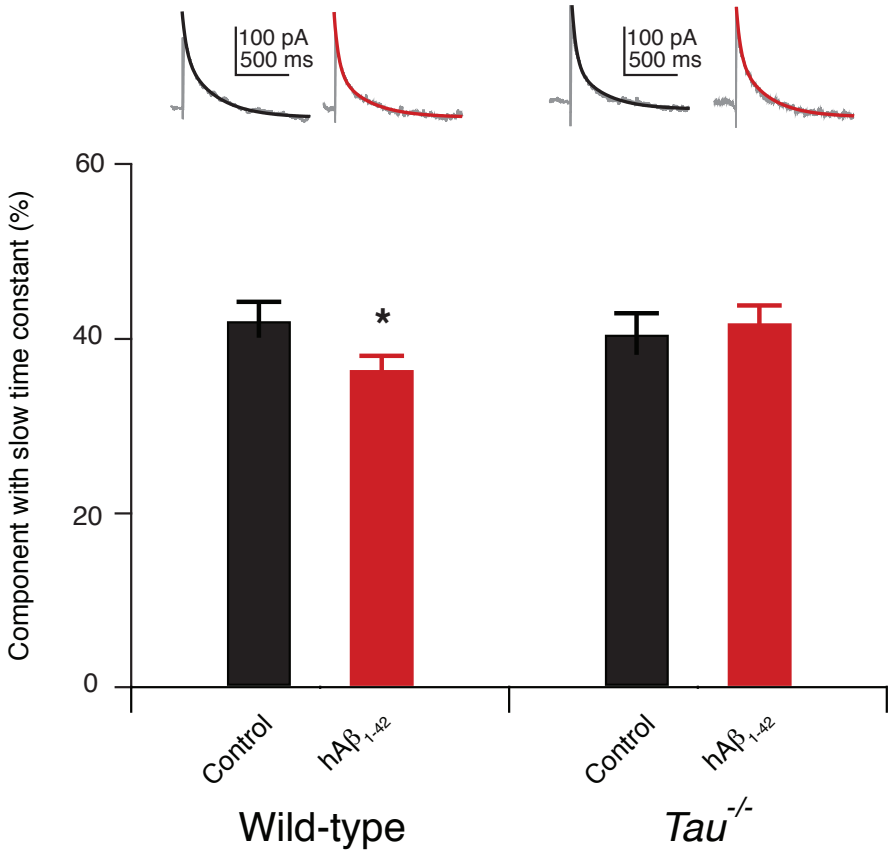

Figure 4.2: Human Aβ_{1-42} increases the contribution of the fast time constant to NMDAR-mediated current in wild-type but not *Tau*$^{-/-}$ mice. Activation of hippocampal Schaffer collateral/commissural projections to CA1 pyramidal neurons allows NMDAR-mediated current to be measured at the CA3-CA1 synapse at a positive holding potential. The contribution of a fast and slow tau to the overall decay time constant can be estimated under control conditions (black) and following incubation with hA$\beta_{1\text{-}42}$ (red). Insets show representative traces of NMDAR-mediated currents (grey) in wild-type (left) and *Tau*$^{-/-}$ mice (right), superimposed with the curve fitted by the double exponential function with fixed fast and slow time constant values before (black) and after (red) incubation with hA$\beta_{1\text{-}42}$. Error bars are s.e.m. * $P < 0.05$.

4.3.2 The effect of Aβ on the GluN1/GluN2B-mediated current in wild-type mice

In order to further investigate a possible subunit selectivity in the hA$\beta_{1\text{-}42}$ effect in wild-type mice, I used pharmacological antagonism to dissociate between NMDAR subunit compositions. There are currently no suitable selective antagonists for GluN2A subunit-containing NMDARs, since NVP-AAM077 only shows a tenfold preference for GluN2A over GluN2B in the rodent (Paoletti and Neyton, 2007); consequently, in order to block all GluN2A subunit-containing NMDARs, there will invariably be some block of GluN2B, which would make it hard to draw conclusions about hA$\beta_{1\text{-}42}$ targeting one subunit.The alternative, Zn^{2+}, is more selective but can interfere with cellular pathways (Smart et al., 2004). In contrast, Ro 25-6981 is a highly selective GluN2B antagonist (Fischer et al., 1997), with a 3000 fold preference for GluN2B (Paoletti and Neyton, 2007). Therefore, in a new set of experiments, I measured the N/A ratio in cells that had undergone a basic treatment of either control aCSF or incubation with 220 nM hA$\beta_{1\text{-}42}$, as before. In addition, a subset of cells in each of these two categories was then exposed to 0.5 μM Ro 25-6981 for at least 30 minutes to block GluN2B subunit-containing NMDARs. A subset of these were performed as wash-on experiments so the N/A ratio could be measured in the same cell before and after 30 minutes of treatment with Ro 25-6981.

In order to test whether such wash-on experiments were feasible in 4-6 month old mice, and that the 30 minute wash on period did not cause changes in the N/A ratio in itself, some test recordings were performed. For these, I patched a CA1 neuron that had been incubated in either control aCSF or hA$\beta_{1\text{-}42}$ and recorded a baseline N/A ratio, and then stopped the recording and held the cell for 30 minutes to mimic the period of acute treatment with Ro 25-7981. I found no significant changes in the N/A ratio following this 30 minute wait for either condition (control baseline: 0.58 ± 0.04, control + 30 min wait: 0.59 ± 0.03, n = 7 cells; hA$\beta_{1\text{-}42}$ baseline: 0.55 ± 0.04, hA$\beta_{1\text{-}42}$ + 30 min wait: 0.59 ± 0.05, n = 4; **Fig. 4.3**). Nevertheless, the N/A ratios within a cell did change and there was an

overall tendency to increase, which may be because of slight increases in series resistance, which have a greater effect on fast currents and therefore will reduce the peak EPSC value which provides the AMPAR-mediated current estimate. A logistical limitation to performing the wash on experiments was that only 100 ml of 220 nM $hA\beta_{1\text{-}42}$ was available each day, so the number of wash-on experiments per day were restricted since 110 nM was required for superfusion in the recording chamber. Therefore, in order to obtain sufficient data per mouse and to ensure that small changes in N/A ratio with time could not explain any results, I also recorded cells in each of the four treatment conditions independently (control + control, control + Ro 25-6981, $hA\beta_{1\text{-}42}$ + control, $hA\beta_{1\text{-}42}$ + Ro 25-6981). For these, slices were treated with Ro 25-6981 for at least 30 minutes in the recording chamber prior to patching.

As expected, a smaller N/A ratio was observed in cells that had been treated with Ro 25-6981, which is attributable to the antagonism of GluN2B subunit-containing NMDARs (control: 0.67 ± 0.03, n = 46 cells; control + Ro 25-6981: 0.48 ± 0.02, n = 24; **Fig. 4.4**(**A**)). In agreement with my earlier results, the N/A ratio in $hA\beta_{1\text{-}42}$-treated cells was also smaller than that recorded in control conditions (control: 0.68 ± 0.03, n = 44 cells; $hA\beta_{1\text{-}42}$: 0.55 ± 0.03, n = 18; **Fig. 4.4**(**A**)). However, strikingly, cells that had been pre-incubated in $hA\beta_{1\text{-}42}$ showed no further reduction in N/A ratio when treated with Ro 25-6981 ($hA\beta_{1\text{-}42}$: 0.55 ± 0.03, n = 18 cells; $hA\beta_{1\text{-}42}$ + Ro 25-6981: 0.55 ± 0.01, n = 12; **Fig. 4.4**(**A**)). ANOVA revealed a main effect of acute treatment ($F_{1,94}$ = 9.20, P = 0.003) and also an interaction between the basic and acute treatment ($F_{1,94}$ = 8.84, P = 0.004) due to an effect of Ro 25-6981 in control slices ($F_{1,94}$ = 28.49, P < 0.001) and the lack of an effect of Ro 25-6981 on the N/A ratio in cells pre-treated with $hA\beta_{1\text{-}42}$ ($F_{1,94}$ = 0.001, P = 0.97). This new dataset also verified the earlier result that $hA\beta_{1\text{-}42}$ causes a reduction in N/A ratio compared to that in control cells (effect of Aβ in control cells $F_{1,94}$ = 9.80, P = 0.002). There was a trend that the N/A ratio recorded in wild-type cells treated with Ro 25-6981 was lower if cells had been pre-incubated in control aCSF than if they had been pre-incubated in $hA\beta_{1\text{-}42}$,

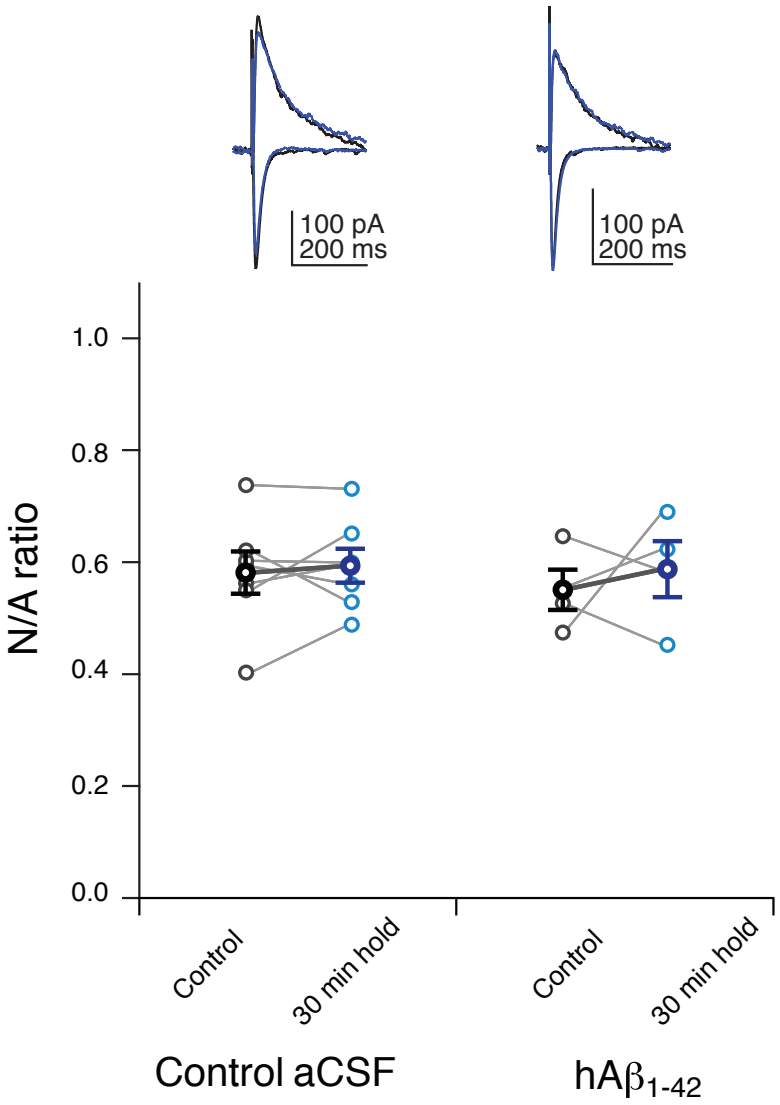

Figure 4.3: CA1 cells can be recorded before and after a 30 minute hold without a change in N/A ratio. Activation of hippocampal Schaffer collateral/commissural projections to CA1 pyramidal neurons allows an N/A ratio to be measured at the CA3-CA1 synapse under control conditions or following incubation with $hA\beta_{1\text{-}42}$ before (black circles represent one cell) and after (blue circles represent one cel) a 30 minute hold of the cell to mimic a Ro 25-6981 wash on period. Pale grey lines show the change for each cell and dark grey lines show the overall average change. Insets show representative traces of AMPAR- and NMDAR-mediated currents in slices pre-treated with control aCSF (left) or $hA\beta_{1\text{-}42}$ (right), before (black) and after (blue) a 30 minute hold; superimposed traces show the same cell before and after hold. Error bars are s.e.m.

but this was not significant (effect of Aβ in Ro 25-6981 treated cells $F_{1,94} = 1.73$, $P = 0.19$). Although the smaller dataset recorded from the same cells before and after wash-on of Ro 25-6981 did not withstand repeated measures ANOVA, it clearly showed a similar pattern of results, with no reduction in N/A ratio following Ro 25-6981 treatment when cells were pre-incubated with $hA\beta_{1\text{-}42}$ (control baseline: 0.65 ± 0.02, control + Ro 25-6981: 0.52 ± 0.02, $n = 10$ cells; $hA\beta_{1\text{-}42}$ baseline: 0.57 ± 0.03, $hA\beta_{1\text{-}42}$ + Ro 25-6981: 0.55 ± 0.01, $n = 9$; **Fig. 4.4(B)**).

The different N/A ratios found in wild-type mice under control conditions and following $hA\beta_{1\text{-}42}$ exposure may reflect a change in either the NMDAR- or AMPAR-mediated current, or a change in the contribution of both these glutamate receptors. However, the finding that the $hA\beta_{1\text{-}42}$-induced reduction in N/A ratio precluded any further reduction by Ro 25-6981 indicates that there is an NMDAR-mediated contribution to this overall N/A ratio reduction. Moreover, they strongly suggest that this reduction can be accounted for primarily by an $hA\beta_{1\text{-}42}$-induced reduction in the current mediated by GluN2B subunit-containing NMDARs following exposure to Aβ.

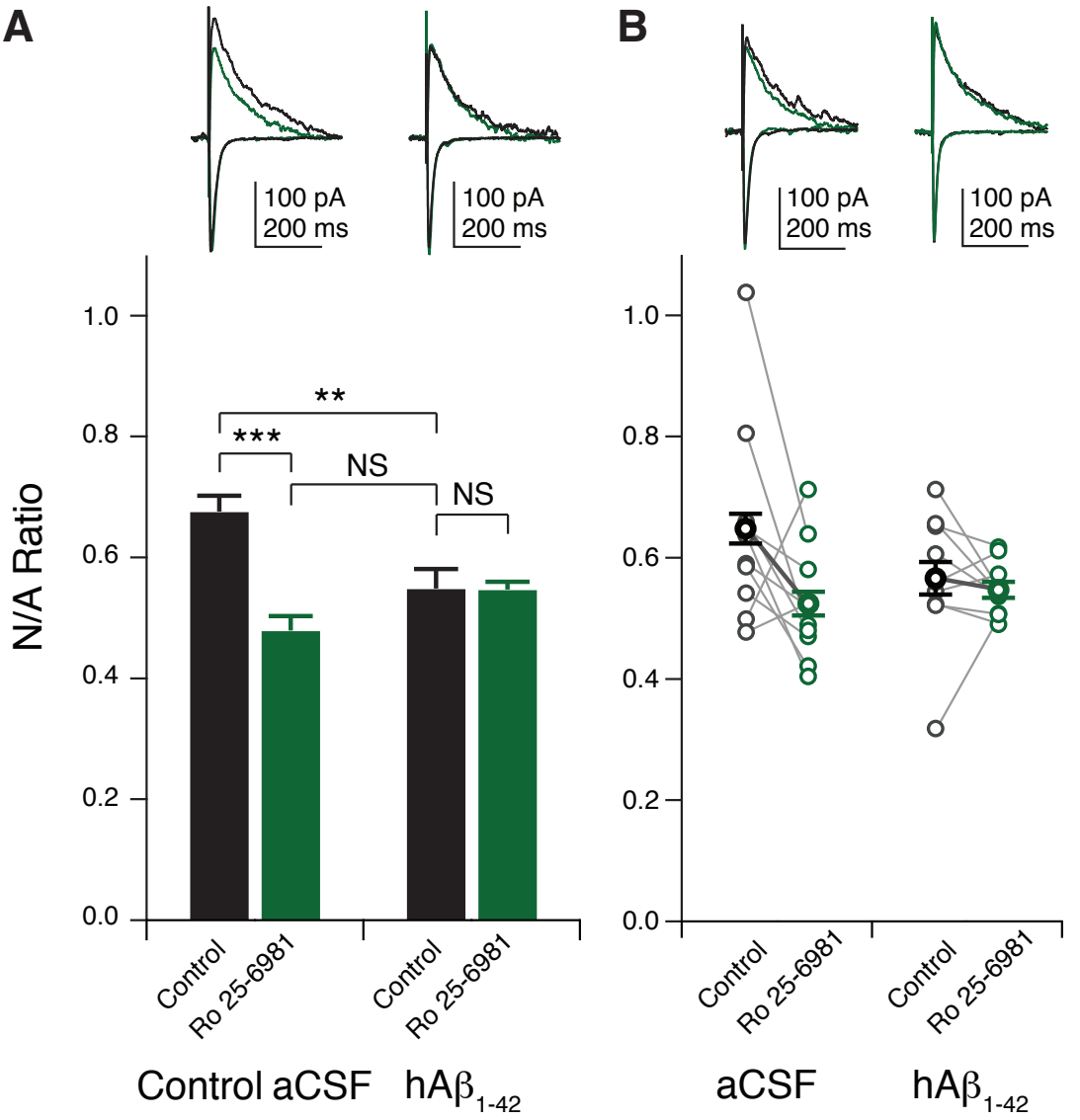

Figure 4.4: Pretreatment with human Aβ_{1-42} prevents a further reduction in the N/A ratio in wild-type mice by Ro 25-6981. (**A**) Slices that had received a basic pre-treatment in control aCSF or 220 nM hA$\beta_{1\text{-}42}$ for 1-3 hours were used to measure the an N/A ratio at CA3-CA1 synapses under acute control conditions (black) or following acute incubation with Ro 25-6981 (green). (**B**) The N/A ratio was recorded under the basic condition of control aCSF or hA$\beta_{1\text{-}42}$ (black circles represent one cell under the basic condition), and then Ro 25-6981 was washed into the superfusing aCSF and the cell was held for 30 minutes to allow for effective block by Ro 25-6981. The N/A ratio was then recorded in this same cell under this new condition (green circles represent one cell in the presence of Ro 25-6981). Pale grey lines show the change in N/A ratio per cell, and dark grey lines show the average change in N/A ratio. Insets show example traces of AMPAR- and NMDAR-mediated currents in slices pre-treated with control aCSF (left) or hA$\beta_{1\text{-}42}$ (right), before (black) and after (green) incubation with Ro 25-6981. Representative traces in (**A**) are from different cells but are shown superimposed to facilitate comparison; superimposed representative traces in (**B**) are from the same cell. Error bars are s.e.m. ** P < 0.01, *** P < 0.001.

4.3.3 Functional GluN2B subunit-containing NMDARs in *Tau*$^{-/-}$ mice

The finding that the hA$\beta_{1\text{-}42}$-induced change in N/A ratio in wild-type mice might be largely accounted for by a reduction in current through GluN2B subunit-containing NMDARs raises the possibility that the explanation for the lack of hA$\beta_{1\text{-}42}$-induced change in N/A ratio in *Tau*$^{-/-}$ mice is because there are no, or a very limited number of, functional GluN2B subunit-containing NMDARs at the synapse to mediate current flow in the age of mouse that I have been using. Therefore, to confirm whether or not these *Tau*$^{-/-}$ mice had GluN2B-subunit containing NMDARs that could have mediated LTP induction, I next tested whether the N/A ratio in *Tau*$^{-/-}$ mice was affected by treatment with Ro 25-6981 for 30 minutes. The experimental conditions used were equivalent to the control and control + Ro 25-6981 conditions that had been used in wild-type mice. I found a reduction in the N/A ratio following treatment with Ro 25-6981 in *Tau*$^{-/-}$ mice that was of a similar magnitude to that which had been recorded in wild-type mice (*Tau*$^{-/-}$ control: 0.66 ± 0.04, n = 16 cells; *Tau*$^{-/-}$ Ro 25-6981: 0.52 ± 0.03, n = 18 cells; t-test P = 0.006; **Fig. 4.5**(**A**)). This reduction was also observed in a small number of paired wash on experiments (control baseline: 0.73 ± 0.06, control + Ro 25-6981: 0.57 ± 0.02, n = 4 cells; **Fig. 4.5**(**B**)). Thus, these data indicate that there were functional GluN2B subunit-containing NMDARs present in *Tau*$^{-/-}$ mice that were the same age as had been used in the LTP experiments.

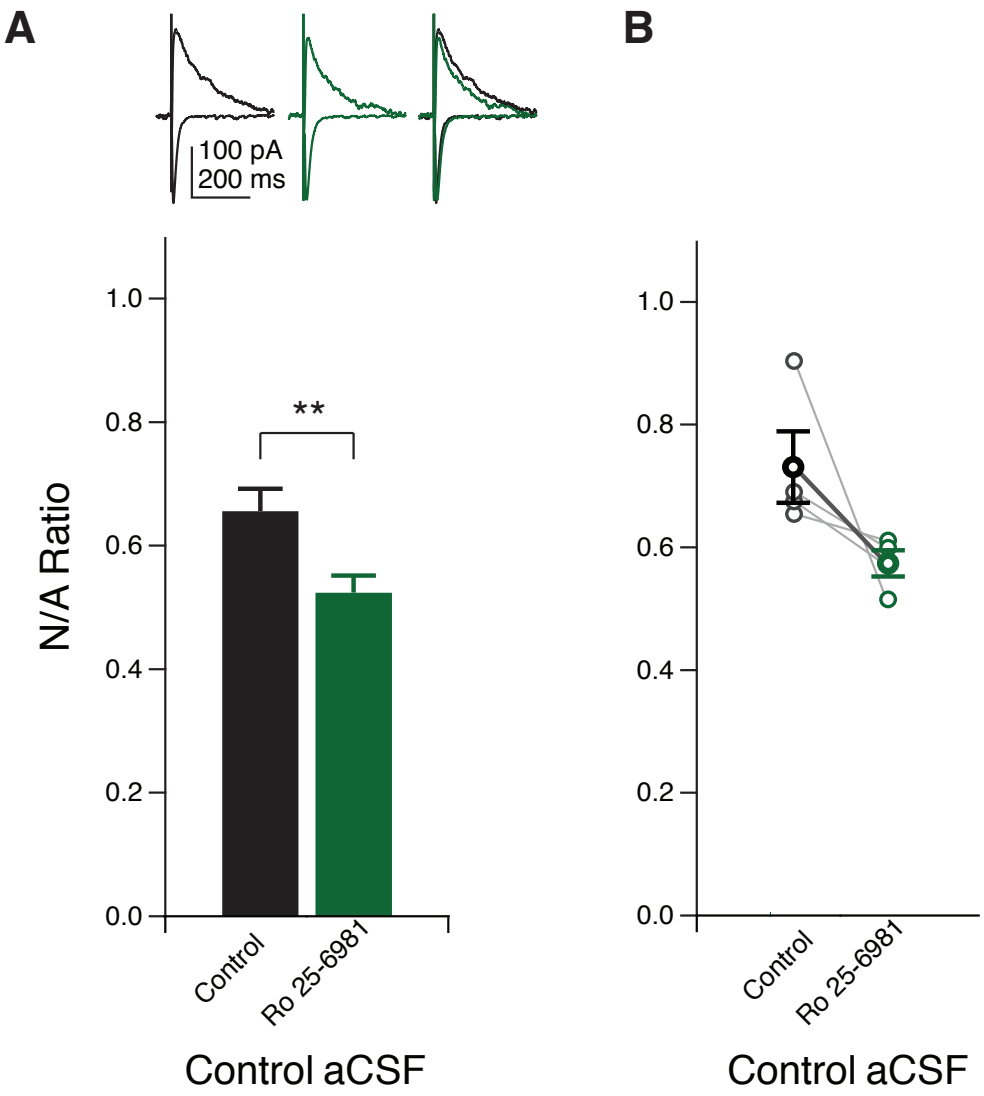

Figure 4.5: Ro 25-6981 causes a reduction in the N/A ratio in *Tau*$^{-/-}$ mice. (**A**) Slices that had received a basic pre-treatment in control aCSF 1-3 hours were used to measure the an N/A ratio at CA3-CA1 synapses under acute control conditions (black) or following acute incubation with Ro 25-6981 (green). (**B**) The N/A ratio was recorded under the basic condition of control aCSF (black circles represent one cell under the basic condition), and then Ro 25-6981 was washed into the superfusing aCSF and the cell was held for 30 minutes to allow for effective block by Ro 25-6981. The N/A ratio was then recorded in this same cell under this new condition (green circles represent one cell in the presence of Ro 25-6981). Pale grey lines show the change in N/A ratio per cell, and dark grey lines show the average change in N/A ratio. Insets show example traces of AMPAR- and NMDAR-mediated currents in slices pre-treated with control aCSF, before (black) and after (green) incubation with Ro 25-6981. Representative traces are from different cells and are shown both separately and superimposed to facilitate comparison. Error bars are s.e.m. ** $P < 0.01$.

4.4 The role of GluN2B subunit-containing NMDARs in tetanus-induced LTP

The lack of an effect of hA$\beta_{1\text{-}42}$ on LTP, slow tau contribution and N/A ratio in *Tau*$^{-/-}$ mice, in contrast to the clear effect found in wild-type mice, is consistent with the interpretation that a reduction in GluN2B subunit-containing NMDARs in wild-type mice is responsible for the hA$\beta_{1\text{-}42}$-induced LTP impairment. However, this presents a conundrum because much previous work has shown that Ro 25-6981 does not impair tetanus-induced LTP in wild-type mice under control conditions, which is the induction protocol that has been used to explore LTP in the preceding chapter. Indeed, I also confirmed that Ro 25-6981 did not cause a significant reduction in the magnitude of tetanus-induced LTP in wild-type mice (control: 151 ± 8%, n = 7; Ro 25-6981: 137 ± 8%, n = 9; t-test P = 0.24; **Fig. 4.6**). Therefore, given that blocking Ca^{2+} influx through GluN2B subunit-containing NMDARs does not block LTP, it suggests that, if an hA$\beta_{1\text{-}42}$-induced reduction in GluN2B subunit-containing receptors does underlie the hA$\beta_{1\text{-}42}$-induced LTP impairment, it is unlikely to be solely due to its role as an ion channel mediating Ca^{2+} influx.

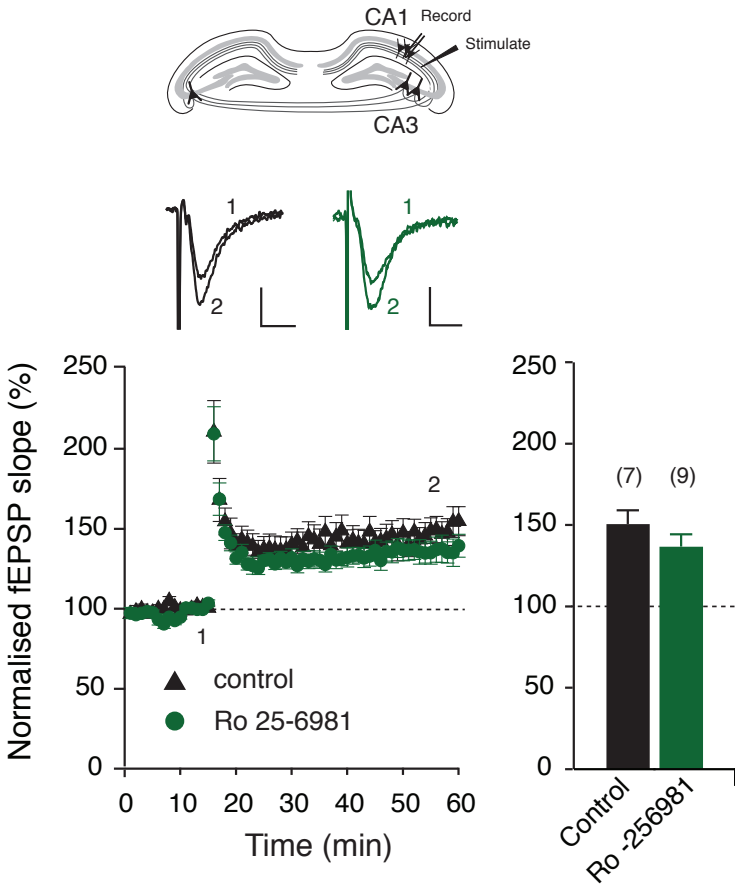

Figure 4.6: Ro 25-6981 does not reduce tetanus-induced LTP in slices from wild-type mice. (**A**) Hippocampal Schaffer collateral/commissural-CA1 LTP induced by electrical stimulation (schematic, top panel) in wild-type mice is equivalent in the presence of control aCSF (black) or after incubation with Ro 25-6981 (green). The insets show superimposed representative fEPSPs at the indicated time points (1, 2), scale bars represent 200 μV and 10 ms. (**B**) Summary of results 40-45 minutes after high-frequency stimulation. The numbers of slices are shown in parentheses. Error bars are s.e.m.

4.4.1 The role of GluN2B-rich synapses in tetanus-induced LTP

The discrepancy between the lack of an effect on tetanus-induced LTP by a GluNB-specific antagonist, and the Aβ-induced LTP impairment correlating with an apparent reduction in GluN2B, raises the possibility that the GluN2B-subunit containing NMDARs play an additional, more fundamental, role in the induction of LTP than simply mediating Ca^{2+} influx. This may be through their molecular association with CaMKII, since the activation of CaMKII is required for LTP (Lisman et al., 2002). In addition, it is conceivable that it is not just the GluN2B subunit-containing NMDARs that are important, but also their synaptic context. CA3-CA1 synapses are not a uniform population, and, even in the adult brain, there are different categories of postsynaptic spine shape that also have distinct receptor signatures (Shinohara et al., 2008). Imaging of individual spines has shown that GluN2B antagonism selectively reduced glutamate uncaging-evoked EPSCs and Ca^{2+} transients in small spines (Sobczyk et al., 2005), indicating that GluN2B is concentrated in such spines. Moreover, these distinct types of spine, with their different NMDAR subunit compositions, may engage differently in plasticity processes and thus could play independent roles even in the mature brain. For example, chronic imaging experiments have revealed that, whilst the volume of all spines increases following an LTP induction protocol, this expansion is only preserved in spines initially classified as small, but is transient in others (Matsuzaki et al., 2004). Therefore, the changes in the extracellular field response to a plasticity protocol and the N/A ratio following incubation with $hA\beta_{1\text{-}42}$ or Ro 25-6981 are the summed changes from this heterogeneous population of synapses, and the different categories of spines within this population may respond differently. Consequently, in order to investigate why there may be a correlation between the $hA\beta_{1\text{-}42}$-induced reduction in GluN2B and LTP magnitude, but no effect of a pharmacological GluN2B antagonist on this form of tetanus-induced LTP, I aimed to investigate whether or not these distinct types of synapses, containing different amounts of GluN2B,

may be differentially able to express tetanus-induced LTP.

Different types of postsynaptic spines are asymmetrically distributed in the adult mouse brain; specifically, postsynaptic CA1 spines receiving input from the left CA3 are mainly those that are small and rich in GluN2B subunit-containing NMDARs, while those receiving right CA3 input tend to be larger and richer in AMPARs (Kawakami et al., 2003; Shinohara et al., 2008). Previous work in our laboratory that I was involved in has shown that synapses that receive left CA3 input show spike timing-dependent LTP (tLTP), while those receiving right CA3 input do not (Kohl et al., 2011). However, this form of tLTP was completely blocked by the same concentration of Ro 25-6981 that does not block tetanus-induced LTP, indicating that GluN2B subunit-containing NMDARs make different contributions to the induction of these two forms of LTP. Therefore, I targeted these different types of spine optogenetically, to test the hypothesis the GluN2B rich postsynaptic spines receiving left CA3 input are also important to mediate tetanus-induced LTP, and that a pathological process which disrupts these would impair such potentiation.

The kinetics of ChR2 do not permit pyramidal neurons to be driven at a sufficiently high frequency to use a tetanus LTP protocol in an optically-activated Schaffer collateral/commissural pathway. Therefore, instead, I established a system that used field recordings with an electrical and optical pathway and maximized the overlap between these two pathways by electrode and optical fibre placement. Thus, not only could the electrical pathway, which recruits fibres originating in both hemispheres indiscriminately, be used as a control pathway, this experimental set up also allowed the use of electrical stimulation to deliver the tetanus while optical stimulation provided hemispheric input-specificity. I injected adult male wild-type mice in the CA3 of one hemisphere with AAV5-CaMKIIα-hChR2(E123T/T159C)-eYFP and 4-6 weeks later coronal slices were prepared for plasticity experiments, which were performed blind to injection side by Mr Mohamady El-Gaby. Once a stable baseline of both the optical and

electrical pathways was recorded for 15 minutes, LTP was induced with electrical stimulation only (100 Hz for 1 s), and a further 45 minutes were recorded to monitor the effect on both pathways. Despite equivalent potentiation in the electrical pathway in both left- and right-injected mice (left: 154 ± 6%, n = 14; right: 149 ± 6%, n = 11; t-test P = 0.50), the optical pathway showed significant potentiation only in left-injected mice (**Fig. 4.7**) and the magnitude of fEPSP increase was significantly greater in left-injected compared to right injected mice (left: 145 ± 7%; right: 113 ± 7%; P = 0.004; (**Fig. 4.7**). This result held when the change in the optical pathway was normalised to the magnitude of electrical LTP (left: 84 ± 11% of electrical; right: 19 ± 15%; P = 0.002). Thus, of all the fibres activated by the electrical tetanus protocol to induce LTP, only those fibres originating in the left CA3 potentiated significantly. Consequently, an asymmetry between the left and right CA3-CA1 synapse in LTP is also found with the standard tetanus induction protocol. This suggests that the GluN2B-rich synapses receiving left CA3 input are important for tetanus-induced LTP, even though blocking GluN2B-mediated current does not prevent this form of plasticity. This is consistent with a requirement for the physical presence of GluN2B subunit-containing receptors at the postsynaptic spine for LTP induction, possibly in order to target CaMKII to the PSD where it can phosphorylate its substrates. Therefore, this further suggests that the hA$\beta_{1\text{-}42}$-induced reduction in N/A ratio and GluN2B found in wild-type, and not in *Tau*$^{-/-}$, mice could explain the different LTP results between these two genotypes.

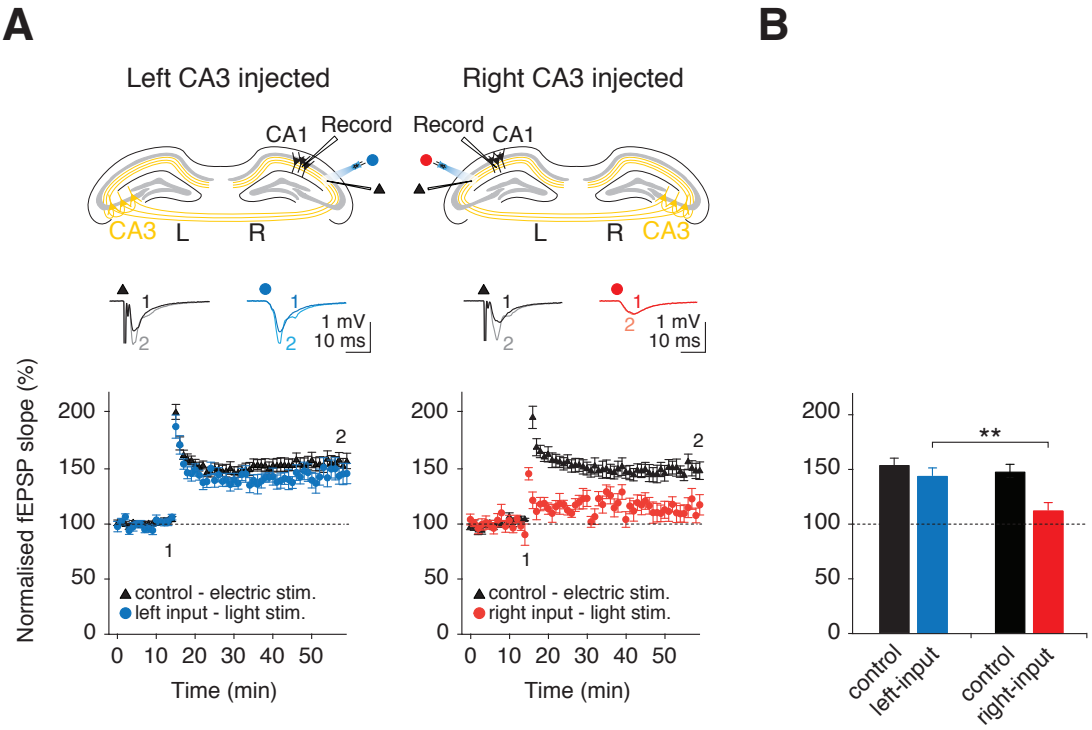

Figure 4.7: Tetanus-induced LTP at the CA3-CA1 pyramidal cell synapse shows hemispheric asymmetry. (**A**) Adeno-associated virus containing channelrhodopsin (hChR2)-eYFP construct under the control of a CaMKIIα promoter was unilaterally injected into the dorsal CA3 region of C57BL/6J mice. WPRE, woodchuck hepatitis post-transcriptional regulatory element. (**B**) Overlapping electrical and optical stimulation in the stratum radiatum (schematic, top panel) enables the effect of high-frequency, electrical stimulation (HFS, arrow) to be measured on selective optical stimulation. This produces robust LTP in the electrical pathway (black triangles), but the optical pathway (circles) only shows LTP when projections originate in the left CA3. Insets show representative fEPSPs at the indicated time points (1, 2). (**C**) Significantly more LTP is observed in left-injected mice than in right-injected mice in the optical pathway. Broken lines represent baseline. Error bars represent s.e.m. ** $P < 0.01$.

4.5 The vulnerability of GluN2B-rich synapses to Aβ

In order to further test this hypothesis, I investigated whether these GluN2B-rich, left CA3-CA1 synapses are particularly vulnerable to acute Aβ exposure in wild-type mice. Therefore, I injected wild-type mice, as before, with an AAV5-CaMKIIα-hChR2(E123T/T159C)-eYFP construct into the right or left CA3. Four-six weeks later, I measured the N/A ratio using optically-evoked EPSCs in left- and right-injected mice with or without pre-incubation in 220 nM $hA\beta_{1\text{-}42}$. There was a reduction in the N/A ratio in left-injected mice following $hA\beta_{1\text{-}42}$ incubation (left-injected control: 0.65 ± 0.03, n = 15 cells, left-injected $hA\beta_{1\text{-}42}$: 0.48 ± 0.03, n = 17 cells; **Fig. 4.8**). However, strikingly, there was no reduction in N/A ratio in right-injected mice in the presence of $hA\beta_{1\text{-}42}$ (right-injected control: 0.65 ± 0.02, n = 12 cells, right-injected $hA\beta_{1\text{-}42}$: 0.70 ± 0.03, n = 14 cells; **Fig. 4.8**). Overall, ANOVA revealed a main effect of hemisphere ($F_{1,54}$ = 13.08, P = 0.001), a trend towards a main effect of treatment ($F_{1,54}$ = 3.66, P = 0.061), but, importantly, a highly significant hemisphere by treatment interaction ($F_{1,54}$ = 12.64, P = 0.001) due to an effect of $hA\beta_{1\text{-}42}$ in left-injected mice ($F_{1,54}$ = 16.69, P < 0.001). Therefore, this shows that the N/A ratio reduction in wild-type mice can be attributed to a reduction in N/A ratio at synapses receiving their input from the left CA3. These synapses are known to be GluN2B-rich (Kawakami et al., 2003; Shinohara et al., 2008; Kohl et al., 2011), which is in agreement with the data presented here, and the most parsimonious explanation is that $hA\beta_{1\text{-}42}$ directly or indirectly targets the synaptic GluN2B subunit-containing NMDARs. Most importantly, synapses activated in left-injected mice show a change in N/A ratio and it is the same input that shows tetanus-induced LTP. Therefore, altogether, this supports the conclusions that the deficit in tetanus-induced LTP in wild-type mice in the presence of $hA\beta_{1\text{-}42}$ is due to changes in GluN2B at the left CA3-CA1 synapses. *Tau*$^{-/-}$ mice appear to have an uncoupling somewhere in the pathway that leads from $hA\beta_{1\text{-}42}$ exposure to GluN2B reduction, which renders them immune to this process.

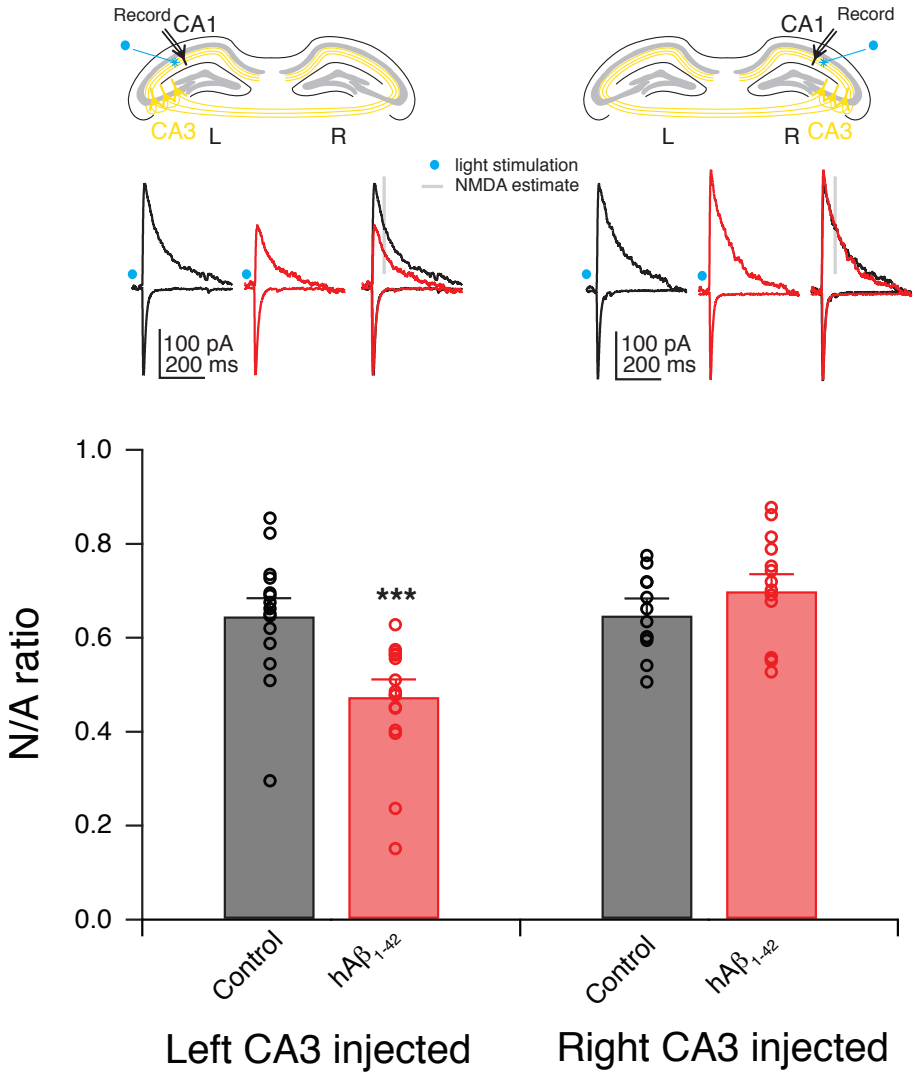

Figure 4.8: Human Aβ_{1-42} reduces the N/A ratio in left-injected but not right-injected wild-type mice. Selective optical activation of hippocampal Schaffer collateral/commissural projections to CA1 pyramidal neurons originating in either the left or right CA3 (schematic, top panel) allows an N/A ratio to be measured at the CA3-CA1 synapse under control conditions (grey) and following incubation with hA$\beta_{1\text{-}42}$ (light red). Individual values for each cell in control conditions (black circles) or after hA$\beta_{1\text{-}42}$ exposure (dark red circles) are illustrated. The insets show representative traces of AMPAR- and NMDAR-mediated currents in left-injected (left side) and right-injected mice (right side), before (black) and after (red) incubation with hA$\beta_{1\text{-}42}$. Representative traces from different cells are shown both individually and superimposed to facilitate comparison. Error bars are s.e.m. *** $P < 0.001$.

4.5.1 The presence of GluN2B-rich synapses in *Tau*$^{-/-}$ mice

It is conceivable that the synaptic context of the GluN2B subunit-containing NMDAR is the important factor in determining why the GluN2B-rich small synapses are important for LTP induction. To provide an indication of whether this synaptic context might be the same in *Tau*$^{-/-}$ mice, I investigated whether they show a similar asymmetry in the distribution of GluN2B subunit-containing NMDARs, since this is known to correlate with morphologically distinct types of synapse. I used optogenetic activation of left and right CA3-CA1 synapses in *Tau*$^{-/-}$ mice and tested the effect of Ro 25-6981. Ideally it would be tested whether the magnitude of the Ro 25-6981-induced reduction in the N/A ratio was significantly different in left- and right-injected mice. However, the power of this test would be low since variability was high and the *n* numbers quite low, and also cells had not been recorded before and after wash-on. Nevertheless, numerically there was a greater reduction in N/A ratio in left-injected mice than in right-injected mice (ratio reduction of 0.24 in left-injected mice but 0.11 in right-injected mice). This N/A ratio reduction in the presence of Ro-256981was significant in left-injected but not in right-injected mice (left-injected control: 0.70 ± 0.07, n = 10 cells, left-injected Ro 25-6981: 0.46 ± 0.05, n = 8 cells; t-test P = 0.016; right-injected control: 0.68 ± 0.07, n = 8 cells, right-injected Ro 25-6981: 0.57 ± 0.07, n = 9 cells; t-test P = 0.27; **Fig. 4.9**). If the NMDAR-mediated current estimate was normalised to a fixed AMPAR-mediated current of -100 pA to facilitate comparisons with the previous findings in wild-type mice in Kohl et al. (2011), then an average reduction of 27 pA was observed in left-injected mice (84 ± 9 to 57 ± 5 pA), but only 10 pA in right-injected mice (78 ± 7 to 68 ± 8 pA). This overall pattern of results in left- and right-injected mice in the presence of a GluN2B antagonist is similar to that which had been observed in wild-type mice (Kohl et al., 2011), despite slight differences in holding potential and time of NMDAR-mediated current estimates, with a large reduction in NMDAR-mediated current in left-injected mice with Ro 25-6981 and a small reduction in

right-injected mice. Therefore, the results hint that *Tau*$^{-/-}$ mice might also have a similar asymmetry to that in wild-type mice, with GluN2B-rich synapses receiving left CA3 input that are important to mediate LTP. Nevertheless, a larger data set is required to confirm this result.

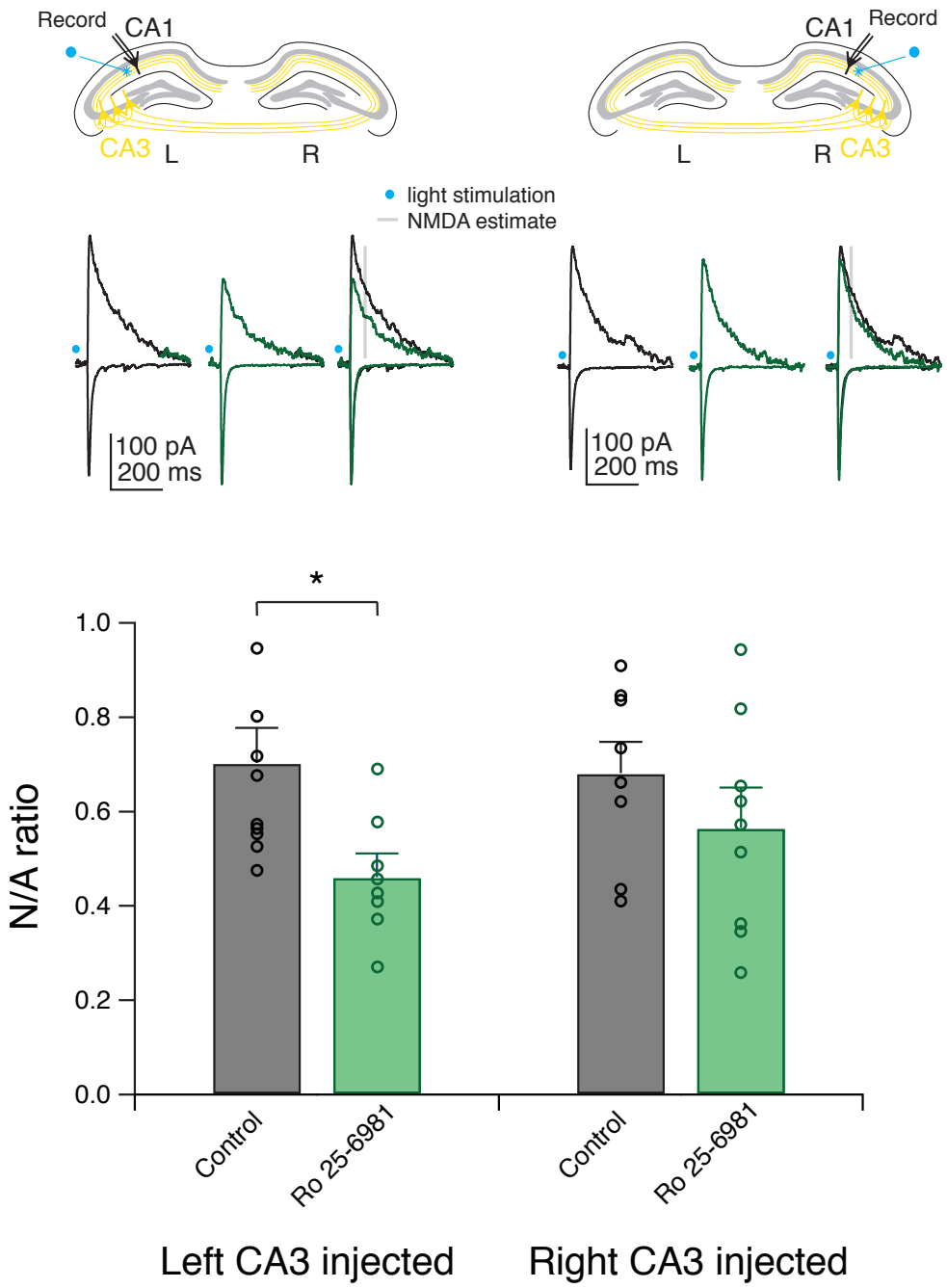

Figure 4.9: Ro 25-6981 significantly reduces the N/A ratio in left-injected but not right-injected *Tau*$^{-/-}$ mice. Selective optical activation of hippocampal Schaffer collateral/commissural projections to CA1 pyramidal neurons originating in either the left or right CA3 (schematic, top panel) allows an N/A ratio to be measured at the CA3-CA1 synapse under control conditions (grey) and following incubation with Ro 25-6981 (pale green). Individual values for each cell in control conditions (black circles) or after Ro 25-6981 treatment (dark green circles) are illustrated. The insets show example traces of AMPAR- and NMDAR-mediated currents in left-injected (left side) and right-injected mice (right side), before (black) and after (green) incubation with Ro 25-6981. Representative traces from different cells are shown both individually and superimposed to facilitate comparison. Error bars are s.e.m. ** $P < 0.01$.

4.6 Discussion

4.6.1 Summary

The data presented in this chapter is consistent with the hypothesis that hA$\beta_{1\text{-}42}$ triggers a reduction in synaptic GluN2B subunit-containing receptors in wild-type mice, but not in *Tau*$^{-/-}$ mice, and that this change can account for why an hA$\beta_{1\text{-}42}$-induced impairment in LTP is present in wild-type mice but not in *Tau*$^{-/-}$ mice. The evidence that supports this conclusion is threefold. Firstly, the hA$\beta_{1\text{-}42}$-induced reduction in N/A ratio is only observed in wild-type, and not in *Tau*$^{-/-}$, mice. This is despite the fact that *Tau*$^{-/-}$ mice have functional GluN2B subunit-containing NMDARs at the age used for the LTP experiments. Moreover, the hA$\beta_{1\text{-}42}$-induced reduction in the N/A ratio in wild-type mice precludes any further effect of a GluN2B subunit-selective blocker. Secondly, it is only in wild-type mice that the contribution of the slow tau to the decay time constant of the NMDAR-mediated current is decreased following hA$\beta_{1\text{-}42}$ treatment, indicative of a decrease in the contribution of GluN2B subunit-containing NMDARs, which have slower decay kinetics. Thirdly, despite no effect of pharmacological GluN2B antagonism on tetanus-induced LTP, it is only the left input with GluN2B-rich synapses that potentiates following this high-frequency protocol, and it is this same set of synapses that show the reduction in N/A ratio following exposure to hA$\beta_{1\text{-}42}$.

4.6.2 Technical considerations

AMPAR- and NMDAR-mediated currents can either be dissociated pharmacologically or by varying the holding potential. The latter technique was favoured due to the ability to measure both currents in the same cell interleaved, but it is important to note that changes in the N/A ratio could be explained by a decrease in NMDAR-mediated current, an increase in AMPAR-mediated current, or both these changes simultaneously. However, evidence only exists that Aβ

may reduce postsynaptic AMPARs (Shemer et al., 2006; Parameshwaran et al., 2007; Ting et al., 2007; Gu et al., 2009; D'Amelio et al., 2011), and therefore it is unlikely that an enhancement in AMPAR-mediated current could explain the results obtained under my experimental conditions. Measurement of miniature AMPAR-mediated EPSCs (mEPSCs) could be used to verify this, but such mEPSCs are still affected by presynaptic changes and the location of synapses along the somato-dendritic axis. Moreover, as with evoked currents, mEPSCs can also come from different synapses in different treatment conditions. Paired recordings are the ideal way to measure changes in synaptic function, but these are technically very challenging at CA3-CA1 synapses in adult mice.

There is considerable variability between studies investigating glutamate receptor-mediated current ratios. The major reasons for this variation are probably the different positive and negative holding potentials used, which influence the magnitude of current flow, the time point or window used to estimate the NMDAR-mediated current and also the location of the extracellular stimulation used to recruit afferent input. Therefore the precise N/A ratio values obtained here are not directly comparable with other similar studies. However, the pattern of results can be compared; the same method was carefully applied to a number of different treatment conditions, and there was no evidence for systematic differences in the series resistance, magnitude of AMPAR-mediated current (used as a normalisation factor), leak at -70 mV, or the number of measurements of each type of glutamate-receptor mediated current per cell (please see table in **Fig. 4.10**). Moreover, any slices with evidence of polysynaptic activity, which could contaminate the NMDAR-mediated current measurement, were rejected.

The use of voltage-clamp to measure current ratios in pyramidal neurons in slices does still have technical drawbacks. Firstly, the use of extracellular stimulation to evoke EPSC responses risks recruiting extrasynaptic NMDARs. In order to minimise this, stimulation strength was kept low, and set at a value where

reliable currents of 100-200 pA were recorded at -70 mV. This value was maintained throughout all measurements in different treatment conditions. Consequently, if the AMPAR-mediated component of the current was reduced by hA$\beta_{1\text{-}42}$, for which there is some evidence (Shemer et al., 2006; Parameshwaran et al., 2007; Ting et al., 2007; Gu et al., 2009; D'Amelio et al., 2011), then a relatively higher stimulation strength would have been used to measure the N-/A ratio following this treatment. Therefore, extrasynaptic NMDARs would be more likely to be recruited. Nevertheless, my results reveal a reduction in N/A ratio, particularly in the GluN2B contribution, which is in the opposite direction to what would be predicted if there was an increased recruitment of extrasynaptic NMDAR following treatment with hA$\beta_{1\text{-}42}$. Consequently, unless extrasynaptic NMDARs became constitutively active, this possible effect would actually result in an underestimation of the hA$\beta_{1\text{-}42}$-induced change of the N/A ratio. Importantly, though, there is no evidence that I was systematically having to use a higher stimulation strength to obtain this magnitude of peak EPSC at -70 mV in the presence of hA$\beta_{1\text{-}42}$, either in wild-type or in *Tau*$^{-/-}$ mice, because in cells recorded interleaved using the same equipment, the average stimulation strengths per cell were very similar (wild-type control: 50 ± 3 μA, n = 29; wild-type hA$\beta_{1\text{-}42}$: 50 ± 3 μA, n = 39; *Tau*$^{-/-}$ control: 50 ± 3 μA, n = 37; *Tau*$^{-/-}$ hA$\beta_{1\text{-}42}$: 49 ± 5 μA, n = 33). An alternative technique to avoid possible recruitment of extrasynaptic NMDARs is measuring mEPSCs in a Mg^{2+} free solution. However, it is possible that residual Mg^{2+} in the tissue may still contribute to NMDAR block, and therefore the N/A ratio would be underestimated. Consequently, this technique may also not be very sensitive to small changes in the NMDAR-mediated current. Furthermore, since GluN2A and GluN2B subunit-containing NMDARs have different open channel probabilities (Erreger et al., 2005), this approach may not be very suitable to investigate subunit-selective changes.

Somatic voltage-clamp is not able to fully control the voltage at the activated synapses, where the current is being generated, due to the passive cable filtering properties of dendrites. Therefore, given this 'space-clamp' limitation,

an additional consideration is whether somatic voltage-clamp is an acceptable way to measure synaptic currents, since there is a distortion of current amplitude, kinetics, slope conductance and reversal potential with distance from the dendrites (Williams and Mitchell, 2008). However, whilst the currents and decay time constants measured here using somatic voltage-clamp are therefore not the true values at the dendrites, they will still be reflective of these values. Moreover, every effort was made to keep the series resistance low and constant and to use equivalent recording conditions in each set of experiments. Therefore, when using somatic voltage-clamp data to make comparisons between the effects of different treatments on the N/A ratio interleaved within one study, the results from such measurements are still informative.

One further consideration when interpreting the data presented here is the nature of the GluN2B-specific antagonist, Ro 25-6981, which has been used. Although Ro 25-6981 is a highly selective blocker, it is activity dependent. Therefore the incubation period was a minimum of 30 minutes, which has previously shown to give effective block in our laboratory, and also is similar to that used in other studies (Kawakami et al., 2003). Nevertheless, even when used at maximum efficacy, Ro 25-6981 is still not expected to block all GluN2B-subunit containing NMDARs, and the extent of this block varies with ambient glutamate concentration (Fischer et al., 1997). Therefore, if $hA\beta_{1\text{-}42}$ were to influence the glutamate concentration in the synaptic cleft, this could complicate the interpretation of results, and this is discussed in more detail in the concluding chapter. Moreover, Ro 25-6981 has low efficacy at blocking triheteromeric NMDARs, which may be the predominant type in the adult hippocampus (Gray et al., 2011; Rauner and Köhr, 2011; Tovar et al., 2013; Volianskis et al., 2013). Therefore, it is encouraging that two different approaches to determining a possible subunit selective effect of $hA\beta_{1\text{-}42}$ that did not involve Ro 25-6981, namely the decay time constant and the N/A ratio in left- compared to right-injected mice, also produced results consistent with the interpretation that $hA\beta_{1\text{-}42}$ targets GluN2B subunit-containing NMDARs in the PSD.

Genotype	Hemisphere	Basic treatment	Acute treatment	Value	AMPA	NMDA	Series resistance	Leak AMPA	No. values per current
Wild-type		control		av	-186.5	110.1	15.1	-158.7	20.7
Wild-type		control		sem	6.4	5.3	0.4	14.7	2.0
Wild-type		$hA\beta_{1-42}$		av	-189.5	91.5	13.8	-169.2	19.8
Wild-type		$hA\beta_{1-42}$		sem	5.3	4.0	0.4	10.9	1.7
Tau$^{-/-}$		control		av	-195.0	115.0	14.2	-183.0	15.6
Tau$^{-/-}$		control		sem	7.0	7.6	0.5	15.3	1.3
Tau$^{-/-}$		$hA\beta_{1-42}$		av	-197.1	114.8	13.0	-165.1	19.7
Tau$^{-/-}$		$hA\beta_{1-42}$		sem	6.4	7.1	0.4	16.0	1.8
Wild-type	left	control		av	-165.0	106.5	13.3	-194.4	14.9
Wild-type	left	control		sem	7.6	7.8	0.6	20.1	1.8
Wild-type	left	$hA\beta_{1-42}$		av	-143.5	69.4	13.1	-130.8	12.3
Wild-type	left	$hA\beta_{1-42}$		sem	7.2	6.3	0.3	14.2	1.8
Wild-type	right	control		av	-167.2	108.3	12.1	-156.9	19.3
Wild-type	right	control		sem	5.1	4.5	0.8	14.7	2.4
Wild-type	right	$hA\beta_{1-42}$		av	-172.8	119.8	12.5	-189.4	15.4
Wild-type	right	$hA\beta_{1-42}$		sem	7.2	5.4	0.5	27.5	2.6
Wild-type		control	control	av	-215.6	142.5	13.8	-184.3	8.1
Wild-type		control	control	sem	7.3	6.0	0.4	12.3	0.6
Wild-type		control	ro 25-6981	av	-195.1	95.1	14.2	-208.7	13.6
Wild-type		control	ro 25-6981	sem	7.3	6.9	0.5	41.3	1.4
Wild-type		$hA\beta_{1-42}$	control	av	-210.6	114.5	13.5	-166.1	10.7
Wild-type		$hA\beta_{1-42}$	control	sem	7.8	6.7	0.4	25.2	1.3
Wild-type		$hA\beta_{1-42}$	ro 25-6981	av	-204.1	111.6	15.2	-109.5	16.8
Wild-type		$hA\beta_{1-42}$	ro 25-6981	sem	10.8	6.5	0.6	12.5	2.9
Tau$^{-/-}$			control	av	-189.0	124.8	14.2	-160.1	12.5
Tau$^{-/-}$			control	sem	14.0	11.0	0.4	19.3	1.1
Tau$^{-/-}$			ro 25-6981	av	-198.6	103.4	15.2	-149.0	13.8
Tau$^{-/-}$			ro 25-6981	sem	9.3	6.3	0.4	22.9	1.9
Tau$^{-/-}$	left		control	av	-179.5	122.9	11.5	-171.4	12.1
Tau$^{-/-}$	left		control	sem	12.1	10.6	0.9	27.6	3.3
Tau$^{-/-}$	left		ro 25-6981	av	-195.4	90.4	12.6	-120.2	15.6
Tau$^{-/-}$	left		ro 25-6981	sem	14.1	11.0	0.6	6.8	2.3
Tau$^{-/-}$	right		control	av	-160.8	107.5	11.4	-176.8	12.9
Tau$^{-/-}$	right		control	sem	12.4	11.7	0.7	9.5	2.0
Tau$^{-/-}$	right		ro 25-6981	av	-163.6	97.2	14.1	-196.7	9.3
Tau$^{-/-}$	right		ro 25-6981	sem	17.2	19.6	0.4	27.3	1.8

Figure 4.10: Table of average values for descriptive parameters in N/A ratio recordings. The average values of NMDAR- and AMPAR-mediated currents for each experimental condition used. Also shown are the average series resistance, leak current at -70 mV, and number of measurements made of each current per cell.

4.6.3 Possible molecular pathways

The discrepancy between the lack of an effect on tetanus-induced LTP from GluN2B block and the importance of GluN2B-rich synapses in potentiation suggests that the physical presence of GluN2B subunit-containing NMDARs at the PSD is important. This is in agreement with the finding of Foster et al. (2010), who found that, at an age when pharmacological inhibition of GluN2B with Ro 25-6981 no longer blocked pairing-induced LTP, LTP was still impaired by RNAi knockdown of GluN2B. Given that hA$\beta_{1\text{-}42}$ impairs LTP, it suggests it might have a similar effect to RNAi or mimic the different type of spine, and actually exert the impairment by reduction of GluN2B content at the PSD. There are many tightly regulated pathways controlling GluN2B internalisation and supply to the PSD with which Aβ could interact in order to mediate such an effect.

4.6.3.1 Fyn and tau

Given the importance of tau protein for the LTP deficit and reduction in N/A ratio, one candidate by which Aβ could interfere with with synaptic GluN2B content is via the tyrosine kinase fyn, since tau is known to target fyn to the dendrite (Ittner et al., 2010). Fyn plays an important role at the synapse, phosphorylating the GluN2B subunit at Y1472 (Rong et al., 2001) and hence strengthening the interaction between the GluN2B subunit-containing NMDAR and PSD-95. The importance of this function is demonstrated by the LTP and spatial learning deficits in *Fyn* mutant mice (Grant et al., 1992; Kojima et al., 1997). In support of a possible pathway involving fyn, an early paper showed that Aβ-induced neuronal death in organotypic hippocampal slices was prevented in $Fyn^{-/-}$ mice (Lambert et al., 1998). Moreover, two recent studies have implicated Aβ binding to the prion protein in the activation of fyn, which leads to tau pathology (Larson et al., 2012) and dendritic loss (Um et al., 2012). Moreover, Um et al. (2012) further showed that, despite an initial increase in NMDARs at the cell surface,

the activation of fyn culminated in an overall loss of NMDARs; the results presented here are consistent with this, since recordings were not made until 1-3 hours after initial Aβ exposure. However, if tau plays a central role in targeting fyn and hence maintaining appropriate GluN2B cogent at the PSD, it is perhaps surprising that loss of tau does not impair LTP (Shipton et al., 2011) and, instead, partial or complete tau reduction actually prevents Aβ-induced neurodegeneration in culture (Rapoport et al., 2002; Jin et al., 2011), LTP deficits (Shipton et al., 2011) and cognitive deficits in hAPP-overexpressing mice (Roberson et al., 2007, 2011). It is possible that the lack of tau, and hence the weaker fyn-mediated anchoring of the GluN2B-subunit containing NMDARs at the PSD, may uncouple GluN2B receptors from the pathways that normally mediate internalisation and thus higher levels of GluN2B remain at the PSD under conditions of acute exposure to $hA\beta_{1\text{-}42}$. However, an alternative explanation might be that the weaker anchoring of the NMDAR, in the absence of the appropriate interaction between fyn and tau, reduces Aβ-induced excitotoxicity (Ittner et al., 2010) and hence maintains appropriate synaptic function for longer in the presence of Aβ.

4.6.3.2 Extrasynaptic overactivation or synaptic underactivation

Excitotoxicity by overactivation of extrasynaptic NMDARs is very likely to play a role in disease progression, especially in triggering neuronal death. However, it has also been suggested that excitotoxicity, via an increase in Ca^{2+} influx through extrasynaptic GluN2B subunit-containing NMDARs, causes the $hA\beta_{1\text{-}42}$-induced LTP impairment (Hu et al., 2009; Li et al., 2011) and the facilitation of LTD induction (Li et al., 2009). The evidence for the LTP effect is that Ro 25-6981 can recover the magnitude of LTP to control levels when co-applied with $hA\beta_{1\text{-}42}$ (Li et al., 2011). However, the data here suggests that the root cause of the LTP impairment may actually be a synaptic effect, and one mediated by a decrease in GluN2B numbers, rather than an extrasynaptic increase in GluN2B-mediated current. The discrepancy between the findings presented here and those showing extrasynaptic GluN2B overactivation may simply arise

from methodological differences if extrasynaptic NMDAR overactivation and synaptic NMDAR reduction occur simultaneously, since the effect that dominates the measurements made will depend on the extent to which extrasynaptic NMDARs are recruited by stimulation.

However, a more interesting possibility is that the findings are not mutually exclusive explanations, and, in fact, may be two aspects of the same pathological pathway with distinct effects of Aβ occurring at different time points following initial exposure, as the results of Um et al. (2012) would suggest. If $hA\beta_{1\text{-}42}$ triggers an overactivation of extrasynaptic GluN2B subunit-containing NMDARs, homeostatic regulatory pathways used to maintain an appropriate level of cellular activation may be recruited and act to reduce synaptic GluN2B subunit-containing receptors to compensate. Indeed, in cultured neurons, extrasynaptic NMDAR overactivity precedes a reduction in evoked- and mini-EPSCs (Talantova et al., 2013). GluN2B subunit-containing receptors may be particularly at risk of compensatory internalisation, since they are known to undergo more frequent endocytosis in neuronal culture (Lavezzari et al., 2004). Therefore, such a compensatory pathway could be intercepted at the initial stage when overactivation occurs, through blockade by Ro 25-6981, as demonstrated by Hu et al. (2009); Li et al. (2011).

It also seems conceivable that the short exposure used by Li et al. (2011), with Aβ preparation only added to the perfusate during recordings, could produce similar effects to those observed by Coan et al. (1989), who demonstrated that using a Mg^{2+} free solution during field recordings where NMDAR activation is enhanced blocked the induction of tetanus-induced LTP; however, this was not through NMDAR internalisation or saturation of LTP since LTP could be induced once an appropriate level of Mg^{2+} was restored. However, longer exposure to Aβ, such as the 1-3 hour pre-incubation used here, may engage compensatory mechanisms that do alter synaptic glutamate receptor composition. It is known that the glutamate re-uptake inhibitor TBOA, which causes

extrasynaptic overactivation, mimics the effect of Aβ on tetanus-induced LTP (Li et al., 2011). Therefore, in order to investigate whether the extrasynaptic overactivation and synaptic reduction might be part of the same pathway, slices from left-injected mice could be pretreated with TBOA to test whether it triggers a reduction in the N/A ratio of optically-evoked synaptic currents that can be attributed to a specific loss in GluN2B subunit-containing NMDARs.

4.6.3.3 Aβ-induced disruption in intracellular trafficking

One possible mechanism for how synaptic GluN2B loss may occur by a process that is partially or fully independent to that involving extrasynaptic NMDAR overactivation relates to GluN2B trafficking. GluN2B internalisation is more frequent than that for GluN2A (Lavezzari et al., 2004) and, unlike GluN2A subunit-containing NMDARs, GluN2B subunit-containing NMDARs are also normally trafficked into recycling endosomes. Therefore, GluN2B subunit-containing NMDARs would be particularly sensitive to Aβ-induced trafficking deficits and this would explain the subunit selectivity after acute Aβ exposure. In support of the possibility that Aβ may interfere with GluN2B supply to the PSD, Aβ has been shown to affect pathways involving CREB (Vitolo et al., 2002). CREB activation is linked to the kinesin protein KIF17, which controls the relative levels of GluN2A and GluN2B at the synapse (Yin et al., 2011). The trafficking hypothesis can also be directly related to tau involvement, since Aβ has been shown to impair axonal transport and this impairment can be prevented by acute inhibition of GSK-3 activity (Decker et al., 2010b) or reduction in tau (Vossel et al., 2010). Under this possible molecular pathway, the lack of tau is not neuroprotective because of weakened interaction of GluN2B subunits at the synapse making them less vulnerable to internalisation, but actually because it prevents tau itself exerting harmful effects. Specifically, Aβ-triggered hyperphosphoylation of tau may cause it to dissociate from microtubules and become mislocalised at high levels in dendrites. Hoover et al. (2010) found that the accumulation of missorted, hyperphosphorylated tau

both impeded delivery of glutamate receptors to the synapse and damaged the anchoring of those already present. Moreover, filamentous tau can impair anterograde fast axonal transport mediated by kinesin through a mechanism that involves GSK-3 activation (LaPointe et al., 2009; Kanaan et al., 2011). If block of GSK-3 permits physiological intracellular transport to continue even in the presence of Aβ and filamentous tau, this may therefore explain why inhibiting GSK-3 can recover the LTP deficit. It is not yet known whether such effects could occur on the timescale of my experiments, with Aβ incubation for 1-3 hours, but this could be addressed using multi-photon imaging with fluorescently labelled tau.

Therefore, there are many possible molecular pathways that could mediate the reduction in synaptic GluN2B. Further investigation should reveal whether the deficit arises through an effect on GluN2B anchoring and likelihood of internalisation, trafficking impairments affecting GluN2B supply, or whether or not the synaptotoxicity is, in fact, part of a larger pathway involving excitotoxicity. It is also important to note that although the data presented here is consistent with a lower levels of GluN2B being present at the synapse in wild-type mice following Aβ exposure, it cannot be excluded that the Aβ peptide could partially reduce NMDAR-mediated Ca^{2+} influx at all GluN1/GluN2B receptors. This would also explain the change in N/A ratio and the occlusion of the effect of Ro 25-6981. Under this scenario, the LTP impairment would arise because an alteration in synaptic NMDAR current would create the low Ca^{2+} influx conditions that encourage the activation of the phosphatase pathways that support LTD (Mucke and Selkoe, 2012).

4.6.4 Aβ effect at different types of synapses

The data presented here suggest that different types of synapses may be differentially vulnerable to the effects of $hA\beta_{1\text{-}42}$. Specifically, the change in N/A ratio is only detected in those synapses receiving left CA3 input which have previ-

ously been shown to be small and rich in GluN2B subunit-containing NMDARs (Kawakami et al., 2003; Shinohara et al., 2008; Kohl et al., 2011). Thus far, the data has been interpreted as a selective reduction in GluN2B subunit-containing NMDARs, which is consistent with why left-injected mice alone show such an effect. This is also in agreement with the work of of Brouillette et al. (2012), which showed a reduction in levels of the GluN2B following repeated intrahippocampal injection of soluble $A\beta_{1-42}$ *in vivo*.

Another hypothesis is also plausible, and this again suggests that the two major types of asymmetrically distributed synapses are differentially vulnerable. In this explanation, however, it is presynaptic release that is affected by Aβ. This would cause a reduction in the release probability that essentially silences small synapses. Therefore, after exposure to $hA\beta_{1\text{-}42}$ a different set of synapses are being recruited and these tend to be the large stable synapses which are less able to mediate the induction of LTP. However, this is less consistent with the available evidence because previous work has shown no overall difference in N/A ratio between these two types of synapse (Kohl et al., 2011), and the EPSC measurements presented in the preceding chapter showed no evidence of presynaptic changes following Aβ exposure.

Either explanation would result in ineffective activation of the GluN2B-rich synapses during the tetanus induction protocol, and these are now known to be required for even high-frequency induced LTP. The reason why these synapses can potentiate may be because of the high level of CaMKII present at the PSD anchored to GluN2B (Strack and Colbran, 1998; Leonard et al., 1999) and because the GluN2B subunit can also recruit additional activated CaMKII that translocates to the synapse following LTP induction (Zhang et al., 2008). The interaction between CaMKII and GluN2B locks CaMKII in its active conformation (Bayer et al., 2001), which is required for CaMKII to phosphorylate its substrates at the PSD and hence to mediate the molecular pathways that mediate the expression of LTP (Barria and Malinow, 2005). The morphology of these

small synapses may also be important in the maintenance of plasticity, since the postsynaptic spine would be amenable to structural enlargement to stabilise the potentiation. In contrast, synapses receiving right CA3 input have been shown to have large, mushroom-shaped postsynaptic spines, that are rich in AMPARs (Shinohara et al., 2008). This type of synapse may not be able to sustain an increased strength (Matsuzaki et al., 2004), and would thus be already saturated. Therefore, a combination of both the synapse morphology and the density or total content of GluN2B subunit-containing NMDARs might mean these types of synapses respond differently to an LTP induction protocol. The importance of the thin, GluN2B-rich spines in LTP, and thus potentially also in learning and memory, may partly explain why compensatory processes that occur during the AD process are unable to fully support cognitive function. For example, DeKosky and Scheff (1990) found that patients with mild to moderate AD had a lower density of synapses, but the synapses which remained were enlarged sufficiently to maintain a constant total synaptic contact within a given volume. It is likely that these enlarged synaptic contacts would be more typical of the synapses receiving right CA3 input and, therefore, not able to potentiate, nor, perhaps, fulfil certain requirements for effective cognition.

Since it seems that the physical presence of GluN2B subunit-containing NMDARs is important, perhaps through molecular anchoring of CaMKII, I would not expect that increasing calcium influx during LTP induction would overcome the hA$\beta_{1\text{-}42}$-induced effect because the necessary downstream molecular cascades would still not be triggered. This hypothesis could be tested by investigating whether increasing Ca^{2+} influx during LTP induction recovers the hA$\beta_{1\text{-}42}$-induced LTP impairment in wild-type mice. For example, using whole-cell current-clamp recordings of CA1 cells where the postsynaptic cell is clamped at -20 mV during tetanic stimulation to maximise opening of NMDARs by removal of the Mg^{2+} block. If LTP cannot be recovered, it suggests that the role of the GluN2B subunit-containing NMDAR is primarily important due to its intracellular molecular associations rather than its role as an ion channel in

mediating Ca^{2+} influx. Therefore, to prevent hA$\beta_{1\text{-}42}$-induced deficits it will be necessary to prevent reduction of GluN2B at the PSD, particularly in the small postsynaptic spines receiving left CA3 input. The same left-right asymmetry seems to be present also in *Tau*$^{-/-}$ mice and, therefore, in order to investigate how best to protect these vulnerable GluN2B-rich synapses, left-injected *Tau*$^{-/-}$ mice could be used to explore the uncoupling of this pathological process in greater detail.

4.6.5 Perspective

AD is associated with episodic memory impairments, and a number of behavioural tasks in rodent models of AD have been used to explore this deficit in more detail. However, to further understand these impairments, it is imperative to investigate how such memory impairments may arise at the synaptic level. A useful model to investigate this aspect of pathology has been the Aβ-induced deficit in hippocampal LTP at the CA3-CA1 synapse, which is postulated to support long-term associative memory in healthy individuals. In this chapter, I have explored the possible mechanism underlying the LTP deficit in wild-type mice following hA$\beta_{1\text{-}42}$ treatment, and also examined why *Tau*$^{-/-}$ mice are not vulnerable. The finding that the plastic GluN2B-rich synapses seem particularly at risk to the effects of hA$\beta_{1\text{-}42}$ opens an avenue to dissect the pathological process in more detail. In addition, it suggests that treatments targeted to protecting this type of synapse may be particularly effective in slowing disease progression at the early stages of AD.

The asymmetry in LTP and in synaptic vulnerability suggests that the left-right difference in the mouse may have implications for hippocampal function and dysfunction, and this will be explored in the next chapter.

CHAPTER 5

Left-right asymmetry in hippocampal memory processes

5.1 Introduction

The hippocampus plays a fundamental role in learning and memory processes, as famously discovered by the study of patient HM, who lost the ability to lay down new declarative memories after surgical removal of the medial temporal lobes (Scoville and Milner, 1957). It is this same type of memory that is affected early in the progression of Alzheimer's disease, where the medial temporal lobe is one of the first brain regions to show pathology (Braak and Braak, 1995). Declarative memories for facts, places and events are now established to require the hippocampus (Squire and Zola-Morgan, 1991) and, not only is the hippocampus required to support these forms of memory, its activity also increases during certain types of memory task. For example, using positron emission tomography (PET), Squire et al. (1992) demonstrated that the hippocampus was significantly active above baseline or priming conditions in a word recall task. Interestingly, this elevated activity was localised in the right hippocampus and this was one of the earliest suggestions that an asymmetry in hippocampal function might exist in humans.

Evidence for a left-right dissociation of human hippocampal function accumulated and suggested that, whilst the left hippocampus is required for episodic, autobiographical memories, the right hippocampus is important for location memory and spatial navigation (Burgess et al., 2002). Further exploration has revealed that this episodic-navigation dissociation may not be entirely separated between hemispheres but, instead, each hippocampus may contribute distinct, but complementary, functions within each of these types of memory. Iglói et al. (2010) used functional magnetic resonance imaging (fMRI) in a spatial navigation task and showed that allocentric place representation was associated with a higher blood-oxygen-level dependent (BOLD) contrast in the right hippocampus, while temporal sequences were associated with greater left hippocampal activity. Moreover, in tasks where the overall cognitive demands are similar, left-right differences still emerge and correlate with whichever information is

the most useful to solve the task. For example, in an object recognition task requiring pattern separation, the BOLD contrast was greater in the left hippocampus when semantic information was most relevant to the nature of the task, but, when spatial information was more pertinent, it was greater in the right hippocampus (Motley and Kirwan, 2012).

Therefore, there is substantial evidence for a left-right asymmetry in human hippocampal function. It has generally been thought that this asymmetry may arise due to the hemispheric asymmetry in language processing (Bishop, 2013). However, asymmetry of bilateral structures would allow functional division of labour and thus would be hypothesised to increase processing power. Indeed, it has recently been shown that a higher degree of lateralisation within certain human memory systems correlated with a higher ability in relevant tasks (Gotts et al., 2013). This raises the question of whether hemispheric asymmetry of memory function may have an evolutionary origin prior to the development of language, and thus might also exist in rodents.

Surgical and pharmacological lesion studies have revealed that the hippocampus is also essential for certain forms of memory in rodents, (Olton and Papas, 1979; Rawlins and Olton, 1982; Morris et al., 1982; Eichenbaum et al., 2012), and there have been some indications that a hemispheric bias may exist. Klur et al. (2009) found that, although unilateral infusion of lidocaine into the left or right dorsal hippocampus of rats did not impair the acquisition of the Morris water maze task, rats which had received left infusions during training were impaired on the retention probe trial; in contrast, when rats had acquired the task in the absence of infusions, a unilateral infusion prior to the probe trial only impaired those animals receiving a right hippocampal infusion. The authors also found a lateralised upregulation of some plasticity-related genes in the CA1 (Klur et al., 2009). In a spatial short-term memory task within a radial maze, Poe et al. (2000) found no evidence of asymmetry in young rats, but a hemispheric dissociation did emerge in a small sample of aged rats, since unilateral left, but not right,

hippocampal inactivation increased errors above control rats.

If an asymmetry in hippocampal function is present in rodents, it could arise from differences in the type of information received by each side, how it is processed, or a combination of both. It is has been proposed that information processing occurs at the dendritic level (Euler and Denk, 2001), and the range of postsynaptic spine morphologies suggests that different dendritic spines could perform distinct information processing functions. As previously described, there is a left-right asymmetry in adult mice that allows populations of the two main types of spine, with their different molecular and morphological characteristics, to be interrogated independently to test the proposal that they perform different functions in the mature brain. It is already established that the synapses receiving left CA3 input show spike timing-dependent LTP (Kohl et al., 2011) and I have extended this work here to show that this hemispheric asymmetry in LTP is robust even with a strong, high-frequency induction protocol. This suggests that hemispheric asymmetry is a fundamental characteristic of plasticity at the CA3-CA1 synapse, rather than an induction protocol-specific phenomenon.

LTP has been proposed as a cellular mechanism that may support learning and memory (Bliss and Collingridge, 1993; Martin et al., 2000; Morris, 2013). In the hippocampus, evidence in support of this hypothesis includes findings that manipulations that alter the magnitude of LTP also lead to changes in learning and memory (Tang et al., 1999; Malleret et al., 2001; Zhou et al., 2007), the acquisition of a behavioural task is associated with increased synaptic weights (Whitlock et al., 2006; Gruart et al., 2006; Valenzuela-Harrington et al., 2007), induction of LTP can occlude learning and learning induced-synaptic strengthening can occlude LTP (Whitlock et al., 2006). Altogether, this suggests that this asymmetry in the plastic properties of CA3-CA1 synapses may have relevance *in vivo*. If a left-right dissociation in hippocampal function exists, this might be useful in delineating AD processes, given that I have found these two types of

synapses are differentially affected by Aβ exposure.

5.1.1 Aim

A left-right dissociation of hippocampal memory function is present in humans, but it is not yet clear if a similar asymmetry is present in rodents. Therefore, I aimed to investigate whether there are any behavioural correlates of the striking difference in LTP between left and right CA3-CA1 synapses in mice. Furthermore, since the plastic synapses receiving left CA3 input are also those that are vulnerable to $hA\beta_{1\text{-}42}$-induced changes, any possible dissociation might be informative about the relevance of the synaptic dysfunction studied in mouse models of Alzheimer's disease to cognitive function.

Effectively mimicking naturalistic activity using ChR2 activation at CA3-CA1 synapses would prove very difficult, and the data might be difficult to interpret. However, optogenetic tools have also been developed to allow regional- and cell type-specific silencing of neurons on a millisecond timescale and, perhaps because circuits do not have sufficient time to adapt, using this technique can reveal new information about circuit involvement in memory processes (Goshen et al., 2011). Therefore, in order to interrogate the role of the left and the right CA3, I used acute optogenetic silencing of either the left or the right CA3 during long- and short-term memory tasks. Given the possible importance of NMDAR-dependent LTP for performance on associative spatial memory tasks (Morris, 2013), I hypothesised that the left CA3 input would be more important for a long-term spatial memory task than the right CA3 input.

5.2 Cell-type specific silencing and behavioural surgery

The light-sensitive chloride pump halorhodopsin (NpHR) is activated by green-yellow light; upon activation, it pumps chloride ions into the cell and thus hyperpolarises and silences them. In order to achieve the most effective silencing, eNpHR3.0 (Gradinaru et al., 2010) was used; this variant of NpHR contains an extra tag that permits more effective trafficking of the chloride pump to its functional location in the plasma membrane. eNpHR3.0 was coexpressed with eYFP to enable the expression to be visualised after behavioural testing finished. The most appropriate control for use with eNpHR3.0-eYFP currently available is using eYFP alone.

5.2.1 Viral expression throughout the dorsal CA3

For effective expression, the eNpHR3.0-eYFP experimental construct and the eYFP control construct were packaged in an adenoassociated virus (AAV) (supplied by UNC Vector Core). The viral serotype can affect the cell-type uptake and expression of the virus; an AAV5 serotype was selected to provide more effective spread of the virus than an AAV2 serotype, and hence maximise coverage of the dorsal CA3. In addition, the CaMKIIα-cre mouse line we have previously used to study excitatory neurons (Kohl et al., 2011), had been generated by pronuclear injection of a construct containing Cre driven by the CaMKIIα promoter (Tsien et al., 1996), rather than by homologous recombination, and therefore the genetic manipulation is less stable. Consequently, I decided that a CaMKIIα promoter should give more consistent levels of expression, which was especially important given the many other likely sources of variability in these experiments and since I could not verify expression levels until after behavioural testing.

To confirm that injecting AAV5-CaMKIIα-eNpHR3.0-eYFP or AAV5-CaMKIIα-eYFP into two sites in the dorsal CA3 of one hemisphere gave sufficient expres-

sion throughout one CA3 and its ipsilateral and contralateral projections to CA1, I injected mice at the two sites planned for behavioural surgery. This dual injection produced expression, detected by the presence of eYFP, throughout the entire CA3 of the dorsal hippocampus in one hemisphere and its Schaffer collateral and commissural projections to CA1 (**Fig. 5.1**(**A**),(**B**),(**C**)). Since eNpHR3.0-eYFP is translated into a single protein, the expression of eYFP was visible in the extracellular membrane of the CA3 pyramidal cells where the eNpHR3.0 functions as a pump, both at the soma (**Fig. 5.1**(**D**),(**E**)) and in the projections to CA1 (**Fig. 5.1**(**D**),(**F**)).

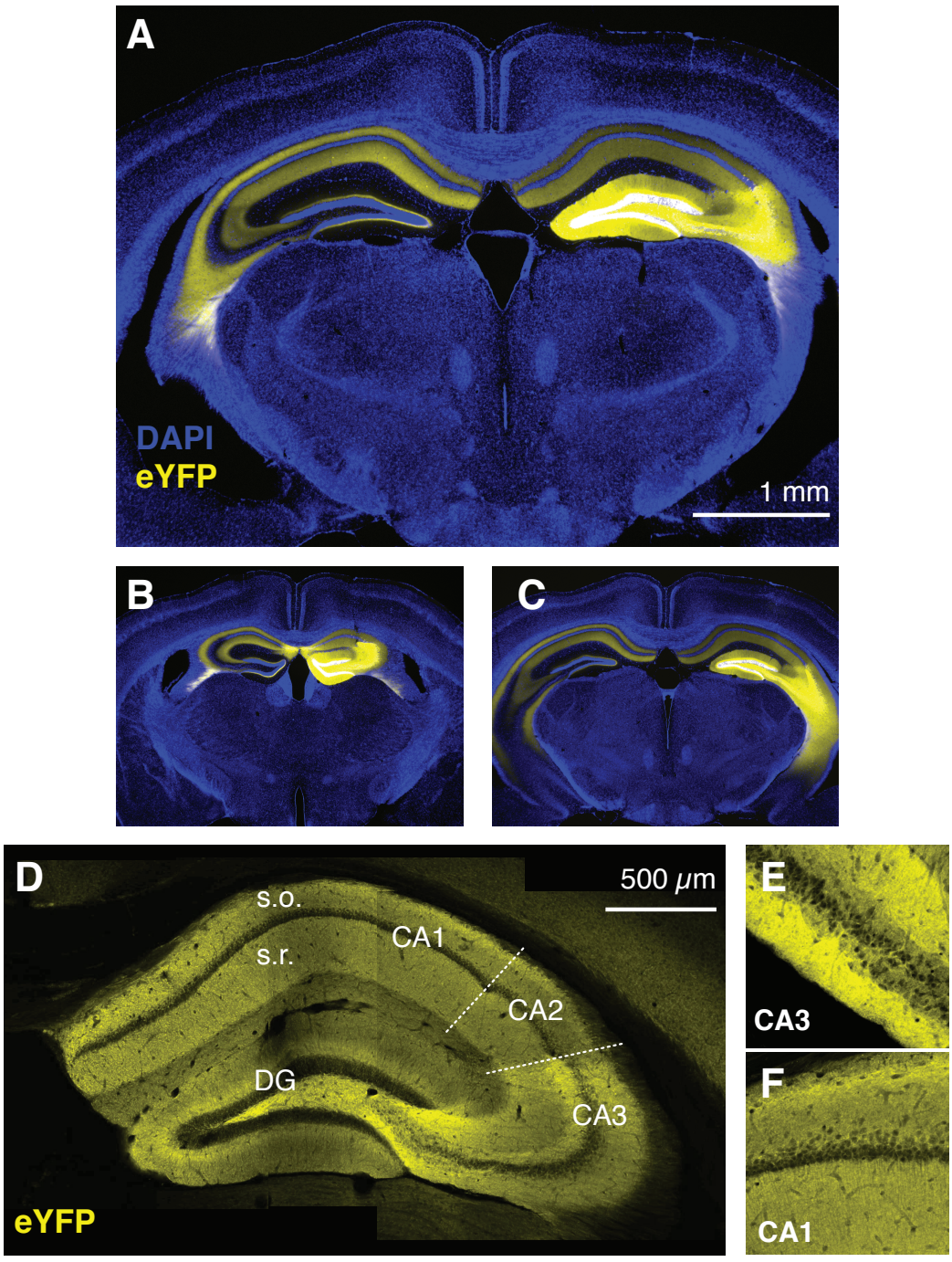

Figure 5.1: Dual unilateral injection of eNpHR3.0-eYFP and YFP gives expression throughout the dorsal CA3 and its projections. (**A**),(**B**),(**C**) Injection of AAV5-CaMKIIα-eNpHR3.0-eYFP or AAV5-CaMKIIα-eYFP into two sites in the dorsal CA3 of one hemisphere produced eYFP expression at the planned implant site (**A**), and also more anterior (**B**), and posterior (**C**), so that the entire dorsal hippocampus was covered. Expression was also visible in the Schaffer collateral (ipsilateral) and commissural (contralateral) projections to the CA1. Images in (**A**),(**B**),(**C**) illustrate a mouse that had been injected with AAV5-CaMKIIα-eYFP. DAPI stain is shown in blue, marking nuclei, and eYFP is shown in yellow. (**D**),(**E**),(**F**) Expression of eYFP in mice injected with AAV5-CaMKIIα-eNpHR3.0-eYFP is targeted to the cell membrane, where the functional pump sits, and is visible in the membranes of pyramidal neurons in the CA3 (**E**) and their projections to the CA1 (**F**). Image in (**D**) is a composite. eYFP is shown in yellow.

5.2.2 Optrode recording to test for silencing *in vivo*

To confirm that it was possible to achieve effective silencing of the CA3 *in vivo*, I injected mice with AAV5-CaMKIIα-eNpHR3.0-eYFP into the two sites planned for behavioural surgery, in the dorsal CA3 of either the left or right hippocampus, and performed optrode recordings in anaesthetised mice. The optrode consisted of an optical fibre that I stripped to the 200 μm core and then tightly glued to a 1 MΩ tungsten monopolar recording electrode. The tip of the recording electrode was positioned to protrude approximately 0.7 mm below the tip of the optical fibre to ensure that the recorded cells received illumination but were not damaged by the presence of the optical fibre.

In order to achieve anaesthesia that was stable for approximately 3 hours, but sufficiently light to record a high amount of neuronal spiking activity, I used urethane topped up with a small amount of ketamine/xylazine mix. The optrode recordings were made at the location where the implant would be located during behavioural testing. In order for results to be comparable with the level of silencing that might be achieved in a behavioural task where trials lasted approximately 20-30 seconds, I tested a 30-second period of silencing and repeated this one to four times at each recording site. This showed effective and reversible silencing of spontaneous spiking in single and multiunit recordings (light on: 8.6 ± 5.1% baseline spiking levels, one-sample *t*-test compared to 100%: $n = 7$ recordings from 2 mice, $P < 0.001$; after light on (30-60 s): 107 ± 12.7% baseline spiking levels; $P = 0.612$; **Fig. 5.2**(**A**)). Moreover, this silencing was repeatable (**Fig. 5.2**(**A**) inset), suggesting that it would still be effective in tasks requiring 10 trials a day. Since behavioural tasks can also last longer than 30 seconds, I injected another set of mice and a 3-minute period of silencing was used. Silencing was stable and reversible even for this extended period of time (light on: 33 ± 9% baseline, one-sample *t*-test compared to 100%: $n = 5$ recordings from 2 mice, $P = 0.002$; after light on: 144 ± 25% baseline; $P = 0.156$; **Fig. 5.2**(**B**)).

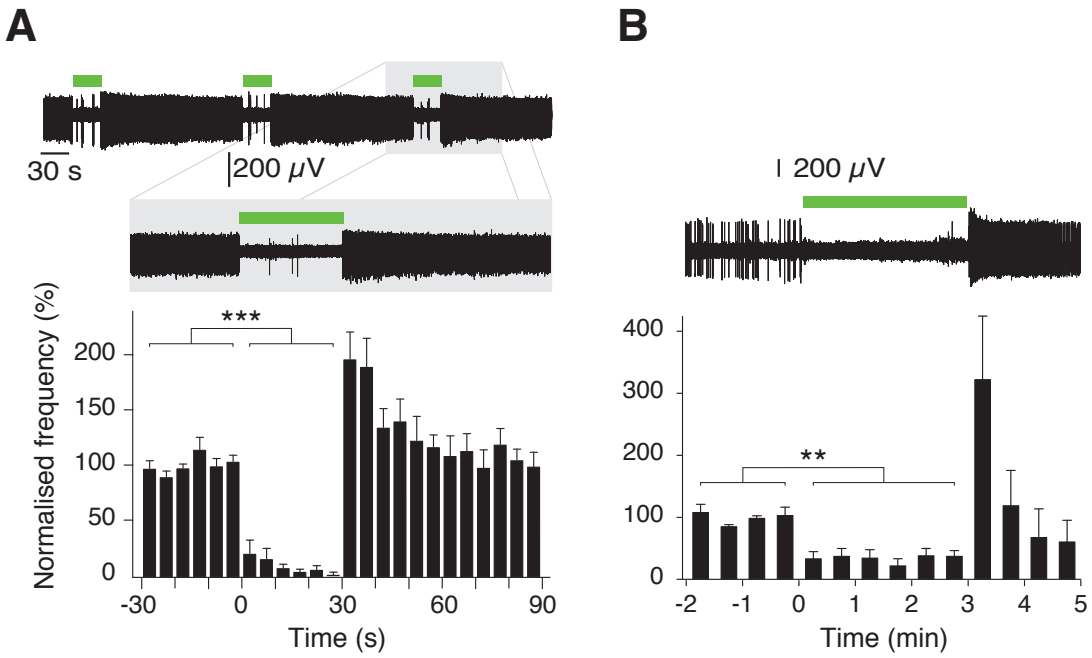

Figure 5.2: Optogenetics enables effective silencing of CA3 activity *in vivo*. (**A**) In mice that had received dual unilateral injections of the AAV construct containing eNpHR3.0, illumination of CA3 neurons in anaesthetised mice with green laser light for 30 seconds resulted in a reversible reduction in spontaneous spiking frequency. The normalised mean frequency of spiking is illustrated in the graph. Inset shows an example recording trace with three periods of silencing; grey window depicts one period of silencing. Green bars depict time with light on (**B**) Illumination of CA3 neurons in eNpHR3.0-expressing mice for 3 minutes also resulted in a reversible reduction in spontaneous spiking frequency. The normalised mean frequency of spiking is illustrated in the graph. Green bar depicts time with light on. Inset shows an example recording trace. Note the rebound activity observed at light offset (Raimondo et al., 2012), which is discussed later. ** $P < 0.01$, *** $P < 0.001$. Error bars represent s.e.m.

5.2.3 Behavioural surgery

To enable me to perform behavioural experiments blind to the group-identity of the mice, Dr Michael Kohl performed the injections and implant surgeries for all batches of mice used in behavioural testing with the exception of half of the last batch which I performed using virus that had been coded so that I could remain blind. Two injections of AAV5-CaMKIIα-eNpHR3.0-eYFP for experimental mice, or AAV5-CaMKIIα-eYFP for control mice, were made into two sites in the dorsal CA3 of either the left or right hippocampus. This ensured that virus delivery could not account for any of the behavioural differences. An optical fibre was then implanted between the two injection sites; the top section of the fibre-optic implant was contained in a metal cannula that could be coupled with patch cords to connect the mice to the light source during testing. The control mice underwent identical implant surgery to ensure that neither cell damage by the fibre-optic implant nor light delivery during testing could account for any behavioural differences. Mice were then left for 8 weeks for sufficient expression of eNpHR3.0-eYFP or eYFP to develop prior to starting handling and behavioural testing.

5.3 Long-term memory

The relationship between LTP at the CA3-CA1 synapse and hippocampus-dependent long-term memory is contentious (Bannerman et al., 2012; Gallistel and Matzel, 2013). Nevertheless, it has been shown that pharmacological and genetic manipulations that reduce the magnitude of CA3-CA1 LTP can also impair performance on long-term associative memory tasks (Tsien et al., 1996; Zhou et al., 2007), while enhancement of LTP is associated with improved performance (Tang et al., 1999; Malleret et al., 2001). Given the hemispheric dissociation in CA3-CA1 LTP in the mouse hippocampus, I aimed to test the effect of acutely silencing the left or the right CA3 during a hippocampus-dependent associative long-term memory task.

5.3.1 Appetitive spatial long-term memory task

In order to investigate whether unilateral dorsal CA3 silencing impairs performance during the acquisition of a hippocampus-dependent long-term memory task, an appetitively-motivated hippocampus-dependent Y-maze task was chosen. In this task, mice had to learn which arm of an elevated Y-maze was rewarded using extra-maze spatial cues. A pseudorandom order of arm starts and maze rotation between trials meant that intra-maze cues provided no information that could be used by the mice to perform the task successfully (Deacon et al., 2002; Reisel et al., 2002). It has been shown that short-term memory errors can impair the acquisition of spatial long-term memory task, but that the contribution of short-term memory errors to learning deficits can be eliminated by preventing arm re-entry during a single trial (Schmitt et al., 2003). Therefore, in order to isolate the long-term memory process in this experiment, mice were only allowed to make one arm choice each trial; if the mouse chose the correct arm, it was allowed to consume the food reward, but if the incorrect arm was chosen the mouse was removed from the maze and the trial was ended (i.e. the mice were not allowed to self-correct).

Mice received blocks of ten trials a day for eleven consecutive days, with five starts from the arm to the left of the designated rewarded arm, and five from the right (**Fig. 5.3**(**A**)) in a pseudorandom order. On the final day of testing, I delivered the food reward only once the arm choice was made, to test whether mice were using the olfactory cues of the reward to solve the task (post-choice baiting). Since the performance of mice did not deteriorate, it indicates they were using extra maze cues to determine arm choice. Light was delivered only for the duration of each trial (10-40 seconds) by manual control of the shutter.

Mice in the two control groups (left-YFP and right-YFP) and in the right-NpHR group acquired the task over the course of testing (**Fig. 5.3**(**B**)), reaching 90-100% accuracy (**Fig. 5.3**(**C**)). In contrast, the left-NpHR group showed impaired performance during acquisition of the task (left-NpHR = 21 mice, right-NpHR = 19 mice, left-YFP = 18 mice, right-YFP = 22 mice; two-way ANOVA; main effect of transgene (NpHR/YFP): $F_{1,76} = 6.01$, $P = 0.017$; transgene by hemisphere interaction: $F_{1,76} = 11.46$, $P = 0.001$; exploration of the interaction by analysis of simple main effects shows this arises due to a significant effect of transgene on the left hemisphere: $F_{1,76} = 16.62$, $P < 0.001$ and a significant effect of hemisphere for NpHR: $F_{1,76} = 13.29$, $P < 0.001$; **Fig. 5.3**(**B**),(**C**)).

In order to further investigate the effect of the optogenetic manipulation on task performance, I analysed the behaviour of the mice on the tenth day of testing, the last day prior to introducing the post-choice baiting control. This revealed that, of the 21 mice in the left-NpHR group, 7 of these mice scored only 4 or 5 correct out of 10 total trials, and thus were still performing entirely at chance level (**Fig. 5.3**(**D**)); no mice scored less than 4. Only two other mice out of the 59 others tested on this task were also performing at chance on this day (scoring 5 or 6), and were right-NpHR mice (**Fig. 5.3**(**D**)). A further three mice in the left-NpHR group performed at an intermediate level with a score of 7 or 8; there was also one mouse in this category in the right-YFP groups. All other mice scored either 9 or 10 (**Fig. 5.3**(**D**)).

Overall, these data demonstrate a differential effect of left and right CA3 silencing on a spatial long-term associative memory task.

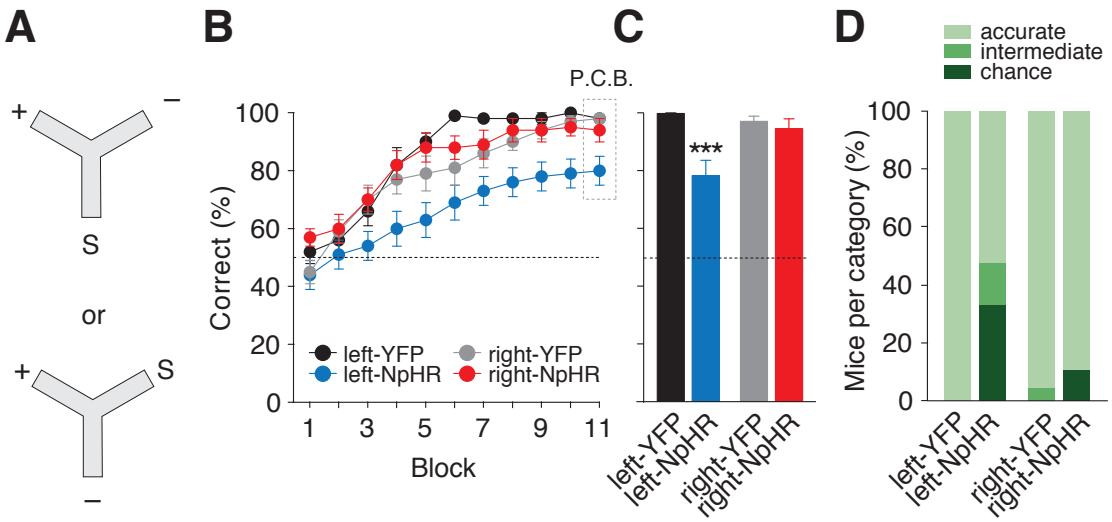

Figure 5.3: Left, but not right, CA3 silencing impairs performance on a spatial long-term memory task. (**A**) Mice were trained to find the rewarded arm (+) of an elevated Y-maze, which remained in a fixed location relative to extramaze cues, by a pseudorandom sequence of starts from the other two arms (S). Mice entering the non-rewarded arm (–) were removed from the maze. (**B**) Mice received blocks of 10 trials a day for eleven days and the number of correct arm entries was recorded. The performance of all four groups of mice improved over the course of testing, but to a different extent. On the final day of testing, the reward was given after the arm choice was made as a control for mice locating reward by odour (box labelled P.C.B.). Broken lines represent chance performance of 50%. (**C**) The average performance on the penultimate day. Broken lines represent chance performance of 50%. (**D**) The performance of each mouse on the penultimate day of testing was divided into three groups: chance performance (a score of 4 to 6 out of 10 correct, pale green), intermediate performance (score of 7 or 8 correct, light green), and accurate performance (9 or 10 correct, dark green) and the graph illustrates the percentage of mice in each group per category. *** $P < 0.001$. Error bars represent s.e.m.

5.3.2 Appetitive visual discrimination long-term memory task

It is possible that unilateral optogenetic silencing or *in vivo* light delivery could cause a generalised sensorimotor or motivational behavioural impairment that could account for the deficit in the left-NpHR group on the spatial long-term memory task. Moreover, lesion experiments have revealed a dissociation between the contribution of the dorsal and ventral hippocampus to behavioural performance: dorsal hippocampal lesions impair spatial learning while ventral hippocampal lesions reduce anxiety (Barkus et al., 2010). The implant location site was chosen to illuminate the dorsal hippocampus, but if there was systematic mistargeting of implants and/or viral injections between the dorsal and ventral hippocampus that differed between groups, behavioural effects that were not due to manipulation of the dorsal hippocampus may explain why the left-NpHR group alone were impaired on the spatial long-term memory task. In addition, each CA3 region projects bilaterally to the lateral septal nucleus (Swanson and Cowan, 1977), which, in turn, relays information to the ventral tegmental area in a reward-related circuit (Luo et al., 2011). Therefore, if only mice in the left-NpHR group had effective silencing of this projection, this might affect learning differentially between groups given the motivational aspect of this rewarded task. To test whether such explanations accounted for the asymmetry, a subset of the same mice, as well as a group of experimentally naïve mice, were trained on an appetitively-motivated, non-spatial visual discrimination T-maze task with the same motor and motivational demands as the appetitive Y-maze task (Reisel et al., 2002; Lyon et al., 2011) with light delivery.

This visual non-spatial long-term memory task was structured in an equivalent manner to the spatial long-term memory task, with a rewarded arm, a non-rewarded arm and a start arm (**Fig. 5.4**(**A**)). However, instead of using extra-maze cues, mice had to learn to associate either a grey or a black/white-striped goal arm with reward. The spatial position of the rewarded arm was varied in a pseudorandom order, and each day mice received a total of five

starts where the rewarded arm was in one position, and five when it was in the other (**Fig. 5.4**(**A**)); this meant that extra-maze spatial information could not be used to solve the task. Everything else was equivalent to the spatial long-term memory task: mice choosing the correct arm were allowed to consume the food reward, but, if the incorrect arm was chosen, the mouse was removed from the maze; light was only delivered for the duration of each trial; training took place over consecutive days; and on the final day I delivered the reward after mice had chosen an arm to confirm mice were not using food odour to solve the task (post-choice baiting).

Since this task has no relevant spatial information, dorsal hippocampal silencing should have no effect on the acquisition of the task. Indeed, all four groups of mice learnt the task and at an equivalent rate (left-NpHR = 15 mice, right-NpHR = 16 mice, left-YFP = 17 mice, right-YFP = 17 mice; two-way ANOVA; main effect of block $F_{7,427} = 80.27$, $P < 0.001$, but no main effect of hemisphere: $F_{1,61} = 0.43$, $P = 0.51$; no main effect of transgene: $F_{1,61} = 0.09$, $P = 0.76$; no hemisphere by transgene interaction: $F_{1,61} = 0.43$, $P = 0.51$; and also no interaction between block and transgene $F_{7,427} = 0.19$, $P = 0.99$, nor between block and hemisphere $F_{7,427} = 1.14$, $P = 0.34$ and no triple interaction $F_{7,427} = 0.36$, $P = 0.93$; **Fig. 5.4**(**A**),(**B**)) and were performing successfully at the end of testing (90-100% correct). This suggests that the impairment following acute silencing of left CA3 in the spatial long-term memory task was not due to a gross asymmetric disruption of sensorimotor or motivational aspects of task performance.

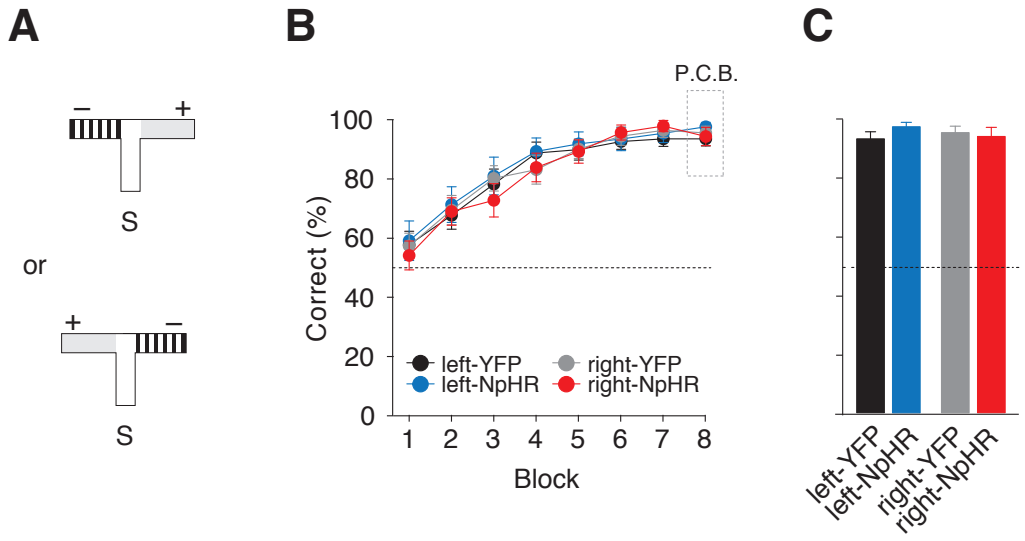

Figure 5.4: Unilateral CA3 silencing does not impair performance on a visual discrimination long-term memory task. (**A**) Mice were trained to find the rewarded arm (+) of a T-maze using visual cues (grey arm vs. black/white striped arm), the position of which was varied in a pseudorandom sequence relative to the position of the start arm (S). Mice entering the non-rewarded arm (-) were removed from the maze. (**B**) Mice received blocks of 10 trials a day for eight days and the number of correct arm entries was recorded. The performance of all four groups of mice improved over the course of testing. On the final day of testing, the reward was given after the arm choice was made as a control for mice locating reward by odour (box labelled P.C.B.). (**C**) The average performance on the penultimate day. Broken lines represent chance performance of 50%. *** $P < 0.001$. Error bars represent s.e.m.

5.4 Short-term memory

5.4.1 Spontaneous alternation T-maze task

The ability to dissociate between short- and long-term memory errors on a spatial task (Schmitt et al., 2003) and the different effects of hippocampal manipulations on tasks with distinct cognitive demands, both suggest that short- and long-term hippocampus-dependent memory may be supported by distinct neural or circuit mechanisms. Given that the left CA3 alone is required to support performance in a long-term memory task, it is further possible that such processes could have a different hemispheric bias. Therefore, I investigated whether a left-right asymmetry in unilateral CA3 silencing was also observed in hippocampus-dependent short-term memory.

I tested the same mice on spontaneous alternation in a T-maze, which is a hippocampus-dependent short-term memory task that harnesses the strong novelty preference displayed by rodents (Deacon et al., 2002; Deacon and Rawlins, 2006). Mice were allowed to make a free arm choice, and then a barrier was placed to contain them in the chosen arm for 30 seconds, allowing them to explore this arm; the mouse was then removed from the arm and immediately placed back in the start arm and the subsequent arm choice was recorded (**Fig. 5.5**(**A**)). Each trial was self-contained and mice received interleaved trials with and without light delivery. All four groups showed equivalent levels of spontaneous alternation with the light off (left-NpHR = 82 ± 3%, right-NpHR = 85 ± 3%, left-YFP = 83 ± 2%, right-YFP = 86 ± 3%), indicating that there was no hemispheric asymmetry in the effect of surgery or tethering to the fibre-optic cable. However, with the light on, striking differences emerged between the groups of animals (left-NpHR = 22, right-NpHR = 21, left-YFP = 21, right-YFP = 22; ANOVA; main effect of transgene: $F_{1,82} = 29.65$, $P < 0.001$; and a main effect of hemisphere: $F_{1,82} = 5.37$, $P = 0.023$; but the two did not interact: $F_{1,82} = 1.46$, $P = 0.23$; (**Fig. 5.5**(**B**)). Therefore, the highly significant main effect of trans-

gene shows that unilateral silencing of either the left or the right CA3 impaired performance on this short-term memory task. It also appeared that there was a trend towards a greater deficit in the right-NpHR group than the left NpHR group; it was notable that there was a main overall effect of hemisphere but it is not clear how to explain this. The fact that right-NpHR mice can exhibit a memory deficit rules out technique-based explanations for why there was only an effect of left CA3 silencing on the hippocampus-dependent long-term memory task. Therefore, this result strengthens the conclusion that the spatial long-term memory task is uniquely dependent on the left CA3.

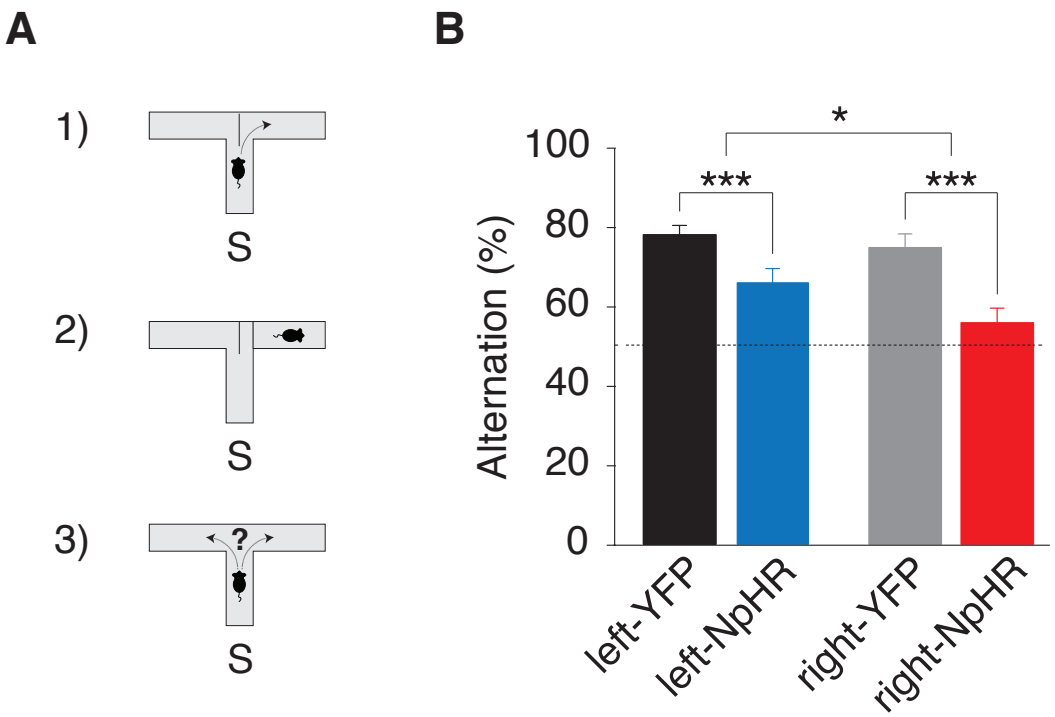

Figure 5.5: Unilateral CA3 silencing impairs performance in a hippocampus-dependent short-term memory task. (**A**) Mice were placed in the start arm (S) and allowed to make a free choice of arm. Once they entered an arm, a barrier was put in place so that they explored the chosen arm for 30 seconds. Mice were then removed and placed immediately back in the start arm and the next arm choice was recorded. If mice chose the novel arm, this was counted as a spontaneous alternation. (**B**) The average rate of alternation in the light on condition. Broken line represents chance performance of 50%. * $P < 0.05$, *** $P < 0.001$. Error bars represent s.e.m.

5.4.2 Novelty preference Y-maze task

The appetitive long-term memory Y-maze task is an explicitly spatial task, since only extramaze cues provide information relevant to the food location. In contrast, extramaze, intramaze and egocentric turning cues all provide information about the arm choices in the spontaneous alternation short-term memory task. Therefore, an additional short-term memory task with a greater contribution of extra-maze cues was also used. This novelty preference task is conducted in a Y-maze with colourless Perspex arms, where each arm remains in a fixed position relative to the extra-maze cues. The first phase of the task is an exploratory phase, and one arm remains blocked off by an opaque barrier, while in the second phase of the task all of the arms are accessible and the time spent in each arm is recorded (**Fig. 5.6**(**A**)). It is thought that primarily extra-maze cues are used to determine novel arm preference in the second phase, since the preference of wild-type mice for the novel arm remained if the maze was rotated between the first and the second phase of the task, but was abolished if the maze was moved to another room with different extramaze cues for the second phase of the task (Sanderson et al., 2007).

Light was delivered throughout the first and the second phases of the task, but was turned off for the minute hold between these phases while the mouse was in the home cage. The results from this task showed a similar pattern to those in the short-term memory spontaneous alternation task, with an impairment of unilateral CA3 silencing irrespective of whether it was the left or right CA3 that was silenced (left-NpHR = 6, right-NpHR = 5, left-YFP = 7, right-YFP = 4; ANOVA, main effect of transgene: $F_{1,18} = 14.91$; $P = 0.001$ but no main effect of hemisphere: $F_{1,18} = 0.39$; $P = 0.54$, and the two did not interact: $F_{1,18} = 0.05$, $P = 0.83$; **Fig. 5.6**(**B**)). Unlike in the spontaneous alternation experiment, however, there was not a trend towards a greater deficit in the right-NpHR group. It is possible that introducing a delay between the first and second phase of the novelty preference Y-maze trial could begin to recruit additional memory

processes that are more dependent on GluN2B subunit-containing receptors, as was suggested by Zhang et al. (2013) using a delayed alternation T-maze task and a delayed matching to place task in the MWM, since GluN2B subunits are concentrated in the postsynaptic spines receiving left CA3 input.

Overall, the deficit in both left-NpHR and right NpHR groups in this additional short-term memory task, which is heavily biased towards the use of extra-maze cues, suggests that the unique impairment in the left-NpHR group in the appetitive spatial long-term memory task might be related to the long-term associative nature of this task rather than its spatial nature alone. This strengthens the dissociation between the hemispheric involvement in short-term memory and long-term associative memory, with hippocampus-dependent short-term memory requiring both the left and the right CA3 for performance, but only the left CA3 being necessary in hippocampus-dependent long-term memory on the appetitive Y-maze task.

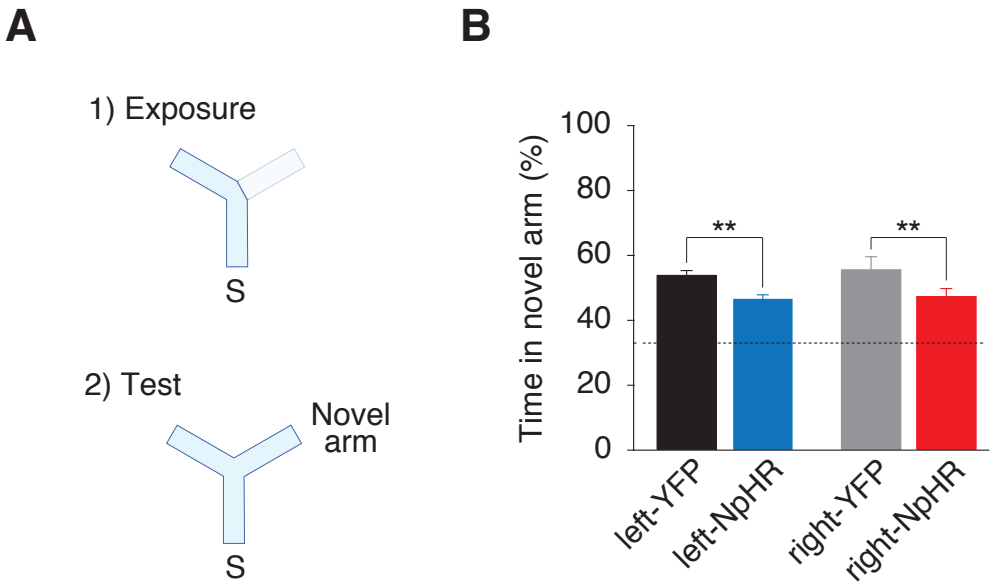

Figure 5.6: Unilateral CA3 silencing impairs performance in a spatial short-term memory task. (**A**) Mice were placed in the start arm (S) and allowed to explore two of the three arms of a colourless Perspex maze for five minutes. The third arm was blocked by an opaque barrier. After a one-minute hold in the home cage, mice were placed back in the start arm and were given access to all three arms for two minutes. The time spent in each arm was recorded. (**B**) The graph shows the average percentage of total time mice spent in the novel arm out of the time spent in all three arms during the two minute test phase of the task. Broken line represents chance performance of 33.3%. ** $P < 0.01$. Error bars represent s.e.m.

5.5 Verification of expression and implant location post-testing

In order to attribute the results to the effect of unilateral CA3 silencing, it was important to confirm that mice expressed sufficient levels of either the experimental eNpHR3.0-eYFP construct or the control eYFP construct, and that such expression was located in the dorsal CA3. In addition, it was necessary to verify that the implant was in a position that was able to illuminate the CA3. Therefore, after behavioural testing, mice were perfused and the fixed brain was sliced to allow imaging. I imaged slices that contained the implant tract under brightfield conditions to determine implant placement. These slices, and an additional series of sections throughout the hippocampus, were also imaged with fluorescence microscopy in order to detect eYFP expression.

All mice were found to have expression in the dorsal CA3 (**Fig. 5.7**(**A**)). The locations of implants were determined by the deepest extent of the implant (**Fig. 5.7**(**B**)), and all were in a position that could illuminate the CA3 (**Fig. 5.7**(**C**)). Moreover, there was no indication that the position of the implants varied systematically between the experimental groups. Although the spread of light and its fall off through tissue can be estimated, very little is known about the power of light necessary to silence neurons with different excitatory drives. Moreover, the way in which a given light power interacts with different expression levels over different distances introduces an additional level of variability in the extent of silencing achieved. A full characterisation of such effects was out of the scope of this work. Therefore, since there are no satisfactory criteria to determine fair exclusions, two broad criteria were used to avoid introducing any bias into the analysis. The first criterion was that expression was present in the dorsal CA3; the second criterion was that the tip of the fibre-optic implant was less than approximately 1.5 mm from the nearest CA3 pyramidal layer. All mice met these criteria, and therefore no exclusions were made.

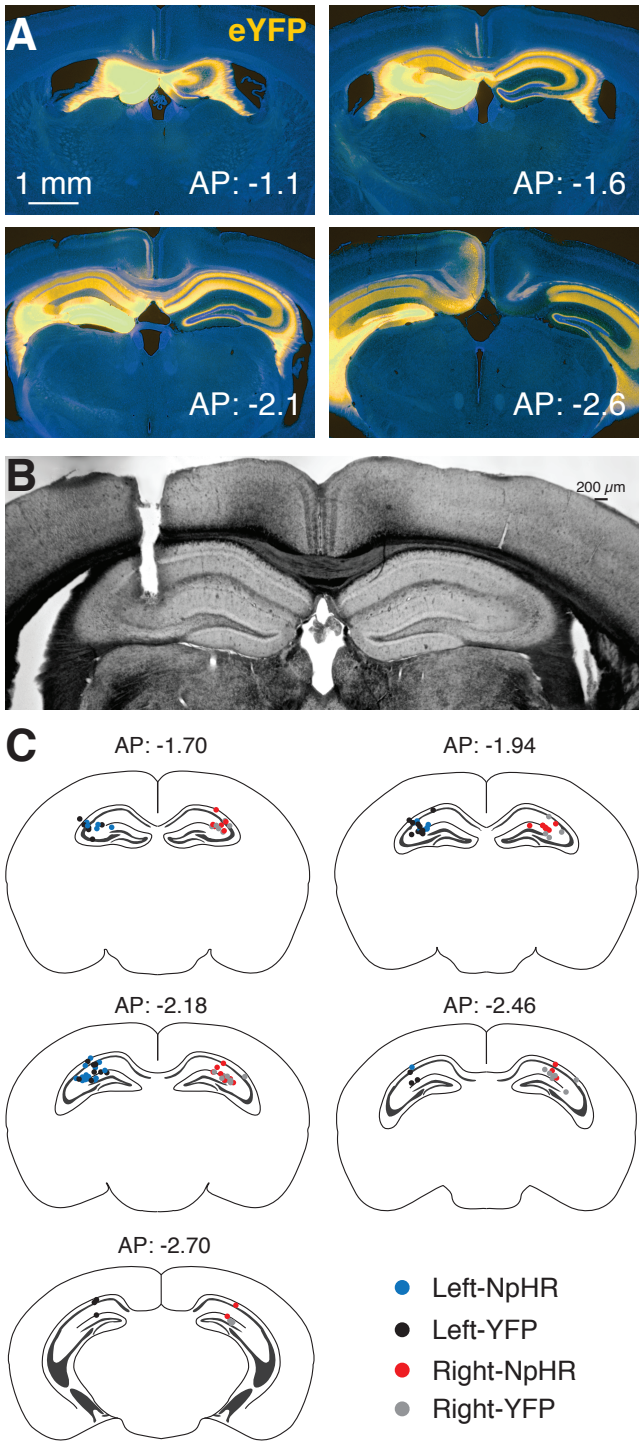

Figure 5.7: Expression and implant placement were verified post-testing. (**A**) An example of the expression pattern obtained, where eYFP was visible throughout the dorsal CA3 in the injected hemisphere and also in the projections to the CA1 both ipsilaterally and contralaterally. (**B**) An example brightfield image used to assign the placement of the implant. (**C**) The approximate locations of the fibre-optic tip for each animal used in behavioural testing.

5.6 Discussion

5.6.1 Summary

Using acute optogenetic silencing of excitatory neurons in either the left or right CA3, I have found that only the silencing of the left CA3 impaired performance on a hippocampus-dependent long-term memory task. In contrast, unilateral silencing of the left or right CA3 impaired performance on hippocampus dependent short-term memory tasks. The unique requirement for the left CA3 to perform a long-term spatial memory task was in stark contrast to the normal performance of mice on a non-spatial, visual long-term memory task, demonstrating the hippocampus-specific nature of this optogenetic manipulation. Overall, these findings suggest that there may be a left-right functional dissociation in hippocampal memory processing in the mouse.

5.6.2 Unilateral lesion experiments

A limited number of studies on the effect of unilateral hippocampal lesions have been published, and have described contrasting results. It was shown by van Praag et al. (1998) that electrolytic unilateral lesions of the right hippocampus in adult rats did slightly impair the acquisition of the MWM, but to a lesser extent than the impairment observed when right lesions had been made at the neonatal stage. However, since lesions were only performed in the right hemisphere, it is not known whether a greater effect of left hippocampus lesions might have been observed. In contrast, a study using pharmacological unilateral lesions of either the left or the right hippocampus of rats, found no effect of either of these manipulations on the acquisition of a MWM task (Klur et al., 2009). Nevertheless, an impairment on the retention probe trial was observed only in rats that had received left infusions during training (Klur et al., 2009), suggesting that left lesions might have slightly impaired learning. However, a different study found that it was only in aged rats where any asymmetries of unilateral pharmacolog-

ical lesions became apparent on a short-term memory task on the radial arm maze (Poe et al., 2000); however, this reported a slight left impairment on this short-term memory task. The only study performing unilateral lesions on mice found that, although these caused a smaller impairment than bilateral lesions on performance in the MWM, there was no clear difference between the left or the right hemisphere (Gerlai et al., 2002). If anything, though, there was a trend to a poorer performance in mice with right hippocampal lesions (Gerlai et al., 2002). Therefore, such studies have not provided conclusive evidence about a functional laterality in the rodent hippocampus. In addition, unpublished work exists showing that unilateral lesions have no effect on spontaneous alternation in a T-maze in rats (pers. comm. Dr. David Bannerman). In addition, surgical and pharmacological lesion studies remove or inactivate both the CA3 and the entire CA1, which receives input from both hemispheres, making it difficult to compare them to the more limited and acute manipulation used here.

5.6.3 Source of the impairments

NpHR is a pump that hyperpolarises the neuron and thus prevents the initiation of spikes. Therefore, during periods of silencing all the outputs of the neuron will be similarly affected. Consequently, the deficits found here could arise from silencing the requisite processing in the recurrent CA3 network, the subcortical output of CA3, or the CA3-CA1 synapse. Given the different pattern of results in the short- and long-term memory tasks, the source of impairment may vary between tasks with different cognitive demands. The possible reasons for the deficits in the short- and long-term memory tasks are discussed below.

5.6.4 Left CA3 involvement in long-term spatial memory

The impaired performance of the left-NpHR group on the spatial long-term memory task suggests that the left CA3 is a necessary component in the hippocampal circuitry that supports long-term memory, whereas the right CA3 is

not. The requirement for the CA3 in this memory task is not in direct agreement with the work of Nakashiba et al. (2008), where the authors found that the trisynaptic pathway (entorhinal cortex to dentate gyrus to CA3 to CA1 to entorhinal cortex) was not necessary for incremental spatial learning on the Morris water maze (MWM), and the monosynaptic pathway (loop between entorhinal cortex and CA1) could suffice. This discrepancy might arise because of the different tasks used, or because long-term nature of the doxycycline-mediated manipulation used to silence the CA3 output permitted adaptive changes to the network.

In order to perform successfully on the appetitive spatial Y-maze task, mice must acquire information about the location of the food reward within the room, recall this information, and make an accurate arm choice. These processes may not be entirely distinct, however, if the hippocampus was required to disambiguate between recalled memories of very similar arms, with one arm being associated with a reward and the other not (Bannerman et al., 2012). The left-NpHR deficit could arise through disruption of any of these components, and further investigation will be required to dissect which aspect, or aspects, of task performance require the left CA3 and are responsible for the impairment.

5.6.4.1 Acquisition

NMDAR-dependent LTP may be one cellular mechanism that supports associative learning (Bliss and Collingridge, 1993; Morris, 2013) and GluN2B subunit-containing NMDARs might be particularly important in this capacity. Rats with RNAi-mediated knock-down of GluN2B in the hippocampus acquired the MWM more slowly (Clayton et al., 2002). Furthermore, the GluN2B subunit-selective antagonist Ro 25-6981 blocked the acquisition of a trace-conditioning task and also the learning-associated increase in synaptic strength in the hippocampus (Valenzuela-Harrington et al., 2007). Moreover, LTP requires the activity of CaMKII (Barria and Malinow, 2005), and mice with a mutation that impairs the interaction between CaMKII and GluN2B exhibit spatial learning

deficits on the MWM task (Zhou et al., 2007). Mice have an asymmetric distribution of GluN2B subunit-containing NMDARs (Kawakami et al., 2003; Shinohara et al., 2008; Kohl et al., 2011) that correlates with a robust left-right asymmetry in LTP. In potentiation induced by both spike timing-dependent (Kohl et al., 2011) and high-frequency paradigms, it is only the GluN2B-rich synapses receiving left CA3 input that express LTP. Therefore, it is tempting to speculate that the left-NpHR group was the only group impaired in this task because synaptic strengthening at the plastic left CA3-CA1 synapses is required for mice to learn the association between food and a spatial location. Nevertheless, the evidence for this is currently purely correlative.

5.6.4.2 Recall

The other possible sources of impairment must also be considered. Recall is difficult to dissociate from acquisition with the present data because each trial provides training as to the reward location and simultaneously tests performance. Instead, it might be possible to test if unilateral light delivery to the CA3 impairs recall in an asymmetric manner by training mice in the absence of light until they acquire the task to a criterion level. At this point, unilateral light delivery could be introduced and the possible change in performance measured. However, necessary controls would need to be performed to account for the possible effects of state-dependency. In addition, using a probe trial to measure the effect on performance might introduce confounds because, unlike in the MWM, there is likely to be a conditioned association between the food itself and the food well as an object. Therefore, persistence at a food well might be more indicative of the strength of this conditioned association, rather than representing recalled knowledge about the spatial location of the reward within the room. Allowing mice to move freely during a probe trial and timing time spent in each arm might also not be ideal, because mice would have learnt that an empty food well signals removal from the maze and so may adopt different behaviour patterns.

Therefore, it might be preferable to use an alternative task to investigate possible left-right differences in recall. Context-dependent fear conditioning has clearly differentiated training (acquisition) and test (recall) periods. This is an aversive memory test and therefore may recruit different processes to the appetitive tasks used here. Nevertheless, new evidence has emerged that recall requires the CA1 region of the hippocampus even weeks after initial training (Goshen et al., 2011). Therefore, by optogenetically silencing either the left or right CA3 in different combinations during the training and test sessions, it might be possible to determine whether the left CA3 is involved in acquisition or recall. It is conceivable that different parts of the hippocampal circuitry might support different phases of this task; for example, the plastic left CA3-CA1 synapses might be hypothesised to support initial acquisition, and consolidatory processes may then transfer information to synapses originating in the right CA3, meaning recall would become dependent on the right CA3. In support of a possible importance of the right hippocampus in information storage, when rats that had acquired the MWM task in the absence of infusions were given a unilateral infusion prior to the probe trial, it was only the animals that had received a right hippocampal infusion which were impaired (Klur et al., 2009), although this study did not control for state-dependency.

5.6.4.3 Accurate choice

Another possible reason for the impaired left-NpHR performance in the spatial long-term memory task is that silencing affects the accuracy of arm choices, causing mice to make more mistakes despite knowing the correct food location. For example, it has recently been shown that mice with knock-out of the GluN1 subunit, and hence NMDARs, in the CA1 and dentate gyrus were impaired on an appetitive Y-maze task and a spatial radial arm maze task, where mice had to learn which of the arms were rewarded using extra-maze cues (Bannerman et al., 2012). Further investigation suggested that this deficit might arise because GluN1 knock-out mice were impaired at using extra-maze spatial information

to select the correct choice when there were similar, and thus competing, immediate cues. The current data does not irrefutably demonstrate whether the observed errors arose through such inaccuracy or because mice did not know the reward location (due to either acquisition or recall deficits). Nevertheless, a more detailed analysis of the performance at the end of testing provides an indication that an increased inaccuracy in the left-NpHR group is not the main explanation for the impairment. As described, most of the left-NpHR mice fell into two categories: either performing at chance, or performing at an equivalent high level of accuracy (9 or 10 correct out of 10 trials) to mice in other groups. Only three left-NpHR mice performed at an intermediate level. Moreover, those performing at chance were following the default behaviour pattern of always turning in a particular direction irrespective of which start arm they were placed in. Many mice in other groups adopted this behavioural pattern for at least one day at the early stages of the task (40-60% of each group), but were able to perform correctly by the end of testing. If inaccuracy were the main reason for the deficit, the pattern that would be expected is a greater number of mice making apparently 'random' errors, and thus falling mainly in the intermediate category. Nevertheless, the data could be reconciled with the findings of Bannerman et al. (2012) if making a correct spatial choice from an array of competing cues, or overcoming a the tendency to perform a default behavioural pattern, involves LTP at the left CA3-CA1 synapse. Alternatively, differences may arise because of the acute vs. chronic nature of these manipulations.

5.6.5 Left and right CA3 involvement in short-term memory

In contrast to the unique requirement for the left CA3 for a long-term memory task, unilateral silencing of either the left or the right CA3 was sufficient to impair short-term memory. Short-term memory deficits are found in mice that have knock-out of the GluN2A (Bannerman et al., 2008) or GluN2B subunit(von Engelhardt et al., 2008), and also in rats with pharmacological antagonism of GluN2A or GluN2B subunit-containing receptors (Zhang et al., 2013). This may

be because short-term plasticity processes that involve GluN2A and GluN2B subunit-containing NMDARs (Volianskis et al., 2013) are required to support short-term memory. Given that GluN2A and GluN2B subunit-containing NMDARs are found in synapses receiving both left and right CA3 input, this may account for why unilateral left or right silencing both cause an impairment. However, if both left- and right CA3-CA1 synapses can support the necessary processing, the considerable magnitude of the short-term memory impairment is perhaps surprising. One explanation might be that short-term memory is particularly demanding on neural networks, possibly recruiting a large proportion of the circuitry; if this were the case, the computational power of both left and right CA3 outputs might be required for effective performance.

It is also possible that the short-term memory deficit does not relate to NMDARs and, instead, unilateral silencing of either CA3 impairs performance because short-term memory requires communication between the left and right CA3, or even output from both the left and right CA3 onto a separate brain structure. Alternatively, the same result could arise if the left and the right CA3 play independent, but equally necessary, roles in the activity required for short-term memory. Consistent with this latter interpretation, gamma oscillations have been closely linked to short-term memory (Fuchs et al., 2007), and, interestingly, a left-right asymmetry of gamma power was recently reported in the CA1 region of the rat hippocampus (Shinohara et al., 2013). Another finding that supports the hypothesis that each hippocampus makes a different contribution to short-term memory function, is the finding of LaMendola and Bever (1997); the authors gave rats prior training on a radial maze in control conditions and then introduced them to a new maze environment but with either the left or the right whisker system anaesthetised. Under these conditions, rats forced to use the left hemisphere (with the right whisker system intact) learnt the new spatial task better. In contrast, those with the right whisker system anaesthetised, and thus using the left whiskers and hence right hemisphere, made more arm re-entry errors, suggesting a short term memory deficit.

5.6.6 The development and role of asymmetry

The contrasting effects of unilateral silencing on memory tasks with distinct cognitive demands suggest that the left and right CA3 perform complementary functions in learning and memory. The separation of these functions could stem from differences in the type of information received by each hemisphere, how it is processed, or a combination of both. It is possible that a link with a peripheral asymmetry may be involved, as the result of LaMendola and Bever (1997) could arise because external whisker inputs to the left hippocampus are more informative than those from the right.

It is not yet known when the left-right hippocampal asymmetry arises in mouse development or how it is maintained, but some mechanistic underpinnings are emerging. For example, Kawahara et al. (2013) showed that hippocampal neurons in wild-type mice express β2-microglobulin, but, if mice lacked this protein (with concomitant loss of expression of major histocompatibility complex class I proteins at the cell surface), they had no morphological or molecular asymmetry at the postsynaptic CA1 spines according to the source of afferent input. These proteins have been implicated in the activity-dependent refinement of neuronal circuitry and the regulation of LTP (Huh et al., 2000). Another mutant with disrupted asymmetry is the *inversus viscerum* mouse, where 50% of mice exhibit *situs inversus* but all mice lack left-right hippocampal asymmetry at the CA3-CA1 synapse, irrespective of the laterality of visceral organs; instead, synapses are characteristic of those receiving right CA3 input in wild-type mice (Kawakami et al., 2008). This suggests that the left-right hippocampal asymmetry may have a fundamental genetic basis, rather than being regulated by activity-dependent mechanisms alone. Moreover, although other interpretations for the deficits are possible, it is notable that these *inversus viscerum* mice are impaired on both spatial long-term memory and the retention of short-term memory (Goto et al., 2010). Not only does this suggest that the left-right asymmetry may be required for normal hippocampal memory

function in adult rodents, it is consistent with the possibility that left CA3-CA1 synapses are required to support for spatial long-term memory.

The asymmetry in human hippocampal function is well established (Burgess et al., 2002). If parallels exist in the rodent, it suggests that, rather than being a simple reflection of the asymmetry in language processing (Bishop, 2013), hippocampal asymmetry might have arisen early in evolution to allow for more efficient use of bilateral brain structures in memory processing.

5.6.7 Silencing with optogenetics

The cell-type specificity and millisecond precision conferred by optogenetic silencing may reveal network mechanisms unforeseen by conventional, genetic and pharmacological lesioning studies (Moser and Moser, 1998; Guscott et al., 2003; Nakashiba et al., 2008), and thus help develop a fuller understanding of memory processes. Nevertheless, there are some important technical considerations that are directly relevant to the interpretation of the work presented in this chapter.

5.6.7.1 The effect of light-delivery

Mice have dichromatic colour vision, with cones of maximum sensitivity to ultraviolet-blue and green light that do provide some capacity for colour vision (Jacobs et al., 2004). Therefore, optogenetic silencing using any of the currently available constructs requires the delivery of light that is within the wavelength range visible to mice. It is not known how the light might be perceived, but the presence of light during tasks could cause a wide range of possible effects on behaviour; these include, but are not limited to, triggering anxiety, acting as a distractor, or even increasing attention. In order to reduce the numbers of mice used in these experiments, all tasks in which mice could be tested only once were conducted with light delivery during all trials. However, mice could be tested repeatedly on the spontaneous alternation task, and therefore a 'light off'

condition was included. If the analysis was extended to include these data, then a significant effect of condition ('light on' vs. 'light off') was found in YFP mice ($F_{1,82}$ = 9.07, P = 0.003), as well as the predicted effect in NpHR ($F_{1,82}$ = 85.53, P < 0.001). Therefore, it is important to consider whether this effect of light could alter the interpretation of the data. In particular, since the results specifically relate to asymmetry, hemispheric differences in the visual stream should be considered. However, there is no indication that the mouse ventral visual stream which projects to the parahippocampal regions has any hemispheric bias (Wang et al., 2012). Another possible consequence of light delivery is thermal effects. The light power used in behavioural experiments is below the damage threshold and permitted repeated periods of silencing in optrode recordings. Nevertheless, heating effects cannot be excluded, and these would be greatest in the implanted hemisphere.

To try and control for any possible visual or thermal effects, NpHR mice were compared to YFP control mice that also received light delivery. Moreover, all comparisons were made within the 'light on' condition, to take any possible asymmetric effects of light delivery into account. The only comparison that could indicate whether there is an asymmetry in the effect of light delivery is that between the left-YFP and right-YFP groups, since any effects in the NpHR groups might arise from CA3 silencing. Importantly, there were no significant differences between these YFP groups in any of the 'light on' experiments, suggesting that left-right effects of light delivery alone cannot explain why only the silencing of the left CA3 impaired performance on the hippocampus-dependent long-term memory task. Furthermore, even if thermal effects, such as altering naturalistic activity patterns, did contribute to the impairments seen, they do not undermine the conclusion that there is a hemispheric asymmetry in memory processing, but the explanation for the results cannot be attributed to silencing.

Red opsins for activation (Lin et al., 2013a) and also for silencing are in development. Once these are available, the advantages of using such opsins in

future work are threefold. Firstly, red wavelength light would scatter less and thus penetrate tissue more effectively. Therefore optogenetic silencing could be achieved in a larger tissue volume; it may even be sufficient to deliver light through the skull in mice and avoid invasive surgery. Secondly, rats and mice are not sensitive to these long wavelengths and therefore it should be possible to avoid the visual effects of light-delivery. Thirdly, opsins with sensitivity to red light alone could be combined with blue light-senstive opsins to independently control two pathways within the same brain region.

5.6.7.2 Characteristics of NpHR-mediated silencing

NpHR, Arch and ArchT are the main types of opsin available for silencing, and when selecting one for use in behavioural experiments there is a trade-off. NpHR has the most persistent and steady hyperpolarising photocurrents over 1 minute of silencing (Mattis et al., 2012) and may even be effective in continuous use for up to 30 minutes (Goshen et al., 2011). Therefore, since the duration of silencing for the various behavioural tests lasted from periods of ten seconds to five minutes, it was deemed necessary to use an opsin where the levels of silencing achieved within each of these periods were as equivalent as possible, so that comparisons between hemispheres could be made across tasks. Therefore, the steady photocurrents of NpHR were considered important.

However, the disadvantage of using NpHR is that it is a chloride pump which pumps Cl^- ions into the cell to generate hyperpolarisation, while Arch and ArchT pump H^+ out of the cell to hyperpolarise it. Therefore, the activation of NpHR causes a build up of Cl^- ions in the cell. This alters the reversal potential for $GABA_A$ receptors such that, after NpHR activation, GABA briefly has a depolarising effect on pyramidal neurons and the frequency of synaptically-evoked spiking is higher than before; this effect increases in magnitude as the duration of silencing increases (Raimondo et al., 2012). Rebound spiking after light delivery was detectable in the optrode recordings, and was much more

pronounced following the extended period of silencing. It is possible that such rebound spiking once the light was turned off at the end of a trial could interfere with the information that had just been encoded and thus affect the performance on the next trial and the rate of acquisition. This would be relevant to the long-term memory task, which requires incremental learning. In the short-term memory tasks, each trial was discrete and therefore rebound spiking is unlikely to influence the performance on other trials. Another possibility is that the rebound spiking would not disrupt previously encoded information, but could occlude future learning. For example, it has been found that induction of LTP at the CA3-CA1 synapse *in vivo* precluded further learning of a trace conditioning task (Gruart et al., 2006). Consequently, an alternative interpretation for why left-NpHR mice alone were impaired on the spatial long-term memory task is that the rebound spiking triggers a high-frequency induced LTP-like phenomenon at the plastic CA3-CA1 synapses receiving left CA3 input, which, in turn, become 'saturated' and cannot support learning. However, even if this effect does account for the left-right difference on the spatial long-term memory task, it still suggests that there is an asymmetry in the function of the hippocampal network with plastic left CA3-CA1 synapses being required to support long-term spatial memory.

5.6.8 Perspective

The results presented in this chapter reveal an unexpected dissociation between the left and the right hippocampus. They are consistent with the conclusion that the left and right CA3 subserve different functions in hippocampus-dependent memory, with only the left CA3 being necessary to mediate long-term associative hippocampus-dependent memory. I have hypothesised that this effect could arise because the left CA3-CA1 synapses are the only synapses able to support LTP, and that potentiation at these synapses is necessary for successful performance on this task. A demonstration of whether this explanation does underpin the left-right difference on the spatial long-term memory task might

be possible if the projections onto CA1 cells could be selectively silenced, rather than all CA3 outputs. The optogenetic toolkit is expanding rapidly and, recently, two optogenetic systems have become available that can inhibit presynaptic release in organotypic hippocampal slices; one technique has harnessed light-responsive mGluR receptors (Levitz et al., 2013) and the other involved the generation of synaptic proteins that inactivate on light exposure (Lin et al., 2013b). Nevertheless, the temporal advantage of opsins has been sacrificed by the second approach, and it is possible that altering mGluR activity may also impact on plasticity processes. Therefore, the most suitable tool to pursue this work further would be one that can mediate silencing at the axon by terminating spikes that have already been generated.

An alternative approach to probe the mechanisms underlying the asymmetry relates to the different types of activity that can be recorded during the short- and long-term memory tasks and also within different phases of the same task. This might reveal whether different strength gamma oscillations are present in the CA3 of each hemisphere during a short-term memory task. Regarding the appetitive long-term memory task, it is known that theta-gamma oscillations are recorded during exploratory behaviours (Bragin et al., 1995), while high-frequency sharp waves have been recorded during consummatory behaviours (Buzsáki et al., 1992). These sharp waves may support a consolidation process (Nakashiba et al., 2009) and, therefore, such activity could mediate synaptic strengthening in an LTP-like process; possibly in a dopamine-dependent manner (Lisman et al., 2011). To investigate this, single and multiunit activity could be recorded during different phases of the long-term memory task, and compared between hemispheres. This might help determine when and where changes in synaptic strength occur. In addition, to test the possible importance of the sharp wave ripples in learning the association between reward and location, silencing could be limited to the time when the mouse is consuming the food reward to test if this causes the same magnitude of impairment as that produced when silencing occurs throughout a trial.

The neural mechanisms, and the location of such mechanisms, that support spatial learning and memory remain contentious (Bannerman et al., 2012; Gallistel and Matzel, 2013). Although care is necessary when interpreting the effects of optogenetic manipulations on behaviour, the cell-type specificity and temporal precision offered by this technique allows new questions to be addressed that should hopefully advance our understanding of hippocampal function in memory processing.

CHAPTER 6

General discussion and conclusion

6.1 Summary of findings

The key findings in this thesis are:

1. Tau protein is required for Aβ to impair tetanus-induced LTP, suggesting that there may be an important interaction between Aβ and tau, with tau acting downstream of Aβ. An increase in tau phosphorylation was observed in the presence of Aβ, and a GSK-3 inhibitor returned this enhanced phosphorylation to control levels and restored LTP. This suggests that the synaptic impairments triggered by the interaction between Aβ and tau may require tau phosphorylation mediated by the tau kinase GSK-3.

2. Acute exposure to Aβ caused a reduction in the N/A ratio in wild-type mice, but not in *Tau*$^{-/-}$ mice; this may explain why *Tau*$^{-/-}$ mice were not vulnerable to the Aβ-induced LTP impairment. The data are consistent with the interpretation that the change in N/A ratio is mediated by a selective reduction by GluN2B subunit-containing NMDARs; a GluN2B selective antagonist caused no further reduction in N/A ratio when applied after pre-treatment with Aβ and, moreover, this N/A ratio reduction was only observed in GluN2B-rich synapses receiving input from left CA3. In addition, these GluN2B-rich left CA3-CA1 synapses were required for tetanus-induced LTP, which suggests that the plastic synapses may be those most vulnerable to Aβ-induced synaptotoxicity and therefore should be the focus of neuroprotective treatments.

3. Acute unilateral silencing has revealed a left-right difference in the requirement for the mouse hippocampus in learning and memory. Silencing the left CA3 impaired performance in a hippocampus-dependent long-term memory task, but silencing the right CA3 had no effect. In contrast, unilateral silencing of the left or the right CA3 impaired performance on hippocampus-dependent short-term memory tasks. This suggests that the

asymmetry in spine morphology, molecular content and ability to potentiate could have implications for hippocampal function, and the results are consistent with the existence of a division of labour between parallel hippocampal networks.

Below, I will briefly discuss the validity of these key findings and suggest how they can be drawn together to contribute towards our understanding of hippocampal function in health and disease.

6.2 Use of rodents as a model system for human disease

In the work presented in this thesis, the mouse has provided the basis of the model system used to study aspects of AD pathology. It is worth questioning whether it is appropriate to use mice for the purpose of studying AD pathology, especially given the limited translational success of these studies. However, we do not yet know why therapies that have proved successful in ameliorating pathology and cognitive deficits in mice models did not translate effectively into the clinic; one possibility is limitations to mouse models, discussed below, but it is also worth noting that clinical trials tend to test novel therapies in patients where the level of pathology is much more advanced than that found in mouse models. This has highlighted the importance of finding fluid biomarkers to help identify early pathology in humans (Blennow et al., 2012).

It is likely that at least some of the underlying molecular mechanisms that mediate pathology will be conserved in mice, but, importantly, transgenic mouse models of AD do not recapitulate the spectrum of pathologies in the human condition. In particular, genetic mutations that cause APP and PSEN overexpression in mice do not promote tau neurofibrillary tangles (LaFerla and Green, 2012); this led to the development of an AD mouse model with an additional tau mutation to study this major aspect of the disease (Oddo et al., 2003). It is not clear why the genetic mutations that cause AD and NFTs in humans do

not also result in NFT formation in mice. It could be because such molecular pathways are relatively poorly conserved, which would have implications for how relevant the findings presented here would be to a possible therapeutic avenue. Another possibility is that the relatively short lifespan of a mouse does not permit full development of NFTs, which may take many years to establish in humans. Alternatively, it may be that, despite becoming hyperphosphorylated, mouse tau has a lower propensity to aggregate; crossing the H1 mouse line with an APP mouse line would help to investigate this possibility. Previous models where hAPP mutations have been expressed in the presence of wild-type human tau do not show NFTs, but this may because mouse tau was still present (Chabrier et al., 2012). Interestingly, it has been reported that mice expressing human tau alone develop hyperphosphorylation and insoluble paired helical fragments of tau in old age, without exogenous Aβ application or endogenous Aβ mutations (Andorfer et al., 2003).

A more promising model to study pathology might be a recently developed transgenic rat model of AD (Cohen et al., 2013), in which APP and PSEN1 mutations lead to tauopathy and neuronal loss, and therefore this model better recapitulates the spectrum of AD pathology. Nevertheless, all animal models created by genetic manipulations will most closely resemble the rarer genetic familial AD condition as opposed to sporadic AD. Whilst the pathologies are indistinguishable between familial and sporadic AD, it remains possible that different molecular pathways mediate the disease progression in each form of AD. One alternative to better model sporadic AD is to use different animal models that naturally develop the pathologies associated with AD. For example, the aged wild-type rodent *Octodon degus* develops the neuropathological hallmarks of AD including amyloid plaques and NFT (Inestrosa et al., 2005), and also disconnectivity of the hippocampus (van Groen et al., 2011). Ardiles et al. (2012) have recently described the functional correlates of this pathology, finding that the age-related increase in Aβ oligomers and phosphorylation of tau is associated with deficits in LTP, and impairments in spatial and object recognition

memory.

An additional approach, that will be useful alongside *in vitro* and *in vivo* studies using rodent models of AD, is the use of human stem cell-derived neurons. While this approach forgoes the ability to investigate a brain structure such as the hippocampus, culture systems do facilitate detailed imaging and molecular manipulations. The major advantage of this technique is that AD is a human disease, and therefore the molecular pathways underlying aspects of this condition might be best investigated or, at least confirmed, in cultures of human-derived neurons.

Overall, whilst it could be argued that mice might not be the best model for AD, they remain useful due to their amenability to experimentation and, especially, because it is not yet established whether the failure to translate findings from mice arises primarily through a species divergence in pathological processes or because of the 'late-stage' nature of clinical trials. However, the disconnect between findings in mice and the results of clinical trials makes further research into predictive biomarkers imperative, particularly given the ethical considerations of testing prophylactic drugs. Therefore, while for the time being it seems that the approach taken here using mice may still have value, it is clear that many approaches must continue in parallel so that the findings that are consistent across species, from human stem cell-derived neuronal cultures to the behavioural level in rodents, can be focussed on as potential therapeutic avenues.

6.3 Use of slices as a model system

The slice model used here is a particularly artificial system to investigate a disease that manifests throughout the entire brain, where there is constant interactivity between different structures. However, many different levels of investigation are required to understand a disease as complex as AD, ranging from the molecular disruption to the behavioural phenotype, and it is not more valid to

investigate one than another. In order to best study each of these levels, different models are required. In this thesis I have chosen to investigate changes at the synaptic level and the processes that underlie them. Therefore, despite the advent of optogenetics meaning that the extent of experimental control possible *in vivo* is increasing, *in vitro* slices remain a useful model system. They provide more direct access for whole-cell patch clamp of pyramidal neurons, and more straightforward pharmacological access that allows for greater consistency in the pharmacological concentrations used between experiments. The primary advantage to using such a reductionist approach is the greater manipulative power afforded *in vitro*, which has enabled me to test the effect of Aβ in combination with different pharmacological agents to start to dissect the mechanisms that account for the involvement of tau in the synaptotoxic effects of Aβ.

Nevertheless, within the constraints of using a slice preparation, it should also be considered whether or not the hippocampus is an appropriate brain region to study. AD does not affect the whole brain uniformly, and the hippocampus is one of the earliest brain regions affected (Braak and Braak, 1995). This suggests that, if one area is to be studied in isolation, the hippocampus is a useful model system. Although the entorhinal cortex shows pathology prior to the hippocampus, the latter has the advantage of our wealth of knowledge about the plasticity processes at the CA3-CA1 synapse and the synaptic mechanisms that support them; these can be used as the basis of investigations into which processes are disrupted. Moreover, despite acute hippocampal slices containing only a small portion of the hippocampus, they can still exhibit some of the oscillatory network properties visible in an intact preparation, and the nature of NMDAR-dependent plasticity induced *in vitro* appears equivalent to that induced *in vivo*. Irrespective of whether LTP proves to be the cellular mechanism underlying learning and memory and, in particular, if LTP at the CA3-CA1 synapses supports associative learning, LTP provides a readout for possible synaptic dysfunction at the *in vitro* level. This measure is more useful than cell death when trying to understand the early pathological changes, especially

since cognitive dysfunction arises before extensive neuronal loss in AD patients (Selkoe, 2002).

Overall, therefore, despite limitations, acute slices are a useful model to investigate synaptic mechanisms and remain useful in the study of disease. However, they are only the starting point, and new techniques such as optogenetics, and improvements to our current techniques such as new lightweight and minimally damaging chronic recording devices, mean it is becoming increasingly possible to transition from findings in *in vitro* work directly to the *in vivo* level.

6.4 Use of acute Aβ application

AD is a progressive neurodegenerative disease; however, rather than use a transgenic AD model where Aβ is naturally processed *in vivo* and exposure is chronic, here I have used short-term incubations with synthetic Aβ. This is clearly a highly artificial system, but one that may still be useful to understand how pathology develops in AD and to elucidate possible early points of interception to slow such progression. With accumulating exposure to Aβ, many molecular pathways are likely to be recruited, and the apparent discrepancy between the findings here of possible synaptic NMDAR reduction with other findings of enhanced low level Ca^{2+} influx and extrasynaptic overactivation (Li et al., 2011) only serve to highlight how pathological changes may progress over relatively short time periods (Um et al., 2012). Therefore, in order to understand the complexity of AD development, very early stage models with acute Aβ application may provide more amenable to determining triggering mechanisms and highly vulnerable neural pathways, such as synapses characteristic of the left CA3-CA1 synapse in mice. Now, however, it will be important to test whether there is degeneration of, or functional changes to, the left CA3-CA1 synapse *in vivo* using chronic transgenic mouse models.

There are also considerations to be taken into account about the precise synthetic Aβ preparation used here. Aβ is a very dynamic molecule that can exist

in equilibrium between many different forms. The inhibition of LTP by Aβ is a well-established phenomenon that has been reported by many different groups (Cullen et al., 1997; Lambert et al., 1998; Walsh et al., 2002; Wang et al., 2004). That this effect was replicated here suggests that Aβ was assembling into the soluble oligomers that are thought to mediate synaptotoxicity under the experimental conditions used. In order to investigate the mechanism underlying the LTP results, this same Aβ preparation and incubation technique was used in the whole-cell patch-clamp work. Two collaborators have independently confirmed using atomic force microscopy that low-N oligomeric molecules are present in the Aβ preparation used. Larger, possibly fibrillar, molecules were also observed, but it is possible these would be less able to penetrate tissue and hence less toxic. One of the main effects of using a mixed Aβ preparation is that the precise composition may vary daily, and this could introduce greater variability into the results. An additional consideration is whether the Aβ preparation used might generate species that ultimately cause the same impairment of LTP, but do so through different molecular pathways to those reported by other groups. Therefore, it is encouraging that the same involvement of GSK-3 in mediating the Aβ-induced LTP inhibition has been found independently in another laboratory, even with many experimental differences, including the use of patch-clamp recordings in organotypic slices of rats, a different Aβ preparation technique and higher concentration, and also using a different GSK-3 inhibitor (CT-99021). Moreover, the importance of tau in mediating synapto- and cytotoxicity has also been very reproducible, having been shown in cultured neurons (Rapoport et al., 2002; Jin et al., 2011), in transgenic mouse models mice overexpressing Aβ (Roberson et al., 2007, 2011) and, more recently, with a particularly aggressive pyroglutamylated form of Aβ (Nussbaum et al., 2012). This reproducibility, extending across transgenic animal models of AD (Roberson et al., 2007, 2011) to extreme measures of cell death (Rapoport et al., 2002), suggests that the processes accessed by the acute Aβ application used here may also be relevant to later stages in the progression of pathology.

It has been suggested that a more unified method of preparation should be used throughout the field of AD research, given the volume of apparently contradictory findings. This would be helpful in many respects and, indeed, in the future it would be important to verify the N/A ratio findings here using a different Aβ preparation. Nevertheless, at least some variation is important. Firstly, it would allow for novel technical developments, for example the fluorescent labelling of Aβ monomers to allow tracking. Secondly, it is not yet known what the best preparation would be, especially given that what is most representative of the species found *in vivo* may change during AD progression. Thirdly, using a variety of preparations may generate new discoveries. Finally, if the same finding is reproduced across laboratories even when many different types of Aβ preparation are used, it suggests that such an effect may be biologically relevant. In addition, the findings here suggest that another possible source of variation contributing to the contradictory conclusions drawn about the effect of Aβ may be because divergent pathological processes take place in different types of spine.

6.5 Use of pharmacology

In order to investigate which molecules might be the components of the pathological pathways causing the LTP deficit in the presence of Aβ, I have used pharmacology to block individual candidate molecules. I have previously discussed the use of GSK-3 inhibitors and concluded that, although it seems GSK-3 may play an important role, the interpretation of data is not entirely straightforward when the enzyme is at the hub of multiple pathways, even if a highly specific GSK-3 antagonist is used. Here I will focus on the use of Ro 25-6981 as the GluN2B antagonist.

Given that Ro 25-6981 did not cause any further reduction in N/A ratio in cells pre-incubated with Aβ, I have attributed at least some of the overall change in N/A ratio following Aβ exposure to a reduction in the current me-

diated by GluN2B subunit-containing receptors. I have also used Ro 25-6981 to show that, although tetanus-induced LTP does not require Ca^{2+} influx through GluN2B subunit containing NMDARs, GluN2B-rich postsynaptic spines support this form of plasticity. Ideally, these results would be balanced with the use of a GluN2A-selective antagonist, to show theoretically a double dissociation. Two possible GluN2A blockers are the competitive antagonist NVP and the non-competitive antagonist Zn^{2+}. However, the limited specificity of the competitive antagonist NVP (Paoletti and Neyton, 2007), and the possible uptake and consequent effect on intracellular signalling pathways by Zn^{2+} (Smart et al., 2004), might make it difficult to interpret data obtained using either antagonist.

Ro 25-6981 has a low maximum efficacy and so does not block all GluN1/GluN2B receptors. Therefore, if Aβ-triggered GluN2B internalisation does underpin the reduction in N/A ratio, the extent of this effect cannot be estimated: the concentration of Ro 25-6981 used here is likely to have achieved close to the maximum possible block, but estimates suggest that this may only be in the order of approximately 60% (Volianskis et al., 2013). Another limitation in the use of Ro 25-6981 is that the magnitude of block which it achieves will vary with agonist concentration, such that 3 μM Ro 25-6981 achieves 93% inhibition of GluN2B in the presence of 100 μM NMDA but only 62% in 10 μM NMDA (Fischer et al., 1997). Nevertheless, given that, if anything, glutamate concentration is likely to increase in the presence of Aβ (Li et al., 2009), it would be predicted that Ro 25-6981 should block more current when slices had been pre-incubated with Aβ. Since the opposite result is observed, this strengthens the validity of the conclusion that Aβ triggers a pathway that targets GluN2B-subunit containing NMDARs.

An additional consideration is that Ro 25-6981 will also affect GluN2B subunit-containing NMDARs located on interneurons (Hanson et al., 2013) and therefore could alter the properties of the inhibitory network. However, there was no in-

dication that effects on interneurons might interact with the changes caused by the acute exposure of Aβ used here, since the same pattern of Aβ-induced LTP deficit was found in the presence of gabazine.

One final, more generally applicable, limitation in the study of the different NMDARs using pharmacology is that there is likely to be a substantial proportion of triheteromeric NMDARs present in the adult brain (Hatton and Paoletti, 2005; Rauner and Köhr, 2011; Gray et al., 2011; Tovar et al., 2013), but these cannot be selectively blocked pharmacologically. A much higher concentration of Ro 25-6981 is required to access this population (Volianskis et al., 2013) than the concentration both used here and in previous studies of hippocampal asymmetry (Kawakami et al., 2003; Kohl et al., 2011). Consequently, it is likely that the effect measured pharmacologically is mediated primarily by GluN1/GluN2B heterodimers. However, the different types of synapse receiving left or right CA3 input accessed optogenetically will not only contain heterodimers but also triheteromers. Very little is known about the possible asymmetry in the distribution of the triheteromeric receptors, and therefore I cannot determine the extent of their contribution in mediating LTP, nor how they are affected by exposure to Aβ.

The results gleaned from experiments involving the use of pharmacology must always be interpreted with caution, especially when there are limitations to the capabilities of the antagonists themselves. However, they provide a useful tool to investigate necessary components of molecular pathways, such as GSK-3. They also provide a more direct way to test for the possible involvement of certain NMDAR subunits than by investigating changes in the decay time constant. Of course, such approaches are most powerful when applied in parallel and there is agreement between different techniques. Here I have used three different approaches to suggest that GluN2B subunits may be particularly implicated in the Aβ-induced LTP impairment.

6.6 Optogenetics as a technique to probe plasticity and memory

The ability to activate and silence neurons has been fundamental to probe neural networks and mechanisms and thus to establish much of our current knowledge about brain function. However, activation by electrical stimulation recruits fibres indiscriminately, and therefore the effects monitored will be generated by multiple cell types and with possible neuromodulatory influence. Silencing by surgical, genetic or pharmacological lesioning or inactivation, even though it can be made cell-type specific, has not previously been possible on the same temporal timescale as activation; therefore, such silencing can be informative about mandatory components in a circuit, but not necessarily about which brain regions and mechanisms are engaged in intact systems during brain function. Therefore, in this thesis, I have begun to use optogenetics; this new technique circumvents some of the complications of interpretation that arise from non-specific activation and chronic silencing and, moreover, allows new questions to be asked.

Optogenetics permits targeting of the projections from the CA3 in one hemisphere, without the use of VHC transection. When an optical pathway is used alone, as in the N/A ratio experiments, it allows the CA3-CA1 pathway to be isolated, such that fibres originating elsewhere than the CA3 will not be recruited. It is possible that electrical stimulation of such non-specific projections, with possible release of neuromodulatory factors, could potentially alter how synapses respond to Aβ or other pharmacological manipulations. Therefore, it is encouraging that both electrical and optical stimulation revealed a reduction in the N/A ratio in the presence of Aβ.

The use of optogenetics in *in vitro* slice experiments does have possible disadvantages, however; in particular, the expression of ChR2 could reduce cell health and cause a reduction of response magnitude during the course of experiments. This makes it important to extract ratios from data where measurements have been alternated between holding potentials, and is also the reason why I

have compared the magnitude of LTP between optical pathways. Therefore, although phototoxicity cannot be excluded, it is very unlikely to account for the distinct effect of Aβ in left- and right-injected mice, nor the different magnitude of LTP between hemispheres. Another important consideration is that optically- and electrically-evoked fEPSPs and EPSCs are not equivalent, since electrical stimulation recruits large-diameter fibres first, but optical stimulation will first trigger action potentials in smaller fibres. Consequently, it was not possible to achieve complete overlap of the electrical and optical input in the LTP experiment. In addition, there is the mechanical limitation of placing the stimulation electrode and optical fibre in the same place. Thus, it was considered necessary to perform these experiments blind so that LTP in left- and right-injected mice was induced under equivalent conditions and no possible bias in fibre placement could explain the LTP data. Nevertheless, if and when new ChR2 constructs to drive pyramidal neurons at very high frequency become available, it would be important to verify that the same effect was observed without relying on the presence of an electrical pathway.

The use of optogenetics to probe plasticity has provided evidence in support of the proposal that the GluN2B subunit plays an important role in LTP. However, the data presented here do not allow a dissociation to be made between the importance of the GluN2B subunit itself and the importance of this subunit within a certain synaptic context. GluN2B subunit-containing NMDARs are also present in synapses that receive right CA3 input (Kohl et al., 2011), yet these synapses do not potentiate. Therefore, the results suggest that, whilst the presence of the GluN2B subunit is a necessary factor in the induction of LTP, the morphological characteristics of left CA3-CA1 synapses may be equally important. The role of GluN2B subunit-containing NMDARs in LTD is controversial, and so it would be interesting to investigate whether LTD could only be induced at right CA3-CA1 synapses. Although NMDARs cannot be completely separated from their synaptic context, the development of optogenetically controlled GluN2A and GluN2B subunit containing NMDARs would permit more

direct testing of the subunit selectivity hypothesis both *in vitro* and *in vivo*.

Optogenetics is not only useful in slice work, and perhaps is most promising as a technique to probe specific pathways *in vivo* and study their role in behaving animals. The two main reasons are, firstly, the cell-type specificity conferred, with either one cell-type being targeted throughout the brain using transgenic mice, or the expression of constructs limited to one cell-type in a particular brain region and, secondly, the ability to activate and silence neurons at a rapid rate. The present pharmacological lesion techniques, such as the $GABA_A$ agonist muscimol, take up to thirty minutes to achieve their full effect and this appears to be sufficient time for adaptive network changes to occur (Goshen et al., 2011). The acute nature of optogenetic lesions should enable better determination of which circuits are actually used during a memory task *in vivo*, rather than which circuits are indispensible. Here I have used optogenetics to silence CaMKII-expressing cells of the CA3 *in vivo*, and the acute nature of this manipulation may be why the work presented here is not in complete agreement with either the current literature on lateralisation in rodents nor the finding of Nakashiba et al. (2008) that the CA3 is not required for incremental spatial learning. In the future, optogenetics may provide a powerful way to probe the functions of the circuits that might be vulnerable in AD.

6.7 Left-right asymmetry of mouse hippocampal function and dysfunction

The work in this thesis reveals a possible asymmetry in the hippocampal function of the mouse, and this left-right difference has relevance to learning and memory in health and disease.

In the mouse hippocampus, GluN2B subunit-containing NMDARs are highly concentrated in the thin postsynaptic spines of CA1 neurons receiving left CA3 input (Shinohara et al., 2008). I have found that these are the synapses which show a change in N/A ratio in response to acute Aβ exposure. My finding that

there is a hemispheric asymmetry in synaptic vulnerability to this Aβ-mediated pathological process is consistent with the recent theoretical proposal of 'molecular nexopathies' by Warren et al. (2013). This hypothesis states that distinct neurodegenerative diseases may be characterised by specific neural pathways being more vulnerable to the changes induced by a pathogenic molecule; in turn, this would explain the different effects on cognitive function. In relation to this neural pathway proposal, there is an intriguing parallel between the asymmetry in the synaptic vulnerability to Aβ-induced changes in the mouse and a finding in humans that the abnormalities in tissue volume and microstructure which develop at least two years before patients progress from mild cognitive impairment to AD are present only the left human hippocampus at this early stage (Douaud et al., 2013). Moreover, given that the early stages of AD are characterised by a failing ability to lay down new long-term memories, it is interesting that the left CA3-CA1 synapses that appear particularly vulnerable to Aβ are also those that potentiate in both tetanus (as described here) and timing-dependent LTP (Kohl et al., 2011), since LTP has been proposed as a cellular model of learning and memory.

I have previously outlined the evidence in support of both this general hypothesis that LTP is a cellular model for learning and memory, with a possibly central role for GluN2B subunit-containing NMDARs, and also the specific proposal that LTP at the CA3-CA1 synapse supports associative spatial learning. Technical limitations have meant the evidence in support of these hypotheses remains correlative and the latter proposal, in particular, is still contentious (Gallistel and Matzel, 2013). With the new technologies available, a major aim for the future will be to test these hypotheses directly and show whether changes in synaptic weights can support learning and memory and where such changes take place in tasks with different cognitive demands. The ideal demonstration would require the artificial introduction of specific synaptic changes to create a memory. Ramirez et al. (2013) have already taken steps in this direction, showing that sets of neurons in the dentate gyrus carry information about a context,

and that re-activating these in combination with a foot shock can create a 'false' association between foot shock and context. Nevertheless, cellular activity is sparse in the dentate gyrus, and the authors found an artificial memory could not be created by manipulating CA1 neurons, since a far higher proportion of these cells are active in a given environment. In addition, the manipulation was not made directly at the synaptic level. The input-specific differences in LTP and the behavioural dissociation described here might open up a new avenue to explore how behaviour maps onto the underlying neural networks and, in particular, to re-investigate a possible link between synaptic plasticity and spatial associative learning and long-term memory. Left-right optogenetic targeting of synapses could be combined with synapse-specific manipulations of recently potentiated synapses. If such manipulations were performed during learning, the effect on task acquisition could be monitored, whereas the effect on information storage could be probed if manipulations were introduced after learning.

The work here is not only relevant to the study of the possible relationship between CA3-CA1 LTP and spatial associative learning. Irrespective of whether this relationship provides the explanation, I have found that the left CA3 is an important component of the network required for effective performance in a task that necessitates long-term hippocampus-dependent associative learning in the mouse. In contrast, both the left and the right CA3 are necessary for performance on short-term memory tasks. This demonstrates that there is a left-right asymmetry in hippocampal function and the work here is consistent with the possibility that the hippocampus might consist of a series of parallel networks, one of which supports the learning of associations. The other networks would be important in short-term memory but, in addition, may perform other roles such as sensory coding and navigation. NMDARs play a role in slow or tonic response components of neural activity; for example, supporting slow responses in the thalamus and sensory tuning in the neocortex. Therefore, it is possible that only a subset of hippocampal NMDARs are engaged in learning and memory, while the rest perform computations similar to those in the

sensory neocortex. The left-right difference could also parallel the better established laterality in human hippocampal function (Burgess et al., 2002). Such asymmetry may be advantageous, perhaps due to the increased efficiency of information processing and storage. Nevertheless, the lack of (pers. comm. Dr. David Bannerman), or much smaller (Poe et al., 2000; Gerlai et al., 2002; Klur et al., 2009), effects caused by complete unilateral hippocampal lesions compared to the considerable impairments seen here with inactivation of only a portion of the CA3 unilaterally, suggest that a high level of adaptive flexibility is maintained in the rodent hippocampus.

6.8 Conclusion and perspective

The work presented in this thesis describes how tau protein and GSK-3 may be important to mediate the well-established Aβ-induced LTP impairment, suggesting possible therapeutic avenues. It also provides further support for a unique role of GluN2B subunit-containing NMDARs in LTP, and shows that an Aβ-induced LTP impairment correlates with a disruption in the synaptic balance of glutamate receptors, specifically GluN2B subunit-containing NMDARs. In addition, it emphasises how crucial the synaptic context might be in determining the contribution that GluN2B subunit-containing NMDARs can make towards plastic changes in synaptic strength. Furthermore, it suggests that GluN2B-rich synapses may be vulnerable to the effects of Aβ and hence suggests such synapses should be the focus of neuroprotective therapies.

The finding that there may be synapses in mice which are particularly at risk from Aβ-induced pathology suggests that knowledge gained from mouse models can generate useful hypotheses that must ultimately be investigated in humans. If a molecular asymmetry is also present in the human hippocampus, and correlates with the left-right differences already known to exist at the cognitive level, this will be hugely valuable in understanding network function and vulnerability. Moreover, the left-right difference in the behaviour and synaptic

effects of Aβ in the mouse would prove a useful new model with which to study the early stages of AD.

The work here is consistent with, though does not demonstrate, a role for GluN2B subunit-containing NMDAR-dependent hippocampal LTP in associative spatial learning. It does, however, lay the foundations for a new approach to investigate this controversial hypothesis in the future. What already seems apparent is that a dissociation of function may exist in the mouse hippocampus; given the asymmetry in the human hippocampus, it is possible that asymmetry of bilateral structures may be conserved across species because of the advantages for supporting efficient network architecture.

In conclusion, despite the huge advances in our understanding of hippocampal function, it seems there is still much more to uncover. The work here will hopefully facilitate the future understanding of one small piece of the puzzle about the neural mechanisms that underlie our incredible ability to generate rich memories that can last a lifetime, as well as how these processes may be affected by disease.

BIBLIOGRAPHY

Abramov E, Dolev I, Fogel H, Ciccotosto GD, Ruff E, Slutsky I (2009) Amyloid-beta as a positive endogenous regulator of release probability at hippocampal synapses. *Nature Neuroscience* 12:1567–1576. 46, 47

Akashi K, Kakizaki T, Kamiya H, Fukaya M, Yamasaki M, Abe M, Natsume R, Watanabe M, Sakimura K (2009) NMDA receptor GluN2B (GluR epsilon 2/NR2B) subunit is crucial for channel function, postsynaptic macromolecular organization, and actin cytoskeleton at hippocampal CA3 synapses. *Journal of Neuroscience* 29:10869–10882. 22, 23

Alcor D, Gouzer G, Triller A (2009) Single-particle tracking methods for the study of membrane receptors dynamics. *European Journal of Neuroscience* 30:987–997. 117

Alexandru A, Jagla W, Graubner S, Becker A, Bäuscher C, Kohlmann S, Sedlmeier R, Raber KA, Cynis H, Rönicke R, Reymann KG, Petrasch-Parwez E, Hartlage-Rübsamen M, Waniek A, Rossner S, Schilling S, Osmand AP, Demuth HU, von Hörsten S (2011) Selective hippocampal neurodegeneration in transgenic mice expressing small amounts of truncated Aβ is induced by pyroglutamate-Aβ formation. *Journal of Neuroscience* 31:12790–12801. 49

Allen B, Ingram E, Takao M, Smith MJ, Jakes R, Virdee K, Yoshida H, Holzer M,

Craxton M, Emson PC, Atzori C, Migheli A, Crowther RA, Ghetti B, Spillantini MG, Goedert M (2002) Abundant tau filaments and nonapoptotic neurodegeneration in transgenic mice expressing human P301S tau protein. *Journal of Neuroscience* 22:9340–9351. 105

Alvarez G, Muñoz-Montaño JR, Satrústegui J, AVILA J, Bogónez E, Díaz-Nido J (1999) Lithium protects cultured neurons against beta-amyloid-induced neurodegeneration. *FEBS letters* 453:260–264. 98

Andorfer C, Kress Y, Espinoza M, De Silva R, Tucker KL, Barde YA, Duff K, Davies P (2003) Hyperphosphorylation and aggregation of tau in mice expressing normal human tau isoforms. *Journal of Neurochemistry* 86:582–590. 200

Ardiles AO, Tapia-Rojas CC, Mandal M, Alexandre F, Kirkwood A, Inestrosa NC, Palacios AG (2012) Postsynaptic dysfunction is associated with spatial and object recognition memory loss in a natural model of Alzheimer's disease. *Proceedings of the National Academy of Sciences* 109:13835–13840. 200

Bahr BA, Hoffman KB, Yang AJ, Hess US, Glabe CG, Lynch G (1998) Amyloid beta protein is internalized selectively by hippocampal field CA1 and causes neurons to accumulate amyloidogenic carboxyterminal fragments of the amyloid precursor protein. *Journal of Comparative Neurology* 397:139–147. 50

Balducci C, Beeg M, Stravalaci M, Bastone A, Sclip A, Biasini E, Tapella L, Colombo L, Manzoni C, Borsello T, Chiesa R, Gobbi M, Salmona M, Forloni G (2010) Synthetic amyloid-beta oligomers impair long-term memory independently of cellular prion protein. *Proceedings of the National Academy of Sciences* 107:2295–2300. 50

Banke TG, Bowie D, Lee H, Huganir RL, Schousboe A, Traynelis SF (2000) Control of GluR1 AMPA receptor function by cAMP-dependent protein kinase. *Journal of Neuroscience* 20:89–102. 8

Bannerman DM, Bus T, Taylor A, Sanderson DJ, Schwarz I, Jensen V, Hvalby Ø, Rawlins JNP, Seeburg PH, Sprengel R (2012) Dissecting spatial knowledge from spatial choice by hippocampal NMDA receptor deletion. *Nature Neuroscience* 15:1153–1159. 39, 170, 185, 187, 188, 196

Bannerman DM, Niewoehner B, Lyon L, Romberg C, Schmitt WB, Taylor A, Sanderson DJ, Cottam J, Sprengel R, Seeburg PH, Köhr G, Rawlins JNP (2008) NMDA receptor subunit NR2A is required for rapidly acquired spatial working memory but not incremental spatial reference memory. *Journal of Neuroscience* 28:3623–3630. 33, 188

Barkus C, McHugh SB, Sprengel R, Seeburg PH, Rawlins JNP, Bannerman DM (2010) Hippocampal NMDA receptors and anxiety: at the interface between cognition and emotion. *European Journal of Pharmacology* 626:49–56. 173

Barria A, Muller D, Derkach V, Griffith LC, Soderling TR (1997) Regulatory phosphorylation of AMPA-type glutamate receptors by CaM-KII during long-term potentiation. *Science* 276:2042–2045. 6

Barria A, Malinow R (2005) NMDA receptor subunit composition controls synaptic plasticity by regulating binding to CaMKII. *Neuron* 48:289–301. 15, 24, 156, 185

Barrow CJ, Yasuda A, Kenny PT, Zagorski MG (1992) Solution conformations and aggregational properties of synthetic amyloid beta-peptides of Alzheimer's disease. Analysis of circular dichroism spectra. *Journal of Molecular Biology* 225:1075–1093. 47

Barry AE, Klyubin I, Mc Donald JM, Mably AJ, Farrell MA, Scott M, Walsh DM, Rowan MJ (2011) Alzheimer's disease brain-derived amyloid-β-mediated inhibition of LTP in vivo is prevented by immunotargeting cellular prion protein. *Journal of Neuroscience* 31:7259–7263. 50

Barten DM, Fanara P, Andorfer C, Hoque N, Wong PYA, Husted KH, Cadelina GW, Decarr LB, Yang L, Liu V, Fessler C, Protassio J, Riff T, Turner H, Janus CG, Sankaranarayanan S, Polson C, Meredith JE, Gray G, Hanna A, Olson RE, Kim SH, Vite GD, Lee FY, Albright CF (2012) Hyperdynamic microtubules, cognitive deficits, and pathology are improved in tau transgenic mice with low doses of the microtubule-stabilizing agent BMS-241027. *Journal of Neuroscience* 32:7137–7145. 52

Bartlett TE, Bannister NJ, Collett VJ, Dargan SL, Massey PV, Bortolotto ZA, Fitzjohn SM, Bashir ZI, Collingridge GL, Lodge D (2007) Differential roles of NR2A and NR2B-containing NMDA receptors in LTP and LTD in the CA1 region of two-week old rat hippocampus. *Neuropharmacology* 52:60–70. 19, 28, 29

Bartlett TE, Lu J, Wang YT (2011) Slice orientation and muscarinic acetylcholine receptor activation determine the involvement of N-methyl D-aspartate receptor subunit GluN2B in hippocampal area CA1 long-term depression. *Molecular Brain* 4:41. 29, 31

Bayer KU, De Koninck P, Leonard AS, Hell JW, Schulman H (2001) Interaction with the NMDA receptor locks CaMKII in an active conformation. *Nature* 411:801–805. 15, 156

Benke TA, Luthi A, Isaac JT, Collingridge GL (1998) Modulation of AMPA receptor unitary conductance by synaptic activity. *Nature* 393:793–797. 6

Berberich S, Jensen V, Hvalby Ø, Seeburg PH, Köhr G (2007) The role of NMDAR subtypes and charge transfer during hippocampal LTP induction. *Neuropharmacology* 52:77–86. 20

Berberich S, Punnakkal P, Jensen V, Pawlak V, Seeburg PH, Hvalby Ø, Köhr G (2005) Lack of NMDA receptor subtype selectivity for hippocampal long-term potentiation. *Journal of Neuroscience* 25:6907–6910. 19

Berndt A, Schoenenberger P, Mattis J, Tye KM, Deisseroth K, Hegemann P, Oertner TG (2011) High-efficiency channelrhodopsins for fast neuronal stimulation at low light levels. *Proceedings of the National Academy of Sciences* 108:7595–7600. 72

Bero AW, Yan P, Roh JH, Cirrito JR, Stewart FR, Raichle ME, Lee JM, Holtzman DM (2011) Neuronal activity regulates the regional vulnerability to amyloid-β deposition. *Nature Neuroscience* 14:750–756. 46, 47

Bettens K, Sleegers K, Van Broeckhoven C (2013) Genetic insights in Alzheimer's disease. *Lancet Neurology* 12:92–104. 45, 105

Bhaskar K, Konerth M, Kokiko-Cochran ON, Cardona A, Ransohoff RM, Lamb BT (2010) Regulation of tau pathology by the microglial fractalkine receptor. *Neuron* 68:19–31. 113

Bhat R, Xue Y, Berg S, Hellberg S, Ormö M, Nilsson Y, Radesäter AC, Jerning E, Markgren PO, Borgegård T, Nylöf M, Giménez-Cassina A, Hernandez F, Lucas JJ, Díaz-Nido J, Avila J (2003) Structural insights and biological effects of glycogen synthase kinase 3-specific inhibitor AR-A014418. *Journal of Biological Chemistry* 278:45937–45945. 69, 100

Bi GQ, Poo MM (1998) Synaptic modifications in cultured hippocampal neu-

rons: dependence on spike timing, synaptic strength, and postsynaptic cell type. *Journal of Neuroscience* 18:10464–10472. 3

Bishop DVM (2013) Cerebral asymmetry and language development: cause, correlate, or consequence? *Science* 340:1230531. 161, 191

Bitan G, Kirkitadze MD, Lomakin A, Vollers SS, Benedek GB, Teplow DB (2003) Amyloid beta -protein (Abeta) assembly: Abeta 40 and Abeta 42 oligomerize through distinct pathways. *Proceedings of the National Academy of Sciences* 100:330–335. 47, 48

Blennow K, Zetterberg H, Fagan AM (2012) Fluid biomarkers in Alzheimer disease. *Cold Spring Harbor Perspectives in Medicine* 2:a006221. 199

Bliss TV, Collingridge GL (1993) A synaptic model of memory: long-term potentiation in the hippocampus. *Nature* 361:31–39. 5, 32, 109, 162, 185

Bliss TV, Lomo T (1973) Long-lasting potentiation of synaptic transmission in the dentate area of the anaesthetized rabbit following stimulation of the perforant path. *Journal of Physiology* 232:331–356. 2

Bliss TVP, Collingridge GL (2013) Expression of NMDA receptor-dependent LTP in the hippocampus: bridging the divide. *Molecular Brain* 6:1–14. 5, 10

Bloodgood BL, Sabatini BL (2007) Nonlinear regulation of unitary synaptic signals by CaV(2.3) voltage-sensitive calcium channels located in dendritic spines. *Neuron* 53:249–260. 10

Bolmont T, Clavaguera F, Meyer-Luehmann M, Herzig MC, Radde R, Staufenbiel M, Lewis J, Hutton M, Tolnay M, Jucker M (2007) Induction of tau pathology by intracerebral infusion of amyloid-beta -containing brain extract and

by amyloid-beta deposition in APP x Tau transgenic mice. *American Journal of Pathology* 171:2012–2020. 89

Bosch M, Hayashi Y (2012) Structural plasticity of dendritic spines. *Current Opinion in Neurobiology* 22:383–388. 8

Bourne J, Harris KM (2007) Do thin spines learn to be mushroom spines that remember? *Current Opinion in Neurobiology* 17:381–386. 42

Braak H, Braak E (1995) Staging of Alzheimer's disease-related neurofibrillary changes. *Neurobiology of Aging* 16:271–84. 45, 160, 202

Bradford MM (1976) A rapid and sensitive method for the quantitation of microgram quantities of protein utilizing the principle of protein-dye binding. *Analytical biochemistry* 72:248–254. 71

Bradley CA, Peineau S, Taghibiglou C, Nicolas CS, Whitcomb DJ, Bortolotto ZA, Kaang BK, Cho K, Wang YT, Collingridge GL (2012) A pivotal role of GSK-3 in synaptic plasticity. *Frontiers in Molecular Neuroscience* 5:13. 111

Bragin A, Jandó G, Nádasdy Z, Hetke J, Wise K, Buzsáki G (1995) Gamma (40-100 Hz) oscillation in the hippocampus of the behaving rat. *Journal of Neuroscience* 15:47–60. 195

Brigman JL, Wright T, Talani G, Prasad-Mulcare S, Jinde S, Seabold GK, Mathur P, Davis MI, Bock R, Gustin RM, Colbran RJ, Alvarez VA, Nakazawa K, Delpire E, Lovinger DM, Holmes A (2010) Loss of GluN2B-containing NMDA receptors in CA1 hippocampus and cortex impairs long-term depression, reduces dendritic spine density, and disrupts learning. *Journal of Neuroscience* 30:4590–4600. 22, 23, 30, 35

Broadbent NJ, Gaskin S, Squire LR, Clark RE (2010) Object recognition memory and the rodent hippocampus. *Learning & Memory* 17:5–11. 33

Brouillette J, Caillierez R, Zommer N, Alves-Pires C, Benilova I, Blum D, De Strooper B, Buée L (2012) Neurotoxicity and memory deficits induced by soluble low-molecular-weight amyloid-β1-42 oligomers are revealed in vivo by using a novel animal model. *Journal of Neuroscience* 32:7852–7861. 156

Burgess N, Maguire EA, O'Keefe J (2002) The human hippocampus and spatial and episodic memory. *Neuron* 35:625–641. 160, 191, 213

Burns A, Iliffe S (2009) Alzheimer's disease. *BMJ (Clinical research ed.)* 338:b158. 4

Buzsáki G, Horváth Z, Urioste R, Hetke J, Wise K (1992) High-frequency network oscillation in the hippocampus. *Science* 256:1025–1027. 195

Cao X, Cui Z, Feng R, Tang YP, Qin Z, Mei B, Tsien JZ (2007) Maintenance of superior learning and memory function in NR2B transgenic mice during ageing. *European Journal of Neuroscience* 25:1815–1822. 23, 36

Cerpa W, Farías GG, Godoy JA, Fuenzalida M, Bonansco C, Inestrosa NC (2010) Wnt-5a occludes Abeta oligomer-induced depression of glutamatergic transmission in hippocampal neurons. *Molecular Neurodegeneration* 5:3. 88, 119

Chabrier MA, Blurton-Jones M, Agazaryan AA, Nerhus JL, Martinez-Coria H, LaFerla FM (2012) Soluble aβ promotes wild-type tau pathology in vivo. *Journal of Neuroscience* 32:17345–17350. 200

Chapman PF, White GL, Jones MW, Cooper-Blacketer D, Marshall VJ, Irizarry M, Younkin L, Good MA, Bliss TV, Hyman BT, Younkin SG, Hsiao KK (1999)

Impaired synaptic plasticity and learning in aged amyloid precursor protein transgenic mice. *Nature Neuroscience* 2:271–276. 117

Chen N, Luo T, Raymond LA (1999) Subtype-dependence of NMDA receptor channel open probability. *Journal of Neuroscience* 19:6844–6854. 12

Chen QS, Wei WZ, Shimahara T, Xie CW (2002) Alzheimer amyloid beta-peptide inhibits the late phase of long-term potentiation through calcineurin-dependent mechanisms in the hippocampal dentate gyrus. *Neurobiology of Learning and Memory* 77:354–371. 118

Chen X, Lin R, Xu S, Wei X, Zhang J, Wang C, Anwyl R, Wang Q (2013) Enhancement of long-term depression by soluble amyloid β protein in rat hippocampus is mediated by metabotropic glutamate receptor and involves activation of p38MAPK, STEP and caspase-3. *Neuroscience* . 51

Chung HJ, Huang YH, Lau LF, Huganir RL (2004) Regulation of the NMDA receptor complex and trafficking by activity-dependent phosphorylation of the NR2B subunit PDZ ligand. *Journal of Neuroscience* 24:10248–10259. 15

Cirrito JR, Yamada KA, Finn MB, Sloviter RS, Bales KR, May PC, Schoepp DD, Paul SM, Mennerick S, Holtzman DM (2005) Synaptic activity regulates interstitial fluid amyloid-beta levels in vivo. *Neuron* 48:913–922. 46

Cissé M, Halabisky B, Harris J, Devidze N, Dubal DB, Sun B, Orr A, Lotz G, Kim DH, Hamto P, Ho K, Yu GQ, Mucke L (2011) Reversing EphB2 depletion rescues cognitive functions in Alzheimer model. *Nature* 469:47–52. 50

Clayton DA, Mesches MH, Alvarez E, Bickford PC, Browning MD (2002) A hippocampal NR2B deficit can mimic age-related changes in long-term potentiation and spatial learning in the Fischer 344 rat. *Journal of Neuro-*

science 22:3628–3637. 23, 35, 185

Coan EJ, Irving AJ, Collingridge GL (1989) Low-frequency activation of the NMDA receptor system can prevent the induction of LTP. *Neuroscience Letters* 105:205–210. 153

Cohen RM, Rezai-Zadeh K, Weitz TM, Rentsendorj A, Gate D, Spivak I, Bholat Y, Vasilevko V, Glabe CG, Breunig JJ, Rakic P, Davtyan H, Agadjanyan MG, Kepe V, Barrio JR, Bannykh S, Szekely CA, Pechnick RN, Town T (2013) A transgenic Alzheimer rat with plaques, tau pathology, behavioral impairment, oligomeric aβ, and frank neuronal loss. *Journal of Neuroscience* 33:6245–6256. 200

Collingridge GL, Kehl SJ, McLennan H (1983) Excitatory amino acids in synaptic transmission in the Schaffer collateral-commissural pathway of the rat hippocampus. *Journal of Physiology* 334:33–46. 5

Corlew R, Wang Y, Ghermazien H, Erisir A, Philpot BD (2007) Developmental switch in the contribution of presynaptic and postsynaptic NMDA receptors to long-term depression. *Journal of Neuroscience* 27:9835–9845. 10

Cui Z, Feng R, Jacobs S, Duan Y, Wang H, Cao X, Tsien JZ (2013) Increased NR2A:NR2B ratio compresses long-term depression range and constrains long-term memory. *Scientific Reports* 3:1036. 23, 30, 36

Cullen WK, Suh YH, Anwyl R, Rowan MJ (1997) Block of LTP in rat hippocampus in vivo by beta-amyloid precursor protein fragments. *Neuroreport* 8:3213–3217. 51, 87, 109, 117, 204

D'Amelio M, Cavallucci V, Middei S, Marchetti C, Pacioni S, Ferri A, Diamantini A, De Zio D, Carrara P, Battistini L, Moreno S, Bacci A, Ammassari-Teule M,

Marie H, Cecconi F (2011) Caspase-3 triggers early synaptic dysfunction in a mouse model of Alzheimer's disease. *Nature Neuroscience* 14:69–76. 51, 118, 147, 148

Dawson HN, Ferreira A, Eyster MV, Ghoshal N, Binder LI, Vitek MP (2001) Inhibition of neuronal maturation in primary hippocampal neurons from tau deficient mice. *Journal of Cell Science* 114:1179–1187. 57, 90

De Felice FG, Vieira MNN, Bomfim TR, Decker H, Velasco PT, Lambert MP, Viola KL, Zhao WQ, Ferreira ST, Klein WL (2009) Protection of synapses against Alzheimer's-linked toxins: insulin signaling prevents the pathogenic binding of Abeta oligomers. *Proceedings of the National Academy of Sciences* 106:1971–1976. 50

De Ferrari GV, Papassotiropoulos A, Biechele T, Wavrant De-Vrieze F, Avila ME, Major MB, Myers A, Sáez K, Henríquez JP, Zhao A, Wollmer MA, Nitsch RM, Hock C, Morris CM, Hardy J, Moon RT (2007) Common genetic variation within the low-density lipoprotein receptor-related protein 6 and late-onset Alzheimer's disease. *Proceedings of the National Academy of Sciences* 104:9434–9439. 88

Deacon RMJ, Bannerman DM, Kirby BP, Croucher A, Rawlins JNP (2002) Effects of cytotoxic hippocampal lesions in mice on a cognitive test battery. *Behavioural Brain Research* 133:57–68. 170, 176

Deacon RMJ, Rawlins JNP (2006) T-maze alternation in the rodent. *Nature Protocols* 1:7–12. 176

Decker H, Jürgensen S, Adrover MF, Brito-Moreira J, Bomfim TR, Klein WL, Epstein AL, De Felice FG, Jerusalinsky D, Ferreira ST (2010a) N-methyl-D-aspartate receptors are required for synaptic targeting of Alzheimer's toxic

amyloid-β peptide oligomers. *Journal of Neurochemistry* 115:1520–1529. 50

Decker H, Lo KY, Unger SM, Ferreira ST, Silverman MA (2010b) Amyloid-beta peptide oligomers disrupt axonal transport through an NMDA receptor-dependent mechanism that is mediated by glycogen synthase kinase 3beta in primary cultured hippocampal neurons. *Journal of Neuroscience* 30:9166–9171. 110, 154

DeKosky ST, Scheff SW (1990) Synapse loss in frontal cortex biopsies in Alzheimer's disease: correlation with cognitive severity. *Annals of Neurology* 27:457–464. 52, 87, 157

Dewachter I, Filipkowski RK, Priller C, Ris L, Neyton J, Croes S, Terwel D, Gysemans M, Devijver H, Borghgraef P, Godaux E, Kaczmarek L, Herms J, Van Leuven F (2009) Deregulation of NMDA-receptor function and down-stream signaling in APP[V717I] transgenic mice. *Neurobiology of Aging* 30:241–256. 118

Dolev I, Fogel H, Milshtein H, Berdichevsky Y, Lipstein N, Brose N, Gazit N, Slutsky I (2013) Spike bursts increase amyloid-β 40/42 ratio by inducing a presenilin-1 conformational change. *Nature Neuroscience* 16:587–595. 48

Douaud G, Menke RAL, Gass A, Monsch AU, Rao A, Whitcher B, Zamboni G, Matthews PM, Sollberger M, Smith S (2013) Brain microstructure reveals early abnormalities more than two years prior to clinical progression from mild cognitive impairment to Alzheimer's disease. *Journal of Neuroscience* 33:2147–2155. 211

Doyere V, Schafe GE, Sigurdsson T, LeDoux JE (2003) Long-term potentiation in freely moving rats reveals asymmetries in thalamic and cortical inputs to the lateral amygdala. *European Journal of Neuroscience* 17:2703–2715. 3

Dudek SM, Bear MF (1992) Homosynaptic long-term depression in area CA1 of hippocampus and effects of N-methyl-D-aspartate receptor blockade. *Proceedings of the National Academy of Sciences* 89:4363–4367. 8

Duffy S, Labrie V, Roder JC (2008) D-serine augments NMDA-NR2B receptor-dependent hippocampal long-term depression and spatial reversal learning. *Neuropsychopharmacology* 33:1004–1018. 29, 37

Dumas TC (2005) Developmental regulation of cognitive abilities: modified composition of a molecular switch turns on associative learning. *Progress in Neurobiology* 76:189–211. 11, 21, 28

Eichenbaum H, Sauvage M, Fortin N, Komorowski R, Lipton P (2012) Towards a functional organization of episodic memory in the medial temporal lobe. *Neuroscience & Biobehavioral Reviews* 36:1597–1608. 161

Emptage NJ, Reid CA, Fine A, Bliss TVP (2003) Optical quantal analysis reveals a presynaptic component of LTP at hippocampal Schaffer-associational synapses. *Neuron* 38:797–804. 10

Erreger K, Dravid SM, Banke TG, Wyllie DJA, Traynelis SF (2005) Subunit-specific gating controls rat NR1/NR2A and NR1/NR2B NMDA channel kinetics and synaptic signalling profiles. *Journal of Physiology* 563:345–358. 12, 13, 20, 21, 148

Esteban JA, Shi SH, Wilson C, Nuriya M, Huganir RL, Malinow R (2003) PKA phosphorylation of AMPA receptor subunits controls synaptic trafficking underlying plasticity. *Nature Neuroscience* 6:136–143. 8

Euler T, Denk W (2001) Dendritic processing. *Current Opinion in Neurobiology* 11:415–422. 162

Fanara P, Husted KH, Selle K, Wong PYA, Banerjee J, Brandt R, Hellerstein MK (2010) Changes in microtubule turnover accompany synaptic plasticity and memory formation in response to contextual fear conditioning in mice. *Neuroscience* 168:167–178. 88

Feng B, Tse HW, Skifter DA, Morley R, Jane DE, Monaghan DT (2004) Structure-activity analysis of a novel NR2C/NR2D-preferring NMDA receptor antagonist: 1-(phenanthrene-2-carbonyl) piperazine-2,3-dicarboxylic acid. *British Journal of Pharmacology* 141:508–516. 17

Fischer G, Mutel V, Trube G, Malherbe P, Kew JN, Mohacsi E, Heitz MP, Kemp JA (1997) Ro 25-6981, a highly potent and selective blocker of N-methyl-D-aspartate receptors containing the NR2B subunit. Characterization in vitro. *Journal of Pharmacology and Experimental Therapeutics* 283:1285–1292. 17, 30, 71, 128, 149, 206

Foster KA, McLaughlin N, Edbauer D, Phillips M, Bolton A, Constantine-Paton M, Sheng M (2010) Distinct roles of NR2A and NR2B cytoplasmic tails in long-term potentiation. *Journal of Neuroscience* 30:2676–2685. 25, 151

Fox CJ, Russell KI, Wang YT, Christie BR (2006) Contribution of NR2A and NR2B NMDA subunits to bidirectional synaptic plasticity in the hippocampus in vivo. *Hippocampus* 16:907–915. 19, 20, 28, 29

Freir DB, Nicoll AJ, Klyubin I, Panico S, Mc Donald JM, Risse E, Asante EA, Farrow MA, Sessions RB, Saibil HR, Clarke AR, Rowan MJ, Walsh DM, Collinge J (2011) Interaction between prion protein and toxic amyloid β assemblies can be therapeutically targeted at multiple sites. *Nature Communications* 2:336. 50

Fuchs EC, Zivkovic AR, Cunningham MO, Middleton S, LeBeau FEN, Bannerman DM, Rozov A, Whittington MA, Traub RD, Rawlins JNP, Monyer H

(2007) Recruitment of parvalbumin-positive interneurons determines hippocampal function and associated behavior. *Neuron* 53:591–604. 189

Futatsugi A, Kato K, Ogura H, Li ST, Nagata E, Kuwajima G, Tanaka K, Itohara S, Mikoshiba K (1999) Facilitation of NMDAR-independent LTP and spatial learning in mutant mice lacking ryanodine receptor type 3. *Neuron* 24:701–713. 10

Gallistel CR, Matzel LD (2013) The neuroscience of learning: beyond the Hebbian synapse. *Annual Review of Psychology* 64:169–200. 39, 170, 196, 211

Gamblin TC, Chen F, Zambrano A, Abraha A, Lagalwar S, Guillozet AL, Lu M, Fu Y, Garcia-Sierra F, LaPointe N, Miller R, Berry RW, Binder LI, Cryns VL (2003) Caspase cleavage of tau: linking amyloid and neurofibrillary tangles in Alzheimer's disease. *Proceedings of the National Academy of Sciences* 100:10032–10037. 53

Gardoni F, Mauceri D, Malinverno M, Polli F, Costa C, Tozzi A, Siliquini S, Picconi B, Cattabeni F, Calabresi P, Di Luca M (2009) Decreased NR2B subunit synaptic levels cause impaired long-term potentiation but not long-term depression. *Journal of Neuroscience* 29:669–677. 23, 25, 30

Ge Y, Dong Z, Bagot RC, Howland JG, Phillips AG, Wong TP, Wang YT (2010) Hippocampal long-term depression is required for the consolidation of spatial memory. *Proceedings of the National Academy of Sciences* 107:16697–16702. 20, 28, 29, 33, 37

Gerkin RC, Lau PM, Nauen DW, Wang YT, Bi GQ (2007) Modular competition driven by NMDA receptor subtypes in spike-timing-dependent plasticity. *Journal of Neurophysiology* 97:2851–2862. 20, 28

Gerlai RT, McNamara A, Williams S, Phillips HS (2002) Hippocampal dysfunction and behavioral deficit in the water maze in mice: an unresolved issue? *Brain Research Bulletin* 57:3–9. 184, 213

Giuffrida ML, Caraci F, Pignataro B, Cataldo S, De Bona P, Bruno V, Molinaro G, Pappalardo G, Messina A, Palmigiano A, Garozzo D, Nicoletti F, Rizzarelli E, Copani A (2009) Beta-amyloid monomers are neuroprotective. *Journal of Neuroscience* 29:10582–10587. 48

Goedert M, Spillantini MG, Jakes R, Rutherford D, Crowther RA (1989) Multiple isoforms of human microtubule-associated protein tau: sequences and localization in neurofibrillary tangles of Alzheimer's disease. *Neuron* 3:519–526. 52

Goedert M, Ghetti B, Spillantini MG (2012) Frontotemporal dementia: implications for understanding Alzheimer disease. *Cold Spring Harbor Perspectives in Medicine* 2:a006254–a006254. 53, 105

Goshen I, Brodsky M, Prakash R, Wallace J, Gradinaru V, Ramakrishnan C, Deisseroth K (2011) Dynamics of retrieval strategies for remote memories. *Cell* 147:678–689. 163, 187, 193, 210

Goto K, Kurashima R, Gokan H, Inoue N, Ito I, Watanabe S (2010) LeftRight Asymmetry Defect in the Hippocampal Circuitry Impairs Spatial Learning and Working Memory in iv Mice. *PLoS ONE* 5:e15468. 190

Goto Y, Niidome T, Akaike A, Kihara T, Sugimoto H (2006) Amyloid beta-peptide preconditioning reduces glutamate-induced neurotoxicity by promoting endocytosis of NMDA receptor. *Biochemical and Biophysical Research Communications* 351:259–265. 118

Gotts SJ, Jo HJ, Wallace GL, Saad ZS, Cox RW, Martin A (2013) Two distinct forms of functional lateralization in the human brain. *Proceedings of the National Academy of Sciences* 110:E3435–44. 161

Gradinaru V, Zhang F, Ramakrishnan C, Mattis J, Prakash R, Diester I, Goshen I, Thompson KR, Deisseroth K (2010) Molecular and cellular approaches for diversifying and extending optogenetics. *Cell* 141:154–165. 73, 164

Granger AJ, Shi Y, Lu W, Cerpas M, Nicoll RA (2013) LTP requires a reserve pool of glutamate receptors independent of subunit type. *Nature* 493:495–500. 7

Grant SG, O'Dell TJ, Karl KA, Stein PL, Soriano P, Kandel ER (1992) Impaired long-term potentiation, spatial learning, and hippocampal development in fyn mutant mice. *Science* 258:1903–1910. 151

Gray JA, Shi Y, Usui H, During MJ, Sakimura K, Nicoll RA (2011) Distinct modes of AMPA receptor suppression at developing synapses by GluN2A and GluN2B: single-cell NMDA receptor subunit deletion in vivo. *Neuron* 71:1085–1101. 12, 149, 207

Gruart A, Muñoz MD, Delgado-García JM (2006) Involvement of the CA3-CA1 synapse in the acquisition of associative learning in behaving mice. *Journal of Neuroscience* 26:1077–1087. 4, 32, 39, 162, 194

Gu Z, Liu W, Yan Z (2009) beta-Amyloid impairs AMPA receptor trafficking and function by reducing Ca2+/calmodulin-dependent protein kinase II synaptic distribution. *Journal of Biological Chemistry* 284:10639–10649. 118, 147, 148

Guscott MR, Clarke HF, Murray F, Grimwood S, Bristow LJ, Hutson PH (2003) The effect of (+/-)-CP-101,606, an NMDA receptor NR2B subunit selective antagonist, in the Morris watermaze. *European Journal of Pharmacol-*

ogy 476:193–199. 191

Gustafsson B, Wigström H (1986) Hippocampal long-lasting potentiation produced by pairing single volleys and brief conditioning tetani evoked in separate afferents. *Journal of Neuroscience* 6:1575–1582. 5

Hafting T, Fyhn M, Molden S, Moser MB, Moser EI (2005) Microstructure of a spatial map in the entorhinal cortex. *Nature* 436:801–806. 47

Halt AR, Dallapiazza RF, Zhou Y, Stein IS, Qian H, Juntti S, Wojcik S, Brose N, Silva AJ, Hell JW (2012) CaMKII binding to GluN2B is critical during memory consolidation. *EMBO* 31:1203–1216. 24, 25, 36

Hanson JE, Weber M, Meilandt WJ, Wu T, Luu T, Deng L, Shamloo M, Sheng M, Scearce-Levie K, Zhou Q (2013) GluN2B antagonism affects interneurons and leads to immediate and persistent changes in synaptic plasticity, oscillations, and behavior. *Neuropsychopharmacology* 38:1221–1233. 18, 34, 206

Hardy J, Selkoe DJ (2002) The amyloid hypothesis of Alzheimer's disease: progress and problems on the road to therapeutics. *Science* 297:353–356. 70, 87

Hartmann T, Bieger SC, Brühl B, Tienari PJ, Ida N, Allsop D, Roberts GW, Masters CL, Dotti CG, Unsicker K, Beyreuther K (1997) Distinct sites of intracellular production for Alzheimer's disease A beta40/42 amyloid peptides. *Nature Medicine* 3:1016–1020. 46

Hatton CJ, Paoletti P (2005) Modulation of triheteromeric NMDA receptors by N-terminal domain ligands. *Neuron* 46:261–274. 207

Hawasli AH, Benavides DR, Nguyen C, Kansy JW, Hayashi K, Chambon P,

Greengard P, Powell CM, Cooper DC, Bibb JA (2007) Cyclin-dependent kinase 5 governs learning and synaptic plasticity via control of NMDAR degradation. *Nature Neuroscience* 10:880–886. 23, 36, 38

Heaulme M, Chambon JP, Leyris R, Molimard JC, Wermuth CG, Biziere K (1986) Biochemical characterization of the interaction of three pyridazinyl-GABA derivatives with the GABAA receptor site. *Brain Research* 384:224–231. 70

Hebb DO (1949) The organization of behavior New York: Wiley & Sons. 2

Hellstrand E, Boland B, Walsh DM, Linse S (2010) Amyloid β-protein aggregation produces highly reproducible kinetic data and occurs by a two-phase process. *ACS Chemical Neuroscience* 1:13–18. 48

Hendricson AW, Miao CLA, Lippmann MJ, Morrisett RA (2002) Ifenprodil and ethanol enhance NMDA receptor-dependent long-term depression. *Journal of Pharmacology and Experimental Therapeutics* 301:938–944. 29

Heneka MT, Kummer MP, Stutz A, Delekate A, Schwartz S, Vieira-Saecker A, Griep A, Axt D, Remus A, Tzeng TC, Gelpi E, Halle A, Korte M, Latz E, Golenbock DT (2013) NLRP3 is activated in Alzheimer's disease and contributes to pathology in APP/PS1 mice. *Nature* 493:674–678. 48

Hernandez F, Borrell J, Guaza C, Avila J, Lucas JJ (2002) Spatial learning deficit in transgenic mice that conditionally over-express GSK-3beta in the brain but do not form tau filaments. *Journal of Neurochemistry* 83:1529–1533. 111

Hill TC, Zito K (2013) LTP-induced long-term stabilization of individual nascent dendritic spines. *Journal of Neuroscience* 33:678–686. 8

Hochgräfe K, Sydow A, Mandelkow EM (2013) Regulatable transgenic mouse

models of Alzheimer disease: onset, reversibility and spreading of Tau pathology. *FEBS* 280:4371–4381. 52, 53

Holtmaat AJGD, Trachtenberg JT, Wilbrecht L, Shepherd GM, Zhang X, Knott GW, Svoboda K (2005) Transient and persistent dendritic spines in the neocortex in vivo. *Neuron* 45:279–291. 42

Hong M, Chen DC, Klein PS, Lee VM (1997) Lithium reduces tau phosphorylation by inhibition of glycogen synthase kinase-3. *Journal of Biological Chemistry* 272:25326–25332. 98

Hooper C, Markevich V, Plattner F, Killick R, Schofield E, Engel T, Hernandez F, Anderton B, Rosenblum K, Bliss T, Cooke SF, Avila J, Lucas JJ, Giese KP, Stephenson J, Lovestone S (2007) Glycogen synthase kinase-3 inhibition is integral to long-term potentiation. *European Journal of Neuroscience* 25:81–86. 111

Hoover BR, Reed MN, Su J, Penrod RD, Kotilinek LA, Grant MK, Pitstick R, Carlson GA, Lanier LM, Yuan LL, Ashe KH, Liao D (2010) Tau mislocalization to dendritic spines mediates synaptic dysfunction independently of neurodegeneration. *Neuron* 68:1067–1081. 154

Hrabetova S, Sacktor TC (1997) Long-term potentiation and long-term depression are induced through pharmacologically distinct NMDA receptors. *Neuroscience Letters* 226:107–110. 17

Hrabetova S, Serrano P, Blace N, Tse HW, Skifter DA, Jane DE, Monaghan DT, Sacktor TC (2000) Distinct NMDA receptor subpopulations contribute to long-term potentiation and long-term depression induction. *Journal of Neuroscience* 20:RC81. 17

Hsiao K, Chapman P, Nilsen S, Eckman C, Harigaya Y, Younkin S, Yang F, Cole G (1996) Correlative memory deficits, Abeta elevation, and amyloid plaques in transgenic mice. *Science* 274:99–102. 89

Hsieh H, Boehm J, Sato C, Iwatsubo T, Tomita T, Sisodia S, Malinow R (2006) AMPAR removal underlies Abeta-induced synaptic depression and dendritic spine loss. *Neuron* 52:831–843. 51, 119

Hu NW, Klyubin I, Anwyl R, Anwy R, Rowan MJ (2009) GluN2B subunit-containing NMDA receptor antagonists prevent Abeta-mediated synaptic plasticity disruption in vivo. *Proceedings of the National Academy of Sciences* 106:20504–20509. 152, 153

Huh GS, Boulanger LM, Du H, Riquelme PA, Brotz TM, Shatz CJ (2000) Functional requirement for class I MHC in CNS development and plasticity. *Science* 290:2155–2159. 190

Hurtado DE, Molina-Porcel L, Carroll JC, Macdonald C, Aboagye AK, Trojanowski JQ, Lee VMY (2012) Selectively silencing GSK-3 isoforms reduces plaques and tangles in mouse models of Alzheimer's disease. *Journal of Neuroscience* 32:7392–7402. 113

Iglói K, Doeller CF, Berthoz A, Rondi-Reig L, Burgess N (2010) Lateralized human hippocampal activity predicts navigation based on sequence or place memory. *Proceedings of the National Academy of Sciences* 107:14466–14471. 160

Inestrosa NC, Reyes AE, Chacón MA, Cerpa W, Villalón A, Montiel J, Merabachvili G, Aldunate R, Bozinovic F, Aboitiz F (2005) Human-like rodent amyloid-beta-peptide determines Alzheimer pathology in aged wild-type Octodon degu. *Neurobiology of Aging* 26:1023–1028. 200

Ishiguro K, Shiratsuchi A, Sato S, Omori A, Arioka M, Kobayashi S, Uchida T, Imahori K (1993) Glycogen synthase kinase 3 beta is identical to tau protein kinase I generating several epitopes of paired helical filaments. *FEBS letters* 325:167–172. 89, 111

Ittner LM, Ke YD, Delerue F, Bi M, Gladbach A, van Eersel J, Wölfing H, Chieng BC, Christie MJ, Napier IA, Eckert A, Staufenbiel M, Hardeman E, Götz J (2010) Dendritic function of tau mediates amyloid-beta toxicity in Alzheimer's disease mouse models. *Cell* 142:387–397. 110, 151, 152

Izumi Y, Auberson YP, Zorumski CF (2006) Zinc modulates bidirectional hippocampal plasticity by effects on NMDA receptors. *Journal of Neuroscience* 26:7181–7188. 19, 28, 29

Jacobs GH, Williams GA, Fenwick JA (2004) Influence of cone pigment coexpression on spectral sensitivity and color vision in the mouse. *Vision Research* 44:1615–1622. 191

Jang H, Arce FT, Ramachandran S, Capone R, Azimova R, Kagan BL, Nussinov R, Lal R (2010) Truncated beta-amyloid peptide channels provide an alternative mechanism for Alzheimer's Disease and Down syndrome. *Proceedings of the National Academy of Sciences* 107:6538–6543. 50

Jin M, Shepardson N, Yang T, Chen G, Walsh D, Selkoe DJ (2011) Soluble amyloid beta-protein dimers isolated from Alzheimer cortex directly induce Tau hyperphosphorylation and neuritic degeneration. *Proceedings of the National Academy of Sciences* 108:5819–5824. 89, 152, 204

Jin Sx, Feig LA (2010) Long-term potentiation in the CA1 hippocampus induced by NR2A subunit-containing NMDA glutamate receptors is mediated by RasGRF2/Erk map kinase signaling. *PLoS ONE* 5:e11732. 16, 25

Jo J, Whitcomb DJ, Olsen KM, Kerrigan TL, Lo SC, Bru-Mercier G, Dickinson B, Scullion S, Sheng M, Collingridge G, Cho K (2011) Aβ(1-42) inhibition of LTP is mediated by a signaling pathway involving caspase-3, Akt1 and GSK-3β. *Nature Neuroscience* 14:545–547. 112

Kamenetz F, Tomita T, Hsieh H, Seabrook G, Borchelt D, Iwatsubo T, Sisodia S, Malinow R (2003) APP processing and synaptic function. *Neuron* 37:925–937. 46, 47

Kameyama K, Lee HK, Bear MF, Huganir RL (1998) Involvement of a postsynaptic protein kinase A substrate in the expression of homosynaptic long-term depression. *Neuron* 21:1163–1175. 8

Kanaan NM, Morfini GA, LaPointe NE, Pigino GF, Patterson KR, Song Y, Andreadis A, Fu Y, Brady ST, Binder LI (2011) Pathogenic forms of tau inhibit kinesin-dependent axonal transport through a mechanism involving activation of axonal phosphotransferases. *Journal of Neuroscience* 31:9858–9868. 155

Kasai H, Matsuzaki M, Noguchi J, Yasumatsu N, Nakahara H (2003) Structure-stability-function relationships of dendritic spines. *Trends in Neurosciences* 26:360–368. 42

Kawahara A, Kurauchi S, Fukata Y, Martínez-Hernández J, Yagihashi T, Itadani Y, Sho R, Kajiyama T, Shinzato N, Narusuye K, Fukata M, Luján R, Shigemoto R, Ito I (2013) Neuronal major histocompatibility complex class I molecules are implicated in the generation of asymmetries in hippocampal circuitry. *Journal of Physiology* . 190

Kawakami R, Dobi A, Shigemoto R, Ito I (2008) Right isomerism of the brain in inversus viscerum mutant mice. *PLoS ONE* 3:e1945. 190

Kawakami R, Shinohara Y, Kato Y, Sugiyama H, Shigemoto R, Ito I (2003) Asymmetrical allocation of NMDA receptor epsilon2 subunits in hippocampal circuitry. *Science* 300:990–994. 43, 44, 138, 141, 149, 156, 186, 207

Kessels HW, Nguyen LN, Nabavi S, Malinow R (2010) The prion protein as a receptor for amyloid-beta. *Nature* 466:E3–4– discussion E4–5. 50

Kim JH, Anwyl R, Suh YH, Djamgoz MB, Rowan MJ (2001) Use-dependent effects of amyloidogenic fragments of (beta)-amyloid precursor protein on synaptic plasticity in rat hippocampus in vivo. *Journal of Neuroscience* 21:1327–1333. 51

Kim T, Vidal GS, Djurisic M, William CM, Birnbaum ME, Garcia KC, Hyman BT, Shatz CJ (2013) Human LilrB2 is a β-amyloid receptor and its murine homolog PirB regulates synaptic plasticity in an Alzheimer's model. *Science* 341:1399–1404. 50

Kirson ED, Yaari Y (1996) Synaptic NMDA receptors in developing mouse hippocampal neurones: functional properties and sensitivity to ifenprodil. *Journal of Physiology* 497 (Pt 2):437–455. 11

Kiyama Y, Manabe T, Sakimura K, Kawakami F, Mori H, Mishina M (1998) Increased thresholds for long-term potentiation and contextual learning in mice lacking the NMDA-type glutamate receptor epsilon1 subunit. *Journal of Neuroscience* 18:6704–6712. 23, 33

Klein PS, Melton DA (1996) A molecular mechanism for the effect of lithium on development. *Proceedings of the National Academy of Sciences* 93:8455–8459. 69, 98

Klur S, Muller C, Pereira de Vasconcelos A, Ballard T, Lopez J, Galani R, Certa

U, Cassel JC (2009) Hippocampal-dependent spatial memory functions might be lateralized in rats: An approach combining gene expression profiling and reversible inactivation. *Hippocampus* 19:800–816. 161, 183, 187, 213

Klyubin I, Betts V, Welzel AT, Blennow K, Zetterberg H, Wallin A, Lemere CA, Cullen WK, Peng Y, Wisniewski T, Selkoe DJ, Anwyl R, Walsh DM, Rowan MJ (2008) Amyloid beta protein dimer-containing human CSF disrupts synaptic plasticity: prevention by systemic passive immunization. *Journal of Neuroscience* 28:4231–4237. 51

Kohl MM, Shipton OA, Deacon RM, Rawlins JNP, Deisseroth K, Paulsen O (2011) Hemisphere-specific optogenetic stimulation reveals left-right asymmetry of hippocampal plasticity. *Nature Neuroscience* 14:1413–1415. 20, 43, 44, 54, 61, 138, 141, 143, 156, 162, 164, 186, 207, 209, 211

Köhr G, Jensen V, Koester HJ, Mihaljevic ALA, Utvik JK, Kvello A, Ottersen OP, Seeburg PH, Sprengel R, Hvalby Ø (2003) Intracellular domains of NMDA receptor subtypes are determinants for long-term potentiation induction. *Journal of Neuroscience* 23:10791–10799. 19, 25, 26

Kojima N, Wang J, Mansuy IM, Grant SG, Mayford M, Kandel ER (1997) Rescuing impairment of long-term potentiation in fyn-deficient mice by introducing Fyn transgene. *Proceedings of the National Academy of Sciences* 94:4761–4765. 151

Kollen M, Dutar P, Jouvenceau A (2008) The magnitude of hippocampal long term depression depends on the synaptic location of activated NR2-containing N-methyl-D-aspartate receptors. *Neuroscience* 154:1308–1317. 29

Konorski J (1948) Conditioned reflexes and neuron organization New York: Cambridge University Press. 2

Korotkova T, Fuchs EC, Ponomarenko A, von Engelhardt J, Monyer H (2010) NMDA receptor ablation on parvalbumin-positive interneurons impairs hippocampal synchrony, spatial representations, and working memory. *Neuron* 68:557–569. 40

Ku HY, Huang YF, Chao PH, Huang CC, Hsu KS (2008) Neonatal isolation delays the developmental decline of long-term depression in the CA1 region of rat hippocampus. *Neuropsychopharmacology* 33:2847–2859. 28

Kurup P, Zhang Y, Xu J, Venkitaramani DV, Haroutunian V, Greengard P, Nairn AC, Lombroso PJ (2010) Abeta-mediated NMDA receptor endocytosis in Alzheimer's disease involves ubiquitination of the tyrosine phosphatase STEP61. *Journal of Neuroscience* 30:5948–5957. 118

Lacor PN, Buniel MC, Furlow PW, Clemente AS, Velasco PT, Wood M, Viola KL, Klein WL (2007) Abeta oligomer-induced aberrations in synapse composition, shape, and density provide a molecular basis for loss of connectivity in Alzheimer's disease. *Journal of Neuroscience* 27:796–807. 51

LaFerla FM, Green KN (2012) Animal models of Alzheimer disease. *Cold Spring Harbor Perspectives in Medicine* 2. 199

Lai AY, McLaurin J (2010) Mechanisms of amyloid-Beta Peptide uptake by neurons: the role of lipid rafts and lipid raft-associated proteins. *International Journal of Alzheimer's Disease* 2011:548380. 50

Lambert MP, Barlow AK, Chromy BA, Edwards C, Freed R, Liosatos M, Morgan TE, Rozovsky I, Trommer B, Viola KL, Wals P, Zhang C, Finch CE, Krafft GA, Klein WL (1998) Diffusible, nonfibrillar ligands derived from Abeta1-42 are potent central nervous system neurotoxins. *Proceedings of the National Academy of Sciences* 95:6448–6453. 51, 87, 109, 117, 151, 204

LaMendola NP, Bever TG (1997) Peripheral and cerebral asymmetries in the rat. *Science* 278:483–486. 189, 190

LaPointe NE, Morfini G, Pigino G, Gaisina IN, Kozikowski AP, Binder LI, Brady ST (2009) The amino terminus of tau inhibits kinesin-dependent axonal transport: implications for filament toxicity. *Journal of Neuroscience Research* 87:440–451. 155

Larson M, Sherman MA, Amar F, Nuvolone M, Schneider JA, Bennett DA, Aguzzi A, Lesné SE (2012) The complex PrP(c)-Fyn couples human oligomeric Aβ with pathological tau changes in Alzheimer's disease. *Journal of Neuroscience* 32:16857–71a. 151

Laurén J, Gimbel DA, Nygaard HB, Gilbert JW, Strittmatter SM (2009) Cellular prion protein mediates impairment of synaptic plasticity by amyloid-beta oligomers. *Nature* 457:1128–1132. 50

Lavezzari G, McCallum J, Dewey CM, Roche KW (2004) Subunit-specific regulation of NMDA receptor endocytosis. *Journal of Neuroscience* 24:6383–6391. 15, 153, 154

Lee AM, Kanter BR, Wang D, Lim JP, Zou ME, Qiu C, McMahon T, Dadgar J, Fischbach-Weiss SC, Messing RO (2013) Prkcz null mice show normal learning and memory. *Nature* 493:416–419. 7

Lee HK, Barbarosie M, Kameyama K, Bear MF, Huganir RL (2000) Regulation of distinct AMPA receptor phosphorylation sites during bidirectional synaptic plasticity. *Nature* 405:955–959. 6

Lee HK, Kameyama K, Huganir RL, Bear MF (1998) NMDA induces long-term synaptic depression and dephosphorylation of the GluR1 subunit of AMPA

receptors in hippocampus. *Neuron* 21:1151–1162. 8

Leonard AS, Lim IA, Hemsworth DE, Horne MC, Hell JW (1999) Calcium/calmodulin-dependent protein kinase II is associated with the N-methyl-D-aspartate receptor. *Proceedings of the National Academy of Sciences* 96:3239–3244. 6, 15, 156

Levitz J, Pantoja C, Gaub B, Janovjak H, Reiner A, Hoagland A, Schoppik D, Kane B, Stawski P, Schier AF, Trauner D, Isacoff EY (2013) Optical control of metabotropic glutamate receptors. *Nature Neuroscience* 16:507–516. 195

Li R, Huang FS, Abbas AK, Wigström H (2007) Role of NMDA receptor subtypes in different forms of NMDA-dependent synaptic plasticity. *BMC Neuroscience* 8:55. 18, 19, 28, 29

Li S, Hong S, Shepardson NE, Walsh DM, Shankar GM, Selkoe D (2009) Soluble oligomers of amyloid Beta protein facilitate hippocampal long-term depression by disrupting neuronal glutamate uptake. *Neuron* 62:788–801. 51, 152, 206

Li S, Jin M, Koeglsperger T, Shepardson NE, Shankar GM, Selkoe DJ (2011) Soluble Aβ oligomers inhibit long-term potentiation through a mechanism involving excessive activation of extrasynaptic NR2B-containing NMDA receptors. *Journal of Neuroscience* 31:6627–6638. 118, 152, 153, 154, 203

Li S, Tian X, Hartley DM, Feig LA (2006) Distinct roles for Ras-guanine nucleotide-releasing factor 1 (Ras-GRF1) and Ras-GRF2 in the induction of long-term potentiation and long-term depression. *Journal of Neuroscience* 26:1721–1729. 16, 29, 31

Limon A, Reyes-Ruiz JM, Miledi R (2012) Loss of functional GABA(A) recep-

tors in the Alzheimer diseased brain. *Proceedings of the National Academy of Sciences* 109:10071–10076. 95, 110

Lin JY, Knutsen PM, Muller A, Kleinfeld D, Tsien RY (2013a) ReaChR: a red-shifted variant of channelrhodopsin enables deep transcranial optogenetic excitation. *Nature Neuroscience* . 192

Lin JY, Sann SB, Zhou K, Nabavi S, Proulx CD, Malinow R, Jin Y, Tsien RY (2013b) Optogenetic inhibition of synaptic release with chromophore-assisted light inactivation (CALI). *Neuron* 79:241–253. 195

Ling Y, Morgan K, Kalsheker N (2003) Amyloid precursor protein (APP) and the biology of proteolytic processing: relevance to Alzheimer's disease. *The International Journal of Biochemistry & Cell Biology* 35:1505–1535. 46

Lisman J (1989) A mechanism for the Hebb and the anti-Hebb processes underlying learning and memory. *Proceedings of the National Academy of Sciences* 86:9574–9578. 9

Lisman J, Schulman H, Cline H (2002) The molecular basis of CaMKII function in synaptic and behavioural memory. *Nature Reviews Neuroscience* 3:175–190. 6, 15, 137

Lisman J, Grace AA, Duzel E (2011) A neoHebbian framework for episodic memory; role of dopamine-dependent late LTP. *Trends in Neurosciences* 34:536–547. 195

Lisman J, Yasuda R, Raghavachari S (2012) Mechanisms of CaMKII action in long-term potentiation. *Nature Reviews Neuroscience* 13:169–182. 6

Liu CC, Liu CC, Kanekiyo T, Xu H, Bu G (2013) Apolipoprotein E and

Alzheimer disease: risk, mechanisms and therapy. *Nature Reviews Neurology* 9:106–118. 45

Liu L, Wong TP, Pozza MF, Lingenhoehl K, Wang Y, Sheng M, Auberson YP, Wang YT (2004) Role of NMDA receptor subtypes in governing the direction of hippocampal synaptic plasticity. *Science* 304:1021–1024. 18, 19, 28, 29

Longordo F, Kopp C, Mishina M, Luján R, Lüthi A (2009) NR2A at CA1 synapses is obligatory for the susceptibility of hippocampal plasticity to sleep loss. *Journal of Neuroscience* 29:9026–9041. 30

Lovestone S, Davis DR, Webster MT, Kaech S, Brion JP, Matus A, Anderton BH (1999) Lithium reduces tau phosphorylation: effects in living cells and in neurons at therapeutic concentrations. *Biological Psychiatry* 45:995–1003. 98

Lucas JJ, Hernández F, Gómez-Ramos P, Morán MA, Hen R, AVILA J (2001) Decreased nuclear beta-catenin, tau hyperphosphorylation and neurodegeneration in GSK-3beta conditional transgenic mice. *EMBO* 20:27–39. 111

Lue LF, Kuo YM, Roher AE, Brachova L, Shen Y, Sue L, Beach T, Kurth JH, Rydel RE, Rogers J (1999) Soluble amyloid beta peptide concentration as a predictor of synaptic change in Alzheimer's disease. *American Journal of Pathology* 155:853–862. 87

Lührs T, Ritter C, Adrian M, Riek-Loher D, Bohrmann B, Döbeli H, Schubert D, Riek R (2005) 3D structure of Alzheimer's amyloid-beta(1-42) fibrils. *Proceedings of the National Academy of Sciences* 102:17342–17347. 48

Luo AH, Tahsili-Fahadan P, Wise RA, Lupica CR, Aston-Jones G (2011) Linking context with reward: a functional circuit from hippocampal CA3 to ventral tegmental area. *Science* 333:353–357. 173

Lüthi A, Wikström MA, Palmer MJ, Matthews P, Benke TA, Isaac JTR, Collingridge GL (2004) Bi-directional modulation of AMPA receptor unitary conductance by synaptic activity. *BMC Neuroscience* 5:44. 6, 8

Lyon L, Burnet PWJ, Kew JNC, Corti C, Rawlins JNP, Lane T, De Filippis B, Harrison PJ, Bannerman DM (2011) Fractionation of spatial memory in GRM2/3 (mGlu2/mGlu3) double knockout mice reveals a role for group II metabotropic glutamate receptors at the interface between arousal and cognition. *Neuropsychopharmacology* 36:2616–2628. 173

Ma T, Du X, Pick JE, Sui G, Brownlee M, Klann E (2012) Glucagon-like peptide-1 cleavage product GLP-1(9-36) amide rescues synaptic plasticity and memory deficits in Alzheimer's disease model mice. *Journal of Neuroscience* 32:13701–13708. 110

Ma T, Hoeffer CA, Capetillo-Zarate E, Yu F, Wong H, Lin MT, Tampellini D, Klann E, Blitzer RD, Gouras GK (2010) Dysregulation of the mTOR pathway mediates impairment of synaptic plasticity in a mouse model of Alzheimer's disease. *PLoS ONE* 5. 88

Ma T, Hoeffer CA, Wong H, Massaad CA, Zhou P, Iadecola C, Murphy MP, Pautler RG, Klann E (2011a) Amyloid β-induced impairments in hippocampal synaptic plasticity are rescued by decreasing mitochondrial superoxide. *Journal of Neuroscience* 31:5589–5595. 110

Ma T, Tzavaras N, Tsokas P, Landau EM, Blitzer RD (2011b) Synaptic stimulation of mTOR is mediated by Wnt signaling and regulation of glycogen synthetase kinase-3. *Journal of Neuroscience* 31:17537–17546. 88

Mairet-Coello G, Courchet J, Pieraut S, Courchet V, Maximov A, Polleux F (2013) The CAMKK2-AMPK kinase pathway mediates the synaptotoxic effects of

Aβ oligomers through Tau phosphorylation. *Neuron* 78:94–108. 112

Malenka RC, Bear MF (2004) LTP and LTD: an embarrassment of riches. *Neuron* 44:5–21. 11

Malleret G, Haditsch U, Genoux D, Jones MW, Bliss TV, Vanhoose AM, Weitlauf C, Kandel ER, Winder DG, Mansuy IM (2001) Inducible and reversible enhancement of learning, memory, and long-term potentiation by genetic inhibition of calcineurin. *Cell* 104:675–686. 162, 170

Mandelkow EM, Mandelkow E (2012) Biochemistry and cell biology of tau protein in neurofibrillary degeneration. *Cold Spring Harbor Perspectives in Medicine* 2:a006247. 52, 53, 88

Markesbery WR, Schmitt FA, Kryscio RJ, Davis DG, Smith CD, Wekstein DR (2006) Neuropathologic substrate of mild cognitive impairment. *Archives of Neurology* 63:38–46. 87

Martin SJ, Grimwood PD, Morris RG (2000) Synaptic plasticity and memory: an evaluation of the hypothesis. *Annual Review of Neuroscience* 23:649–711. 162

Matsuzaki M, Honkura N, Ellis-Davies GCR, Kasai H (2004) Structural basis of long-term potentiation in single dendritic spines. *Nature* 429:761–766. 8, 42, 137, 157

Mattis J, Tye KM, Ferenczi EA, Ramakrishnan C, O'Shea DJ, Prakash R, Gunaydin LA, Hyun M, Fenno LE, Gradinaru V, Yizhar O, Deisseroth K (2012) Principles for applying optogenetic tools derived from direct comparative analysis of microbial opsins. *Nature Methods* 9:159–172. 193

McGuinness L, Taylor C, Taylor RDT, Yau C, Langenhan T, Hart ML, Christian H, Tynan PW, Donnelly P, Emptage NJ (2010) Presynaptic NMDARs in the hippocampus facilitate transmitter release at theta frequency. *Neuron* 68:1109–1127. 10, 93

Merino-Serrais P, Benavides-Piccione R, Blazquez-Llorca L, Kastanauskaite A, Rábano A, Avila J, DeFelipe J (2013) The influence of phospho-τ on dendritic spines of cortical pyramidal neurons in patients with Alzheimer's disease. *Brain* 136:1913–1928. 53

Moechars D, Dewachter I, Lorent K, Reversé D, Baekelandt V, Naidu A, Tesseur I, Spittaels K, Haute CV, Checler F, Godaux E, Cordell B, Van Leuven F (1999) Early phenotypic changes in transgenic mice that overexpress different mutants of amyloid precursor protein in brain. *Journal of Biological Chemistry* 274:6483–6492. 89

Monyer H, Burnashev N, Laurie DJ, Sakmann B, Seeburg PH (1994) Developmental and regional expression in the rat brain and functional properties of four NMDA receptors. *Neuron* 12:529–540. 11, 14, 21

Moody TD, Watabe AM, Indersmitten T, Komiyama NH, Grant SGN, O'Dell TJ (2011) Beta-adrenergic receptor activation rescues theta frequency stimulation-induced LTP deficits in mice expressing C-terminally truncated NMDA receptor GluN2A subunits. *Learning & Memory* 18:118–127. 26

Morishita W, Lu W, Smith GB, Nicoll RA, Bear MF, Malenka RC (2007) Activation of NR2B-containing NMDA receptors is not required for NMDA receptor-dependent long-term depression. *Neuropharmacology* 52:71–76. 29

Morris RG, Anderson E, Lynch GS, Baudry M (1986) Selective impairment of learning and blockade of long-term potentiation by an N-methyl-D-aspartate

receptor antagonist, AP5. *Nature* 319:774–776. 5, 39

Morris RG, Garrud P, Rawlins JN, O'Keefe J (1982) Place navigation impaired in rats with hippocampal lesions. *Nature* 297:681–683. 5, 161

Morris RGM, Schenk F, Tweedie F, Jarrard LE (1990) Ibotenate Lesions of Hippocampus and/or Subiculum: Dissociating Components of Allocentric Spatial Learning. *European Journal of Neuroscience* 2:1016–1028. 5

Morris RGM (2013) NMDA receptors and memory encoding. *Neuropharmacology* 74:32–40. 40, 162, 163, 185

Moser MB, Moser EI (1998) Distributed encoding and retrieval of spatial memory in the hippocampus. *Journal of Neuroscience* 18:7535–7542. 191

Motley SE, Kirwan CB (2012) A parametric investigation of pattern separation processes in the medial temporal lobe. *Journal of Neuroscience* 32:13076–13085. 161

Mucke L, Selkoe DJ (2012) Neurotoxicity of amyloid β-protein: synaptic and network dysfunction. *Cold Spring Harbor Perspectives in Medicine* 2:a006338. 48, 155

Mulkey RM, Endo S, Shenolikar S, Malenka RC (1994) Involvement of a calcineurin/inhibitor-1 phosphatase cascade in hippocampal long-term depression. *Nature* 369:486–488. 8, 51

Mulkey RM, Herron CE, Malenka RC (1993) An essential role for protein phosphatases in hippocampal long-term depression. *Science* 261:1051–1055. 8

Mulkey RM, Malenka RC (1992) Mechanisms underlying induction of homosynaptic long-term depression in area CA1 of the hippocampus. *Neu-*

ron 9:967–975. 8

Nabavi S, Kessels HW, Alfonso S, Aow J, Fox R, Malinow R (2013) Metabotropic NMDA receptor function is required for NMDA receptor-dependent long-term depression. *Proceedings of the National Academy of Sciences* 110:4027–4032. 31

Nakashiba T, Buhl DL, McHugh TJ, Tonegawa S (2009) Hippocampal CA3 output is crucial for ripple-associated reactivation and consolidation of memory. *Neuron* 62:781–787. 195

Nakashiba T, Young JZ, McHugh TJ, Buhl DL, Tonegawa S (2008) Transgenic inhibition of synaptic transmission reveals role of CA3 output in hippocampal learning. *Science* 319:1260–1264. 185, 191, 210

Ng D, Pitcher GM, Szilard RK, Sertié A, Kanisek M, Clapcote SJ, Lipina T, Kalia LV, Joo D, McKerlie C, Cortez M, Roder JC, Salter MW, McInnes RR (2009) Neto1 is a novel CUB-domain NMDA receptor-interacting protein required for synaptic plasticity and learning. *PLoS Biology* 7:e41. 23, 33

Ngo-Anh TJ, Bloodgood BL, Lin M, Sabatini BL, Maylie J, Adelman JP (2005) SK channels and NMDA receptors form a Ca2+-mediated feedback loop in dendritic spines. *Nature Neuroscience* 8:642–649. 10

Nicholson AM, Ferreira A (2009) Increased membrane cholesterol might render mature hippocampal neurons more susceptible to beta-amyloid-induced calpain activation and tau toxicity. *Journal of Neuroscience* 29:4640–4651. 88

Nicholson AM, Methner DNR, Ferreira A (2011) Membrane cholesterol modulates beta-amyloid-dependent tau cleavage by inducing changes in the membrane content and localization of N-methyl-D-aspartic acid receptors. *Journal*

of Biological Chemistry 286:976–986. 50

Nomura I, Takechi H, Kato N (2012) Intraneuronally injected amyloid β inhibits long-term potentiation in rat hippocampal slices. *Journal of Neurophysiology* 107:2526–2531. 48

Nussbaum JM, Schilling S, Cynis H, Silva A, Swanson E, Wangsanut T, Tayler K, Wiltgen B, Hatami A, Rönicke R, Reymann K, Hutter-Paier B, Alexandru A, Jagla W, Graubner S, Glabe CG, Demuth HU, Bloom GS (2012) Prion-like behaviour and tau-dependent cytotoxicity of pyroglutamylated amyloid-β. *Nature* 485:651–655. 49, 110, 204

O'Brien RJ, Lau LF, Huganir RL (1998) Molecular mechanisms of glutamate receptor clustering at excitatory synapses. *Current Opinion in Neurobiology* 8:364–369. 14

Oddo S, Caccamo A, Shepherd JD, Murphy MP, Golde TE, Kayed R, Metherate R, Mattson MP, Akbari Y, LaFerla FM (2003) Triple-transgenic model of Alzheimer's disease with plaques and tangles: intracellular Abeta and synaptic dysfunction. *Neuron* 39:409–421. 199

Oddo S, Caccamo A, Tseng B, Cheng D, Vasilevko V, Cribbs DH, LaFerla FM (2008) Blocking Abeta42 accumulation delays the onset and progression of tau pathology via the C terminus of heat shock protein70-interacting protein: a mechanistic link between Abeta and tau pathology. *Journal of Neuroscience* 28:12163–12175. 113

O'Keefe J, Dostrovsky J (1971) The hippocampus as a spatial map. Preliminary evidence from unit activity in the freely-moving rat. *Brain Research* 34:171–175. 5

Oliet SH, Malenka RC, Nicoll RA (1997) Two distinct forms of long-term depression coexist in CA1 hippocampal pyramidal cells. *Neuron* 18:969–982. 6

Olsen KM, Sheng M (2012) NMDA receptors and BAX are essential for Aβ impairment of LTP. *Scientific Reports* 2:225. 112

Olton DS, Papas BC (1979) Spatial memory and hippocampal function. *Neuropsychologia* 17:669–682. 5, 161

Opazo P, Choquet D (2011) A three-step model for the synaptic recruitment of AMPA receptors. *Molecular and Cellular Neurosciences* 46:1–8. 7

Opazo P, Labrecque S, Tigaret CM, Frouin A, Wiseman PW, De Koninck P, Choquet D (2010) CaMKII triggers the diffusional trapping of surface AMPARs through phosphorylation of stargazin. *Neuron* 67:239–252. 7

Otmakhov N, Tao-Cheng JH, Carpenter S, Asrican B, Dosemeci A, Reese TS, Lisman J (2004) Persistent accumulation of calcium/calmodulin-dependent protein kinase II in dendritic spines after induction of NMDA receptor-dependent chemical long-term potentiation. *Journal of Neuroscience* 24:9324–9331. 6, 16

Palop JJ, Chin J, Roberson ED, Wang J, Thwin MT, Bien-Ly N, Yoo J, Ho KO, Yu GQ, Kreitzer A, Finkbeiner S, Noebels JL, Mucke L (2007) Aberrant excitatory neuronal activity and compensatory remodeling of inhibitory hippocampal circuits in mouse models of Alzheimer's disease. *Neuron* 55:697–711. 95, 110

Palop JJ, Mucke L (2010) Amyloid-beta-induced neuronal dysfunction in Alzheimer's disease: from synapses toward neural networks. *Nature Neuroscience* 13:812–818. 95, 110

Paoletti P, Neyton J (2007) NMDA receptor subunits: function and pharmacology. *Current Opinion in Pharmacology* 7:39–47. 17, 128, 206

Papasozomenos SC, Binder LI (1987) Phosphorylation determines two distinct species of Tau in the central nervous system. *Cell Motility and the Cytoskeleton* 8:210–226. 53

Parameshwaran K, Sims C, Kanju P, Vaithianathan T, Shonesy BC, Dhanasekaran M, Bahr BA, Suppiramaniam V (2007) Amyloid beta-peptide Abeta(1-42) but not Abeta(1-40) attenuates synaptic AMPA receptor function. *Synapse* 61:367–374. 118, 147, 148

Park SY, Ferreira A (2005) The generation of a 17 kDa neurotoxic fragment: an alternative mechanism by which tau mediates beta-amyloid-induced neurodegeneration. *Journal of Neuroscience* 25:5365–5375. 53, 88

Pastalkova E, Serrano P, Pinkhasova D, Wallace E, Fenton AA, Sacktor TC (2006) Storage of spatial information by the maintenance mechanism of LTP. *Science* 313:1141–1144. 7

Pei JJ, Braak E, Braak H, Grundke-Iqbal I, Iqbal K, Winblad B, Cowburn RF (1999) Distribution of active glycogen synthase kinase 3beta (GSK-3beta) in brains staged for Alzheimer disease neurofibrillary changes. *Journal of Neuropathology and Experimental Neurology* 58:1010–1019. 89

Peineau S, Taghibiglou C, Bradley C, Wong TP, Liu L, Lu J, Lo E, Wu D, Saule E, Bouschet T, Matthews P, Isaac JTR, Bortolotto ZA, Wang YT, Collingridge GL (2007) LTP inhibits LTD in the hippocampus via regulation of GSK3beta. *Neuron* 53:703–717. 9, 111

Pellarin R, Schuetz P, Guarnera E, Caflisch A (2010) Amyloid fibril poly-

morphism is under kinetic control. *Journal of the American Chemical Society* 132:14960–14970. 49

Plant K, Pelkey KA, Bortolotto ZA, Morita D, Terashima A, McBain CJ, Collingridge GL, Isaac JTR (2006) Transient incorporation of native GluR2-lacking AMPA receptors during hippocampal long-term potentiation. *Nature Neuroscience* 9:602–604. 7

Poe GR, Teed RG, Insel N, White R, McNaughton BL, Barnes CA (2000) Partial hippocampal inactivation: effects on spatial memory performance in aged and young rats. *Behavioral Neuroscience* 114:940–949. 161, 184, 213

Puzzo D, Privitera L, Leznik E, Fà M, Staniszewski A, Palmeri A, Arancio O (2008) Picomolar amyloid-beta positively modulates synaptic plasticity and memory in hippocampus. *Journal of Neuroscience* 28:14537–14545. 46

Qi-Takahara Y, Morishima-Kawashima M, Tanimura Y, Dolios G, Hirotani N, Horikoshi Y, Kametani F, Maeda M, Saido TC, Wang R, Ihara Y (2005) Longer forms of amyloid beta protein: implications for the mechanism of intramembrane cleavage by gamma-secretase. *Journal of Neuroscience* 25:436–445. 46

Raimondo JV, Kay L, Ellender TJ, Akerman CJ (2012) Optogenetic silencing strategies differ in their effects on inhibitory synaptic transmission. *Nature Neuroscience* 15:1102–1104. 168, 193

Ramirez S, Liu X, Lin PA, Suh J, Pignatelli M, Redondo RL, Ryan TJ, Tonegawa S (2013) Creating a false memory in the hippocampus. *Science* 341:387–391. 211

Rammes G, Hasenjäger A, Sroka-Saidi K, Deussing JM, Parsons CG (2011) Therapeutic significance of NR2B-containing NMDA receptors and mGluR5

metabotropic glutamate receptors in mediating the synaptotoxic effects of β-amyloid oligomers on long-term potentiation (LTP) in murine hippocampal slices. *Neuropharmacology* 60:982–990. 118

Rapoport M, Dawson HN, Binder LI, Vitek MP, Ferreira A (2002) Tau is essential to beta -amyloid-induced neurotoxicity. *Proceedings of the National Academy of Sciences* 99:6364–6369. 89, 109, 152, 204

Rauner C, Köhr G (2011) Triheteromeric NR1/NR2A/NR2B receptors constitute the major N-methyl-D-aspartate receptor population in adult hippocampal synapses. *Journal of Biological Chemistry* 286:7558–7566. 12, 149, 207

Rawlins JN, Olton DS (1982) The septo-hippocampal system and cognitive mapping. *Behavioural Brain Research* 5:331–358. 161

Reisel D, Bannerman DM, Schmitt WB, Deacon RMJ, Flint J, Borchardt T, Seeburg PH, Rawlins JNP (2002) Spatial memory dissociations in mice lacking GluR1. *Nature Neuroscience* 5:868–873. 170, 173

Renner M, Lacor PN, Velasco PT, Xu J, Contractor A, Klein WL, Triller A (2010) Deleterious effects of amyloid beta oligomers acting as an extracellular scaffold for mGluR5. *Neuron* 66:739–754. 119

Resenberger UK, Harmeier A, Woerner AC, Goodman JL, Müller V, Krishnan R, Vabulas RM, Kretzschmar HA, Lindquist S, Hartl FU, Multhaup G, Winklhofer KF, Tatzelt J (2011) The cellular prion protein mediates neurotoxic signalling of β-sheet-rich conformers independent of prion replication. *EMBO* 30:2057–2070. 50

Rhinn H, Fujita R, Qiang L, Cheng R, Lee JH, Abeliovich A (2013) Integrative genomics identifies APOE ε4 effectors in Alzheimer's disease. *Na-*

ture 500:45–50. 45

Roberson ED, Halabisky B, Yoo JW, Yao J, Chin J, Yan F, Wu T, Hamto P, Devidze N, Yu GQ, Palop JJ, Noebels JL, Mucke L (2011) Amyloid-β/Fyn-induced synaptic, network, and cognitive impairments depend on tau levels in multiple mouse models of Alzheimer's disease. *Journal of Neuroscience* 31:700–711. 89, 110, 152, 204

Roberson ED, Scearce-Levie K, Palop JJ, Yan F, Cheng IH, Wu T, Gerstein H, Yu GQ, Mucke L (2007) Reducing endogenous tau ameliorates amyloid beta-induced deficits in an Alzheimer's disease mouse model. *Science* 316:750–754. 89, 110, 152, 204

Rodríguez-Moreno A, Kohl MM, Reeve JE, Eaton TR, Collins HA, Anderson HL, Paulsen O (2011) Presynaptic induction and expression of timing-dependent long-term depression demonstrated by compartment-specific photorelease of a use-dependent NMDA receptor antagonist. *Journal of Neuroscience* 31:8564–8569. 10

Romberg C, Raffel J, Martin L, Sprengel R, Seeburg PH, Rawlins JNP, Bannerman DM, Paulsen O (2009) Induction and expression of GluA1 (GluR-A)-independent LTP in the hippocampus. *European Journal of Neuroscience* 29:1141–1152. 19

Rong Y, Lu X, Bernard A, Khrestchatisky M, Baudry M (2001) Tyrosine phosphorylation of ionotropic glutamate receptors by Fyn or Src differentially modulates their susceptibility to calpain and enhances their binding to spectrin and PSD-95. *Journal of Neurochemistry* 79:382–390. 151

Rönicke R, Mikhaylova M, Rönicke S, Meinhardt J, Schröder UH, Fändrich M, Reiser G, Kreutz MR, Reymann KG (2011) Early neuronal dysfunction by

amyloid β oligomers depends on activation of NR2B-containing NMDA receptors. *Neurobiology of Aging* 32:2219–2228. 118

Rubin JE, Gerkin RC, Bi GQ, Chow CC (2005) Calcium time course as a signal for spike-timing-dependent plasticity. *Journal of Neurophysiology* 93:2600–2613. 10

Saito T, Suemoto T, Brouwers N, Sleegers K, Funamoto S, Mihira N, Matsuba Y, Yamada K, Nilsson P, Takano J, Nishimura M, Iwata N, Van Broeckhoven C, Ihara Y, Saido TC (2011) Potent amyloidogenicity and pathogenicity of Aβ43. *Nature Neuroscience* 14:1023–1032. 49

Sakimura K, Kutsuwada T, Ito I, Manabe T, Takayama C, Kushiya E, Yagi T, Aizawa S, Inoue Y, Sugiyama H (1995) Reduced hippocampal LTP and spatial learning in mice lacking NMDA receptor epsilon 1 subunit. *Nature* 373:151–155. 23, 32

Sanderson DJ, Gray A, Simon A, Taylor AM, Deacon RMJ, Seeburg PH, Sprengel R, Good MA, Rawlins JNP, Bannerman DM (2007) Deletion of glutamate receptor-A (GluR-A) AMPA receptor subunits impairs one-trial spatial memory. *Behavioral Neuroscience* 121:559–569. 178

SantaCruz K, Lewis J, Spires T, Paulson J, Kotilinek L, Ingelsson M, Guimaraes A, DeTure M, Ramsden M, McGowan E, Forster C, Yue M, Orne J, Janus C, Mariash A, Kuskowski M, Hyman B, Hutton M, Ashe KH (2005) Tau suppression in a neurodegenerative mouse model improves memory function. *Science* 309:476–481. 87, 88

Santucci DM, Raghavachari S (2008) The effects of NR2 subunit-dependent NMDA receptor kinetics on synaptic transmission and CaMKII activation. *PLoS Computational Biology* 4:e1000208. 21

Sanz-Clemente A, Matta JA, Isaac JTR, Roche KW (2010) Casein kinase 2 regulates the NR2 subunit composition of synaptic NMDA receptors. *Neuron* 67:984–996. 15

Schimanski LA, Nguyen PV (2004) Multidisciplinary approaches for investigating the mechanisms of hippocampus-dependent memory: a focus on inbred mouse strains. *Neuroscience & Biobehavioral Reviews* 28:463–483. 32

Schmitt WB, Deacon RMJ, Seeburg PH, Rawlins JNP, Bannerman DM (2003) A within-subjects, within-task demonstration of intact spatial reference memory and impaired spatial working memory in glutamate receptor-A-deficient mice. *Journal of Neuroscience* 23:3953–3959. 80, 170, 176

Scoville WB, Milner B (1957) Loss of recent memory after bilateral hippocampal lesions. *Journal of neurology, neurosurgery, and psychiatry* 20:11–21. 4, 160

Selkoe DJ (2002) Alzheimer's disease is a synaptic failure. *Science* 298:789–791. 11, 42, 47, 87, 203

Shankar GM, Bloodgood BL, Townsend M, Walsh DM, Selkoe DJ, Sabatini BL (2007) Natural oligomers of the Alzheimer amyloid-beta protein induce reversible synapse loss by modulating an NMDA-type glutamate receptor-dependent signaling pathway. *Journal of Neuroscience* 27:2866–2875. 51

Shankar GM, Li S, Mehta TH, Garcia-Munoz A, Shepardson NE, Smith I, Brett FM, Farrell MA, Rowan MJ, Lemere CA, Regan CM, Walsh DM, Sabatini BL, Selkoe DJ (2008) Amyloid-beta protein dimers isolated directly from Alzheimer's brains impair synaptic plasticity and memory. *Nature Medicine* 14:837–842. 46, 48, 51, 117

Shemer I, Holmgren C, Min R, Fülöp L, Zilberter M, Sousa KM, Farkas T, Härtig

W, Penke B, Burnashev N, Tanila H, Zilberter Y, Harkany T (2006) Non-fibrillar beta-amyloid abates spike-timing-dependent synaptic potentiation at excitatory synapses in layer 2/3 of the neocortex by targeting postsynaptic AMPA receptors. *European Journal of Neuroscience* 23:2035–2047. 118, 147, 148

Shi S, Hayashi Y, Esteban JA, Malinow R (2001) Subunit-specific rules governing AMPA receptor trafficking to synapses in hippocampal pyramidal neurons. *Cell* 105:331–343. 7

Shinohara Y, Hirase H, Watanabe M, Itakura M, Takahashi M, Shigemoto R (2008) Left-right asymmetry of the hippocampal synapses with differential subunit allocation of glutamate receptors. *Proceedings of the National Academy of Sciences* 105:19498–19503. 42, 43, 137, 138, 141, 156, 157, 186, 210

Shinohara Y, Hosoya A, Hirase H (2013) Experience enhances gamma oscillations and interhemispheric asymmetry in the hippocampus. *Nature Communications* 4:1652. 189

Shipton OA, Leitz JR, Dworzak J, Acton CEJ, Tunbridge EM, Denk F, Dawson HN, Vitek MP, Wade-Martins R, Paulsen O, Vargas-Caballero M (2011) Tau protein is required for amyloid beta-induced impairment of hippocampal long-term potentiation. *Journal of Neuroscience* 31:1688–1692. 92, 152

Shouval HZ, Bear MF, Cooper LN (2002) A unified model of NMDA receptor-dependent bidirectional synaptic plasticity. *Proceedings of the National Academy of Sciences* 99:10831–10836. 9

Singh P, Hockenberry AJ, Tiruvadi VR, Meaney DF (2011) Computational investigation of the changing patterns of subtype specific NMDA receptor activation during physiological glutamatergic neurotransmission. *PLoS Computational Biology* 7:e1002106. 13

Sjöström PJ, Turrigiano GG, Nelson SB (2003) Neocortical LTD via coincident activation of presynaptic NMDA and cannabinoid receptors. *Neuron* 39:641–654. 10

Small SA, Duff K (2008) Linking Abeta and tau in late-onset Alzheimer's disease: a dual pathway hypothesis. *Neuron* 60:534–542. 88, 114

Smart TG, Hosie AM, Miller PS (2004) Zn2+ ions: modulators of excitatory and inhibitory synaptic activity. *The Neuroscientist* 10:432–442. 128, 206

Snyder EM, Nong Y, Almeida CG, Paul S, Moran T, Choi EY, Nairn AC, Salter MW, Lombroso PJ, Gouras GK, Greengard P (2005) Regulation of NMDA receptor trafficking by amyloid-beta. *Nature Neuroscience* 8:1051–1058. 65, 118

Sobczyk A, Scheuss V, Svoboda K (2005) NMDA receptor subunit-dependent [Ca2+] signaling in individual hippocampal dendritic spines. *Journal of Neuroscience* 25:6037–6046. 13, 14, 38, 42, 137

Sprengel R, Suchanek B, Amico C, Brusa R, Burnashev N, Rozov A, Hvalby O, Jensen V, Paulsen O, Andersen P, Kim JJ, Thompson RF, Sun W, Webster LC, Grant SG, Eilers J, Konnerth A, Li J, McNamara JO, Seeburg PH (1998) Importance of the intracellular domain of NR2 subunits for NMDA receptor function in vivo. *Cell* 92:279–289. 25

Squire LR, Ojemann JG, Miezin FM, Petersen SE, Videen TO, Raichle ME (1992) Activation of the hippocampus in normal humans: a functional anatomical study of memory. *Proceedings of the National Academy of Sciences* 89:1837–1841. 4, 160

Squire LR, Zola-Morgan S (1991) The medial temporal lobe memory system.

Science 253:1380–1386. 4, 160

Stéphan A, Laroche S, Davis S (2001) Generation of aggregated beta-amyloid in the rat hippocampus impairs synaptic transmission and plasticity and causes memory deficits. *Journal of Neuroscience* 21:5703–5714. 117

Strack S, Colbran RJ (1998) Autophosphorylation-dependent targeting of calcium/ calmodulin-dependent protein kinase II by the NR2B subunit of the N-methyl- D-aspartate receptor. *Journal of Biological Chemistry* 273:20689–20692. 6, 15, 156

Swanson LW, Cowan WM (1977) An autoradiographic study of the organization of the efferent connections of the hippocampal formation in the rat. *Journal of Comparative Neurology* 172:49–84. 173

Sydow A, Van der Jeugd A, Zheng F, Ahmed T, Balschun D, Petrova O, Drexler D, Zhou L, Rune G, Mandelkow E, D'Hooge R, Alzheimer C, Mandelkow EM (2011) Tau-induced defects in synaptic plasticity, learning, and memory are reversible in transgenic mice after switching off the toxic Tau mutant. *Journal of Neuroscience* 31:2511–2525. 88

Tackenberg C, Brandt R (2009) Divergent pathways mediate spine alterations and cell death induced by amyloid-beta, wild-type tau, and R406W tau. *Journal of Neuroscience* 29:14439–14450. 51, 98, 113, 114

Takami M, Nagashima Y, Sano Y, Ishihara S, Morishima-Kawashima M, Funamoto S, Ihara Y (2009) gamma-Secretase: successive tripeptide and tetrapeptide release from the transmembrane domain of beta-carboxyl terminal fragment. *Journal of Neuroscience* 29:13042–13052. 46

Talantova M, Sanz-Blasco S, Zhang X, Xia P, Akhtar MW, Okamoto Si,

Dziewczapolski G, Nakamura T, Cao G, Pratt AE, Kang YJ, Tu S, Molokanova E, McKercher SR, Hires SA, Sason H, Stouffer DG, Buczynski MW, Solomon JP, Michael S, Powers ET, Kelly JW, Roberts A, Tong G, Fang-Newmeyer T, Parker J, Holland EA, Zhang D, Nakanishi N, Chen HSV, Wolosker H, Wang Y, Parsons LH, Ambasudhan R, Masliah E, Heinemann SF, Piña-Crespo JC, Lipton SA (2013) Aβ induces astrocytic glutamate release, extrasynaptic NMDA receptor activation, and synaptic loss. *Proceedings of the National Academy of Sciences* 110:E2518–27. 153

Tampellini D, Rahman N, Lin MT, Capetillo-Zarate E, Gouras GK (2011) Impaired β-amyloid secretion in Alzheimer's disease pathogenesis. *Journal of Neuroscience* 31:15384–15390. 47

Tang TTT, Yang F, Chen BS, Lu Y, Ji Y, Roche KW, Lu B (2009) Dysbindin regulates hippocampal LTP by controlling NMDA receptor surface expression. *Proceedings of the National Academy of Sciences* 106:21395–21400. 23, 30

Tang YP, Shimizu E, Dube GR, Rampon C, Kerchner GA, Zhuo M, Liu G, Tsien JZ (1999) Genetic enhancement of learning and memory in mice. *Nature* 401:63–69. 23, 36, 162, 170

Tanzi RE (2012) The genetics of Alzheimer disease. *Cold Spring Harbor Perspectives in Medicine* 2. 45, 105

Terry RD, Masliah E, Salmon DP, Butters N, DeTeresa R, Hill R, Hansen LA, Katzman R (1991) Physical basis of cognitive alterations in Alzheimer's disease: synapse loss is the major correlate of cognitive impairment. *Annals of Neurology* 30:572–580. 52, 87

Ting JT, Kelley BG, Lambert TJ, Cook DG, Sullivan JM (2007) Amyloid precursor protein overexpression depresses excitatory transmission through

both presynaptic and postsynaptic mechanisms. *Proceedings of the National Academy of Sciences* 104:353–358. 118, 147, 148

Tomita S, Adesnik H, Sekiguchi M, Zhang W, Wada K, Howe JR, Nicoll RA, Bredt DS (2005a) Stargazin modulates AMPA receptor gating and trafficking by distinct domains. *Nature* 435:1052–1058. 7

Tomita S, Stein V, Stocker TJ, Nicoll RA, Bredt DS (2005b) Bidirectional synaptic plasticity regulated by phosphorylation of stargazin-like TARPs. *Neuron* 45:269–277. 8

Tonini R, Ferraro T, Sampedro-Castañeda M, Cavaccini A, Stocker M, Richards CD, Pedarzani P (2013) Small-conductance Ca2+-activated K+ channels modulate action potential-induced Ca2+ transients in hippocampal neurons. *Journal of Neurophysiology* 109:1514–1524. 10

Tovar KR, McGinley MJ, Westbrook GL (2013) Triheteromeric NMDA receptors at hippocampal synapses. *Journal of Neuroscience* 33:9150–9160. 12, 149, 207

Townsend M, Shankar GM, Mehta T, Walsh DM, Selkoe DJ (2006) Effects of secreted oligomers of amyloid beta-protein on hippocampal synaptic plasticity: a potent role for trimers. *Journal of Physiology* 572:477–492. 91, 109

Tsien JZ, Chen DF, Gerber D, Tom C, Mercer EH, Anderson DJ, Mayford M, Kandel ER, Tonegawa S (1996) Subregion- and cell type-restricted gene knockout in mouse brain. *Cell* 87:1317–1326. 164

Tsien JZ, Huerta PT, Tonegawa S (1996) The essential role of hippocampal CA1 NMDA receptor-dependent synaptic plasticity in spatial memory. *Cell* 87:1327–1338. 5, 170

Tycko R (2006) Molecular structure of amyloid fibrils: insights from solid-state NMR. *Quarterly Reviews of Biophysics* 39:1–55. 48

Um JW, Kaufman AC, Kostylev M, Heiss JK, Stagi M, Takahashi H, Kerrisk ME, Vortmeyer A, Wisniewski T, Koleske AJ, Gunther EC, Nygaard HB, Strittmatter SM (2013) Metabotropic glutamate receptor 5 is a coreceptor for Alzheimer aβ oligomer bound to cellular prion protein. *Neuron* 79:887–902. 50

Um JW, Nygaard HB, Heiss JK, Kostylev MA, Stagi M, Vortmeyer A, Wisniewski T, Gunther EC, Strittmatter SM (2012) Alzheimer amyloid-β oligomer bound to postsynaptic prion protein activates Fyn to impair neurons. *Nature Neuroscience* 15:1227–1235. 151, 153, 203

Valenzuela-Harrington M, Gruart A, Delgado-García JM (2007) Contribution of NMDA receptor NR2B subunit to synaptic plasticity during associative learning in behaving rats. *European Journal of Neuroscience* 25:830–836. 4, 32, 36, 39, 162, 185

van Groen T, Kadish I, Popović N, Popović M, Caballero-Bleda M, Baño-Otálora B, Vivanco P, Rol MÁ, Madrid JA (2011) Age-related brain pathology in Octodon degu: blood vessel, white matter and Alzheimer-like pathology. *Neurobiology of Aging* 32:1651–1661. 200

van Praag H, Qu PM, Elliott RC, Wu H, Dreyfus CF, Black IB (1998) Unilateral hippocampal lesions in newborn and adult rats: effects on spatial memory and BDNF gene expression. *Behavioural Brain Research* 92:21–30. 183

Verdoorn TA, Burnashev N, Monyer H, Seeburg PH, Sakmann B (1991) Structural determinants of ion flow through recombinant glutamate receptor channels. *Science* 252:1715–1718. 121

Verret L, Mann EO, Hang GB, Barth AMI, Cobos I, Ho K, Devidze N, Masliah E, Kreitzer AC, Mody I, Mucke L, Palop JJ (2012) Inhibitory interneuron deficit links altered network activity and cognitive dysfunction in Alzheimer model. *Cell* 149:708–721. 95, 110

Vicini S, Wang JF, Li JH, Zhu WJ, Wang YH, Luo JH, Wolfe BB, Grayson DR (1998) Functional and pharmacological differences between recombinant N-methyl-D-aspartate receptors. *Journal of Neurophysiology* 79:555–566. 12, 67, 125, 126

Vitolo OV, Sant'Angelo A, Costanzo V, Battaglia F, Arancio O, Shelanski M (2002) Amyloid beta -peptide inhibition of the PKA/CREB pathway and long-term potentiation: reversibility by drugs that enhance cAMP signaling. *Proceedings of the National Academy of Sciences* 99:13217–13221. 112, 154

Vlassenko AG, Vaishnavi SN, Couture L, Sacco D, Shannon BJ, Mach RH, Morris JC, Raichle ME, Mintun MA (2010) Spatial correlation between brain aerobic glycolysis and amyloid-β (Aβ) deposition. *Proceedings of the National Academy of Sciences* 107:17763–17767. 47

Volianskis A, Bannister N, Collett VJ, Irvine MW, Monaghan DT, Fitzjohn SM, Jensen MS, Jane DE, Collingridge GL (2013) Different NMDA receptor subtypes mediate induction of long-term potentiation and two forms of short-term potentiation at CA1 synapses in rat hippocampus in vitro. *Journal of Physiology* 591:955–972. 5, 12, 21, 40, 149, 189, 206, 207

Volk LJ, Bachman JL, Johnson R, Yu Y, Huganir RL (2013) PKM-ζ is not required for hippocampal synaptic plasticity, learning and memory. *Nature* 493:420–423. 7

von Engelhardt J, Doganci B, Jensen V, Hvalby Ø, Göngrich C, Taylor A,

Barkus C, Sanderson DJ, Rawlins JNP, Seeburg PH, Bannerman DM, Monyer H (2008) Contribution of hippocampal and extra-hippocampal NR2B-containing NMDA receptors to performance on spatial learning tasks. *Neuron* 60:846–860. 22, 34, 35, 37, 188

Vossel KA, Zhang K, Brodbeck J, Daub AC, Sharma P, Finkbeiner S, Cui B, Mucke L (2010) Tau reduction prevents Abeta-induced defects in axonal transport. *Science* 330:198. 110, 154

Walsh DM, Klyubin I, Fadeeva JV, Cullen WK, Anwyl R, Wolfe MS, Rowan MJ, Selkoe DJ (2002) Naturally secreted oligomers of amyloid beta protein potently inhibit hippocampal long-term potentiation in vivo. *Nature* 416:535–539. 51, 87, 91, 109, 117, 204

Wang D, Cui Z, Zeng Q, Kuang H, Wang LP, Tsien JZ, Cao X (2009) Genetic enhancement of memory and long-term potentiation but not CA1 long-term depression in NR2B transgenic rats. *PLoS ONE* 4:e7486. 23, 30, 36

Wang HY, Lee DH, Davis CB, Shank RP (2000) Amyloid peptide Abeta(1-42) binds selectively and with picomolar affinity to alpha7 nicotinic acetylcholine receptors. *Journal of Neurochemistry* 75:1155–1161. 50

Wang Q, Walsh DM, Rowan MJ, Selkoe DJ, Anwyl R (2004) Block of long-term potentiation by naturally secreted and synthetic amyloid beta-peptide in hippocampal slices is mediated via activation of the kinases c-Jun N-terminal kinase, cyclin-dependent kinase 5, and p38 mitogen-activated protein kinase as well as metabotropic glutamate receptor type 5. *Journal of Neuroscience* 24:3370–3378. 51, 87, 91, 109, 112, 204

Wang Q, Sporns O, Burkhalter A (2012) Network analysis of corticocortical connections reveals ventral and dorsal processing streams in mouse visual

cortex. *Journal of Neuroscience* 32:4386–4399. 192

Ward B, McGuinness L, Akerman CJ, Fine A, Bliss TVP, Emptage NJ (2006) State-dependent mechanisms of LTP expression revealed by optical quantal analysis. *Neuron* 52:649–661. 10, 93

Warren JD, Rohrer JD, Schott JM, Fox NC, Hardy J, Rossor MN (2013) Molecular nexopathies: a new paradigm of neurodegenerative disease. *Trends in Neurosciences* . 211

Waxman EA, Giasson BI (2011) Induction of intracellular tau aggregation is promoted by α-synuclein seeds and provides novel insights into the hyperphosphorylation of tau. *Journal of Neuroscience* 31:7604–7618. 88

Wei W, Nguyen LN, Kessels HW, Hagiwara H, Sisodia S, Malinow R (2010) Amyloid beta from axons and dendrites reduces local spine number and plasticity. *Nature Neuroscience* 13:190–196. 52, 87

Welander H, Frånberg J, Graff C, Sundström E, Winblad B, Tjernberg LO (2009) Abeta43 is more frequent than Abeta40 in amyloid plaque cores from Alzheimer disease brains. *Journal of Neurochemistry* 110:697–706. 49

Whitlock JR, Heynen AJ, Shuler MG, Bear MF (2006) Learning induces long-term potentiation in the hippocampus. *Science* 313:1093–1097. 4, 32, 39, 162

Williams SR, Mitchell SJ (2008) Direct measurement of somatic voltage clamp errors in central neurons. *Nature Neuroscience* 11:790–798. 149

Woo NH, Teng HK, Siao CJ, Chiaruttini C, Pang PT, Milner TA, Hempstead BL, Lu B (2005) Activation of p75NTR by proBDNF facilitates hippocampal long-term depression. *Nature Neuroscience* 8:1069–1077. 31

Wu Y, Kawakami R, Shinohara Y, Fukaya M, Sakimura K, Mishina M, Watanabe M, Ito I, Shigemoto R (2005) Target-cell-specific left-right asymmetry of NMDA receptor content in schaffer collateral synapses in epsilon1/NR2A knock-out mice. *Journal of Neuroscience* 25:9213–9226. 43

Yang SN, Tang YG, Zucker RS (1999) Selective induction of LTP and LTD by postsynaptic [Ca2+]i elevation. *Journal of Neurophysiology* 81:781–787. 10

Yao J, Du H, Yan S, Fang F, Wang C, Lue LF, Guo L, Chen D, Stern DM, Gunn Moore FJ, Xi Chen J, Arancio O, Yan SS (2011) Inhibition of amyloid-beta (Abeta) peptide-binding alcohol dehydrogenase-Abeta interaction reduces Abeta accumulation and improves mitochondrial function in a mouse model of Alzheimer's disease. *Journal of Neuroscience* 31:2313–2320. 110

Yashiro K, Philpot BD (2008) Regulation of NMDA receptor subunit expression and its implications for LTD, LTP, and metaplasticity. *Neuropharmacology* 55:1081–1094. 11, 21, 28

Yasuda R, Sabatini BL, Svoboda K (2003) Plasticity of calcium channels in dendritic spines. *Nature Neuroscience* 6:948–955. 10

Yin X, Feng X, Takei Y, Hirokawa N (2012) Regulation of NMDA receptor transport: a KIF17-cargo binding/releasing underlies synaptic plasticity and memory in vivo. *Journal of Neuroscience* 32:5486–5499. 22, 23, 35

Yin X, Takei Y, Kido MA, Hirokawa N (2011) Molecular motor KIF17 is fundamental for memory and learning via differential support of synaptic NR2A/2B levels. *Neuron* 70:310–325. 22, 23, 30, 35, 154

Yoshida H, Crowther RA, Goedert M (2002) Functional effects of tau gene mutations deltaN296 and N296H. *Journal of Neurochemistry* 80:548–551. 105

Youle RJ, Strasser A (2008) The BCL-2 protein family: opposing activities that mediate cell death. *Nature Reviews Molecular Cell Biology* 9:47–59. 112

Zalutsky RA, Nicoll RA (1990) Comparison of two forms of long-term potentiation in single hippocampal neurons. *Science* 248:1619–1624. 6

Zempel H, Thies E, Mandelkow E, Mandelkow EM (2010) Abeta oligomers cause localized Ca(2+) elevation, missorting of endogenous Tau into dendrites, Tau phosphorylation, and destruction of microtubules and spines. *Journal of Neuroscience* 30:11938–11950. 88

Zhang S, Edelmann L, Liu J, Crandall JE, Morabito MA (2008) Cdk5 regulates the phosphorylation of tyrosine 1472 NR2B and the surface expression of NMDA receptors. *Journal of Neuroscience* 28:415–424. 15

Zhang XH, Liu SS, Yi F, Zhuo M, Li BM (2013) Delay-dependent impairment of spatial working memory with inhibition of NR2B-containing NMDA receptors in hippocampal CA1 region of rats. *Molecular Brain* 6:13. 33, 34, 79, 179, 188

Zhang XH, Wu LJ, Gong B, Ren M, Li BM, Zhuo M (2008) Induction- and conditioning-protocol dependent involvement of NR2B-containing NMDA receptors in synaptic potentiation and contextual fear memory in the hippocampal CA1 region of rats. *Molecular Brain* 1:9. 20

Zhang Y, McLaughlin R, Goodyer C, LeBlanc A (2002) Selective cytotoxicity of intracellular amyloid beta peptide1-42 through p53 and Bax in cultured primary human neurons. *The Journal of cell biology* 156:519–529. 49

Zhang YP, Holbro N, Oertner TG (2008) Optical induction of plasticity at single synapses reveals input-specific accumulation of alphaCaMKII. *Proceedings of*

the National Academy of Sciences 105:12039–12044. 156

Zhang Y, Kurup P, Xu J, Carty N, Fernandez SM, Nygaard HB, Pittenger C, Greengard P, Strittmatter SM, Nairn AC, Lombroso PJ (2010) Genetic reduction of striatal-enriched tyrosine phosphatase (STEP) reverses cognitive and cellular deficits in an Alzheimer's disease mouse model. *Proceedings of the National Academy of Sciences* 107:19014–19019. 118

Zhao WQ, Santini F, Breese R, Ross D, Zhang XD, Stone DJ, Ferrer M, Townsend M, Wolfe AL, Seager MA, Kinney GG, Shughrue PJ, Ray WJ (2010) Inhibition of calcineurin-mediated endocytosis and alpha-amino-3-hydroxy-5-methyl-4-isoxazolepropionic acid (AMPA) receptors prevents amyloid beta oligomer-induced synaptic disruption. *Journal of Biological Chemistry* 285:7619–7632. 50, 51

Zhou Q, Homma KJ, Poo Mm (2004) Shrinkage of dendritic spines associated with long-term depression of hippocampal synapses. *Neuron* 44:749–757. 8

Zhou Y, Takahashi E, Li W, Halt A, Wiltgen B, Ehninger D, Li GD, Hell JW, Kennedy MB, Silva AJ (2007) Interactions between the NR2B receptor and CaMKII modulate synaptic plasticity and spatial learning. *Journal of Neuroscience* 27:13843–13853. 24, 31, 36, 162, 170, 186